THE UNIVERSITY
OF MICHIGAN

SEP 14 1962

ENGINEERING
LIBRARY

АВТОМАТИКА
и
ТЕЛЕМЕХАНИКА

Vol. 22, No. 7, July, 1961

Translation Published December, 1961

SOVIET INSTRUMENTATION AND
CONTROL TRANSLATION SERIES

Automation and Remote Control

(The Soviet Journal *Avtomatika i Telemekhanika* in English Translation)

■ This translation of a Soviet journal on automatic control is published as a service to American science and industry. It is sponsored by the Instrument Society of America under a grant in aid from the National Science Foundation, continuing a program initiated by the Massachusetts Institute of Technology.

SOVIET INSTRUMENTATION AND CONTROL TRANSLATION SERIES

Instrument Society of America

Philip A. Sprague
President
Dr. Ralph H. Tripp
Past President
Nathan Cohn
President-elect-Secretary
Henry J. Noebels
Dept. Vice President
Dr. Benjamin W. Thomas
Dept. Vice President-elect
E. A. Adler
Dept. Vice President
Francis S. Hoag
Dept. Vice President
John J. McDonald
Dept. Vice President
John R. Mahoney
Dept. Vice President-elect
John C. Koch
Treasurer
Alonzo B. Parsons
Dist. I Vice President
H. Kirk Fallin
Dist. II Vice President
Harold J. Bowman
Dist. III Vice President
Fred R. Gilmer
Dist. IV Vice President
Charles H. Callier
Dist. V Vice President
Otto J. Lessa
Dist. VI Vice President
J. Howard Park, III
Dist. VII Vice President
C. Roy Horton
Dist. VIII Vice President
Max Curtis
Dist. IX Vice President
Kenneth S. Vriesen
Dist. X Vice President
Allan E. Lee
Dist. XI Vice President

International Headquarters

William H. Kushnick
Executive Director
Charles W. Covey
Editor, ISA Journal
Herbert S. Kindler
Director, Tech. & Educ. Services

ISA Publications Committee

Charles O. Badgett, *Chairman*

Jere E. Brophy	George A. Larsen	Joshua Stern
Dr. Enoch J. Durbin	Thomas G. MacAnespie	Frank S. Swan
Prof. Richard W. Jones	John E. Read	Richard A. Ter

Translations Advisory Board of the Publications Committee

Jere E. Brophy, *Chairman*

T. J. Higgins	S. G. Eskin	G. Werbizky

■ This translation of the Soviet Journal *Avtomatika i Telemekh nika* is published and distributed at nominal subscription rates und a grant in aid to the Instrument Society of America f.om the N tional Science Foundation. This translated journal, and others i the Series (see back cover), will enable American scientists and e gineers to be informed of work in the fields of instrumentati measurement techniques, and automatic control reported in t Soviet Union.

The original Russian articles are translated by competent techni personnel. The translations are on a cover-to-cover basis and t Instrument Society of America and its translators propose to tra late faithfully all of the scientific material in *Avtomatika i Te mekhanika*, permitting readers to appraise for themselves the sco status, and importance of the Soviet work. All views expressed in t translated material are intended to be those of the original auth and not those of the translators nor the Instrument Society of Ameri

Publication of *Avtomatika i Telemekhanika* in English translati started under the present auspices in April, 1958, with Russian V 18, No. 1 of January, 1957. The program has been continued wi the translation and printing of the 1958-1961 issues.

Transliteration of the names of Russian authors follows the syst known as the British Standard. This system has recently achie wide adoption in the United Kingdom, and is currently being adopt by a large number of scientific journals in the United States.

Readers are invited to submit to the Instrument Society of Ameri comments on the quality of the translations and the content of t articles. Pertinent correspondence will be published in the Society monthly publication, the ISA JOURNAL. Space will also be ma available in the ISA JOURNAL for such replies as may be recei from Russian authors to comments or questions by the readers.

1961 Volume 22 Subscription Prices:

Per year (12 issues), starting with Vol. 22, No. 1

General:	*United States and Canada*	$35.0
	Elsewhere	38.0
Libraries of nonprofit academic institutions:		
	United States and Canada	$17.5
	Elsewhere	20.0
Single issues to everyone, each		$ 6.0

1957 Volume 18, 1958 Volume 19, 1959 Volume 20, and 1960 Volum 21 issues also available. Prices upon request.

See back cover for combined subscription to entire Series.

Subscriptions and requests for information on back issues should be addressed to the:

Instrument Society of America
530 William Penn Place, Pittsburgh 19, Penna.

Translated and printed by Consultants Bureau Enterprises, Inc.

Copyright © 1961 by the Instrument Society of America

Automation and Remote Control

A translation of Avtomatika i Telemekhanika, a publication of the Academy of Sciences of the USSR

EDITORIAL BOARD OF AVTOMATIKA I TELEMEKHANIKA

D. I. Ageikin
M. A. Aizerman
A. B. Chelyustkin *(Assoc. Editor)*
E. G. Dudnikov
N. Ya. Festa
V. A. Ilin
A. G. Iosuf'yan
V. V. Karibskii
A. V. Khramoi
B. Ya. Kogan
V. S. Kulebakin
S. A. Lebedev
A. Ya. Lerner
A. M. Letov *(Assoc. Editor)*
V. S. Malov
B. N. Petrov
Yu. P. Portnov-Sokolov
B. S. Sotskov
A. A. Tal' *(Corresp. Secretary)*
V. A. Trapeznikov *(Editor in Chief)*
Ya. Z. Tsypkin
G. M. Ulanov
A. A. Voronov
S. V. Yablonskii

Vol. 22, No. 7 | Russian Original Dated July, 1961 | December, 1961

CONTENTS

	PAGE	RUSS. PAGE
On the Application of Lyapunov's Direct Method to Differential Equations With Ambiguous Right Sides. Yu. I. Alimov	713	817
Concerning the Problem of Determining the Stability-Sector Boundaries in Nonlinear Control Systems. A. K. Bedel'baev	726	831
The Problem of Speed of Response without Switching for an Arbitrary Number of Control Functions. A. N. Filatov	729	834
On a Certain Problem in the Theory of Processes with an Optimal Speed of Response in Linear Systems. F. Al'brekht	733	838
Optimization of Automatic Systems by Statistical Criteria. S. A. Doganovskii	739	845
Automatic Optimization of Space Distribution. II. L. N. Fitsner	750	857
Optimum Control Characteristics of a Pulsed Relay System in the Presence of Random Disturbances. V. N. Novosel'tsev	758	865
The Description of Multidimensional Linear Systems in Matrix Form. I. Matyáš and Y. Silhánek	768	876
The Analysis of Periodic States Due to Level Quantization of Signal in Automatic Digital Systems. Yu. M. Korshunov	778	885
Investigating Nonsteady-State Processes in a Pulse System with a Step Motor. V. M. Kolesnikov	788	896
Precision Transistor Integrator. Yu. L. Kurkin and N. S. Kurkina	799	907
On the "Reversal" Conditions of Relay Semiconductor Devices. S. V. Kulikov	806	914
Determining the Optimal Parameters for Certain Types of Magnetic Logic Elements. N. P. Vasil'eva and I. Gashkovets	811	919
A Transmitting Device for Pulse-Frequency Telemetering. I. A. Lyubinskii, V. A. Milyutina, and N. V. Pozin	827	934
Tables and Formulas for Determining the Accuracy Characteristic for the Operation of a Linear Stationary Dynamic System. A. N. Sklyarevich	831	939
The SRP-3 Industrial Remote Control System. M. G. Geshelin, B. M. Levin, and A. G. Mamikonov	843	950
INFORMATION		
Modern Trends in the Development of Dispatcher Monitoring on the Basis of Digital Techniques. Ya. A. Kupershmidt, V. S. Malov, and I. M. Shenbrot	847	954

ON THE APPLICATION OF LYAPUNOV'S DIRECT METHOD TO DIFFERENTIAL EQUATIONS WITH AMBIGUOUS RIGHT SIDES*

Yu. I. Alimov

(Sverdlovsk)

Translated from Avtomatika i Telemekhanika, Vol. 22, No. 7,
pp. 817-830, July, 1961
Original article submitted November 26, 1960

Physical considerations are presented by virtue of which the dynamical equations of relay control systems may be considered as contingent equations [1,2] with ambiguous and continuous, in a certain sense, right sides. The theory of contingent differential equations is used to apply the direct method of Lyapunov to "relay" differential equations.

1. The dynamical equations of a relay control system,

$$\dot{\mathbf{x}} = \mathbf{f}(t, \mathbf{x}), \tag{1}$$

where $\mathbf{x}$ and $\mathbf{f}$ are n-dimensional column matrices [3], are as a rule considered as differential equations with discontinuous right sides. This point of view does not always correspond to the physical sense of the problem and leads to a very sharp line of demarcation between classical and "relay" differential equations as objects of mathematical investigation. Another approach, completely justified physically, is possible in which one bases the study of relay control systems on the strict theory of contingent equations; this theory has been developed sufficiently well by Zaremba [1] and Marchaud [2]. The following considerations, repeatedly put forth by many authors in a manner suitable to the particular case of relay systems, may serve as our guiding principle.

In composing the equations of motion of a relay system, each relay link is often considered as some union of "continuous" links, described ordinarily by differential equations (possibly with retarded arguments or partial derivatives, although such cases will not be considered) and, in general, by certain inertialess relay elements with a single input and a single output. Then the equations of motion, being put into normal form, may be written in the form of a system:

$$\dot{\mathbf{x}} = \mathbf{f}(t, \mathbf{x}) = \mathbf{f}[t, \mathbf{x}, \varphi(\sigma)], \qquad \sigma = \sigma(t, \mathbf{x}), \tag{2}$$

where $\mathbf{f}(t, \mathbf{x}, \varphi)$ and $\sigma(t, \mathbf{x})$ are continuous functions, and $\varphi(\sigma)$ is the characteristic of the relay element. For convenience in exposition, we shall meanwhile limit ourselves to the case of a single relay element. Here and in what follows, the continuity of functions is understood as continuity with respect to all their explicitly described arguments.

In any working regime, both the input $\sigma = \sigma(t)$ and the output $\varphi = \varphi[\sigma(t)]$ coordinate of each real link approximated by an inertialess relay element are continuous functions of time. Without going into a detailed description of the form of the characteristic $\varphi(\sigma)$ near the so-called switching thresholds

$$\sigma = \sigma(t, \mathbf{x}) = \sigma_k \qquad (k = k_1, k_2, \ldots), \tag{3}$$

the function $\varphi(\sigma)$ may be considered discontinuous in (3) only in regimes accompanied by sufficiently rapid traversal of the coordinate $\sigma(t)$ through the switching surfaces (3), when the magnitude of $\varphi(t) = \varphi[\sigma(t)]$ changes exceedingly rapidly near (3) in comparison with other regions of the $t, \mathbf{x}$ space (the meaning of inexact terminology such as "suf-

* The contents of this paper were briefly presented on June 30, 1960 at the First Congress of the IFAK.

ficiently rapid" is more precisely given for the class of problems considered in [4]). In the t, x phase space of model (2), these regimes correspond either to those portions of the surfaces (3) which are threaded through by trajectories of the corresponding ordinary system of differential equations

$$\dot{x} = f[t, x, \varphi(\sigma)], \quad \sigma = \sigma(t, x) \neq \sigma_k \quad (k = k_1, k_2, \ldots), \tag{4}$$

in one direction, or those portions from which the trajectories of the local system corresponding to (4) diverge toward different sides, each into "its own", from the subspaces

$$\sigma(t, x) \neq \sigma_k \quad (k = k_1, k_2, \ldots). \tag{5}$$

But to neglect the continuous change of the output coordinate $\varphi(t)$ is inadmissible in describing those motions of a real system (sliding regimes, motions with delays) which are connected with the coordinate $\sigma(t)$ lingering near the switching thresholds. The discontinuous idealization of the function $\varphi(\sigma)$ leads to the appearance of the surfaces (3) of portions threaded through by trajectories of system (4) passing from one subspace (5) into another, changing directions in so doing. The construction of the correct model within the framework of the chosen structural scheme now requires a more accurate expression of the dependence of $\varphi(\sigma)$ near the surfaces (3).

Before proceeding to this more accurate expression, it is of interest to test, directly from the discontinuous idealization, the following simple approximation to the relay characteristic at switching points:

$$\varphi(\sigma_k) = \xi_k. \quad (k = k_1, k_2, \ldots). \tag{6}$$

where ξ_k may be an arbitrary number in the interval

$$\left[\underline{\lim}_{\sigma \to \sigma_k} \varphi(\sigma), \quad \overline{\lim}_{\sigma \to \sigma_k} \varphi(\sigma)\right]. \tag{7}$$

Here and below, $\underline{\lim}$ and $\overline{\lim}$ are the least and greatest limit points respectively [5]. Such an approximation, already used successfully by Coulomb in studying dry friction, retains all the advantages of the discontinuous idealization, yet being in a certain sense continuous: the equations $\varphi = \varphi(\sigma)$ determines on the σ, φ plane a line, any portion of which in general may be sketched without lifting the pencil from the paper (see, for example, Fig. 2a).

The goal of this paper is to show how approximations of the type (6), (7) may be used in constructing a "continuous" variant of the theory of relay control systems (2).

It is easy to see that approximations (6), (7) are strongly connected with a representation of the relay characteristic $\varphi(\sigma)$, as well as of discontinuous functions, as limits of nonuniformly convergent sequences $\{\varphi_k(\sigma)\}$ of continuous functions, monotone and changing sharply near (3). The validity of such representations is discussed, and the representations themselves used, in many papers having to do with the theory of relay differential equations. Actually, the characteristic $\varphi(\sigma)$ under approximations (6), (7) may be considered as a point set in the σ, φ plane, the limit of the same sequence $\{\varphi_k(\sigma)\}$ when each term of this sequence is also considered a set of points (σ, φ); and as a measure of the nearness of sets, their mutual deviation according to Hausdorff [6] is taken in the closed region of the σ, φ plane with which we are dealing. We note that the comparison of characteristics $\varphi_k(\sigma)$ with the aid of their mutual deviation in the σ, φ plane certainly corresponds better to one's intuitive idea of the nearness of curves than does the comparison of the functions $\varphi_k(\sigma)$ for the same values of their argument σ, as is done in the theory of series of functions.

2. Employing the usual geometrical interpretation [7], we shall say some more about the direction field of system (2); the directions of the field at a given point (t, x) shall be thought of as corresponding to the vector $f(t, x)$, and considered as a point of some n-dimensional space $E(f)$—the space of directions of the system (2).

Taking the approximation (6), (7) for the relay characteristic $\varphi(\sigma)$, it is natural to consider that on the switching surfaces (3) the right sides of system (2) give not one, but a whole cone of directions (Fig. 1); namely: the set $\{f[t, x, \varphi(\sigma_k)]\}$ of vectors $f(t, x, \xi_k)$ corresponding to all numbers ξ_k from the interval (7). We note that at points (t^0, x^0) of the surface (3) the inequalities

$$\underline{\lim}_{(t, x) \to (t^0, x^0)} f_i(t, x) \leqslant f_i(t, x) \leqslant \overline{\lim}_{(t, x) \to (t^0, x^0)} f_i(t, x) \quad (i = 1, 2, \ldots, n) \tag{8}$$

for components of the vector function $\mathbf{f}(t,\mathbf{x})$ might not be fulfilled. An integral curve of the relay system (2) may now be defined as any continuous curve $\mathbf{x}(t)$ about which it may be said that motion along it proceeds at each moment of time t in some direction of the cone $\{\mathbf{f}(t, \mathbf{x}(t))\}$. Such a definition would seem in the present case to be a simple and accurate analog of the definition of integral curve of ordinary differential equations.

The system obtained does not possess complete information for the determination of the velocity $\mathbf{x}(t)$ as function of the coordinates $t, \mathbf{x}$. The possible violation of uniqueness of the solution will be payment for the comparative simplicity of the model, reflecting the insufficiency of the information contained in the latter. The criterion of how successful such a simplified model will be is in the final analysis found by comparison with experiments.

The assumed conception of a system with incomplete information naturally also includes those cases when the direction field determined by the functions $\mathbf{f}(t, \mathbf{x})$ is "washed away" not only on the surfaces defined, but also on certain sets in phase space with nonzero volume. This latter circumstance is very essential, since for no single link in a real system may the output be characterized exactly for any lengthy period of time in the form of a single-valued functional or differential dependence of the input and time. For instance, the results of repeatedly photographing static characteristics of an electromagnetic relay often have an appearance like Fig. 2b rather than Fig. 2a. Relay switching proceeds in different experiments under differing values of the input σ (the line density in the rectangle 1234 is proportional to the relative frequency of relay switching at the corresponding value of σ in the interval 12). In the first approximation, one considers a strictly determined characteristic (Fig. 2a), which is some kind of average or another of the real characteristic (Fig. 2b). A different approximation involves the consideration of characteristics in a form represented in Fig 2c. Here the coordinates σ and φ may define any point in the blacked out rectangle 1234, covering the hysteresis zone of a real dependence $\varphi(\sigma)$. Further improvements in the model may consist in accounting for the statistical inhomogeneity of the region 1234.

The above sketched principle for constructing mathematical models of relay systems reveal a definite similarity to the theory of equations in contingents and paratingents [1, 2, 8]. We shall give a short exposition of the fundamentals of this theory.* The exposition is given in terms as near as possible to the formalism occuring in the theory of ordinary differential equations.

3. All spaces considered below are Euclidean. We recall that the distance $\rho(\mathbf{p}, \mathbf{q})$ between points $\mathbf{p} = (p_1, p_2, \ldots, p_m)$ and $\mathbf{q} = (q_1, q_2, \ldots, q_m)$ of m-dimensional Euclidean space is given by the formula

$$\rho(\mathbf{p}, \mathbf{q}) = \left[\sum_{i=1}^{m} (p_i - q_i)^2\right]^{0.5}, \tag{9}$$

and the distance $\rho(A, B)$ between point set A and B of such a space is taken as the exact lower bound [5] of the set of quantities $\rho(\mathbf{p}, \mathbf{q})$ where $\mathbf{p}$ and $\mathbf{q}$ are any points in the sets A and B respectively.

An abstract function which assigns to a point $\mathbf{p} = (p_1, p_2, \ldots, p_m)$ a nonempty bounded closed connected set $\{\mathbf{f}(\mathbf{p})\}$ in some n-dimensional space $E(\mathbf{f})$ is called a many-valued n-dimensional vector function $\mathbf{f}(\mathbf{p})$. In the scalar case (n = 1) the set $\{\mathbf{f}(\mathbf{p})\}$ is a segment, for which we introduce the special notation $[mf(\mathbf{p}), Mf(\mathbf{p})]$. It is further considered that the analytical expressions on the right side of systems (2), (6) and (7) provide some many-valued vector functions $\mathbf{f}(t, \mathbf{x})$ by the superposition of the ordinary functions $\mathbf{f}(t, \mathbf{x}, \varphi)$ and the scalar many-valued functions $\varphi = \varphi[\sigma(t, \mathbf{x})]$, which were given in sec. 2. In accordance with this natural definition, and with account taken of one additional convention formulated in sec. 4, a completely determined sense is given also to such expressions as the sum $\varphi_1(\sigma) + \varphi_2(\sigma)$ of scalar many-valued functions $\varphi_1(\sigma)$ and $\varphi_2(\sigma)$ [superposition of the single-valued function $u = v + w$ and the many-valued functions $v = \varphi_1(\sigma)$ and $w = \varphi_2(\sigma)$], the scalar product of two many-valued vector-functions of the same dimensionality and so on. The relations

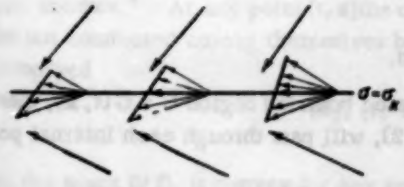

Fig. 1

$$mV(\mathbf{p}) \geqslant 0 \quad \text{and} \quad MV(\mathbf{p}) \leqslant 0 \tag{10}$$

for scalar many-valued functions $V(\mathbf{p})$ are customarily written in the form of the corresponding inequalities

*A more detailed theory of equations in contingents is given in [9].

$$V(p) \geqslant 0 \quad \text{and} \quad V(p) \leqslant 0 \tag{11}$$

(strict inequality in (10) will correspond to strict inequality in (11) and conversely).

If the right side of equation (1) determines in some fashion an n-dimensional many-valued function of the variables $t, \mathbf{x}$, then this equation will be considered as an equation in contingents. The space $E(f)$ for the function $f(t, \mathbf{x})$ we have already essentially agreed to call the direction space of system (1), and the sets $\{f(t, \mathbf{x})\}$, the direction cones.

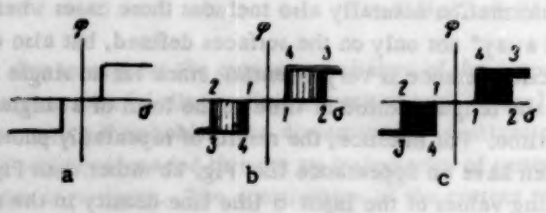

Fig. 2

As is known, the contingent kont $\mathbf{x}(t_1)$ of the curve $\mathbf{x} = \mathbf{x}(t)$ at the point $(t, \mathbf{x}(t_1))$ of the space $t, \mathbf{x}$ is defined as the set of all limiting directions of the chord spanning the points $(t_1, \mathbf{x}(t_1))$ and $(t_2, \mathbf{x}(t_2))$ of this curve when $t_2 \to t_1$.

Definition 1. Following [1, 2, 8], we define a solution to the equation in contingents (1) passing through the point $(t_0, \mathbf{x}_0)$ and defined on some interval

$$t_0 - \alpha < t < t_0 + \alpha \quad (\alpha > 0,) \tag{12}$$

as any continuous vector function $\mathbf{x}(t) = \mathbf{x}(t_0, \mathbf{x}_0, t)$ for which $\mathbf{x}(t_0) = \mathbf{x}_0$ and whose contingents, considered as a point set in the direction space $E(f)$ are included in the direction cone $\{f[t, \mathbf{x}(t)]\}$ everywhere in the interval (12):

$$\operatorname{kont} \mathbf{x}(t) \subset \{f[t, \mathbf{x}(t)]\}, \qquad t_0 - \alpha < t < t_0 + \alpha. \tag{13}$$

It is easily seen that definition 1 in its application to the relay equation (2), (6) and (7) corresponds very well with the considerations presented in sec. 1 and sec. 2.

The ϵ-neighborhood $S(\epsilon, A)$ of the point set A is taken to mean the set of all points p of the given space for which $\rho(p, A) < \epsilon$.

Definition 2. The many-valued function $f(p)$ is called β-continuous at the point p_0 if for any $\epsilon > 0$ there exists a $\delta = \delta(p_0, \epsilon) > 0$ such that the set $\{f(p)\}$ lies in the ϵ-neighborhood of the set $\{f(p_0)\}$, provided the point p lies in the δ-neighborhood of the point p_0. α-continuity shall require, in addition to the above, that the set $\{f(p_0)\}$ in turn lie in the ϵ-neighborhood of the set $\{f(p)\}$.

This terminology is connected with the concepts of semideviation [6] β and deviation α of sets and we borrow them from the work of Yu. K. Solntsev [10]. The term "semicontinuity from above with respect to deviation" [8] appears to be less convenient as it is more cumbersome.

If at each point of the region $G = G(t, \mathbf{x})$ of $t, \mathbf{x}$ space the many-valued function $f(t, \mathbf{x})$ is β-continuous in the variables $t, \mathbf{x}$ and the set $\{f(t, \mathbf{x})\}$ is convex, then we shall say that the contingent equation $\mathbf{x} = f(t, \mathbf{x})$ satisfies condition A in the region G.

Following papers [1, 2 and 8] one may formulate this existence theorem.

Theorem 1. If the contingent equation (1) satisfies condition A in a closed bounded region $\overline{G} = \overline{G}(t, \mathbf{x})$, then at least one solution of this equation, defined on some interval of the form (12), will pass through each internal point of the region $\overline{G}$.

This theorem is very easily proved by the method of Peano, if, carrying through the discussion according to the scheme in [7], in the concluding portion of the proof one uses, in place of the mean value theorem of integral calculus, the fact that the direction of the chord subtending the Euler broken arc belongs to the least convex cone which contains the directions of all links of this arc. It is apparently not possible to weaken significantly the requirement on the convexity of the set $\{f(t, \mathbf{x})\}$.

Further construction of the theory of contingent equations is conveniently carried out under the following assumptions (integrals are to be understood in the sense of Lebesgue).

Theorem 2. Suppose the contingent equation (1) is given and satisfies the condition A in the closed and bounded region $\overline{G} = \overline{G}(t, \mathbf{x})$. The vector function $\mathbf{x}(t)$ is a solution of this equation on the interval (t_1, t_2) if and only if the following conditions are fulfilled for every t', t'' in the interval (t_1, t_2):

$$(t', \mathbf{x}(t')) \in \overline{G}, \qquad \mathbf{x}(t'') = \mathbf{x}(t') + \int_{t'}^{t''} \varphi(\xi)\, d\xi, \tag{14}$$

where $\varphi(t)$ is some summable function for which

$$\varphi(t) \in \{\mathbf{f}[t, \mathbf{x}(t)]\} \quad \text{for} \quad t_1 < t < t_2. \tag{15}$$

4. Starting from Theorems 1 and 2, it is not difficult to obtain for contingent equations a theorem on the continuability of solutions, analogous to the corresponding proposition in the theory of ordinary differential equations, and, in the case of continuability of solutions, to prove that the axiom of E. A. Barbashin on the generalized dynamic system [6] is fulfilled. The usual theorems on substitution of variables (analogous, for example, to Theorems 1 and 2 of [11]), are easily extended to contingent equations.

Thus the consideration of system (2) as a contingent equation, based on approximations (6) and (7) allows one to obtain a correct model for a relay system without having recourse each time to a detailed construction of its phase space. This latter circumstance is fairly significant, since the construction indicated is cumbersome with two or more intersecting switching surfaces and is not too useful for "strongly washed away" characteristics $\varphi(\sigma)$, similar to that depicted in Fig. 2c. In fact, however, such an approach is admissible only under the condition that for the system examined the requirements of the existence theorem are satisfied. We briefly consider how natural these requirements are in the case, encountered most often in practice, when the relay system may be described by equations of the form (2).

Under an approximation of the type (6), (7), the characteristic $\varphi(\sigma)$ of real links (of the same number and similar to Fig. 2c), and also the jump-forming external disturbances are β-continuous, so that the right side of equation (2), being a superposition of continuous and β-continuous functions, is always β-continuous.

The requirement of convexity of the set $\{\mathbf{f}(t, \mathbf{x})\}$ is far more limiting. Actually, from the convexity of the set $\{\varphi(\sigma)\}$ and the continuity (single-valued of the function $\mathbf{f}(t, \mathbf{x}, \varphi)$ the convexity of the set $\{\mathbf{f}(t), \mathbf{x}, \varphi(\sigma)]\}$ does not in general follow. In this connection, we return to the question of what one should understand by the result $\mathbf{f}(t, \mathbf{x}) = \mathbf{f}[t, \mathbf{x}, \varphi(t, \mathbf{x})]$ of superimposing a many-valued and a single function $\mathbf{f}(t, \mathbf{x}, \varphi)$ and $\varphi(\sigma) = \varphi(t, \mathbf{x})$. Here the following two limiting points of view are possible. The first, actually occurring in [12], reduces to the definition of the cone $\{\mathbf{f}[t, \mathbf{x}, \varphi(t, \mathbf{x})]\}$ at points $(t^\circ, \mathbf{x}^\circ)$ of the surface (3) as a set of vectors defined by the ordinary vector function

$$(t^\circ, \mathbf{x}^\circ, \xi_k) = (f_1(t^\circ, \mathbf{x}^\circ, \xi_k^{(1)}), \ldots, f_n(t^\circ, \mathbf{x}^\circ, \xi_k^{(n)}))' \tag{16}$$

under the condition that the numbers $\xi_k^{(i)}$ $(i = 1, 2, \ldots, n)$ take on all values from the segment (7) independently of one another.* At any point $(t, \mathbf{x})$ the components $f_i(t, \mathbf{x}, \varphi)$ $(i = 1, 2, \ldots, n)$ of the right side of system (2) prove to be not connected among themselves by scalar many-valued functions, and the set $\{\mathbf{f}(t, \mathbf{x}, \varphi)\}$, a rectangular parallelopiped

$$mf_i(t, \mathbf{x}, \varphi) \leqslant f_i \leqslant Mf_i(t, \mathbf{x}, \varphi) \qquad (i = 1, 2, \ldots, n)$$

in the space $E(\mathbf{f})$, is convex for any system (2). Definition 1 becomes near in substance to the definition of E. E. Viktorovskii [12].

The opposite point of view, taken in one form or another in almost all papers on the theory of relay equations (see, for example [11]) and characterized above in sec. 2, reduces to this: that only those vectors (16) for which $\xi_k^{(1)} = \xi_k^{(2)} = \ldots = \xi_k^{(n)} = \xi_k$ are included in the cone $\{\mathbf{f}(t, \mathbf{x}, \varphi(t, \mathbf{x}))\}$. The cone $\{\mathbf{f}(t, \mathbf{x}, \varphi)\}$ degenerates into the arc of some curved line in the space $E(\mathbf{f})$ and therefore is convex only when this curve is a straight line. Thus this approach comprises only those systems (2) which are representable in the form

*In (16) and below the sign $'$ denotes the transposed matrix.

$$\dot{x} = f_1(t, x) + f_2(t, x)\varphi(\sigma) \quad (\sigma = \sigma(t, x)),$$

where $f_1(t, x)$, $f_2(t, x)$ and $\sigma(t, x)$ are ordinary continuous functions according to Definition 1, and Theorem 1 becomes more effective than in the preceding case, when each system (2) was often considered as a system in n relay elements. In particular, the method of constructing Lyapunov functions, worked out for control systems with one nonlinear link, is not applicable to relay system (2) with the Viktorovskii definition of solution.

The latter point of view corresponds, strictly speaking, only to the situation when the real link actually has one output (one pair of contacts on the relay, one point for removing the voltage from the trigger, etc.) whereas the first of the limiting approaches considered assumes the existence of n outputs from the link, independent at moments of switching. Such an assumption will apparently be natural in most cases; however, there may occur cases (when the relay has several groups of contacts, the output voltages of the trigger are taken at various points in its scheme, etc.), when it may prove useful to have some intermediate point of view, employing not one and not n, but two or three characteristics, identical everywhere with the exclusion of the sliding regimes, for the description of the real link. Then a compromise is attained between the necessity of describing the link by several characteristics, and the endeavor to simplify the equations of motion. All the approaches given to determining the cones $\{f(t, x)\}$ involve alike the theory of contingent equations. Results near in substance to the results [11, 12], are obtained from this theory, as was already noted above, in the form of limiting particular cases. We note that the theory developed in [11, 12], was presented in a form difficult for its application to the problem of automatic control, and the Solntsev definition [10] does not correspond to the physical considerations presented above.

Uniqueness may be attained in determining the direction field for relay systems of the form

$$\dot{x} = f[t, x, \varphi_1(\sigma_1), \varphi_2(\sigma_2), \ldots, \varphi_m(\sigma_m)],$$
$$\sigma_j = \sigma_j(t, x) \quad (j = 1, \ldots, m), \tag{17}$$

under the condition that the second, more effective of the limiting approaches examined takes place for those and only those functions $\varphi(\sigma)$ which are designated in (17) by undistinguished symbols. Thus, for example, the definition of solution according to Viktorovskii means that each system (2) is considered as a system

$$\dot{x} = (f_1[t, x, \varphi_1(\sigma)], \ldots, f_n[t, x, \varphi_n(\sigma)])',$$

and in the examples introduced below (see secs. 5, 6) the cones $\{f(t, x)\}$ are segments of straight lines in the space $E(f)$ (compare with [11], page 105).

5. In the extension to contingent equations of Lyapunov's direct method, it is useful to use the following assertion.

Theorem 3. Suppose the contingent equation (1) satisfies condition A in a closed bounded region $\overline{G}(t, x)$, and the continuous and continuously differentiable function $V = V(t, x)$ is such that for the scalar many-valued function

$$W(t, x) = \frac{\partial V}{\partial t} + \frac{\partial V}{\partial x} f(t, x) \tag{18}$$

the following inequality is satisfied everywhere in $\overline{G}(t, x)$:

$$W(t, x) \leqslant 0. \tag{19}$$

Suppose, further, that some arc of some integral curve $x(t)$ of system (1), corresponding to the segment

$$t_1 \leqslant t \leqslant t_2, \tag{20}$$

is completely situated in $\overline{G}(t, x)$. Then the function $V(t) = V[t, x(t)]$ does not increase in (20), and we have the following estimate:

$$V(t_2) - V(t_1) \leqslant (t_2 - t_1) \sup_{t_1 < \tau < t_2} [MW[\tau, x(\tau)]]. \tag{21}$$

The proof of Theorem 3 is given in Appendix 1. The scalar product $\frac{\partial V}{\partial x} f(t, x)$ of the row matrix $\frac{\partial V}{\partial x} = \left(\frac{\partial V}{\partial x_1}, \ldots, \frac{\partial V}{\partial x_n}\right)$ and the many valued function $\mathbf{f}(t, \mathbf{x})$ is to be understood in (18) in relation to that mentioned in sec. 3: the set $\left\{\frac{\partial V}{\partial x} f(t, x)\right\}$ is a segment formed by numbers which are scalar products of n-dimensional vectors $\partial V / \partial x$ and $\xi(t, \mathbf{x})$ under the condition that $\xi(t, \mathbf{x})$ is an arbitrary vector of the cone $\{\mathbf{f}(t, \mathbf{x})\}$. The computation of the function (18) for system (2) is accomplished completely analogously to the method in the case of ordinary differential equations.

If stability is understood in the sense of the usual definition [13], then on the basis of Theorems 1-3, considering the many valued function (18) in place of the ordinary derivative of the Lyapunov V-function, it is easy to establish the validity of Lyapunov's theorems on the stability and instability of motion in the supplemented formulation introduced in [13] for contingent equations. The proof is a verbatim repetition of the proof of the classical theorem.

In the way of an example, we investigate, by the method of Lur'e, the stability in the large of the equilibrium of the system of contingent equations

$$\dot{\mathbf{x}} = \mathbf{A}\mathbf{x} + \mathbf{a}\varphi(\sigma), \quad \sigma = \mathbf{k}'\mathbf{x}, \tag{22}$$

describing normal modes of motion of a control system with one nonlinear link ($\mathbf{A}$ is a square, and $\mathbf{x}$, $\mathbf{a}$, $\mathbf{k}$ column n-dimensional matrices). We assume that the linear part $\dot{\mathbf{x}} = \mathbf{A}\mathbf{x}$ is asymptotically stable, and that the function $\varphi(\sigma)$ is δ-continuous and satisfies the condition $\varphi(\sigma)\sigma \geq 0$, i.e. has, for example, the form represented in Fig. 2c (the blacked out regions cover the hysteresis zone or the possible rapid fluctuation and drift characteristics of the nonlinear link). Taking the V-function as a quadratic form $V(\mathbf{x}) = \mathbf{x}'\mathbf{H}\mathbf{x}$ ($\mathbf{H} = \mathbf{H}'$), we find that the many-valued function (18) is determined in the given case by the equations

$$W(\mathbf{x}) = -\mathbf{x}'\mathbf{G}\mathbf{x} + 2\mathbf{a}'\mathbf{H}\mathbf{x}\varphi(\sigma), \quad \mathbf{G} = -\mathbf{H}\mathbf{A} - \mathbf{A}'\mathbf{H}, \quad \mathbf{H} = L(\mathbf{G}).$$

Suppose the relation

$$2L(\mathbf{G})\,\mathbf{a} = -\mathbf{k},$$

holds, where $\mathbf{G}$ is some symmetric matrix for which

$$\mathbf{x}'\mathbf{G}\mathbf{x} > 0 \quad \text{for} \quad \mathbf{x} \neq 0. \tag{23}$$

Then

$$\dot{W}(\mathbf{x}) = -\mathbf{x}'\mathbf{G}\mathbf{x} - \sigma\varphi(\sigma), \tag{24}$$

so that

$$\dot{W}(\mathbf{x}) < 0 \quad \text{for} \quad \mathbf{x} \neq 0. \tag{25}$$

Since the form $\mathbf{x}'L(\mathbf{G})\mathbf{x}$ is positive definite (Lyapunov's theorem), the stability of the equilibrium $\mathbf{x} = 0$ in the large will follow, in accordance with the above, from Lyapunov's theorem [13]. Inequality (23) is satisfied if

$$\mathbf{x}'\mathbf{G}\mathbf{x} = \mathbf{x}'\mathbf{G}_1\mathbf{x} + (\mathbf{u}'\mathbf{x})^2 \quad (\mathbf{G} = \mathbf{G}_1 + \mathbf{u}\mathbf{u}'), \tag{26}$$

where $\mathbf{x}'\mathbf{G}_1\mathbf{x}$ is some positive definite form, and $\mathbf{u}$ a real column matrix. Representation (26) is possible under the condition that the equation for $\mathbf{u}$

$$2L(\mathbf{u}\mathbf{u}')\,\mathbf{a} + \mathbf{k} + 2L(\mathbf{G}_1)\,\mathbf{a} = 0 \tag{27}$$

admits a real solution. This is known to take place for any matrix $\mathbf{G}_1$ with sufficiently small elements, as well as for those which correspond to the positive definite form $\mathbf{x}'\mathbf{G}_1\mathbf{x}$, if the shortened resolving equation

$$2L(\mathbf{u}\mathbf{u}')\mathbf{a} + \mathbf{k} = 0 \tag{28}$$

possesses simple roots. The method of investigating equation (28) is indicated in [14]. We have generalized the results obtained in [15] for systems of the form (22) with $\varphi(\sigma) = \varphi(\sigma, t)$: in the example analyzed, the nonlinear characteristic may depend in a different manner on time along different trajectories of the system (this occurs, for example, in the reversal of magnetization in magnetic relays).

In order to extend the contingent equations, the theorems of Barbashin and Krasovskii ([13], Theorem 14.1), Krasovskii ([13], Theorem 15.1), Wechsler [16], and other applications of the direct method of Lyapunov, which permit one to weaken the requirements on the V-function and their derivatives, it is necessary to use also the fact that contingent equations under certain natural restrictions (see sec. 4) determine a generalized dynamic system. An illustration of this is the proof of the following theorem given in Appendix II.

Theorem 4. Suppose the contingent equation

$$\dot{x} = f(x), \qquad 0 \in \{f(0)\} \tag{29}$$

satisfies condition A over the entire t, x space, and all its solutions $x(t)$ are continuous for $-\infty < t < +\infty$. If there exists a continuous positive definite function $V = V(x)$, infinitely large for $x \to \infty$, not increasing along any solution $x(t)$ and such that no one of the surfaces $V(x) = c$ for $c > 0$ contains any solution $x(t)$ completely, then the equilibrium $x = 0$ of the system (29) is asymptotically stable in the large.

6. As is shown by the investigation of system (22) carried through above, significant information on the solutions of equation (2) may be obtained comparatively simply if the function (18) is considered in place of the $\dot{V}$ in the theorems of the direct method of Lyapunov. However, the limitations imposed here on the V-function are not known to be excessively rigid except under the condition that motion resulting from the system studied actually may proceed at each point (t, x) in any direction belonging to the cone $\{f(t, x)\}$. If the right side is ambiguous only on certain surfaces of the t, x space, then this latter condition is violated. In accordance with Definition 1, the motion often proceeds in one definite direction, and to make the stability condition more precise, the measurements of the V-function should be restricted to this direction only.

A possible procedure for making the investigation of stability in the given situation more precise will be considered in connection with the contingent equations

$$\dot{x} = F(x) + a\varphi(x), \qquad F(0) = 0, \qquad 0 \in \{\varphi(0)\}, \tag{30}$$

given over the entire phase space x. Here $F(x)$ is a continuous single-valued vector function, a is a constant column matrix, $\varphi(x)$ is a β-continuous scalar function, ambiguous only on the sufficiently smooth surfaces S_k, determined by the equations

$$\sigma_k(x) = 0 \quad (k = \ldots, -1, 0, 1, \ldots)$$

and separating the x space into nonintersecting regions. We denote the regions separated by the surface S_k as G_k^+ and G_k^-, supposing that $\sigma_k(x) > 0$ in G_k^+, and $\sigma_k(x) < 0$ in G_k^-.

The equations of a controlled system with one link with ambiguous characteristic may be brought into the form (30).

By definition 1, motion in the regions $G_k^{\pm}$ proceeds in accordance with the equations

$$\dot{x} = F(x) + a\varphi_k^{\pm}(x) = f_k^{\pm}(x),$$
$$\varphi(x) = \begin{cases} \varphi_k^+(x) & \text{в } G_k^+, \\ \varphi_k^-(x) & \text{в } G_k^- \end{cases} \tag{31}$$

(the superscript signs are chosen to be the same in G_k and $\varphi_k(x)$), and within the set

$$\sigma_k(x) = 0, \quad \dot{\sigma}_k^+(x) \cdot \dot{\sigma}_k^-(x) \leqslant 0, \quad \dot{\sigma}_k^+(x) \neq \dot{\sigma}_k^-(x), \tag{32}$$

in accordance with the system $\dot{\sigma}_k^{\pm}(x) = \dfrac{\partial \sigma_k}{\partial x}[F(x) + a\varphi_k^{\pm}(x)]$

$$\dot{x} = f_k^\circ(x) = F(x) + a\xi_k^\circ(x), \tag{33}$$

for which

$$\dot{\sigma}_k^\circ(x) = \frac{\partial \sigma_k}{\partial x} f_k^\circ(x) \equiv 0. \tag{34}$$

From (34) it follows that

$$\xi^\circ{}_k(x) = -\frac{\partial \sigma_k}{\partial x} F(x) \cdot \left(\frac{\partial \sigma_k}{\partial x} a\right)^{-1}, \tag{35}$$

$$m\varphi(x) \leqslant \xi_k^\circ(x) \leqslant M\varphi(x). \tag{36}$$

It is easy to see that from (32) the relation

$$\frac{\partial \sigma}{\partial x} a \neq 0 \tag{37}$$

follows.

If, on the surface S_k

$$m\varphi(x) = \min\{\varphi_k^+(x), \varphi_k^-(x)\}, \quad M\varphi(x) = \max\{\varphi_k^+(x), \varphi_k^-(x)\}, \tag{38}$$

which is always fulfilled for the characteristic of a real link, then (36) is valid only in the set (32).

On those portions of the switching surfaces where

$$\begin{gathered}\sigma_k(x) = \dot{\sigma}_k^+(x) = \dot{\sigma}_k^-(x) = \dot{\sigma}_k(x) = 0, \\ \ddot{\sigma}_k^+(x) \cdot \ddot{\sigma}_k^-(x) \leqslant 0, \quad \ddot{\sigma}_k^+(x) \neq \ddot{\sigma}_k^-(x), \\ \ddot{\sigma}_k^\pm(x) = \frac{\partial \dot{\sigma}}{\partial x}[F(x) + a\varphi_k^\pm(x)],\end{gathered} \tag{39}$$

Definition 1 leads to the system

$$\dot{x} = F(x) + a\xi_k^{\circ\circ}(x) = f_k^{\circ\circ}(x), \tag{40}$$

for which

$$\dot{\sigma}_k^{\circ\circ}(x) = \frac{\partial \dot{\sigma}_k^{\circ\circ}}{\partial x} f_k^{\circ\circ}(x) \equiv 0, \quad \dot{\sigma}_k^{\circ\circ}(x) = \frac{\partial \dot{\sigma}_k}{\partial x} \cdot f_k^{\circ\circ}(x). \tag{41}$$

Since on the set (39) necessarily $\frac{\partial \sigma_k}{\partial x} a = 0$ and

$$\frac{\partial}{\partial x}\left(\frac{\partial \sigma_k}{\partial x} F(x)\right) a \neq 0, \tag{42}$$

then on this set $\sigma_k^{\circ\circ}(x) = \dot{\sigma}_k(x) = 0$ and $m\varphi(x) \leqslant \xi_k^{\circ\circ}(x) \leqslant M\varphi(x)$,

$$\xi^{\circ\circ}{}_k(x) = -F(x)\frac{\partial}{\partial x}\left(\frac{\partial \sigma_k}{\partial x} F(x)\right)\left[\frac{\partial}{\partial x}\left(\frac{\partial \sigma_k}{\partial x} F(x)\right) a\right]^{-1}. \tag{43}$$

When inequalities (42) are satisfied over all space, the motion on those portions of the surfaces S_k which enter into none of the sets (32) or (39) proceeds under condition (38) along the semitrajectories of the local system (31).

The structure of the phase space of system (30) on the boundaries of the sets (32), (39) is not explained in detail here, since the existence and continuability of the solution of this system is always guaranteed in practice by the general theorems of contingent equations. Definition 1 leads in the given case basically to those representations of the trajectories which are usually used in writings on the theory of relay systems. The difference consists in the following: it is usually considered that, moving along the system's trajectories, it is impossible to fall into the zone of dynamic indeterminacy

$$\sigma_k(x) = 0, \qquad \dot{\sigma}_k^+(x) > 0 > \dot{\sigma}_k^-(x), \tag{44}$$

from which the trajectories of system (31) diverge to different sides. According to Definition 1, there is a trajectory of system (33) lying on the surface S_k passing through each point of zone (44) (see Fig. 3a). Such an approach is better founded since the phase picture of a relay system near the zone (44) should be considered a limiting case of the phase picture of an ordinary dynamical system with sharp dependence of the solution on initial conditions (Fig. 3b). This difference presents no obstacle to carrying over directly to contingent equations many results (in particular, those obtained in [3]) of the theory of differential equations with discontinuous right sides.

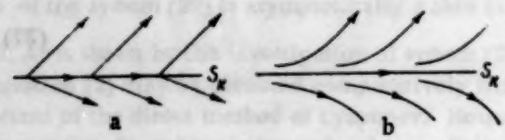

Fig. 3

Suppose the equation of the switching surface S_k for system (30) is represented in the form

$$x_n = \psi_k(t, x_1, x_2, \ldots, x_{n-1}), \tag{45}$$

and there is constructed a continuous positive definite function $V(x)$, growing to infinity as $x \to \infty$, with continuous partial derivatives $\partial V/\partial x$ in the regions G_k^+, and the partial derivatives $\partial V_k^\circ/\partial x$ of the function $V_k^\circ(x_1, x_2, \ldots, x_{n-1})$, obtained from $V(x)$ by the substitution (45), are also continuous. We introduce the notation:

$$\dot{V}_k^+(x) = \frac{\partial V}{\partial x} f_k^+(x), \qquad \dot{V}_k^-(x) = \frac{\partial V}{\partial x} f_k^-(x),$$
$$\dot{V}_k^\circ(x) = \frac{\partial V_k^\circ}{\partial x} f_k^\circ(x), \qquad \dot{V}_k^{\circ\circ}(x) = \frac{\partial V_k^{\circ\circ}}{\partial x} f_k^{\circ\circ}(x), \tag{46}$$

where $f_k^\pm$, f_k°, $f^{\circ\circ}$ are the right sides of systems (31), (33) and (40) respectively. If the inequality $\dot{V}(x) \leq 0$ is valid over the entire space x for the function

$$\dot{V}(x) = \begin{cases} \dot{V}_k(x) & \text{in the region } G_k^+, \\ \dot{V}_k^\circ(x) & \text{in the region } S_k^\circ, \\ \dot{V}_k^{\circ\circ}(x) & \text{in the region } S_k^{\circ\circ}, \end{cases} \tag{47}$$

where S_k° and $S_k^{\circ\circ}$ are given by the relations

$$\sigma_k(x) = 0, \qquad \frac{\partial \sigma_k}{\partial x} a \neq 0,$$
$$\sigma_k(x) = \frac{\partial \sigma_k}{\partial x} a = 0, \qquad \frac{\partial}{\partial x}\left(\frac{\partial \sigma_k}{\partial x} F(x)\right) a \neq 0, \tag{48}$$

and $\dot{V}(x) = 0$ only on some set M not containing whole trajectories of system (30), different from the equilibrium $x = 0$, then one may consider that Theorem 4 is applicable. We use this fact for transferring Lur'e's algorithm [14] to the particular case of system (30):

$$\dot{x} = Ax + a\varphi(\sigma), \qquad \dot{\sigma} = b'x - \rho\varphi(\sigma),$$
$$\rho \geq 0, \qquad \Gamma^2 = \rho + b'A^{-1}a > 0, \tag{50}$$

assuming that the eigenvalues of matrix A have negative real parts, and the function $\varphi(\sigma)$ is such that $\varphi(\sigma)\sigma > 0$ for $\sigma \neq 0$ and

$$\int_0^\infty \varphi(\sigma)d\sigma = \infty \tag{51}$$

We shall prove that if the equation in the column matrix u

$$2L(uu')a + 2\sqrt{\rho}\,u + b = 0 \qquad (\rho \geqslant 0), \tag{52}$$

where the matrix L(G) is determined for a symmetric matrix G by the relation

$$G = -L(G)A - A'L(G),$$

has a simple real solution, then the equilibrium $x = 0$, $\sigma = 0$ of the system (50) considered is asymptotically stable in the large.

If equation (52) is soluble in the indicated sense, then the equation

$$2L(uu')a + 2\sqrt{\rho}\,u + b + 2L(G_1)a = 0 \tag{53}$$

is also soluble, where $G_1 = G_1'$ is any square matrix with sufficiently small elements. We choose G_1 such that the form $x'G_1x$ is positive definite. Then for the positive definite Lyapunov function

$$V(x, \sigma) = x'L(G)x + \int_0^\sigma \varphi(\sigma)\,d\sigma, \qquad G = uu' + G_1$$

the function (46) assumes the form

$$\dot{V}_k(x, \sigma) = \dot{V}_k = \dot{V}_k^{-}(x, \sigma) = -x'G_1x - (u'x + \sqrt{\rho}\varphi(\sigma))^2, \tag{54}$$

$$\dot{V}_k^{\circ}(x, \sigma) = -x'Gx - 2a'L(G)\,x\xi_k^{\circ}(x, \sigma), \tag{55}$$

$$\dot{V}_k^{\circ\circ}(x, \sigma) = -x'Gx + 2a'L(G)\,x\xi_k^{\circ\circ}(x, \sigma), \tag{56}$$

and the regions S_k° (48) and $S_k^{\circ\circ}$ (49) are determined respectively by the relations

$$\sigma = \sigma_k, \qquad \rho > 0, \tag{57}$$

$$\sigma = \sigma_k = \rho = 0, \qquad b'a \neq 0. \tag{58}$$

For $\rho > 0$ the set (58) is empty and in set (57) $\dot{\sigma}_k^{\circ} = b'x - \rho\xi_k^{\circ}(x, \sigma) = 0$, so that the function (55) is representable in the form

$$\dot{V}_k^{\circ}(x, \xi^{\circ}) = -x'Gx + 2a'L(G)\,\xi_k^{\circ}x + \xi_k^{\circ}[b'x - \rho\xi_k^{\circ}] = -x'G_1x - (u'x + \sqrt{\rho}\xi_k^{\circ})^2$$

and proves to be negative definite. According to (51) the function (55) vanishes only at the point $x = 0, \sigma = 0$. The conditions of applicability of Theorem 4 are satisfied (the set M coincides with the origin $x = 0$, $\sigma = 0$).

According to (53) in the case $\rho = 0$ in the set (58),

$$\dot{V}_k^{\circ\circ}(x, \sigma) = -x'Gx,$$

and the set (57) is empty. By the substitution $x(t) = 0\,(t_1 < t < t_2)$ we convince ourselves that the straight line $x = 0$, on which only the equations $\dot{V} = 0$, $V = \text{const}$ are possible, does not contain a single arc $x = x(t)$, $\sigma = \sigma(t)\,(t_1 < t < t_2)$ of any trajectory of system (50) different from the equilibrium $x = 0$, $\sigma = 0$. Again the conditions of applicability of Theorem 4 hold.

The author thanks E. A. Barbashin for guidance in completing this project.

APPENDIX I.

We prove Theorem 3. Consider an arc of the solution $\mathbf{x}(t)$, spoken of in the conditions of the theorem. Since the function $\mathbf{x}(t)$ is absolutely continuous on the interval (20) (Theorem 2), and the function $V(t, \mathbf{x})$ by virtue of continuous differentiability satisfies in $\overline{G}(t, \mathbf{x})$ a Lipschitz condition in t and $\mathbf{x}$, then the compound function $V(t) = V[t, \mathbf{x}(t)]$ is absolutely continuous on (20), since for any $t' \in [t_1, t_2]$

$$V(t') = V(t_1) + \int_{t_1}^{t'} \dot{V}(\xi)\, d\xi. \tag{59}$$

On the segment (20) the vector function $\left(\frac{\partial V}{\partial \mathbf{x}}\right)_{\mathbf{x}=\mathbf{x}(t)}$ and the partial derivative $\left(\frac{\partial V}{\partial t}\right)_{\mathbf{x}=\mathbf{x}(t)}$ are continuous; therefore according to the chain rule of differentiation, the derivative $\dot{V}(t) = \frac{d}{dt} V[t, \mathbf{x}(t)]$ coincides with the function below (60) at points where the derivative $\dot{\mathbf{x}}(t)$ exists, i.e. almost everywhere on the segment (20):

$$U(t) = \left(\frac{\partial V}{\partial t}\right)_{\mathbf{x}=\mathbf{x}(t)} + \left(\frac{\partial V}{\partial x}\right)_{\mathbf{x}=\mathbf{x}(t)} \dot{\mathbf{x}}(t). \tag{60}$$

Moreover, at these points $\dot{\mathbf{x}}(t) \in \{f[t, \mathbf{x}(t)]\}$ (Definition 1), so that according to the definition of algebraic operations on many-valued functions (sec. 3), almost everywhere in (20) the relation

$$U(t) \in \left\{\left(\frac{\partial V}{\partial t}\right)_{\mathbf{x}=\mathbf{x}(t)} + \left(\frac{\partial V}{\partial \mathbf{x}}\right)_{\mathbf{x}=\mathbf{x}(t)} f(t, \mathbf{x}(t))\right\} \tag{61}$$

is satisfied, as well as the inequality

$$mW(t, \mathbf{x}(t)) \leqslant \dot{V}(t) \leqslant MW(t, \mathbf{x}(t)). \tag{62}$$

The assertion of Theorem 3, in particular the estimate (21), follows from (62) and (59) by the mean value theorem of integral calculus.

APPENDIX II.

We prove Theorem 4. From the conditions of the theorem, it follows that for any solution $\mathbf{x}(t) = \mathbf{x}(\mathbf{x}_0, t)$ [$\mathbf{x}(\mathbf{x}_0, 0) = \mathbf{x}_0$] of equation (29), the limit

$$\lim_{t \to +\infty} V[\mathbf{x}(\mathbf{x}_0, t)] = V_\infty(\mathbf{x}_0) \tag{63}$$

exists and the semitrajectory $\mathbf{x}(\mathbf{x}_0, t)$, $0 \leq t < +\infty$ is situated in the region

$$V(\mathbf{x}) \leqslant V(\mathbf{x}_0), \tag{64}$$

the region (64) being bounded and shrinking to the origin as $\mathbf{x}_0 \to 0$. Thus stability of the equilibrium $\mathbf{x} = 0$ in the sense of Lyapunov is present, and the set $\Omega(\mathbf{x}_0)$ of ω-limit points [6] of the trajectory $\mathbf{x}(\mathbf{x}_0, t)$ is nonempty. According to (63) and the continuity of the function $V(\mathbf{x})$

$$V(q) = V_\infty(\mathbf{x}_0), \quad \text{if} \quad q \in \Omega(\mathbf{x}_0). \tag{65}$$

By following papers [1, 2], it is not difficult to show that under the conditions indicated in Theorem 4, the mapping accomplished in the space $\mathbf{x}$ by trajectories of equation (29) satisfies the axiom of a generalized dynamic system [6], so that the theory developed in [6] is completely applicable to this equation. In particular, according to Theorem 3 of [6], for each point $q \in \Omega(\mathbf{x}_0)$ there exists a trajectory $\varphi(q, t)$ satisfying the condition

$$\varphi(q, t) \in \Omega(\mathbf{x}_0) \qquad (-\infty < t < +\infty). \tag{66}$$

From (65) and (66) for this trajectory, there follows the equation

$$V[\varphi(q, t)] = V_\infty(x_0) = \text{const} \qquad (-\infty < t < +\infty),$$

from which in correspondence with the conditions of this theorem, it follows that $V_\infty(x_0) = 0$. The validity of the equation $\lim_{t\to+\infty} x(x_0, t) = 0$ now becomes clear, if one bears in mind the positive definiteness and continuity of the function $V(x)$.

LITERATURE CITED

1. Zaremba, S. C. Sur les equations au paratingent. Bulletin des Sciences mathematiques, vol. 60, 1936.
2. Marchaud, A. Sur les champs continus de demi-cônes convexes et leurs integrales. Compositio Mathematica, vol. 3, f. 1, 1936.
3. Aizerman, M. A. and Gantmakher, F. R. On the stability of periodic motion. Prikl. matem. i mekh., vol. 22, No. 6 (1958).
4. Andronov, A. A., Vitt, A. A. and Khaikin, S. E. Theory of Vibrations [in Russian] Fizmatgiz, 1958.
5. Fikhtengol'ts, G. M. Course in Differential and Integral Calculus, Vol. 1 [in Russian] Gostekhizdat, 1948.
6. Barbashin, E. A. On the theory of generalized dynamical systems, Uch. Zapiski M.G.U., No. 135, Matemika, Vol. 2 (1949).
7. Petrovskii, I. G. Lectures on the Theory of Ordinary Differential Equations. [in Russian] Gostekhizdat, 1952.
8. Myshkis, A. L. On regions of uniqueness of solutions of systems of linear partial differential equations. Matem. Sbornik, Vol. 19 (61), No. 3 (1946).
9. Barbashin, E. A. and Alimov, Yu. I. On the theory of relay differential equations. Izv. byssh. uchebn. zaved., Matematika (to appear).
10. Solntsev, Yu. K. On continuous dependence on initial conditions of the solutions of systems of differential equations with piecewise continuous right sides. Uch. zapiski M.G.Y., No. 186, Matematika, Vol. 9, 1959.
11. Filippov, A. F. Differential equations with discontinuous right sides. Matem. Sbornik. Vol. 51 (93), No. 1 (1960).
12. Viktorovskii, E. E. On a generalized concept of integral curves. Matem. Sbornik, Vol. 34 (76), No. 2, 1954.
13. Krasovskii, N. N. Certain Problems in the Theory of Stability of Motion. [in Russian] Fizmatgiz, 1959.
14. Lur'e, A. I. Certain Nonlinear Problems in the Theory of Automatic Control. [in Russian] Gostekhizdat, 1951.
15. Rozenvasser, E. N. On the question of the stability of nonlinear control systems. Avtomatika i Telemekhanika, Vol. XX, No. 6 (1959).
16. Wechsler, D. On stability theorems for systems of stationary differential equations. Revue de Mathematiques pures et Appliques, vol. 3, No. 1, 1958.

CONCERNING THE PROBLEM OF DETERMINING THE STABILITY-SECTOR BOUNDARIES IN NONLINEAR CONTROL SYSTEMS*

A. K. Bedel'baev

(Alma-Ata)

Translated from Avtomatika i Telemekhanika, Vol. 22, No. 7,
pp. 831-833, July, 1961
Original article submitted November 9, 1960

A method is presented for determining the boundaries of the sector in which a system of automatic control is stable "in the large".

Let a system of indirect control be described by the equations [1]

$$\dot{\eta}_s = \sum_{k=1}^{n} b_{sk}\eta_k + n_s\xi \quad (s = 1, 2, \ldots, n),$$
$$\dot{\xi} = f(\sigma), \qquad \sigma = \sum_{k=1}^{n} j_k\eta_k - r\xi, \tag{1}$$

where b_{sk}, n_s, j_k and r are constants, and $f(\sigma)$ is a nonlinear function the accuracy of which is restricted by the relationships

$$f(0) = 0, \qquad m\sigma^2 < \sigma f(\sigma) < M\sigma^2. \tag{2}$$

In the inequalities (2), m and M ($0 < m < M < \infty$) are certain constants which are to be determined. In accordance with (2), we shall consider system (1) as being absolutely stable over the sector (m, M), provided it is asymptotically stable at any initial deviations and at any nonlinear function $f(\sigma)$, as long as it satisfies the conditions (2). In the following we describe a method of determining the boundaries of sector (m, M) in which the system (1) is absolutely stable.

Let the roots $\lambda_1, \lambda_2, \ldots, \lambda_n$ of equation

$$(-1)^n D(\lambda) = \|b_{sk} - \lambda\delta_{sk}\| = 0 \tag{3}$$

have the negative real parts

$$\operatorname{Re}\lambda_s < 0 \quad (s = 1, 2, \ldots, n) \tag{4}$$

and be such that the condition [1]

$$\Gamma^2 = r + \sum_{s=1}^{n} j_s \frac{N_s(0)}{D(0)} > 0 \tag{5}$$

is satisfied.

*We wish to state that this is not a new problem, and that it has been investigated earlier by a number of authors, including M. A. Aizerman, B. S. Razumikhin, V. M. Popov, V. A. Pliss, E. N. Rozenvasser, and others.

Then the solution of the equilibrium-position stability ($\eta_1 = \eta_2 = \ldots \eta_n = \xi = 0$) of system (1) can be obtained from an analysis of the equations

$$\dot{x}_s = \sum_{k=1}^{n} b_{sk} x_k + n_s \psi(\sigma)\,\sigma \quad (s = 1, 2, \ldots, n), \quad \dot{\sigma} = \sum_{k=1}^{n} j_k x_k - r\psi(\sigma)\,\sigma, \tag{6}$$

where

$$x_s = \dot{\eta}_s, \quad \psi(\sigma) = \frac{1}{\sigma} f(\sigma).$$

Let us examine the positively defined Lyapunov function

$$v = \sum_{s=1}^{n} \sum_{k=1}^{n} \sigma_{sk} x_s x_k + \frac{1}{2}\sigma^2,$$

where σ_{sk} are determined from the formulas (2.54) of work [3]. The time derivative of this function, computed from (6), will be

$$-\dot{v} = \sum_{s=1}^{n} \sum_{k=1}^{n} a_{sk} x_s x_k + 2\sigma \sum_{k=1}^{n} \rho_k x_k + r\psi(\sigma)\,\sigma^2,$$

where

$$-2\rho_k = j_k + p_k \psi(\sigma), \quad p_k = \sum_{s=1}^{n} (\sigma_{sk} + \sigma_{ks})\, n_s,$$

and a_{sk} are arbitrary constants selected in conformity with Silvester's inequalities:

$$\begin{vmatrix} a_{11} & a_{12} & \ldots & a_{1k} \\ a_{21} & a_{22} & \ldots & a_{2k} \\ \ldots & \ldots & \ldots & \ldots \\ a_{k1} & a_{k2} & \ldots & a_{kk} \end{vmatrix} > 0 \quad (k = 1, 2, \ldots, n). \tag{8}$$

Consequently, the expression for $-\dot{v}$ will be a positively definite form of the variables $x_1, x_2, \ldots, x_n, \sigma$, provided its discriminant is larger than zero:

$$\begin{vmatrix} a_{11} & a_{12} & \ldots & a_{1n} & \rho_1 \\ a_{21} & a_{22} & \ldots & a_{n2} & \rho_2 \\ \ldots & \ldots & \ldots & \ldots & \ldots \\ a_{n1} & a_{n2} & \ldots & a_{nn} & \rho_n \\ \rho_1 & \rho_2 & \ldots & \rho_n & r\psi(\sigma) \end{vmatrix} > 0.$$

From here, it is readily found that [3]

$$\sum_{s=1}^{n} \sum_{k=1}^{n} A_{sk} \rho_s \rho_k < rA\psi(\sigma), \tag{9}$$

where A is a determinant composed of a_{sk}, and A_{sk} are the determinant's minors with signs. Let

$$a = \sum_{s=1}^{n}\sum_{k=1}^{n} A_{sk}p_s p_k, \qquad c = \sum_{s=1}^{n}\sum_{k=1}^{n} A_{sk}j_s j_k, \tag{10}$$

$$2b = \sum_{s=1}^{n} g_s j_s - 4rA, \qquad g_s = \sum_{k=1}^{n} (A_{sk} + A_{ks})\, p_k. \tag{11}$$

On the basis of (7), the inequality (9) will then have the form

$$az^2 + 2bz + c < 0 \quad (z = \psi(\sigma)). \tag{12}$$

It is evident from (8) and (10) that $a > 0$ and $c > 0$. Hence the inequality (12) is valid only at the condition $b < 0$, i.e.,

$$\sum_{s=1}^{n} g_s j_s < 4rA. \tag{13}$$

This being established, we write inequality (12) in the form

$$m < \psi(\sigma) < M, \tag{14}$$

where $\underline{m}$ and M are defined by the formulas

$$m = \frac{-b - \sqrt{b^2 - ac}}{a}, \qquad M = \frac{-b + \sqrt{b^2 - ac}}{a}, \tag{15}$$

with the provision that the condition $b^2 \geq ac$, which follows from the fact that values of function $\psi(\sigma)$ are real values, is satisfied. From (14) it is now easy to obtain the inequalities (2), at which, as we see, the system (1) is absolutely stable.

In conclusion, we note that the expressions for $\underline{m}$ and M contain a_{sk} values which satisfy only the condition (8). By varying these values, we can both extend and restrict the boundaries of the sector (m, M) in accordance with the conditions of practical problems.

LITERATURE CITED

1. Lur'e, A. I. Certain nonlinear problems in the theory of automatic control. Gostekhizdat, 1951.
2. Rozenvasser, E. N. Concerning the construction of Lyapunov's function for a certain class of nonlinear systems. Izv. AN SSSR, OTN. Mekhanika i mashinostroenie, No. 2, 1960.
3. Bedel'baev, A. K. Stability of nonlinear automatic-control systems. Izd. AN KazSSR, Alma-Ata, 1960.

THE PROBLEM OF SPEED OF RESPONSE WITHOUT SWITCHING FOR AN ARBITRARY NUMBER OF CONTROL FUNCTIONS

A. N. Filatov

(Tashkent)

Translated from Avtomatika i Telemekhanika, Vol. 22, No. 7,
pp. 834-837, July, 1961
Original article received March 3, 1961

The author demonstrates the existence of a certain class of linear systems for which the optimal processes with respect to speed of response are performed without switching of the control functions for transition of the image point from any specified point on the phase plane onto a specified manifold.

The problem of speed of response in the theory of optimal processes resides, as we know, in the following [1].

Assume the equations of motion for the image point $(x_1, x_2, \ldots, x_n)$ in the n-dimensional phase space X_n have the following form:

$$\dot{x}_i = f_i(x_1, x_2, \ldots, x_n, u(t)) \quad (i = 1, \ldots, n). \tag{1}$$

Here u(t) is a piecewise-continuous control function, and $|u(t)| \leq M$. The functions $f_i(x_1, x_2, \ldots, x_n, u)$ are continuous over the set of variables $x_1, x_2, \ldots, x_n, u$ and are continuously differentiable with respect to $x_1, x_2, \ldots, x_n$.

It is necessary to choose the function u(t) in such a way that the image point in leaving a specified position $(x_1^0, x_2^0, \ldots, x_n^0)$ reaches another a priori specified position $(x_1^1, x_2^1, \ldots, x_n^1)$ in the least possible time.

If the right sides of equations (1) are linear functions with respect to the variables $x_1, x_2, \ldots, x_n$ with constant coefficients (the case of linear systems), then the control function u(t) must as a rule change its sign (switch) during the process of movement; this is, of course, provided that the initial conditions are not chosen in any special manner. For example, even for the very simple system

$$\dot{x}_1 = x_2, \quad \dot{x}_2 = u(t)$$

it is impossible to proceed from the arbitrary point (x_1^0, x_2^0) on the phase plane to (for example) the origin in the shortest possible time without switching (with the exception of those cases where the initial point is located on the switching curve). However, if we pose the analogous problem (for linear systems) with the requirement that the image point of the phase space X_n must make the transition from the specified position $(x_1^0, x_2^0, \ldots, x_n^0)$ onto a smooth manifold of dimensionality $s<n$ specified in this space, then it is possible to indicate the conditions for which the control function will not switch during the entire period of movement for any initial data provided only that there exists an allowed control function which transfers the image point from this initial position onto the specified manifold.

This paper is devoted to finding the above-mentioned conditions. The analysis is performed for two variables (we study a phase plane). A straight line is taken as the smooth manifold.

1. Assume the system of equations according to which the image point on the phase plane $x_1 0 x_2$ moves is written in the form

$$\dot{x}_1 = a_{11}x_1 + a_{12}x_2 + b_{11}u_1 + b_{12}u_2 + \ldots + b_{1r}u_r,$$
$$\dot{x}_2 = a_{21}x_1 + a_{22}x_2 + b_{21}u_1 + b_{22}u_2 + \ldots + b_{2r}u_r, \tag{2}$$

where a_{ij} and b_{ij} are constant; $u_k(t)$ ($k = 1, \ldots, r$) are control functions; here $|u_k(t)| \leq M_k$ for $t_0 \leq t \leq t_1$. We shall assume that the functions $u_k(t)$ are piecewise-continuous. The problem resides in the following: it is required to find the conditions for which the image point moving in accordance with equations (2) from any a priori specified position (x_1^0, x_2^0) will arrive on the specified straight line $x_1 = 0$ (i.e., on the $0x_2$ axis) during the briefest possible time without switching of the control functions $u_k(t)$ (of course, for the condition that an allowed control function which transfers the image point from the specified state onto the specified manifold exists). We shall use t_0 to denote the instant at which the image point leaves the specified state, and t_1 to denote the instant at which it arrives on the specified manifold.

We shall solve the problem formulated above using the principle of the maximum and the transversality conditions [1]. We shall formulate the auxiliary system of equations

$$\dot{\psi}_1 = -a_{11}\psi_1 - a_{21}\psi_2, \qquad \dot{\psi}_2 = -a_{12}\psi_1 - a_{22}\psi_2. \tag{3}$$

Solving the system of equations (3), we find

$$\psi_1(t) = -\frac{c_1(a_{22}-\lambda_1)}{a_{12}}e^{\lambda_1 t} - \frac{c_2(a_{22}+\lambda_2)}{a_{12}}e^{\lambda_2 t}, \quad \psi_2(t) = c_1 e^{\lambda_1 t} + c_2 e^{\lambda_2 t}, \tag{4}$$

where $\lambda_1 < \lambda_2$ are the roots of the characteristic equation

$$\lambda^2 + (a_{11} + a_{22})\lambda + (a_{11}a_{22} - a_{12}a_{21}) = 0 \tag{5}$$

for the system (3). In accordance with the transversality conditions we have the equation

$$c_1 e^{\lambda_1 t_1} + c_2 e^{\lambda_2 t_1} = 0, \tag{6}$$

at the instant t_1, from which it follows that

$$c_2 = -c_1 e^{-(\lambda_2 - \lambda_1)t_1}. \tag{7}$$

Therefore

$$\begin{aligned} \psi_1(t) &= -c_1 e^{\lambda_1 t_1}\left[\frac{a_{22}-\lambda_1}{a_{12}}e^{-\lambda_1(t_1-t)} - \frac{a_{22}+\lambda_2}{a_{12}}e^{-\lambda_2(t_1-t)}\right], \\ \psi_2(t) &= c_1 e^{\lambda_1 t_1}\left[e^{-\lambda_1(t_1-t)} - e^{-\lambda_2(t_1-t)}\right]. \end{aligned} \tag{8}$$

In accordance with the principle of the maximum,

$$u_k(t) = M_k \operatorname{sign}(b_{1k}\psi_1 + b_{2k}\psi_2) \quad (k = 1, \ldots, r). \tag{9}$$

We formulate the expression

$$b_{1k}\psi_1 + b_{2k}\psi_2 = c_1 e^{\lambda_1 t_1}\left(b_{2k} - b_{1k}\frac{a_{22}+\lambda_1}{a_{12}}\right)e^{-\lambda_1(t_1-t)} - c_1 e^{\lambda_1 t_1}\left(b_{2k} - b_{1k}\frac{a_{22}+\lambda_2}{a_{12}}\right)e^{-\lambda_2(t_1-t)}. \tag{10}$$

Introducing the substitutions

$$b_{2k} - b_{1k}\frac{a_{22}+\lambda_1}{a_{12}} = \sigma_{1k}, \qquad b_{2k} - b_{1k}\frac{a_{22}+\lambda_2}{a_{12}} = \sigma_{2k}, \tag{11}$$

we write (10) in the form

$$b_{1k}\psi_1 + b_{2k}\psi_2 = \frac{c_1 e^{\lambda_1 t_1}}{e^{\lambda_2(t_1-t)}}\left[\sigma_{1k}e^{(\lambda_2-\lambda_1)(t_1-t)} - \sigma_{2k}\right]. \tag{12}$$

Thus, the change in the sign of the function $u_k(t)$ depends only on the change in the sign of the expression

$$\sigma_{1k}e^{(\lambda_2-\lambda_1)(t_1-t)} - \sigma_{2k}, \tag{13}$$

where

$$(\lambda_2 - \lambda_1)(t_1 - t) \geqslant 0.$$

Expression (13) does not change sign in the following cases:

$$\begin{aligned} &\text{a) } \sigma_{1k} \geqslant 0, \quad \sigma_{2k} < 0, && \text{b) } \sigma_{1k} > 0, \quad \sigma_{2k} \leqslant 0; \\ &\text{c) } \sigma_{1k} \leqslant 0, \quad \sigma_{2k} < 0; && \text{d) } \sigma_{1k} < 0, \quad \sigma_{2k} \geqslant 0, \\ &\text{e) } \sigma_{1k} \geqslant \sigma_{2k} > 0, && \text{f) } \sigma_{2k} \leqslant \sigma_{1k} < 0. \end{aligned} \tag{14}$$

We shall clarify the conditions for which inequalities (14) are valid. As an example, we shall study the inequality "a" in (14):

$$b_{2k} - b_{1k}\frac{a_{22}+\lambda_1}{a_{12}} \geqslant 0, \qquad b_{2k} - b_{1k}\frac{a_{22}+\lambda_2}{a_{12}} < 0.$$

From this it follows that

$$\frac{b_{2k}a_{12} - b_{1k}a_{22}}{b_{1k}} \geqslant \lambda_1, \qquad \frac{b_{2k}a_{12} - b_{1k}a_{22}}{b_{1k}} < \lambda_2 \quad \text{for } \frac{b_{1k}}{a_{12}} > 0;$$

$$\frac{b_{2k}a_{12} - b_{1k}a_{22}}{b_{1k}} \leqslant \lambda_1, \qquad \frac{b_{2k}a_{12} - b_{1k}a_{22}}{b_{1k}} > \lambda_2, \quad \text{for } \frac{b_{1k}}{a_{12}} < 0.$$

Therefore condition "a" in (14) is valid only when the inequalities

$$\text{a) } \frac{b_{1k}}{a_{12}} > 0, \qquad \lambda_1 \leqslant \frac{b_{2k}a_{12} - b_{1k}a_{22}}{b_{1k}} < \lambda_2 \tag{15}$$

are satisfied.

In analogous fashion we find the inequalities on whose fulfillment the remaining conditions in (14) depend:

$$\text{b) } \frac{b_{1k}}{a_{12}} > 0, \qquad \lambda_1 < \frac{b_{2k}a_{12} - b_{1k}a_{22}}{b_{1k}} \leqslant \lambda_2; \tag{16}$$

$$\text{c) } \frac{b_{1k}}{a_{12}} < 0, \qquad \lambda_1 \leqslant \frac{b_{2k}a_{12} - b_{1k}a_{22}}{b_{1k}} < \lambda_2; \tag{17}$$

$$\text{d) } \frac{b_{1k}}{a_{12}} < 0, \qquad \lambda_1 < \frac{b_{2k}a_{12} - b_{1k}a_{22}}{b_{1k}} \leqslant \lambda_2; \tag{18}$$

$$\text{e) } \frac{b_{1k}}{a_{12}} > 0, \qquad \lambda_1 < \lambda_2 < \frac{b_{2k}a_{12} - b_{1k}a_{22}}{b_{1k}}; \tag{19}$$

$$\text{f) } \frac{b_{1k}}{a_{12}} > 0, \qquad \frac{b_{2k}a_{12} - b_{1k}a_{22}}{b_{1k}} < \lambda_1 < \lambda_2. \tag{20}$$

Note that the equality sign in conditions "e" and "f" in (14) is reached either for $b_{1k} = 0$ or for $\lambda_1 = \lambda_2$. The latter is impossible by assumption (the roots of the characteristic equation (5) are assumed to be real and different). For the case $b_{1k} = 0$ ($k = 1, \ldots, r$) it is evident that $\sigma_{1k} = \sigma_{2k}$, and expression (13) does not change sign.

Furthermore, it is evident that in finding the solution (4) we assumed $a_{12} \neq 0$. However, if $a_{12} = 0$, then the system (3) becomes

$$\dot{\psi}_1 = -a_{11}\psi_1 - a_{21}\psi_2, \qquad \dot{\psi}_2 = -a_{22}\psi_2,$$

from which it follows that

$$\psi_2(t) = c_2 e^{-a_{22}t}.$$

In view of the transversality condition, $\psi_2(t_1) = 0$, i. e. $\psi_2(t) \equiv 0$.

Therefore, $\psi_1 = c_1 e^{-a_{11}t}$ and

$$u_k(t) = M_k \operatorname{sign} b_{1k}\psi_1 = M_k \operatorname{sign} b_{1k}c_1 e^{-a_{11}t}. \tag{21}$$

From (21) it is evident that the functions $u_k(t)$ will not change sign.

All of the above can be formulated in the form of the following theorem.

Theorem. If the image point on the phase plane moves in accordance with equations (2), and if the transition from the a priori specified position (x_1^0, x_2^0) on to the straight line $x_1 = 0$ is possible by means of an allowed control function, then for arrival on the specified straight line from the specified point by means of an optimal control function without switching during the shortest possible time, it is necessary and sufficient that one of the following conditions be satisfied:

1) $\dfrac{b_{1k}}{a_{12}} > 0$,

2) $\lambda_1 \leqslant \dfrac{b_{2k}a_{12} - b_{1k}a_{22}}{b_{1k}} < \lambda_2$,

3) $\lambda_1 < \dfrac{b_{2k}a_{12} - b_{1k}a_{22}}{b_{1k}} \leqslant \lambda_2$,

4) $b_{1k} = 0$,

5) $a_{12} = 0$.

Here $k = 1, \ldots, r$ throughout.

Remark 1. The conditions of the theorem are also retained for the case where any straight line parallel to the $0x_2$ axis is used as the specified straight line.

Remark 2. If the straight line onto which the image point arrives is assumed to be a straight line of the form $\alpha_1 x_1 + \alpha_2 x_2 + \alpha_3 = 0$, then by performing a transformation of variables in (2) according to the formulas

$$x_1 = X_1\cos\varphi - X_2\sin\varphi, \qquad x_2 = X_1\sin\varphi + X_2\cos\varphi,$$

where

$$\varphi = \arctan\left(-\frac{\alpha_1}{\alpha_2}\right),$$

we reduce the problem to that just treated above.

LITERATURE CITED

1. V. G. Boltyanskii, R. V. Gamkrelidze and L. S. Pontryagin. "The Theory of Optimal Processes," Izvestiya Akad. Nauk SSSR, Ser. matem., 24, No. 1, 1960.

ON A CERTAIN PROBLEM IN THE THEORY OF PROCESSES WITH AN OPTIMAL SPEED OF RESPONSE IN LINEAR SYSTEMS

F. Al'brekht

(Bucharest)

Translated from Avtomatika i Telemekhanika, Vol. 22, No. 7,
pp. 838-844, July, 1961
Original article submitted December 12, 1960

1. We shall study the equation

$$\frac{dx}{dt} = Ax + bu, \tag{1}$$

which is defined in the n-dimensional space R^n, where $\underline{b}$ is a fixed vector in R^n and A is a linear transformation of R^n which does not depend on time. The class of allowed functions from which we choose the control function u(t) is the class of piecewise-continuous functions with $|u(t)| \leq 1$. We assume that the nondegeneracy condition (cf. [2]) is satisfied, i.e., $\underline{b}$ does not belong to any invariant sub-space with the dimensionality $\leq n-1$ of the transformation A.

Assume $F \subset R^n$ is a closed convex set. We shall state that the control law $u(t)$ $(0 \leq t \leq T)$ transfers the point $x_0 \in R^n - F$ to F if the corresponding solution $x(t; x_0, u(t))$ of Eq. (1) satisfies the conditions $x(0; x_0, u(t)) = x_0$, $x(T; x_0, u(t)) \in F$.

The control law $u(t)$ $(0 \leq t \leq T)$ which transfers the point x_0 into this set F shall be called optimal if for any allowed control law $u^*(t)$ $(0 \leq t \leq T^*)$ which transfers x_0 into F the condition $T^* - T \geq 0$ is satisfied.

Such a statement of the problem of optimization with respect to speed of response (when the final point on the trajectory belongs to a specific closed set) has been studied with a varying degree of generality by the authors of [1, 4, 5 and 6] who dealt with the theorems for the existence and uniqueness of an optimal control law. However, in certain engineering respects we can only assume that the problem has been finally solved when it has been established that a moving point which has "passed due to inertia" through the final point on the optimal trajectory and is continuing its motion along a new optimal trajectory does not emerge from the vicinity of the set F, i.e., it must be established that the optimization is in a certain sense "stable". In the case where the set F can be reduced to a point, such stability is assured by the conditions which are imposed for the possibility of synthesis [2, 3]. This paper is devoted to an investigation of this problem; the most complete results are obtained for the case where n = 2 and F is a straight line.

2. If u(t) is an optimal control law which transfers x_0 into F, and $x(T; x_0, u(t)) = x_1 \in F$, then the corresponding optimal trajectory intersects F only at the point x_1 and u(t) is an optimal control law in the sense of [2, 3] that transfers x_0 to x_1. From this it follows that the optimal control law under study satisfies the maximum principle derived by L. S. Pontryagin [3].

The following propositions [1, 4, 5 and 6] apply.

A. If $u(t)$ $(0 \leq t \leq T)$ is the optimal control law that transfers x_0 into F, then there exists a solution $\psi(t)$ of the equation $\dot{\psi} = -A^*\psi$ (where A^* is a transformation which is conjugate with respect to A) such that $u(t) = \operatorname{sign} \psi(t) \cdot b$, $\psi(T) \cdot (y - x_1) \geq 0$ for all $y \in F$, where $x_1 = x(T; x_0, u(t))$; here $m \cdot n$ denotes the scalar product of the vectors $\underline{m}$ and $\underline{n}$.

B. The optimal control law which transfer x_0 into F is unique if it exists.

C. If there exists an allowed control law u(t) which transfers x_0 into F, then there also exists such a control law which is optimal.

The propositions formulated above make it possible to synthesize an optimal control law for Eq. (1) if the set F is an (n-1)-dimensional hyperplane (or a convex smooth hypersurface). As we know [3], this synthesis problem consists of finding the function $v(x) = u_x(0)$ where $u_x(t)$ is the control law which transfers the point $\underline{x}$ into F; $v(x)$ enters into the equation

$$\frac{dx}{dt} = Ax + bv(x) \tag{2}$$

for the optimal trajectories of Eq. (1).

In proposition "A" the latter relationship becomes

$$\psi(T) = a, \tag{3}$$

where $\underline{a}$ is a vector normal to the hyperplane F and directed in the opposite direction from x_0; therefore the vector $\psi(T)$ is defined in a single-valued fashion. This leads to the following method for plotting the optimal trajectories of Eq. (1).

Assume that the hyperplane F passes through the point $x = 0$ and that the real parts of all the eigenvalues of the matrix A are negative. Then for any point in space there exists an "allowed" (and therefore an optimal) control law which transfers it into F. Assume also that the scalar products $a \cdot b \neq 0$; moreover, it is easy to establish the fact that the analysis given below can also be adapted to the case $a \cdot b = 0$. Assume $\underline{x}$ is some point on the hyperplane F that is the end of a certain optimal trajectory. If the corresponding control law is such that $u(T) = \operatorname{sign} a \cdot b$, it follows from proposition "A" and relationship (3) that $a \cdot (Ax + b \operatorname{sign} a \cdot b) = aA \cdot x + |a \cdot b| \geq 0$. Analogously, if $u(T) = -\operatorname{sign} a \cdot b$, then $a \cdot (Ax - b \operatorname{sign} a \cdot b) = aA \cdot x - |a \cdot b| \leq 0$. Therefore the set S of points on the hyperplane F that are simultaneously the ends of two optimal trajectories (located in the respective half-spaces into which F subdivides the space R^n), is determined by the inequalities

$$aA \cdot x + |a \cdot b| \geqslant 0, \qquad aA \cdot x - |a \cdot b| \leqslant 0,$$

with the possible exception of the points at which these inequalities become equalities. The set S is never empty since it contains the origin. It coincides with the entire hyperplane F if the vectors $\underline{a}$ and aA are linearly dependent; it reduces to a single point if $a \cdot b = 0$*.

Assume F_1 is one of the half-spaces into which F subdivides R^n, and assume $\underline{a}$ is the vector representing the external normal to F with respect to F_1. We shall assume that $u(t) = \operatorname{sign} \psi(t) \cdot b (t \leq 0)$, where $\psi(t)$ is determined by expression (3). In order to be specific we shall assume that $a \cdot b = +1$.

We shall always move in the direction of negative $\underline{t}$. Assume $\tau_1 < 0$ is the initial instant of the step discontinuity of the control u(t). We shall use P_1 to denote the set of points $p \in F$ from which the semi-trajectories $x(t; p, u(t))$ $(t \leq 0)$ penetrate into the half-space F_1. We shall continue these semi-trajectories to the instant τ_1, or until they first return to F if this occurs earlier. It is clear that each of them is optimal for any point on it.

Assume Γ_1 is the set of points $x(\tau_1; p, u(t))$, $p \in P_1$ belonging to F_1. We find that this set is located on an (n-1)-dimensional hyperplane. If Γ_1 is empty, then in view of the propositions cited above and our proposition, the semi-trajectories which have been plotted fill the entire half-space F_1. If Γ_1 is not empty, then our semi-trajectories form a set R_1^+ which is bound by P_1, Γ_1 and the semi-trajectories originating from the boundary (on F) points P_1. Repeating the reasoning cited above, we construct the set Γ_1 by originating from R_2^-; this set is formed by the semi-trajectories $x(t-\tau_1; q, u(t))$, $t \leq \tau_1$, $q \in \Gamma_1$ which are continued to the next point τ_2, the step of discontinuity for the control u(t), or until the instant at which they leave $F_1 - R_1^+$, etc. Such a geometric construction leads to subdividing the half-space F_1 into mutually non-intersecting sets on each of which the value of the function v(x) is constant ($v(x) = \pm 1$ for $x \in R_1^{\pm}$).

Repeating this procedure exactly for the vector $-\underline{a}$ and the corresponding set P_2, we obtain the analogous subdivision of the second half-space F_2.

---

*From the nondegeneracy conditions cited in section 1, it follows that these two conditions are incompatible.

Examples. We shall examine the following system* in the plane R^2:

$$\frac{dx}{dt} = -y + u, \qquad \frac{dy}{dt} = x - u,$$

where we shall take the axis 0x as F, and the unit length of the 0y axis as the vector $\underline{a}$. The optimal control law for the points in the lower half-plane is written as

$$u(t) = \operatorname{sign}(-\sin t - \cos t) \qquad (t \leqslant 0).$$

The graphical construction described above leads to the pattern of optimal trajectories shown in Fig. 1. These trajectories consist of circular arcs with centers at (1, 1) and (-1, -1); the step discontinuities occur on the straight line $x+y = \pm(\sqrt{2}-2)$. The solid lines depict the trajectories corresponding to u = 1, and the dotted lines represent trajectories corresponding to u = -1. Solid lines are used to draw the trajectories which pass through the points (1, 0) and (-1, 0) and are part of the boundaries for the regions R_1^+ and R_1^-. The set S coincides with the segments [-1, 1] of the 0x axis.

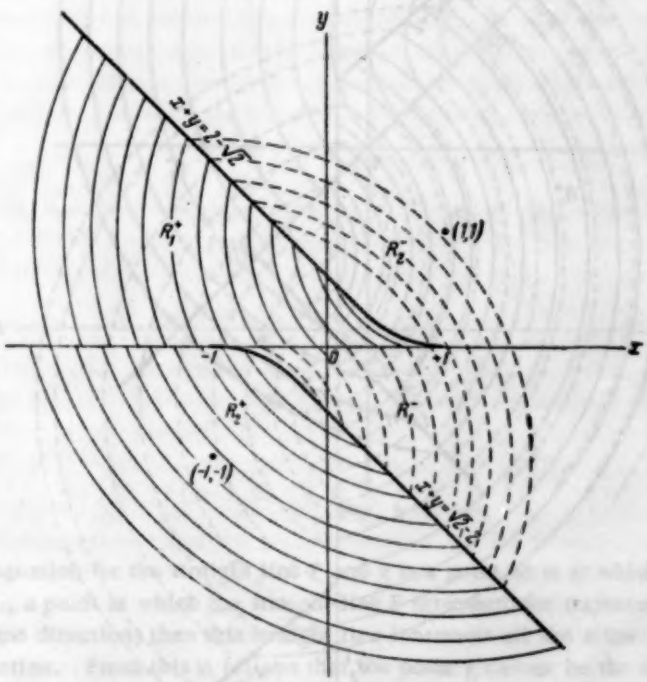

Fig. 1

If we choose the axis 0y of the straight line x-y = 0 as the straight line F, then the pattern for the optimal trajectories will be as shown in Figs. 2 and 3, respectively.

3. We shall now proceed to a study of the "stability" of the synthesis achieved in this manner. As we have already said, for stability of this kind, the trajectories which originate from the vicinity of the end of an arbitrary optimal trajectory must remain in the vicinity of the set F. The examples cited above demonstrate that this stability is not always present; it is violated at external points of the set S. Thus it is natural to introduce the following definition.

*Although here the matrix A does not satisfy the condition of negative real parts for the eigenvalues, this can easily be achieved by an obvious modification of the right sides of the system without altering the qualitative pattern of the optimal trajectories; this pattern is especially easy to depict for the system under study.

If $v(x)$ ($|v(x)| \leq 1$) is a function which is defined on R^n-C, where C is a closed convex set in F, and satisfies the following conditions:

a) each trajectory of the equation

$$\frac{dx}{dt} = Ax + bv \quad (x)$$

reaches C; the first point of its intersection with C is called the end of that trajectory;

b) for each $x_0 \in R^n$-C the function $u_{x0}(t) = v(x(t; x_0))$, where $\dot{x}(t; x_0)$ is a solution of Eq. (2) with the initial conditions $x(0; x_0) = x_0$, is studied only up to its end $p(x_0)$ and is an allowed control for Eq. (1).

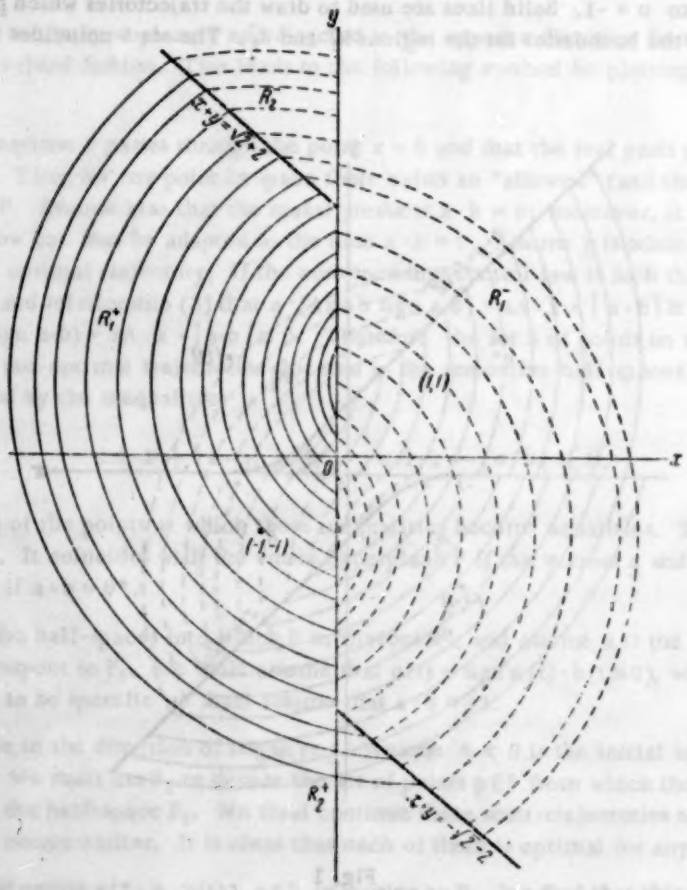

Fig. 2

Such a function $v(x)$ shall be called a synthesizing function relative to F for Eq. (1).

This synthesizing function can always be deteremined by means of the optimal control laws $u_x(t)$ which transfer the point $x \in R^n$-C into C, if we assume $v_C(x) = u_x(0)$. For example, the optimal control laws which transfer the points in the space into the set F determine the synthesizing function $v_F(x)$.

Definition. The synthesizing function $v(x)$ is called stable if for any $x \in R^n$-C and any $\epsilon > 0$ there exists an $\eta > 0$ such that all trajectories of Eq. (2) which originate from the η-vicinity of the point $p(x)$ remain in the ϵ-vicinity of the set F.

As our examples show, the synthesizing function $v_F(x)$ is, generally speaking, not stable. But if F is a hyperplane passing through the origin, and if the real parts of all the eigenvalues of the matrix A are negative, then it is easy to see that the synthesizing function $v_0(x)$ defined by optimal control laws that transfer the points in the space

to the origin is stable [2, 3]. Thus the problem arises of finding the "optimal" stable synthesizing function if such a function exists.

We shall limit our analysis to the case of n = 2, when F is a straight line passing through the origin. Certain of the arguments cited below can obviously be generalized to include the case of arbitrary n when F is an (n-1)-dimensional hyperplane. In addition to the propositions cited above, we shall also postulate that the vectors $\underline{a}$ and aA are linearly independent; it is easy to deduce the fact that in the contrary case the synthesizing function $v_F(x)$ is stable.

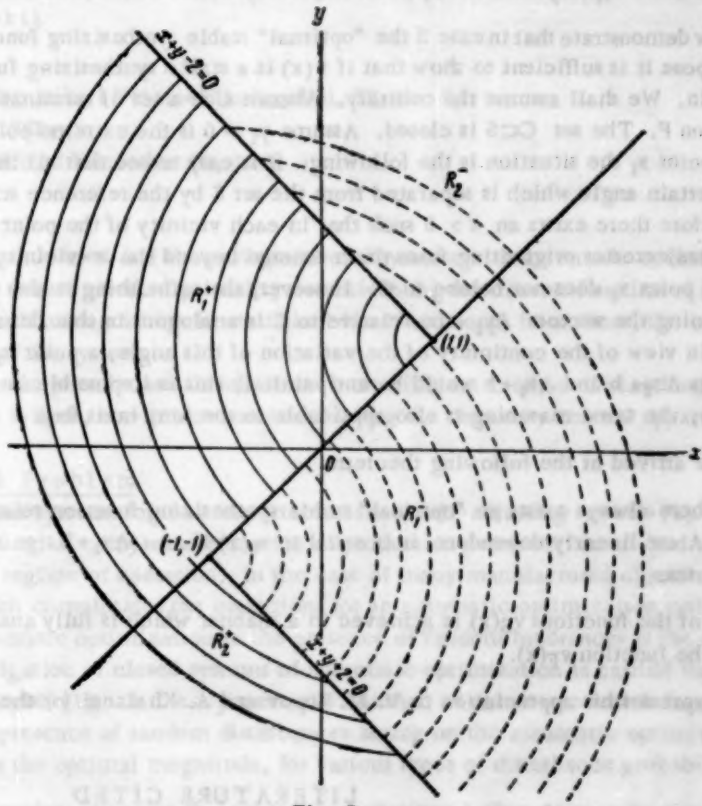

Fig. 3

If $a \cdot x = 0$ is the equation for the straight line F and $\underline{x}$ is a point on it at which $aA \cdot x + |a \cdot b|$ and $aA \cdot x - |a \cdot b|$ have identical signs (i.e., a point at which the straight line F intersects the trajectories of the equations $\dot{x} = Ax + b$ and $\dot{x} = Ax - b$ in the same direction) then this straight line intersects all the allowed trajectories passing through the point $\underline{x}$ in the same direction. From this it follows that the point $\underline{x}$ cannot be the end of a trajectory of Eq. (2) with the stable synthesizing function v(x). In fact, it is easy to see than when ϵ is sufficiently small, any vicinity of such a point contains points with a property such that allowed trajectories originating from them emerge beyond the ϵ-vicinity of the straight line F before they reach F. Therefore, the ends of the trajectories in Eq. (2) which are determined by a stable synthesizing function definitely lie on the segment S of the straight line F with the ends x_1 and x_2 which are respectively determined by the equations $aA \cdot x_1 + |a \cdot b| = 0$ and $aA \cdot x_2 - |a \cdot b| = 0$. Since for $a \cdot b = 0$ the set S evidently consists solely of the origin, it follows that in this case the function $v_0(x)$ will be an "optimal" stable synthesizing function. However, if $a \cdot b \neq 0$, then the following three cases are possible.

1. $Ax_1 + b \operatorname{sign} a \cdot b = 0$, i.e., the point x_1 is singular for the equation $\dot{x} = Ax + b \operatorname{sign} a \cdot b$ (cf. Fig. 3).

2. $aA \cdot (Ax_1 + b \operatorname{sign} a \cdot b) > 0$, i.e., the trajectory of the equation $\dot{x} = Ax + b \operatorname{sign} a \cdot b$ in passing through the point x_1 passes into the half-plane F_2 (relative to which $\underline{a}$ is a vector internal normal with respect to the straight line F; cf. Fig. 2) for both increasing and decreasing values of t.

3. $aA \cdot (Ax_1 + b \operatorname{sign} a \cdot b) < 0$, i.e., the trajectory passing through the point x_1 penetrates into the second half-plane F_1 (cf. Fig. 1)* for both directions of variation for t.

* The case $aA \cdot (Ax_1 + b \operatorname{sign} a \cdot b) = 0$ cannot arise, since the vectors $\underline{a}$ and aA are linearly independent; this is also obvious from purely geometric considerations.

Since $x_2 = -x_1$, it follows that each of these cases involves the satisfaction of analogous relationships for the trajectories of the equations $\dot{x} = Ax - b \operatorname{sign} a \cdot b$ at the point x_2.

Simple reasoning demonstrates that in cases 1 and 2, the synthesizing function $v_S(x)$, which is determined by means of the optimal control laws that transfer the points of the plane onto the segment S, is stable. Under these conditions it is "optimal" in the sense that no trajectory of Eq. (2) with a different synthesizing function that is stable relative to F is traversed during a shorter time. In fact, since the end of such a trajectory must lie on S, it cannot be traversed more rapidly than the optimal trajectory which transfers the initial point under study to S.

We shall now demonstrate that in case 3 the "optimal" stable synthesizing function relative to F is the function $v_0(x)$. For this purpose it is sufficient to show that if $v(x)$ is a stable synthesizing function, then all trajectories of Eq. (2) end at the origin. We shall assume the contrary. Assume C is a set of terminations of the trajectories of the corresponding Eq. (2) on F. The set $C \subset S$ is closed. Assume $y_1 \neq 0$ is the extreme point in this set and lies on the semi-axis $0x_1$. At the point x_1 the situation is the following: it is easy to see that all the vectors $Ax_1 + bu$, $-1 \leq u \leq 1$ are located within a certain angle which is separated from the set S by the reference straight line of this set, which passes through x_1. Therefore there exists an $\epsilon > 0$ such that in each vicinity of the point x_1 there can be found points for which all allowed trajectories originating from them emerge beyond the ϵ-vicinity of the straight line F before they reach S. Thus, the point x_1 does not belong to C. However, the same thing is also valid for y_1, since the location of the angle containing the vectors $Ay_1 + bu$ relative to C is analogous to that described above for x_1. In fact, in the contrary case, in view of the continuity of the variation of this angle, a point z_1 would exist on the segment $\overline{y_1 x_1}$ at which the vectors $Az_1 + b$ and $Az_1 - b$ would be antiparallel; this is impossible in case 3. Therefore the point y_1 cannot be non-zero; the same reasoning is also applicable to the semi-axis $0x_2$.

Thus we have arrived at the following theorem.

Theorem. There always exists an "optimal" stable synthesizing function relative to F. It is equal to $v_F(x)$ if the vectors $\underline{a}$ and aA are linearly dependent; it is equal to $v_0(x)$ if $aA \cdot (Ax_1 + b \operatorname{sign} a \cdot b) < 0$, and is equal to $v_S(x)$ in the remaining cases.

The plotting of the functions $v_S(x)$ is achieved in a manner which is fully analogous to the procedure described above for plotting the function $v_F(x)$.

The author expresses his appreciation to V. M. Popov and A. Khalanai for their interesting discussion and valuable remarks.

LITERATURE CITED

1. V. G. Boltyanskii, R. V. Gamkrelidze and L. S. Pontryagin. "Theory of Optimal Processes", Izvestiya Akad. Nauk SSSR, Seriya Mathematicheskaya, 24, 1 (1960).
2. R. V. Gamkrelidze, "Theory of Processes which are Optimal with Respect to Speed of Response in Linear Systems", Izvestiya Akad. Nauk SSSR, Seriya Matematicheskaya, 22, 4 (1958).
3. L. S. Pontryagin, "Optimal Control Processes", Uspekhi Matematicheskikh Nauk, 14, 1 (1959).
4. L. I. Rozonoér, "On Sufficient Conditions for Optimalness", Doklady Akad. Nauk SSSR, 127, 3 (1959).
5. L. I. Rozonoér, "The L. S. Pontryagin Principle of the Maximum in the Theory of Optimal Systems", Avtomatika i Telemekhanika, 20, Nos. 10, 11 and 12, (1959).
6. A. F. Filippov, "On Certain Problems in the Theory of Optimal Control", Vestnik Moskovskovo Gosudarstvennovo Universiteta, 2 (1959).

OPTIMIZATION OF AUTOMATIC SYSTEMS BY STATISTICAL CRITERIA

S. A. Doganovskii

(Moscow)

Translated from Avtomatika i Telemekhanika, Vol. 22, No. 7,
pp. 845-856, July, 1961
Original article submitted December 31, 1960

Statistical criteria are defined and the performance of systems with automatic optimization by statistical criteria is investigated. Optimality conditions for the transfer function of a compensator are found, as well as conditions for statistical invariance and, from these, the conditions for non-interaction of the system.

This investigation permits one to select the most efficient method of searching for the optimal regime of a system, and guides one in designing the necessary control apparatus.

I. Formulation of the Problem

Automatic optimization systems form an important class of self-adjusting systems [1]. The use of such systems allows one to solve the problem of complex automation of production processes connected with the maintenance of the most suitable (optimal) regime of operation. In the case of many manufactured objects, random disturbances play an important role, which complicates the conditions for an automatic optimization system. The question of investigating a system of automatic optimization in the presence of random hindrances is the subject of a fair number of papers [1-5]. The investigation of closed systems of automatic optimization is carried through in the paper of A. A. Fel'dbaum (see, for example, [1]). In these papers, the question of automatic search for extrema and the stabilization of the system in the presence of random disturbances acting on the automatic optimizer is considered, and the error determined, as well as the optimal magnitude, for various types of disturbance probability distribution functions.

The influence of obstacles acting on the automatic optimizer A (Fig. 1) may be significantly lowered when the system is optimized under statistical criteria of the form

$$\varphi = \psi\left\{\sum_{j=1}^{n}\sum_{i=1}^{m} M\,[\alpha_i x_i(t)\,F_{ij}(t+\tau_{ij})] + \sum_{j=1}^{n}\sum_{i=1}^{m} M\,[\beta_i x(t)\,x_i(t+\tau_i)]\right\} = \min, \qquad (1)$$

where M is the symbol for mathematic expectancy; ψ is the symbol for the functional transformation; F, the values of the controlled disturbances acting on the system; α_i and β_i, certain weight functions; x_i, the controlled variables of the system; and $\underline{x}$ the value of the regulated variable. By optimization of the system (Fig. 1) one understands minimization of the magnitude of φ, formed by the block for the formation of the minimized quantity BFMQ according to formula (1). The minimization of φ is accomplished by the automatic optimizer A, which carries out an automatic search for the necessary values Z_i of controlled actions on the object O, and values τ_{ij}. The computing device BFMQ and the optimizer A constitute the computing device for optimization of the regime of the system CDORS.

The main purpose of this article is the investigation of questions concerning the automatic optimization of a system (Fig. 1) by different statistical criteria φ. The investigation is limited to the case of the search for the optimal regime in several variables, for a class of steady random disturbances. Methods are shown for designing an apparatus for the automatic optimization by statistical criteria.

II. Equations and Methods for Investigating the System

An illustration of the method of investigation and a derivation of the equations of the system in Fig. 1 are outlined for the example involving the correction of the parameters k_0, τ_0 and T_0 of the compensating device $K_0(p)$ of

a linear system with control by a disturbance F_1 (Fig. 2). Here F_2 is the uncontrolled equivalent disturbance; $K_1(p)$, $K_2(p)$, $K_3(p)$ are the corresponding transfer functions for the system; and $\underline{x}$ is the controlled quantity. The results obtained and the method of investigation are applicable to a wide class of systems, including automatic control systems with automatic control by deviation, and combined systems.

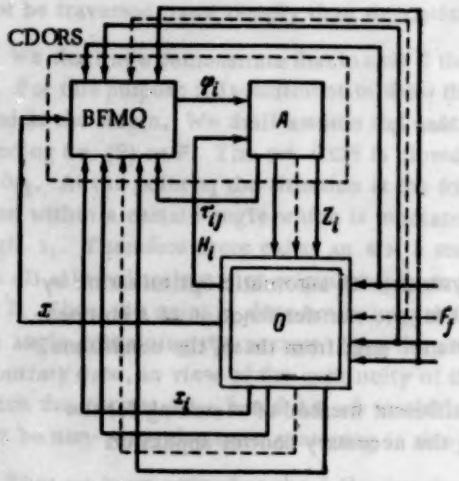

Fig. 1

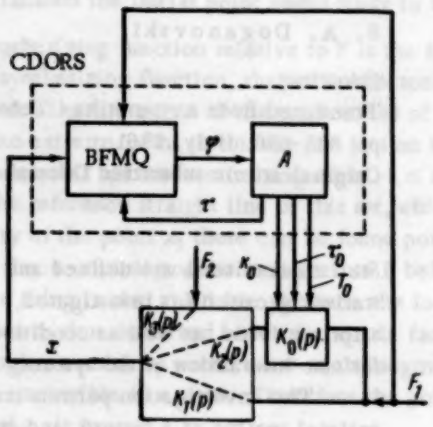

Fig. 2

We consider the problem of forming various statistical criteria φ and demonstrating the system's extremal characteristics obtained as functions of the control variables ($z_1, z_2, \ldots, z_m; \tau_1, \tau_2, \ldots, \tau_n$) in the presence of functions $H_i(z_1, z_2, \ldots, z_m; \tau_1, \tau_2, \ldots, \tau_n)$ limiting the variables mentioned.

The knowledge of similar characteristics allows one then to choose the most efficient (for example, in the sense of rapidity in searching out the extremals) method of searching for the optimal regime, and also to select principles for constructing the control apparatus CDORS.

The control systems, in which the conditions of invariance are realized, reduce, as shown in many articles (see, for example,[5]) to the structural scheme of Fig. 2, with two channels for the propagation of the controlled disturbing action F_1. In the case when the transfer functions $K_1(p)$ and $K_2(p)K_0(p)$ in the two channels are equal in magnitude and opposite in sign, complete invariance (independence) of the regulated output of variable $\underline{x}$ in relation to the disturbance F_1 occurs. If the mentioned transfer functions are not subjected to this condition, then a shift in the controlled quantity $\underline{x}$ appears at the output, this shift being due to the controlling signal F_1. Moreover, the quantity $\underline{x}$ shifts under the action of uncontrolled disturbances, reduced to the equivalent disturbance F_2. Adjustment of the parameters of the compensating device with transfer function $K_0(p)$ allows one to reduce the magnitude of the statistical criterion φ to a minimum. In the case of a linear operator $K_0(p)$ the variable parameters adjustable by the automatic optimizer A are the values of the amplification coefficient k_0, the delay time τ_0 and the constant times T_0 (Fig. 2). The magnitude of φ is formed by the computing device BFMQ in accordance with expression (1), the argument τ_{ij} of which may in general be corrected by the automatic optimizer A.

We consider the definition of the criterion φ as the mean square of the regulated quantity $\underline{x}$ for the class of stationary random input disturbances F_1, assuming that uncontrolled disturbances are absent, i.e. $F_2 = 0$. In this case the expression

$$\varphi = M[x^2(t)] = \lim_{T\to\infty} \frac{1}{T}\int_0^T [x(t)]^2\,dt = \frac{1}{\pi}\int_0^\infty S_F(\omega)\,|K(j\omega)|^2\,d\omega$$

$$= \frac{1}{\pi}\int_0^\infty S_F(\omega)\,|K_1(j\omega) - K_0(j\omega)K_2(j\omega)|^2\,d\omega, \qquad (2)$$

is valid, where $S_F(\omega)$ is the spectral density of the input disturbance, $|K(j\omega)|$ is the modulus of the amplitude-phase

characteristic (a.p.c.) of the system; $K_1(\omega)$, $K_2(j\omega)$, the a.p.c. of the system; and $K_0(j\omega)$, the a.p.c. of the compensating device.

We consider the adjustment of the parameters of a compensating device $K_0(p)$ with the following a.p.c.:

$$K_1(j\omega) = \frac{k_1}{1 + j\omega T_1} e^{-j\omega\tau_1}, \tag{3}$$

$$K_2(j\omega) = \frac{k_2}{1 + j\omega T_2} e^{-j\omega\tau_2}. \tag{4}$$

The quantity φ is determined from the expression

$$\varphi = \frac{1}{\pi}\int_0^\infty S_F(\omega)\frac{k_1^2(k_2^*)^2 A(\omega) + (k_1^*)^2 k_2^2 B(\omega) - 2k_1k_2k_1^*k_2^* Q(\omega)}{(k_2^*)^2 C(\omega)}\,d\omega, \tag{5}$$

where

$$A(\omega) = (1 - \omega^2 T_1^* T_2)^2 + \omega^2 (T_1^* + T_2)^2,$$

$$B(\omega) = (1 - \omega^2 T_1 T_2^*)^2 + \omega^2 (T_1 + T_2^*)^2,$$

$$C(\omega) = \omega^6 (T_1 T_1^* T_2)^2 + \omega^4 [(T_1 T_1^*)^2 + (T_1 T_2)^2 + (T_1^* T_2)^2] + \omega^2 [T_1^2 + (T_1^*)^2 + T_2^2] + 1.$$

Here asterisks indicate parameters of $K_0(j\omega)$, and Q is determined by the formula

$$\begin{aligned} Q = {} & (\cos\omega\tau_1 \cos\omega\tau + \sin\omega\tau_1 \sin\omega\tau)\,[\omega^2 (T_1^* + T_2)(T_1 + T_2^*) \\ & + (1 - \omega^2 T_1 T_2)(1 - \omega^2 T_1 T_2^*)] + \omega(\cos\omega\tau_1 \sin\omega\tau - \sin\omega\tau_1 \cos\omega\tau) \\ & \times [(T_1 + T_2^*)(1 - \omega^2 T_1^* T_2) - (T_1^* + T_2)(1 - \omega^2 T_1 T_2^*)], \end{aligned} \tag{6}$$

where $\tau = \tau_1^* - \tau_2^* + \tau_2$.

We consider further particular cases obtained from the equation (5).

1. For the case of an inertialess object with coefficients k_1 and k_2, the compensating device is an amplifier with variable amplification coefficient k_0.

Considering that $T_1 = T_1^* = T_2 = T_2^* = \tau_1 = \tau_2 = 0$, and setting $k_0 = k_1^*/k_2^*$, we arrive at the expression

$$\varphi = \frac{1}{\pi}\int_0^\infty S_F(\omega)\frac{k_1^2(k_2^*)^2 + (k_1^*)^2 k_2^2 - 2k_1k_2k_1^*k_2^*}{(k_2^*)^2} = \frac{1}{\pi}\int_0^\infty S_F(\omega)(k_1 - k_0k_2)^2\,d\omega = D_{FF}(k_1 - k_0k_2)^2, \tag{7}$$

where D_{FF} is the dispersion of the input signal.

An investigation of the process by which such a system moves to its optimal regime with an automatic optimizer of step type, and a formula for choosing the necessary time of averaging T and the mathematical expectation of the required steps of the search are given in [8]. The expressions indicated may be used for investigating the process by which a system moves to its optimal regime for other particular cases considered below.

2. For the case of an inertialess object $T_1 = T_1^* = T_2 = T_2^* = 0$ in the presence of pure retardation $\tau_0 = \tau_1^* - \tau_2^*$ with $k_1 = k_2$, we find

$$\begin{aligned} \varphi &= \frac{1}{\pi}\int_0^\infty S_F(\omega)\frac{k_1^2(k_2^*)^2 + (k_1^*)^2 k_2^2 - 2k_1k_2k_1^*k_2^*(\cos\omega\tau_1\cos\omega\tau + \sin\omega\tau_1\sin\omega\tau)}{(k_2^*)^2}\,d\omega \\ &= 2k_1^2[D_{FF} - R_{FF}(\Delta\tau)], \end{aligned} \tag{8}$$

where $R_{FF}(\Delta\tau)$ is the correlation function of the input signal $\Delta\tau = \tau_1 - \tau$.

Setting $R_{FF}(\Delta\tau) = e^{-\mu(\Delta\tau)^2}$ and $k_1 = 1/\sqrt{2}$, from formula (8) we obtain

$$\varphi = 1 - e^{-\mu(\Delta\tau)^2}. \tag{9}$$

Approximating a portion of the correlation function by a parabola, we arrive at the expression

$$\varphi = D_{FF}\,[1 - \gamma\,(\tau_1 - \tau_2 - \tau_0)^2], \tag{10}$$

where γ is the scale factor coefficient, and τ_0 is bounded by the values $\tau_1 - \tau_2 \pm 1/\sqrt{\gamma}$.

We find the equation of motion for the system in this case, using the expression considered in [8]. Introducing the notations $\theta = \tau_1 - \tau_2 - \tau_0$, we may write

$$\delta\theta_i = \frac{k_{fd}}{RC}\int_0^{\tau_{os}} \Delta\varphi_i\,dt = \frac{k_{fd}}{RC}\,T_{os}\cdot 2\Delta\theta\gamma\theta_i D_{FF} = BD_{FF}\theta_i, \tag{11}$$

where

$$B = 2\gamma\,\frac{k_{fd}}{RC}\,T_{os}\quad\Delta\theta, \tag{12}$$

$$\begin{aligned}\delta\theta_i = BD_{FF}\theta_i = BD_{FF}\,(\theta_{i-1} - \delta\theta_{i-1}) = BD_{FF}[\theta_0\,(1 - BD_{FF})^{i-1}\\ - BD_{FF}\theta_0\,(1 - BD_{FF})^{i-1}] = BD_{FF}\theta_0\,(1 - BD_{FF})^i,\\ \theta\,[n] = \theta_0\,(1 - BD_{FF})^n.\end{aligned} \tag{13}$$

Substituting the value of θ, we find

$$\tau_0\,[n] = (\tau_1 - \tau_2)\,[1 - (1 - BD_{FF})^n] + \tau_0\,(0)\,(1 - BD_{FF})^n. \tag{14}$$

The condition for convergence of the search process may be written out in the form

$$\gamma\,\frac{k_{fd}}{RC}\,T_{os}\quad\Delta\tau_0 D_{FF} < 1 \tag{15}$$

or

$$|\,1 - BD_{FF}\,| < 1. \tag{16}$$

Considering the condition of boundedness, we find the equation of the search process of the optimal regime from its bounds in the form

$$\tau_0\,[n] = (\tau_1 - \tau_2)\,[1 - (1 - BD_{FF})^n] + \left(\tau_1 - \tau_2 + \frac{1}{\sqrt{\gamma}}\right)(1 - BD_{FF})^n. \tag{17}$$

The corresponding mathematical expectation of the number of steps in the search is determined from the expression

$$M\,[n] = \ln\left(\frac{\Delta\tau_0}{2\sqrt{\gamma}}\right)\int_{-\infty}^{\infty}\frac{p(D_T)}{\ln(1 - BD_T)}\,dD_T. \tag{18}$$

3. For the case of an inertialess object ($k_1 \neq k_2$) in the presence of pure retardation, and considering that $T_1 = T_1^\circ = T_2 = T_2^\circ = 0$ and $k_0 = k_1^\circ/k_2^\circ$, we obtain the expression

$$\varphi = \frac{1}{\pi}\int_0^\infty S_F(\omega)\,[k_1^2 + k_0^2k_2^2 - 2k_1k_2k_0\,(\cos\omega\tau_1\cos\omega\tau$$

$$+ \sin\omega\tau_1\sin\omega\tau)]\,d\omega = D_{FF}\,(k_1 - k_0k_2)^2 + 2k_1k_2k_0\,[D_{FF} - R_{FF}\,(\tau_1 - \tau)], \qquad (19)$$

where D_{FF} is the dispersion, and $R_{FF}(\tau_1 - \tau)$ the correlation function of the input signal. Thus formula (19) determines a surface $\varphi = \varphi(k_0, \tau_0)$ with a minimum at definite values τ_0 and k_0. In the case when $R_{FF}(\Delta\tau) = D_{FF}e^{-\mu(\Delta\tau)^2}$, expression (19) may be written in the form

$$\varphi = D_{FF}\,[(k_1 - k_0k_2)^2 + 2k_1k_2k_0\,(1 - e^{-\mu(\Delta\tau)^2})]. \qquad (20)$$

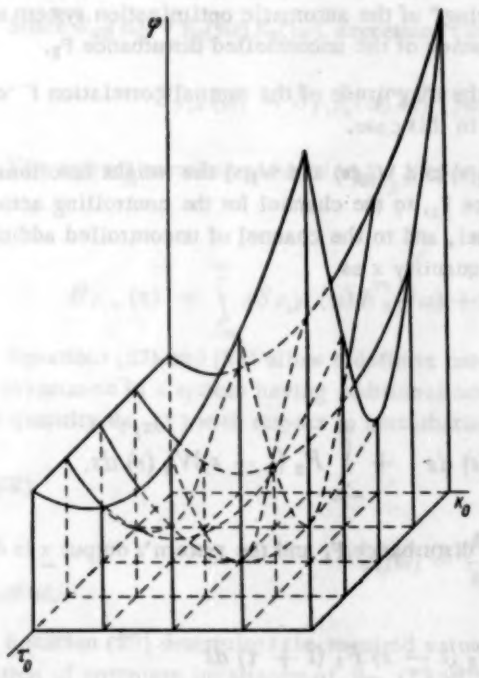

Fig. 3

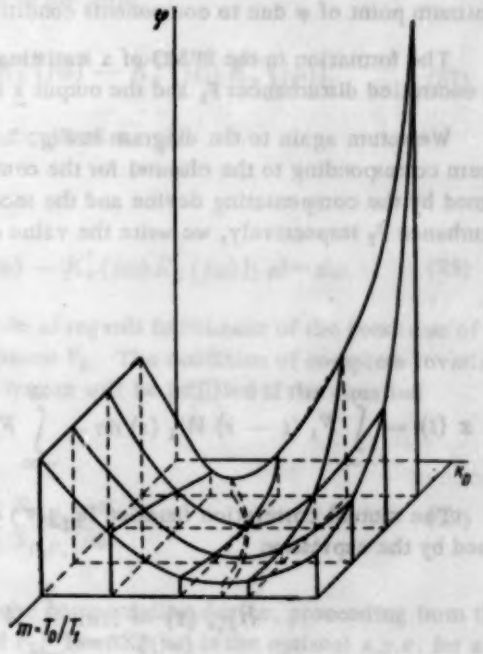

Fig. 4

Figure 3 illustrates the shape of a similar surface, whose sections at k_0 = const are curves described by correlation function equations of the form (9) and whose section at τ_0 = const are parabolas analogous to the curves described by equations (7). The bound functions H_i are planes bounding the admissible values of k_0 and τ_0 in the system.

4. For the case of an inertial object, setting $\tau_1 = \tau_1 = T_2 = T_2^* = 0$ in formula (5), we obtain the expression

$$\varphi = \frac{1}{\pi}\int_0^\infty S_F(\omega)\,\frac{(k_1 - k_0k_2)^2 + \omega^2\,(k_1T_0 - k_0k_2T_1)^2}{(\omega^2T_1^2 + 1)\,(\omega^2T_0^2 + 1)}\,d\omega$$

$$= \frac{(k_1 - k_0k_2)^2}{\pi}\int_0^\infty \frac{S_F(\omega)}{(\omega^2T_1^2 + 1)\,(\omega^2T_0^2 + 1)}\,d\omega + \frac{(k_1T_0 - k_0k_2T_1)^2}{\pi}\int_0^\infty \frac{S_F(\omega)\,\omega^2}{(\omega^2T_1^2 + 1)\,(\omega^2T_0^2 + 1)}\,d\omega. \qquad (21)$$

Expression (21) determines the form of the surface $\varphi = \varphi(k_0, m)$, where $m = T_0/T_1$. For $S_F(\omega) = S_0$, after expanding the fractional integrand, we obtain the expression

$$\varphi = \frac{S_0}{\pi}\left[(k_1 - k_0k_2)^2\int_0^\infty \frac{d\omega}{(m^2\omega^2T_1^2+1)(\omega^2T_1^2+1)}\right.$$

$$\left. + T_1^2(k_1m - k_0k_2)^2\int_0^\infty \frac{\omega^2 d\omega}{(m^2\omega^2T_1^2+1)(\omega^2T_1^2+1)}\right] = \frac{S_0}{2T_1(1+m)}\left[(k_1 - k_0k_2)^2 + \frac{1}{m}(k_1m - k_0k_2)^2\right]. \quad (22)$$

Fig. 4 illustrates the shape of the surface $\varphi = \varphi(k_0, m)$, corresponding to the expression (22). The bounding function is represented by planes bounding the admissible values of $\underline{m}$ and k_0.

The definition of the statistical criterion φ by the magnitude of the mean square of the regulated quantity is inefficient in those cases when the system is under the action of additional noncontrolled disturbances F_2 causing changes in the regulated quantity $\underline{x}$. The correction of the parameters of the compensating device $K_0(p)$ according to the criterion of mean square of the quantity $\underline{x}$ leads to a "yawing" of the automatic optimization system near the minimum point of φ due to components conditioned by the influence of the uncontrolled disturbance F_2.

The formation in the BFMQ of a statistical criterion φ as the magnitude of the mutual correlation function of the controlled disturbances F_1 and the output $\underline{x}$ is more efficient in this case.

We return again to the diagram in Fig. 2. Denoting by $W_1(s)$ and $W_{02}(s)$ and $W_3(s)$ the weight functions of the system corresponding to the channel for the controlled disturbance F_1, to the channel for the controlling action formed by the compensating device and the second object channel, and to the channel of uncontrolled additional disturbance F_2 respectively, we write the value of the regulated quantity $\underline{x}$ as

$$x(t) = \int_{-\infty}^{\infty} F_1(t-s)\,W_1(s)\,ds - \int_{-\infty}^{\infty} F_1(t-s)\,W_{02}(s)\,ds + \int_{-\infty}^{\infty} F_2(t-s)W_3(s)\,ds. \quad (23)$$

The mutual correlation function $R_{F_1x}(\tau)$ of the controlled disturbance F_1 and the system's output $\underline{x}$ is determined by the expression

$$R_{F_1x}(\tau) = \lim_{T\to\infty}\int_{-\infty}^{\infty} W_1(s)\,ds\frac{1}{2T}\int_{-T}^{T} F_1(t-s)\,F_1(t+\tau)\,dt$$

$$- \lim_{T\to\infty}\int_{-\infty}^{\infty} W_{02}(s)\,ds\frac{1}{2T}\int_{-T}^{T} F_1(t-s)\,F_1(t+\tau)\,dt$$

$$+ \lim_{T\to\infty}\int_{-\infty}^{\infty} W_3(s)\,ds\frac{1}{2T}\int_{-T}^{T} F_2(t-s)\,F_1(t+\tau)\,dt$$

$$= \int_{-\infty}^{\infty} W_3(s)\,R_{F_1F_2}(\tau+s)\,ds + \int_{-\infty}^{\infty} W_1(s)\,R_{F_1F_1}(\tau+s)\,ds$$

$$- \int_{-\infty}^{\infty} W_{02}(s)\,R_{F_1F_1}(\tau+s)\,ds. \quad (24)$$

The mutual spectral density $S_{F_1X}(\omega)$ is determined by the expression

$$S_{F_1x}(\omega) = \int_{-\infty}^{\infty} R_{F_1F_2}(\tau + s)\, e^{-j\omega(\tau+s)}\, d\tau \int_{-\infty}^{\infty} W_3(s)\, e^{j\omega s}\, ds$$

$$+ \int_{-\infty}^{\infty} R_{F_1F_1}(\tau + s)\, e^{-j\omega(\tau+s)}\, d\tau \int_{-\infty}^{\infty} W_1(s)\, e^{j\omega s}\, ds$$

$$- \int_{-\infty}^{\infty} R_{F_1F_1}(\tau + s)\, e^{-j\omega(\tau+s)}\, d\tau \int_{-\infty}^{\infty} W_{02}(s)\, e^{j\omega s}\, ds. \qquad (25)$$

Bearing in mind that the second integral of each of the terms represents a quantity conjugate to the corresponding transfer function of the object and compensating device, we arrive at the expression

$$S_{F_1x}(\omega) = S_{F_1F_2}(\omega)\, K_3^*(j\omega) + S_{F_1F_1}(\omega)\, [K_1^*(j\omega) - K_{02}^*(j\omega)]. \qquad (26)$$

Since $K_{02}(j\omega) = K_0(j\omega)\, K_2(j\omega)$, expression (26) may be written in the form

$$S_{F_1x}(\omega) = S_{F_1F_2}(\omega)\, K_3^*(j\omega) + S_{F_1F_1}(\omega)\, [K_1^*(j\omega) - K_0^*(j\omega)\, K_2^*(j\omega)]. \qquad (27)$$

The mutual correlation function $R_{F_1X}(\tau)$ is determined by the expression

$$R_{F_1x}(\tau) = \int_{-\infty}^{\infty} [S_{F_1F_2}(\omega)\, K_3^*(j\omega) + S_{F_1F_1}(\omega)\, [K_1^*(j\omega) - K_0^*(j\omega)\, K_2^*(j\omega)]]\, e^{j\omega\tau}\, d\omega. \qquad (28)$$

Equations (27) and (28) allow a definite conclusion to be made as regards fulfillment of the condition of complete invariance in a system having additional uncontrolled disturbance F_2. The condition of complete invariance of the quantity $R_{F_1X}(\tau)$ with respect to perturbations acting on the system will be fulfilled if the equation

$$K_0^*(j\omega) = \frac{K_1^*(j\omega)}{K_2^*(j\omega)} + \frac{K_3^*(j\omega)}{K_2^*(j\omega)} \frac{S_{F_1F_2}(j\omega)}{S_{F_1F_1}(j\omega)} \qquad (29)$$

is satisfied.

Equation (29) determines the required value of the a.p.c. of the compensating device, proceeding from the condition of complete invariance of $R_{F_1X}(\tau)$ with respect to F_1 and F_2. Thus $K_0^*(j\omega)$ is the optimal a.p.c. for a linear control system with disturbance F_1 (Fig. 2).

In the case when there is no correlation between the perturbations F_1 and F_2, equation (29) may be written in the usual form

$$K_0(j\omega) = \frac{K_1(j\omega)}{K_2(j\omega)}. \qquad (30)$$

One may consider that the perturbation F_2, correlated with F_1, forms an additional channel for the basic controlled disturbance F_1, determined by the a.p.c. of $K_3(j\omega)$ and the mutual spectral density $S_{F_1F_2}(j\omega)$. Therefore in the diagram of Fig. 2 the parameters a.p.c. $K_0(j\omega)$ will now already be determined by the parallel union of the direct and supplementary channels of the basic controlled disturbance F_1.

Aside from the condition of complete statistical invariance (29) formulated above, one may consider the problem of choosing definite classes of functions $K_3(j\omega)$, $S_{F_1F_2}(j\omega)$ and values of the argument τ which will guarantee fulfillment of the equation

$$\int_{-\infty}^{\infty} W_3(s)\, R_{F_1F_2}(\tau + s)\, ds = 0. \qquad (31)$$

The fulfillment of equation (31) for definite values of the argument τ means preservation of the condition of complete invariance, determined by equation (30), and the independence of $R_{F_1x}(\tau)$ with respect to additional uncontrolled disturbance F_2. In other words, in this case each of the terms of expression (27) attains the value zero.

The equation defining the statistical criterion φ as the magnitude of the mutual correlation function of the controlled perturbation F_1 and the regulated quantity $\underline{x}$ is written for a system of automatic control by F_1 (Fig. 2) in the form

$$\varphi = \psi\left\{\int_{-\infty}^{\infty}[S_{F_3F_3}(\omega)K_3^*(j\omega)+S_{F_1F_1}(\omega)[K_1^*(j\omega)-K_0^*(j\omega)K_2^*(j\omega)]]\,e^{j\omega\tau}d\omega\right\}=\min, \tag{32}$$

where ψ represents some function of $R_{F_1x}(\tau)$.

The condition of physical realizability of the optimal a.p.c. (29) is determined by the general methods of the theory of optimal filters of Wiener and Kolmogorov [2].

We consider a concrete particular case when the fulfillment of these conditions is comparatively simple.

1. Case of an inertialess object. Setting in equation (32)

$$K_1^*(j\omega)=k_1,\quad K_2^*(j\omega)=k_2,\quad K_0^*(j\omega)=k_0,\quad K_3^*(j\omega)=k_3$$

we arrive at the following expression, determining the criterion φ:

$$\varphi=\psi\{k_3R_{F_3F_3}(\tau)+(k_1-k_0k_2)R_{F_1F_1}(\tau)\}. \tag{33}$$

Suppose ψ is a quadratic transformation; then we obtain the following formula determining the surface $\varphi = \varphi(k_0, \tau)$:

$$\varphi=\varphi(k_0,\tau),\quad \varphi=[k_3R_{F_3F_3}(\tau)+(k_1-k_0k_2)R_{F_1F_1}(\tau)]^2. \tag{34}$$

In the case when an uncontrolled disturbance F_2 exerts an influence on the system, one may guarantee minimization of the chosen criterion φ by accounting for the change of two parameters of the system: the coefficient of the compensating device k_0 and the argument of the correlation function τ [see formula (31)].

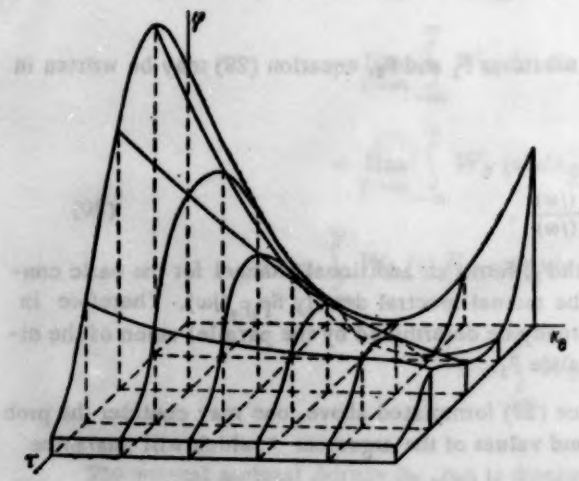

Fig. 5

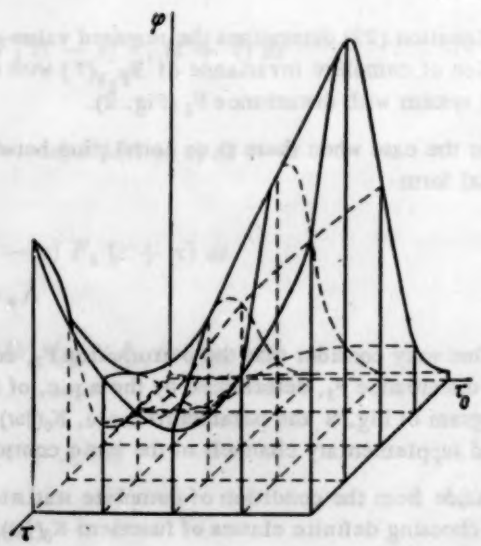

Fig. 6

Fig. 5 illustrates the character of the surface $\varphi(k_0, \tau)$ obtained for correlation functions of the type $e^{-\mu\tau^2}$ having a minimum on the surface (k_0, τ). The bounding functions H_i are represented by planes bounding the admissible values of k_0 and τ.

2. Case of an inertialess object with pure retardation. Setting

$$K_3^*(j\omega) = k_3,$$
$$K_1(j\omega) = e^{-j\omega\tau_1},$$
$$K_2(j\omega) = e^{-j\omega\tau_2},$$
$$K_0(j\omega) = e^{-j\omega\tau_0},$$

we arrive at the expression

$$\varphi = \psi\left[k_3 R_{F_1F_2}(\tau) + R_{F_1F_1}(\tau_1 + \tau) - R_{F_1F_1}(\tau_2 + \tau_0 + \tau)\right] \tag{35}$$

or

$$\varphi = \left[k_3 R_{F_1F_2}(\tau) + R_{F_1F_1}(\tau_1 + \tau) - R_{F_1F_1}(\tau_2 + \tau_0 + \tau)\right]^2. \tag{36}$$

By way of example, the shape of the surface obtained for correlation functions of exponential type is given in Fig. 6. This surface is constructed according to expression (36). The boundings planes are shown there also. In the case when the correlation functions have the form $e^{-\mu\tau^2}\cos\alpha\tau$, the surfaces in Figs. 3, 4, 5 and 6 take on a more complicated form and several minima are attained for φ. This complicates the problem of searching for the least of the values φ, and leads to the required use of some automatic optimizer of a global type [1].

By analogous methods, one may construct formulas and surfaces for many different cases determined by expressions (1), (31) and (32) and answer the question of the physical realizability of the optimal operators obtained. Thus the investigation of the problem of defining a statistical criterion by the magnitude of the mutual correlation function between the input, representing controlled disturbances, and the regulated quantity of the system allows one to clarify the conditions of complete statistical invariance of the criterion φ with respect to the controlled and uncontrolled disturbances acting on the system. The determination of the conditions of complete statistical invariance of the system allows one to solve the problem of non-interaction and compensation for the influence of disturbances conditioned by the control in a connected system with many inputs and outputs, since [1, 5] the conditions for non-interaction follow from the conditions of invariance.

We consider, by way of example, a system consisting of the two diagrams of Fig. 2, the output of which is the sum of outputs of the individual diagrams. Then, writing the disturbance, weight functions and output signals of each diagram as in Fig. 2, and denoting the output quantity by $\underline{x}$, we obtain the following expression for the mutual correlation functions $R_{F_{11}x}(\tau_1)$ and $R_{F_{21}x}(\varphi_2)$:

$$R_{F_{11}x}(\tau_1) = \int_{-\infty}^{\infty} [W_{11}(s) - W_{102}(s)]\, R_{F_{11}F_{11}}(s + \tau_1)\, ds + \int_{-\infty}^{\infty} W_{13}(s)\, R_{F_{13}F_{11}}(s + \tau_1)\, ds + \int_{-\infty}^{\infty} [W_{21}(s) - W_{202}(s)]\, R_{F_{21}F_{11}}(s + \tau_1)\, ds + \int_{-\infty}^{\infty} W_{23}(s)\, R_{F_{23}F_{11}}(s + \tau_1)\, ds, \tag{37}$$

$$R_{F_{21}x}(\tau_2) = \int_{-\infty}^{\infty} [W_{21}(s) - W_{202}(s)]\, R_{F_{21}F_{11}}(s + \tau_2)\, ds + \int_{-\infty}^{\infty} W_{23}(s)\, R_{F_{23}F_{11}}(s + \tau_2)\, ds + \int_{-\infty}^{\infty} [W_{11}(s) - W_{102}(s)]\, R_{F_{11}F_{11}}(s + \tau_2)\, ds + \int_{-\infty}^{\infty} W_{13}(s)\, R_{F_{13}F_{11}}(s + \tau_2)\, ds. \tag{38}$$

For further simplification of expressions (37) and (38), one may neglect the influence of $F_{i2}(t)$, since the action of one circuit on the other is equivalent to a similar disturbance. In this case, the necessary conditions for independence in the construction of parameters of the compensating device of each circuit may be written in the form

$$\int_{-\infty}^{\infty} [W_{21}(s) - W_{202}(s)] R_{F_2F_{11}}(s + \tau_1)\, ds = 0, \tag{39}$$

$$\int_{-\infty}^{\infty} [W_{11}(s) - W_{102}(s)] R_{F_{11}F_2}(s + \tau_2)\, ds = 0. \tag{40}$$

The fulfillment of conditions (39) and (40) is determined, as for (31), for definite classes of integrands and values of the arguments τ_1 and τ_2.

The arguments given may be generalized to the case of n circuits, which leads to the expression

$$\sum_{i=1}^{n} \int_{-\infty}^{\infty} [W_{i1}(s) - W_{i02}(s)] R_{F_iF_j}(s + \tau_j)\, ds\, \delta_{ij} = 0, \tag{41}$$

where $j = 1, 2, \ldots, n$, and δ_{ij} is defined by the conditions

$$\delta_{ij} = 0 \text{ for } i = j, \quad \delta_{ij} = 1 \text{ for } i \neq j. \tag{42}$$

The reasoning may also be generalized to other structures and object diagrams, including systems with negative feedback.

Equations (41)–(42) are analogous in structure to the system of equations associated with ordinary autonomous control systems (see [1]). However, equations (41) determine conditions for non-interaction of not the regulated variables themselves, but rather the statistical criteria, representing the mutual correlation functions of the controlled disturbances and the quantity x. The question of the physical realizability of similar conditions, depending on the choice of necessary classes of integrand and values of the arguments, is, as for ordinary coupled automatic control systems, an independent problem.

III. Certain Possibilities for Application of the Results Obtained

As an example of the correction of the parameters of the compensating device of a linear control system, a method is shown of defining statistical criteria. The characteristics of an automatic optimization system have been found and illustrated by a series of examples, and also the condition of complete statistical invariance and a method for determining the optimal transfer function of a compensating device have been found, as well as the condition of non-interaction following from them. The investigation which has been carried out allows one to choose the most efficient method of searching for the optimal regime of a system, and also of designing the necessary apparatus.

1. Since the characteristics of the system examined are to a definite extent known, in order to hurry the process it is expedient to organize the search in the form of a combination of the method of extrapolation and the method of gradients. The application of the method of gradients is most useful, as is known [1], when the system is initially not too far from the extremum point.

2. In IAT AN SSSR an apparatus for the automatic optimization of a system of statistical criteria, named the computing device for optimization of the regime of a system (CDORS) [6] is described. Such a device, as is evident from Fig. 1, consists of a block for the formation of the minimized quantity φ_i on the basis of the statistical criterion taken, and an automatic many-channeled optimizer performing a search for such values of the variables of the system Z_i and quantities τ_{ij} for which minimization of the criterion φ_i chosen is guaranteed.

The application of CDORS for a continuous search is illustrated in Fig. 7, where the structural scheme of the control system with object (OP) having an extremal static characteristic of the form $Y = -kx^2$ is depicted. In Fig. 7 the notation Y is used for the regulated quantity, and X for the regulating quantity. The variation of the quantity X may be considered slow (secular) in comparison with the variations of the quantity ΔX, which represents perturbations

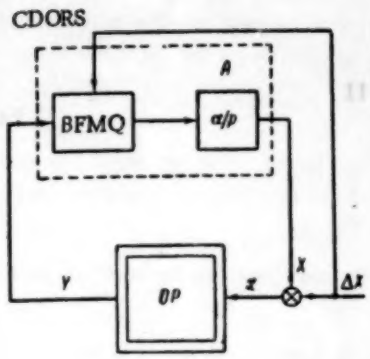

Fig. 7

obeying a normal distribution law with zero mathematical expectancy. We suppose the control process starts with the value X not in the optimal regime. In this case the following expressions are valid:

$$\varphi = M[\Delta XY] = -2kXM[\Delta X^2],$$

$$X = m\frac{M[\Delta XY]}{M[\Delta X^2]} \quad (m = -1/2\,k).$$

Since the rate of change of the controlling signal is proportional to the output signal of BFMQ, the equation $dX/dt = -2k\alpha M[\Delta X^2]X$, is valid, whose solution determines the exponential decay curve for the variation in X, i.e. the searching process for the optimal regime of the system converges.

SUMMARY

1. In this article, the questions of automatic optimization of a system by statistical criteria are examined, the advantages of forming the criterion by the mutual correlation function of controlled input perturbations and regulated output quantities are shown, and the characteristics of an automatic optimization system and conditions for statistical invariance of the system are found. The optimal transfer function for the example of a system of control by perturbation with correction of the parameters of the compensating device is found.

2. The investigation carried out here allows one to determine the most efficient method of searching for the optimal regime and of designing the control apparatus.

The author thanks N. S. Taubman for reading the manuscript and N. S. Varaks for carrying out the numerical calculations and construction of the φ-surfaces.

LITERATURE CITED

1. Fel'dbaum, A. A. Computing Devices in Automatic Systems [in Russian], Fizmatgiz, 1959.
2. Pugachev, V. S. Theory of Random Functions and Its Application to the Problem of Automatic Control [in Russian], Fizmatgiz, 1960.
3. Chelustkin, A. B. The Design and Application of Correlation Control. Automatic Control. May, 1958.
4. Krasovskii, A. A. Dynamics of continuous systems of extremal control with random search signals. Izv. AN SSSR, OTN, Énergetika i avtomatika, No. 3, 1960.
5. Ulanov, G. M. Control by Perturbation (Compensation of Perturbations and Invariance) [in Russian] Gosénergoizdat, 1960.
6. Doganovskii, S. A. Automatic correction of the parameters of compensating devices for objects with changing characteristics. Proceedings of the First Congress of IFAK, Vol. I, 1960.
7. Doganovskii, S. A. Automatic adjustment of the parameters of compensators in systems involving control by perturbation. Avtomatika i Telemekhanika, Vol. XX, No. 8, 1959.
8. Doganovskii, S. A. Automatic optimization of the regime of one class of systems by means of a statistical quality criterion. Avtomatika i Telemekhanika, Vol. XXI, No. 8, 1960.

AUTOMATIC OPTIMIZATION OF SPACE DISTRIBUTION. II

L. N. Fitsner

(Moscow)

Translated from Avtomatika i Telemekhanika, Vol. 22, No. 7,
pp. 857-864, July, 1961
Original article submitted October 11, 1960

For the extremal system considered in [1], a method is described for designing a coordinate converter. The effects of lag elements, dry friction, backlash, and dead-zones on the stability of the search process are evaluated. Some considerations on the influence of random noise are presented.

1. Coordinate Converter

In [1] we have considered automation of the process of the space distribution of some physical quantity in a three-dimensional space, using an automatic search system. As the basic example, we consider the process of the automatic distribution of the cutting allowance for blanks of complicated parts. In the method chosen, a number of parameters of the mechanical parts of the setup and random effects have an appreciable influence on the search process. This gave rise to the need to find the conditions permitting stable operation of the system and small search error.

The present article considers solutions to these questions.

It was proved in [1] that the process of searching for the extremal of a function characterizing the position of a blank piece in space depends essentially on the directions of the test motions.

In searching for the extremal of a function Q of the variables $x_1, \ldots, x_n$, it is frequently possible to approximate this function in the neighborhood of the extremal by a quadratic form

$$Q = \sum_{i=1}^{n} \sum_{j=1}^{n} a_{ij} x_i x_j. \tag{1}$$

The search for the extremal is substantially facilitated if this quadratic form has a canonical form

$$Q^* = \sum_{i=1}^{n} b_i y_i^2. \tag{2}$$

In this case, a single optimization cycle over each variable y_i individually is sufficient. The search is thus substantially accelerated. The problem then arises of converting the quadratic form (1) to the canonical form (2). However, since the coefficients a_{ij} are originally unknown, this transformation must be realized automatically during the search for the minimum itself.

For n = 3 the transformation to the coordinates (y_1, y_2, y_3) of a three-dimensional y-space from the coordinates (x_1, x_2, x_3) of a three-dimensional x-space is realized by the formula

$$y_k = \sum_{l=1}^{3} x_l \cos \alpha_{lk} \quad (k = 1, 2, 3), \tag{3}$$

where α_{lk} are the angles between corresponding axes in the old and new coordinate systems.

Since we have the relations

$$\sum_{k=1}^{3} \cos^2 \alpha_{lk} = 1 \quad (l = 1, 2, 3) \tag{4}$$

and

$$\sum_{k=1}^{3} \cos \alpha_{1k} \cos \alpha_{2k} = 0,$$

$$\sum_{k=1}^{n} \cos \alpha_{1k} \cos \alpha_{3k} = 0, \tag{4'}$$

$$\sum_{k=1}^{n} \cos \alpha_{2k} \cos \alpha_{3k} = 0,$$

the nine factors $\cos \alpha_{lk}$ are connected by the six relations (4) and (4'). Consequently there are three independent factors. It is therefore suffient to carry out the process with respect to three parameters, denoted below by q_1, q_2, q_3. A supplementary automatic optimizer is used for the selection of these parameters.

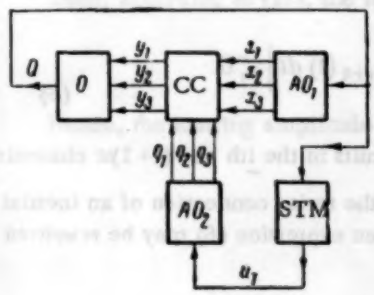

Fig. 1

A block diagram of a setup including an automatic coordinate converter is given in Fig. 1. The system consists of the object O, at whose output the function Q of the input quantities y_1, y_2 and y_3 is obtained, the coordinate converter CC, the basic optimizer AO_1, carrying out automatic determination of the variables x_1, x_2 and x_3, minimizing Q, with a search time meter STM and the auxiliary optimizer AO_2. In this circuit, aside from the basic optimization process, i.e., minimization of the function Q, a second, slower optimization process takes place, consisting in the determination of those parameters q_1, q_2, and q_3 for which the search time is minimized. After a series of parts of a single type has been worked, the second optimizer automatically finds that coordinate transformation for which the search time is reduced.

The automatic coordinate converter consists of a circuit transforming the three input parameters q_1, q_2, q_3 into the nine coefficients $\cos \alpha_{lk}$ according to formulae (4) and (4'). These coefficients correspond to the gain factors of circuits transmitting the x_l (l = 1, 2, 3). Summing the outputs of the three circuits according to formula (3), the quantities y_k are obtained.

2. The Effect of Inertial Elements in the System on the Search Process

In the present system, the drive elements, the carriage holding the part, and the relay for measuring the direction of motion of the drive organ are, as a rule, inertial elements. Position indicators may be considered practically inertialess.

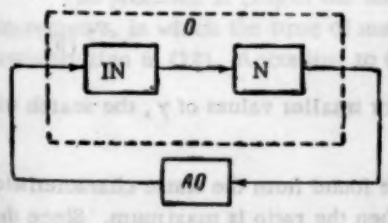

Fig. 2.

A block diagram of the optimization system is given in Fig. 2. Here O is the object of search, IN is a linear inertial part, N is the nonlinear inertialess part, AO is the automatic optimizer.

Consider a drive organ consisting of a separately excited dc motor. To a sufficient degree of exactness, such a motor may be described by a third-order equation [4]. The relay in the automatic optimizer introduces delay into the system. The stability of the search for partial extremes with respect to each of the variables with this search method depends primarily on the parameters of the inertial part of the system. For the search to be stable, the time intervals T between measurements of increments of Q must be correctly chosen. This question is considered in [5]. Unstable search can also result from incorrect choice of the time intervals necessary to pass

from the search over the ith to the (i + 1)st variable. Let us denote the durations of these intervals by T_i. The search will be stable if during the time T_i the increment to Q due to the change in x_i does not exceed the increment to Q caused by the change in x_{i+1}. The inertial part of the system (drive organ and carriage) for the ith channel can be represented, as a rule, in the form of a chain of inertial circuits with output coordinate μ_i and an integrating circuit with output coordinate x_i.

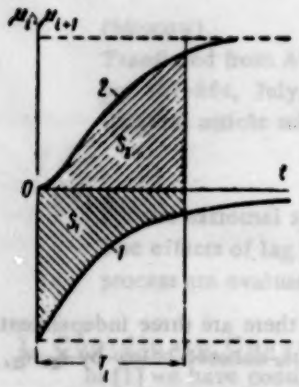

Fig. 3

The change in μ_i after disconnection of the drive organ (curve 1) and the change in μ_{i+1} after connection of the drive organ in the channel of variable x_{i+1} (curve 2) are shown in Fig. 3.

The value of T_i providing stable search can be found from the condition

$$\left|\frac{\partial Q}{\partial x_i} S_1\right| \leqslant \left|\frac{\partial Q}{\partial x_{i+1}} S_2\right|.$$

Here S_1, S_2 are the areas under the curves shown in Fig. 3 (with $\xi_i = \xi_{i+1}$, where ξ_i, ξ_{i+1} are the coefficients of the integrating networks in the ith and (i + 1) st channels, respectively).

Expanding (5), we have

$$\left|\frac{\partial Q}{\partial x_i}\xi_i \int_0^{T_i} [1-\eta_i(t)]\,dt\right| - \left|\frac{\partial Q}{\partial x_{i+1}}\xi_{i+1}\int_0^{T_i}\eta_{i+1}(t)\,dt\right| \leqslant 0. \tag{6}$$

In expression (6) $\eta_i(t)$ and $\eta_{i+1}(t)$ are the transfer functions of the inertial circuits in the ith and (i + 1)st channels.

Let the inertial part of the ith channel of the system be constituted by the series connection of an inertial circuit with time constant τ_i and an integrating circuit with coefficient ξ_i. Then expression (6) may be rewritten in the form

$$\left|\frac{\partial Q}{\partial x_i}\xi_i \int_0^{T_i} e^{-\frac{t}{\tau_i}}dt\right| - \left|\frac{\partial Q}{\partial x_{i+1}}\xi_{i+1}\int_0^{T_i}\left(1-e^{-\frac{t}{\tau_{i+1}}}\right)dt\right| \leqslant 0. \tag{7}$$

Substituting $\frac{\tau_{i+1}}{\tau_i} = \theta$, $\frac{T_i}{\tau_i} = \gamma$, we have

$$\left|\frac{\partial Q}{\partial x_i}(1-e^{-\gamma})\right| - \left|\frac{\partial Q}{\partial x_{i+1}}\left(\gamma + \theta\left(e^{-\frac{\gamma}{\theta}}-1\right)\right)\right| \leqslant 0. \tag{8}$$

If $\frac{\partial Q}{\partial x_i} = \frac{\partial Q}{\partial x_{i+1}}$, and $\xi_i = \xi_{i+1}$, then

$$|1-e^{-\gamma}| - |\gamma - 2e^{-\frac{\gamma}{2}} - 2| \leqslant 0. \tag{9}$$

From this, for the boundary of the region of stable search, $\gamma = 2.25$. For smaller values of γ, the search will be unstable.

According to (7) the required relationship of dQ/dx_i to dQ/dx_{i+1} can be found from the static characteristics of the search object. The calculation should be oriented on the best case, when the ratio is maximum. Since the parameters of the inertial elements in the various channels are not identical, the interval T_i should be found from formulas (6), (7) and the formulas presented in [5] individually for each of the channels.

3. Estimating the Influence of Dead Zones

Let it be necessary to find the extremal value of the function Q = Q(x) using an automatic optimizer with dead zone δ_d. Motion of the system in an incorrect direction will be detected only in a region for which the increment of Q(x) during the time T exceeds δ_d, i.e.,

$$\frac{\partial Q(x)}{\partial x}\Delta x > \delta_d, \tag{10}$$

where

$$\Delta x = \mu_{max} T. \tag{11}$$

From (10) and (11) we obtain

$$\frac{\partial Q}{\partial x}\mu_{max} T > \delta_d. \tag{12}$$

From (12) we can find the values of the amplitudes x_0 and the period of hunting T_0 caused by the presence of δ_d. Let, for example,

$$Q(x) = ax^2 + c. \tag{13}$$

Then, according to (12), the system will deviate from the extremal point for

$$2ax\mu_{max} T < \delta_d. \tag{14}$$

Hence, the hunting amplitude

$$x_0 < \frac{\delta_d}{2a\mu_{max} T} + \mu_{max} T. \tag{15}$$

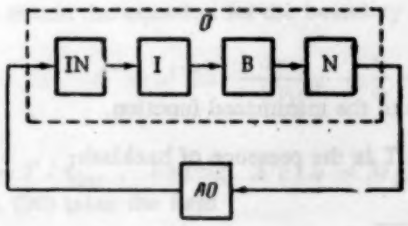

Fig. 4

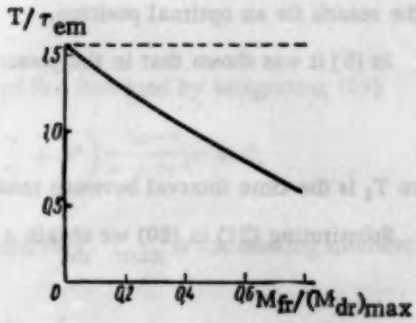

Fig. 5

The presence in (15) of the term $\mu_{max} T$ is explained by the adoption of a discrete method of measuring the increments, in which the time of measuring the increment does not coincide with the time of reversal of the inequality sign in (12). According to (15) the hunting period

$$T_0 = 4\frac{x}{\mu_{max}} < 4\frac{\delta_d}{2a\mu_{max}^2 T} + 4T. \tag{16}$$

These formulae permit finding the dependence of amplitude and period of hunting on the magnitude of the dead zone. In those cases where the amplitude and period of hunting (and consequently, the error and time of research for the optimal position) become unacceptably great due to the presence of the dead zone, the latter can usually be decreased at the price of a somewhat more complicated automatic optimizer circuit.

4. The Effect of Backlash

As a rule, backlash arises in the mechanical transmission between the drive organ and the carriage.

A circuit representing the search dynamics in the presence of backlash is given in Fig. 4. In the diagram we have: O) the search object; AO) the automatic optimizer; IN) the inertial circuit; I) the integrating circuit; B) the backlash circuit; N) a nonlinear element whose characteristic presents an extreme.

Following the method adopted in [5], it is easily shown that this system can operate if the inequality

$$\mu_{\max}\xi\int_0^T [2\eta(t)-1]\,dt-\delta>0 \tag{17}$$

is respected.

Here $\mu_{\max}$ is the maximum value at the output of the inertial circuit; ξ is the gain factor of the integrating circuit; $\eta(t)$ is the transfer function of the inertial circuit; δ is the magnitude of backlash.

Let

$$\eta(t)=1-e^{-\frac{t}{\tau}}. \tag{18}$$

Substituting (18) in (17), we obtain

$$\frac{T}{2\tau}+e^{\frac{T}{\tau}}-1-\frac{\delta}{2\xi\mu_{\max}\tau}>0. \tag{19}$$

If the inertial part consists of the series connection of a delay network with delay time t_d and an integrating network, condition (17) may be written in the form

$$T-2t_d-\frac{\delta}{\xi\mu_{\max}}>0. \tag{20}$$

From expressions (17), (19), and (20) it follows that the backlash increases the time T and thus the total time for the search for an optimal position.

In [5] it was shown that in the presence of delay and the absence of backlash an extremal system is stable with

$$T_1\geqslant 2t_d \tag{21}$$

where T_1 is the time interval between measurements of increments to the minimized function.

Substituting (21) in (20) we obtain a formula for determining T in the presence of backlash:

$$T=T_1+\frac{\delta}{\xi\mu_{\max}}. \tag{22}$$

5. The Influence of Drive Friction on the Search Process

In the present extremal system, drive friction acts in the mechanical transmission between the drive organ and the carriage.

Let the drive organ employ a separately excited dc motor.

For such a system the following equations are valid:

$$M_{dr}-M_{fr}=J\frac{d\omega}{dt}, \tag{23}$$

$$M_{fr}=A\ \text{sign}\ \omega, \tag{24}$$

$$M_{dr} = c_2 I_a \tag{25}$$

$$I_a = \frac{u - c_1\omega}{R_a}. \tag{26}$$

Here M_{dr} is the drive moment; M_{fr} is the moment of friction; ω is the angular velocity of the drive; J is the moment of intertia reduced to the drive shaft; A is the absolute value of the moment of friction; I_a is the armature winding current; U is the voltage across the armature winding; c_1, c_2 are constants.

Employing (23) - (26), the equation of motion is written in the form

$$\tau_{em}\frac{d\omega}{dt} + \omega = \frac{u}{c_1} + A^* \quad \text{for} \quad \omega < 0, \tag{27}$$

$$\tau_{em}\frac{d\omega}{dt} + \omega = \frac{u}{c_1} - A^* \quad \text{for} \quad \omega > 0,$$

where $\tau_{em} = \frac{JR_a}{c_1c_2}$ is the electromechanical time constant, $A^* = \frac{AR_a}{c_1c_2}$.

Integrating (27) for two segments of the trajectory, we obtain

$$\omega = \begin{cases} -\frac{2u}{c_1}e^{-\frac{t}{\tau_{em}}} + \frac{u}{c_1} + A^* & \text{for} \quad \omega < 0, \\ \left(-\frac{u}{c_1} + A^*\right)e^{-\frac{t-t_1}{\tau_{em}}} + \frac{u}{c_1} - A^* & \text{for} \quad \omega > 0. \end{cases} \tag{28}$$

From (5) it follows that the present extremal system can function (has hunting of the first kind) when the inequality

$$\int_0^{t_1}\left(-\frac{2u}{c_1}e^{-\frac{t}{\tau_{em}}} + \frac{u}{c_1} + A^*\right)dt < \int_{t_1}^{T}\left[\left(-\frac{u}{c_1} + A^*\right)e^{-\frac{t-t_1}{\tau_{em}}} + \frac{u}{c_1} - A^*\right]dt \tag{29}$$

is observed.

Here t_1 is the time corresponding to $\omega = 0$.

We obtain the equation for the boundary of the region of hunting of the first kind by integrating (29):

$$A^* + A^* \ln\frac{2u}{u + c_1A^*} - \frac{u}{c_1} + \frac{1}{2}\left(\frac{u}{c_1} - A^*\right)\nu - \left(-\frac{u}{c_1} + A^*\right)\frac{ue^{-\nu}}{u + c_1A^*} = 0, \tag{30}$$

where $\nu = T/\tau_{em}$. Putting $A^*c/u = M_{fr}/(M_{dr})_{max} = \lambda$, where $(M_{dr})_{max}$ is the starting moment of the drive, (30) takes the form

$$1 + \ln\frac{2}{1+\lambda} - \frac{1}{\lambda} + \frac{(1-\lambda)\nu}{2\lambda} + \frac{(1-\lambda)e^{-\nu}}{\lambda(1+\lambda)} = 0. \tag{31}$$

Let us consider the influence of friction in a system whose inertial part contains, aside from inertial and integrating networks, a delay element with a delay time t_d. This circuit takes into account the delay occurring in the drive organ commutator. The motion of such a system is described by the expression

$$\left(-\frac{u}{c_1} + A^*\right)t_d + \int_0^{t_1}\left(-\frac{2u}{c_1}e^{-\frac{t}{\tau_{em}}} + \frac{u}{c_1} + A\right)dt + \tag{32}$$

$$+ \int_{t_1}^{T}\left(-\frac{u}{c_1} + A^*\right)e^{-\frac{t-t_1}{\tau_{em}}} + \left(\frac{u}{c_1} - A^*\right)dt = 0,$$

Integrating in (32), we obtain

$$\left(-\frac{u}{c_1}+A^*\right)t_d+2\tau_{em}A^*+2A^*\tau_{em}\ln\frac{2u}{u+c_1A^*}-$$
$$-\frac{2u\tau}{c_1}+\left(\frac{u}{c_1}-A^*\right)T-\left(-\frac{u}{c_1}+A^*\right)\tau\frac{2u}{u-c_1A^*}e^{-\frac{T}{\tau_{em}}}=0. \tag{33}$$

Putting $t_d/\tau_{em}=\theta$, we write (33) in the form

$$\frac{1}{2}\left(-\frac{1}{\lambda}+1\right)\theta+1+\ln\frac{2}{1+\lambda}-\frac{1}{\lambda}+\frac{(1-\lambda)\nu}{2\lambda}+\frac{(1-\lambda)e^{-\nu}}{\lambda(1+\lambda)}=0. \tag{34}$$

The curve $\nu=f(\lambda)$, obtained as the solution of equation (31) is given in Fig. 5. From the graph it follows that drive friction broadens the region of hunting of the first kind in which the extremal system can function. Other conditions being equal, drive friction therefore permits decreasing T, and thus the total search time.

However it does not follow from this that in such systems it is alway useful to increase the friction, since the latter is connected with the need for a more powerful drive, having a larger value of τ_{em}.

6. Considerations of the Influence of Random Disturbances

In [1] it was noted that the basic source of noise affecting the search process is the unevenness of the surface of the blank to be positioned. The effect on the search process of protuberances and indentations in the surface depends substantially on the choice of criteria for the search.

In search according to criterion Q_1 (minimization of the maximum deviation),indentations do not as a rule lead to false motions of the system. Protuberances exceeding the increment of the optimized function ΔQ can cause a false direction of motion in the system; however, in accordance with the adopted criterion, in the next search cycle the system leaves the protuberance. In search according to criterion Q_2 (maximization of the minimum deviation) protuberances have no effect on the search process; the presence of indentation, as a rule, does not lead to an incorrect result, although connected with false movement of the system, which increases the search time.

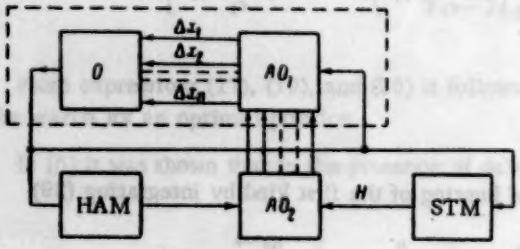

Fig. 6

The criterion Q_3 (minimization of the difference Q_1-Q_2) is poorer from the point of view of noise resistance, since in this case both protuberances and indentation affect the search process. Comparison of criteria Q_1 and Q_2 with respect to noise resistance can be done only if data on the statistics of protuberances and indentations on the surface of the blank are available.

The proposed system for automatic search of an optimum position of the blank is distinguished by relatively high noise resistance.

If the dimensions of the protuberances (indentations) do not exceed Δx_j, the optimum position will be missed only in cases of very low probability, where the two indicators fall simultaneously during the search process on protuberances (indentations) and find themselves on opposite sides. In this case the system will hunt about the protuberances or indentations exactly as about an extremal point. However, even in this case it is possible to leave the false extremum in any other direction, as a result of the regular shift in the direction of motion.

The permissible search time for the best position is usually given by technological conditions.

The basic problem of investigating the effects of noise in this case consists in determining the magnitudes of change in each of n variables (Δx_j) between measurements of increments (magnitudes of the steps in the stepping method), at which the search error is minimum, while the search time does not exceed an acceptable value.

This problem can be solved directly on the automatic search system, using an automatic synthesizer.

An automatic search system including the search object O and an automatic optimizer AO_1 as well as an automatic synthesizer consisting of an automatic optimizer AO_2, a search time meter STM and a hunting amplitude meter HAM, is shown in Fig. 6. The automatic optimizer of the synthesizer AO_2 minimizes the hunting amplitude (and therefore the search error) by acting on the magnitude of the increments Δx_j given by the automatic optimizer AO_1. Search is carried out under the condition that the mean duration of the search process (for differing initial conditions) not exceed a prescribed quantity $(T_s)_{pres}$. A voltage H, proportional to T, is applied to AO_2 and a decision is made to carry out the search only in regions for which $T_s < (T_s)_{pres}$.

SUMMARY

The formulas presented permit estimating the effects on the search process of individual parameters of an extremal system. Such estimates are necessary for the design and adjustment of systems. In more complicated cases, for example, estimating the influence of random noise, the influence on the search process of the simultaneous action of several system parameters, and others, analytical methods become practically inapplicable.

This indicates that for the solution of these problems it is necessary to develop a special computer, which we have termed the automatic synthesizer. It will be described in the succeeding article of the present series.

LITERATURE CITED

1. L. N. Fitsner, Automatic Optimization of a Space Distribution, I [in Russian], Avtomatika i Telemekhanika, 22, No. 1, 1961.
2. I. M. Gel'fand, Lectures on Linear Algebra [in Russian] (Gostekhizdat, 1951).
3. B. Ya. Kogan, Electronic Models and Their Application in the Investigation of Automatic Control Systems [in Russian] (Fizmatgiz, 1959).
4. L. N. Fitsner, On the Choice of Power Source in Optimal Automatic Control Systems [in Russian], Avtomatika i Telemekhanika 19, No. 12 (1958).
5. L. N. Fitsner, On the Design Principles and Methods of Analysis of Certain Types of Extremal Systems [in Russian]; in Proceedings of the Conference on the Theory and Application of Discrete Automatic Systems, September 22-26 (1958); Izd-vo AN SSSR, 1960.

OPTIMUM CONTROL CHARACTERISTICS OF A PULSED RELAY SYSTEM IN THE PRESENCE OF RANDOM DISTURBANCES

V. N. Novosel'tsev

(Moscow)

Translated from Avtomatika i Telemekhanika, Vol. 22, No. 7,
pp. 865-875, July, 1961
Original article submitted March 9, 1961

The problem of optimum speed control in second-order pulsed relay (number) systems is investigated. The optimum control in such systems is discussed for random disturbances that are given in the form of a transfer matrix. An optimizing control algorithm for certain types of matrices is determined.

1. Optimum Control in Continuous Second-Order Pulsed Systems

Optimum speed control in application to continuous second-order systems (see, for example, [1]) evolves down to the construction of an optimum control function F(s, v). Optimum control response is determined by the expression w = -N sign F, changing its sign when the function F converges through zero. For a system which controls a member described by the equations

$$w = \frac{dv}{dt}, \quad v = \frac{ds}{dt}, \tag{1}$$

at a restriction $|w| \leq N$, the optimum control function has the form

$$F(s,v) = s - \frac{v^2}{2}\operatorname{sign} v \tag{2}$$

(the finite point coincides with the origin of the coordinates). Figure 1 shows the block diagram of such a system. Optimum control can be effected by plotting on the phase plane an optimum switching curve (see, for example, [1])

$$s = -\frac{1}{2}v^2 \operatorname{sign} v. \tag{3}$$

It is readily conceived that for the restriction $|w| = N$, the optimum control in such a system does not differ in any way from the case $|w| \leq N$.

As has been shown by N. N. Krasovskii [2], in the optimum control of pulsed systems it is not possible to limit the control response only to its extremal values, because the amplitude of control response depends upon the initial state of the system, assuming all possible values within the range $|w| \leq N$. Optimum control in pulsed relay systems of the type $|w| = N$ differs therefore considerably from that in pulsed systems in which the modulus of acceleration has a limitation of the type $|w| \leq N$. Moreover, from the engineering point of view, it is better to have a control response that depends upon the coordinates of a system at a given moment of time than a control response that is a function of the initial state of the system and time. According to the results of [2] such a dependence is not easily obtained even for second-order systems, while in the particular case of pulsed systems using switching curves of the type described in (3), such a dependence is not feasible at all.

For a pulsed control system in which the controlled member is described by equation (1), it is possible to obtain a system of difference equations valid for any repetition period, by making use of the concept of a grid function [3]. At T = 1, this system has the form

$$\begin{aligned} s[n+1] - s[n] &= v[n] + \frac{w[n]}{2}, \\ v[n+1] - v[n] &= w[n] \end{aligned} \tag{4}$$

where the limitation of the value w[n] with respect to the modulus is preserved.

Let us introduce the following notations at arbitrary values of T:

$$x_n = \frac{s[nT]}{NT^2}, \quad y_n = \frac{v[nT]}{NT}, \quad u_n = \frac{w[nT]}{N}. \tag{5}$$

Then the equation (4) takes the form

$$x_{k+1} - x_k = y_k + \frac{u_k}{2}, \quad y_{k+1} - y_k = u_k, \quad |u_k| \leqslant 1. \tag{6}$$

For small repetition periods it is possible to obtain another system of equations by employing the well-known relation

$$\left(\frac{df}{dt}\right)_{t=kT} \approx \frac{f([k+1]T) - f(kT)}{T}.$$

In this case the difference equations would have the form

$$x_{k+1} - x_k = y_k, \quad y_{k+1} - y_k = u_k. \tag{7}$$

The system (7) has been investigated in the works [4] and [5], and the obtained results can be readily applied to system (6). In the following, the system (6) is investigated for a restriction $|u| \leq 1$.

2. Optimum Control in a Pulsed Relay System in the Absence of Random Disturbances

In all practical cases, the accuracy required in performing any operation or process is limited by a certain value ε. Hence it is natural to formulate the problem of optimum control in regard to speed as a problem of minimum-time displacement of the image point in the system phase-space from an arbitrary initial position to the proximity of the origin of coordinates, limited by the value $\pm\varepsilon$. Here it is necessary that the final velocity of the point be strictly equal to zero, so as to allow the image point to maintain its motionless state after reaching the above proximity.

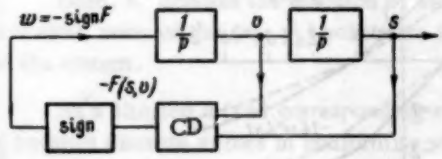

Fig. 1. Optimum second-order relay system.

When discrete equidistant values of the control response are used, the number of the (2n + 1) levels is defined as a function of the value of ε by the equation

$$n = \begin{cases} \frac{1}{2\varepsilon}, & \text{if } \frac{1}{2\varepsilon} \text{ is an integer,} \\ E\left[\frac{1}{2\varepsilon}\right] + 1 & \text{in all other cases} \end{cases} \tag{8}$$

(Here E[α] denotes the integral part of α.)

If $2\varepsilon = 1$, then two or three discrete control-response levels may be used in the pulsed relay system. The optimum control of system (7) at two values of the control response is investigated in work [4]. In work [5], an expression for the optimum control in such a system has been obtained at $2\varepsilon = 1$ and three levels of control response, and the advantages of such a method of control have been demonstrated.

The presence of only discrete values of control response at ambiguous optimum-control characteristics permits the plotting of switching curves analogous to (3), which divide the system phase plane into two or three zones having values of u equal to +1 and -1 or +1, 0 and -1, respectively. The equation of the switching curve obtained in [4] for the system (7) may be written for system (6) in the following form:

$$F(y) = -\frac{y^2 + 4|y| + 1}{2} \operatorname{sign} y. \tag{9}$$

In this case, the optimum control has the form

$$u^{\circ}_{k+1} = -\operatorname{sign}\,[x_k - F(y_k)].$$

At ternary control (for three discrete control-response levels), the phase plane is divided into three parts of the same type as shown in [5]. The boundaries between them are the following two switching curves:

$$x = F_1(y) \equiv \begin{cases} -\frac{1}{2}(y^2 + 4|y| + 1), & \text{if} \quad y \leqslant 0, \\ +\frac{1}{2}(y^2 + 2|y| - 1), & \text{if} \quad y > 0 \end{cases} \tag{10}$$

and

$$x = F_2(y) \equiv \begin{cases} +\frac{1}{2}(y^2 + 4|y| + 1), & \text{if} \quad y \geqslant 0, \\ -\frac{1}{2}(y^2 + 2|y| - 1), & \text{if} \quad y < 0. \end{cases}$$

Here

$$u^{\circ} = \begin{cases} -1 & x \geqslant F_1(y) \\ 0 & F_1(y) > x \geqslant F_2(y), \\ +1 & F_2(y) > x. \end{cases} \tag{11}$$

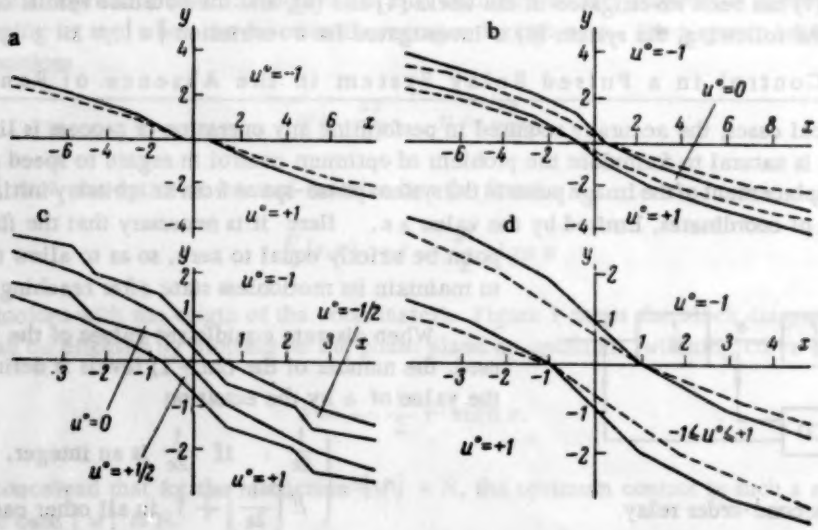

Fig. 2. Optimum switching curves for the systems (7) and (4) shown by the solid and dotted lines, respectively.

A switching curve (and a phase trajectory) is understood to be the discrete points (of the corresponding equations) that are obtained at integral values of the coordinates, connected by straight lines. Here the x coordinate is assumed to be continuous while the y coordinate may take on only integral values. For a control response having two or three values, such an assumption is natural. Similarly, in the uniform division of the integral $|u| \leq 1$ into 2n parts, it is assumed that y takes on values that are multiples of 1/2n. In this case, it is these points that should be connected by straight lines.

Optimum control when using 2n + 1 discrete levels may be constructed in the same manner as shown in [4] and [5] for the case of two and three levels. In performing this construction, the points having the coordinates $(x_0, 0)$ and $(x_0, 1/2n)$ are considered first, and then the obtained results are generalized to include arbitrary points of the phase plane. Speaking generally, optimum control is ambiguous, and among all the possible algorithms of control it is necessary to select the one that leads to 2n optimum switching curves. These divide the phase plane into 2n + 1 zones, in each of which the control-response value is constant.

With increasing n of a switching curve, the dividing neighboring zones approach each other so that in the limit defined by $n \to \infty$, the phase plane is found to be divided into three regions. In two of these the control response assumes limit values, while in the third region, located between them, there takes place a continuous dependence of the control-response value upon the system coordinates. Figure 2, a, b, c, d show the optimum switching curves for a number of levels equal to 2, 3, 5, 8, and ∞, respectively.

In the case of Fig. 2d the optimum trajectory begins in an arbitrary point $(x_0, 0)$ on the x axis of the phase plane, and intersects twice the zone of continuous dependence of u upon the system coordinates. As a result, at $x_0 < 0$, the optimum control has the form shown in Fig. 3. Here the dotted lines denote the moments of the first and second intersection of the trajectories with the $|u| < 1$ zone. (In this case, obviously, $\varepsilon = 0$.) An exception are the trajectories which begin in the points $(x_0 = n^2, y_0 = 0)$. For such points, the optimum control has the "canonical" form given in [4]:

$$u_k^\circ = -\operatorname{sign}\left[\frac{K^\circ}{2} - k\right].$$

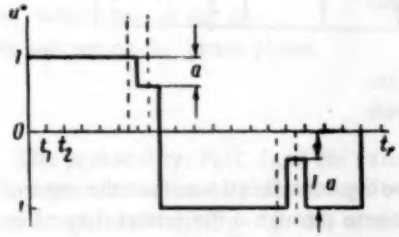

Fig. 3. Optimum control u_k°.

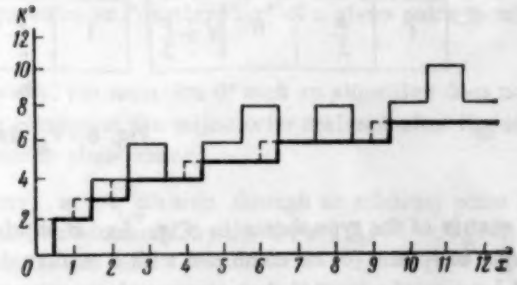

Fig. 4. Dependence of K° upon the initial conditions in pulsed relay systems.

Here, K° denotes the duration of the optimum transition process in a system with arbitrary values of n. In this case, none of the (x_k, y_k) points are located within the region of continuous dependence of u upon the coordinates of the system.

At a limited n (and corresponding $\varepsilon > 0$), the optimum trajectory also intersects twice this region $(x_0 \neq n^2)$, and u assumes discrete values in conformity with the switching curves.

Thus the optimum control over nearly the entire duration of the transition process (with the exception of two steps, at the most) consists in maintaining the limit values of the control response. It should be noted that as $h \to 0$, the zone of continuous dependence of u on the system coordinates grows narrower, and the optimum control is reduced to the retainment of limit values for u over the duration of the entire transition process.

The duration of the optimum process (number of K° steps) as a function of the initial deviation of the image point from the origin of the coordinates at zero value of the initial velocity $(y_0 = 0)$ is defined in Fig. 4, where the dependence of K° upon x_0 is shown for the cases: $\varepsilon = 1/2$, $n = 2$ (thin line), $n = 3, 5, 7, \ldots, \infty$ (thick line), and $\varepsilon = 0$, $n = \infty$ (dotted line). It can be seen from the figure that the pulsed relay system having three control-response levels has an exceptional position among the totality of such systems. A system having three control-response levels provides for a transition process shorter than that in any system with an even number of levels (in the figure, $n = 2$), while a further increase in the number of levels relative to $n = 3$, for a given accuracy, does not result in decreased duration of the transition process. With decreasing ε, the number of levels will increase in conformity with (8), so that the duration of the transition process will slightly increase. In the limit case, this dependence will take the form shown by the dotted line in Fig. 4. The realization of pulsed relay systems of control having two and three control-response levels is discussed in [5]. A pulsed relay system with three levels of control response is the easiest to realize (the system with $n = 2$ being an exception). The following discussion deals mainly with a system of this type.

3. Optimum Control in the Presence of Random Disturbances

In a control analysis of pulsed relay systems in the presence of random disturbances, the latter are readily described by the transfer matrix $\| P_{ij} \|$, which defines the probabilities of the error-induced transitions from the ith to the jth value of the control response. Fortuitious distortions at each step are assumed to be independent.

The control analysis of a pulsed relay system in the presence of random disturbances of the type described by the matrix shown in Fig. 5a leads to results typical for such systems. A comparison analysis of the matrices shown in Fig. 5b, c leads to similar results.

$u_i \backslash u_j$	−1	0	1
−1	$q+\frac{p}{2}$	0	$\frac{p}{2}$
0	$\frac{p}{2}$	q	$\frac{p}{2}$
1	$\frac{p}{2}$	0	$q+\frac{p}{2}$

a

$u_i \backslash u_j$	−1	0	1
−1	q	$\frac{p}{2}$	$\frac{p}{2}$
0	$\frac{p}{2}$	q	$\frac{p}{2}$
1	$\frac{p}{2}$	$\frac{p}{2}$	q

b

$u_i \backslash u_j$	−1	0	1
−1	$q+\frac{p}{2}$	$\frac{p}{2}$	0
0	0	1	0
1	0	$\frac{p}{2}$	$q+\frac{p}{2}$

c

Fig. 5. P_{ij} transfer matrices.

A matrix of the type shown in Fig. 5a is obtained from the following considerations: Let the control response at the input of system (6) be combined with a random disturbance. We denote through q the probability of undistorted passage of a symbol that corresponds to any control-response level. Suppose, further, that the disturbance effect is reduced to an independent distortion of the control signals, so that, with the same degree of probability (equal to $p/2$), the resulting signal can resolve into a limit value of the control response. The matrices of the type shown in Fig. 5b, c are obtained upon similar assumptions.

If in the absence of random disturbances, the optimum trajectory (at the selected algorithm) was uniquely determined in the system phase space, then, in the presence of disturbances, instead of a single trajectory being produced from the initial point, the latter produces a whole "bunch" of such trajectories, each of which can have its own probability defined by the transfer matrix. This bunch can be characterized over each mth step by a certain point in the phase space of the system, the point coordinates being determined by the expressions

$$\begin{aligned} x_m &= [Ex]_m(u_1,\ u_2,\ldots,\ u_m, p), \\ y_m &= [Ey]_m(u_1,\ u_2,\ldots,\ u_m,\ p), \end{aligned} \tag{12}$$

where $[Ex]_m$ and $[Ey]_m$ denote the ensemble average of the coordinate values after m steps.

A sequence of (x_i, y_i) points upon the phase plane forms an "ensemble-average trajectory." The character of this trajectory is dependent on the algorithm of u_i-production, the form of the transfer matrix, and the value of p.

We will determine the optimum control in a pulsed relay system as follows:

At an initial moment of time let the image point of the system be situated in an arbitrary point of the phase plane with the coordinates (x_0, y_0). Together with the control response, at the system output arrives a random disturbance which causes control distortion in correspondence to a certain transfer matrix. It is required to satisfy the equality

$$[Ex]_{K_m} = [Ey]_{K_m} = 0 \tag{13}$$

for a minimum number of K_m steps elapsed. K_m we shall denote as the duration of the optimum process, and the method of u_i-production that provides for such duration we shall term the optimizing algorithm of control.

For the system under discussion having disturbances described by any of the matrices given in Fig. 5 the optimizing algorithm of control evolves down to the application of two switching curves shifted with regard to their position in the absence of disturbances.

Such a formulation of the problem differs fundamentally from the well-known formulation in which the criterion for high-speed optimization is the determination of the minimum of the ensemble average of steps necessary to reach a given point. Let us, therefore, examine this criterion in more detail.

Previously, we have said that in the presence of disturbances the initial point produces a whole bunch of trajectories instead of one. If under the effect of disturbances there can occur a jump in the produced command, then after the first step, the image point, under the effect of the disturbance and control, can make the transition to one of the three phase-space points. The totality of these points we shall denote through D_1. After the second step, the region of possible states can already contain 9 points. Generalizing, the region of possible states after the kth step (let us denote it through D_k) can contain a number of points less than or equal to n^k, where n is the number of the discrete levels of the control response, i.e., the number of commands. Figure 6 shows a schematic of these regions. By optimum control we understand one that provides an "overlapping" of a given point in minimum time.

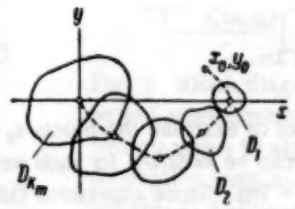

Fig. 6. Schematic of the optimum process on the phase plane.

Speaking generally, the selection of such an algorithm does not necessarily provide for the passage of the trajectories realized after K_m steps through the given point in phase space.

The probability, $P_k(i, j)$, of the passage of the trajectory, at the kth step, through an arbitrary point (i, j) of the D_k region, is defined by the chosen control algorithm and, subsequently, by the set $u_1, u_2, \ldots, u_k$. It can be readily conceived that as $p \to 0$, the distribution $P_{K_m}(i, j)$ takes the form

$$P_{Km}(i, j) = \delta(x)\,\delta(y)$$

and the problem resolves to the regular problem of high-speed optimization in the absence of random disturbances, discussed in the first part of this paper. In this case $K_m = K^*$, while

$$P_{K_m}(i, j) = \begin{cases} 1, & \text{if } x = y = 0, \\ 0 & \text{in all other cases.} \end{cases}$$

Plotting of Optimum Switching Curves

In the plotting of switching curves we shall use the same sequence of operations as was used in the work [4] and [5] in the absence of disturbances.

We shall determine the expression for the maximum of the ensemble average of the value for x and y over m steps at $y_0 = x_0 = 0$. Making use of the non-dependence between control response and disturbance, we may write $[Ey]_m$ in the form of the sum

$$[Ey]_m = [Ey(u_i)]_m + [E\Delta y(p)]_m,$$

$$\max_{u_i} [Ey]_m = \max_{u_i} [Ey(u_i)]_m + \max_{u_i} [E\Delta y(p)]_m, \quad i = 1, 2, \ldots, m.$$

The first term attains the maximum at $u_i = 1$; $i = 1, 2, \ldots, m$; the second term does not depend on u_i, and is equal to pm. Finally, we have

$$\max_{u_i} [Ey]_m = qm. \tag{14}$$

For the ensemble average of the x-coordinate, we find in the same manner as above that $\max_{u_i} [Ex]_m$ is attained at $u_i = 1$, $i = 1, \ldots, m$, and equals

$$\max_{u_i} [Ex]_m = \sum_{i=1}^{m} \max [Ey]_m = \frac{qm^2}{2}.$$

For the maximum of the ensemble average of the quantity x_{2m}, provided $x_0 = y_0 = 0$, $[Ey]_{2m} = 0$, we get the expression

$$\max_{u_i} [Ex]_{2m} = qm^2. \tag{15}$$

The maximum is reached at

$$u_i = \operatorname{sign} [m - i] \quad (i \neq m, \operatorname{sign} 0 = 1), \quad i = 1, 2, \ldots, 2m. \tag{16}$$

It is now possible to determine the quantity k_m for the points on the x axis. Let us examine the points $x_0 = -qm^2$, $y_0 = 0$, where m is an integer. It is readily conceived that the equality (13) can be satisfied for such points over 2m steps when using the control defined by expression (16). For such points $K_m = 2m$. Since expression (15) determines the maximum value of $[Ex]_{2m}$, then at $x_0 = -q(m^2 + l)$, $l > 0$, the duration of the transition process must be larger, i.e., in this case

$$K_m > 2m.$$

At the same time for $x_0 \leq -q(m + 1)^2$, according to (14),

$$K_m \geqslant 2(m + 1).$$

Hence, at $-qm^2 > x_0 \geq -q(m + 1)^2$, we have

$$2m < K_m \leqslant 2(m + 1).$$

We select within these limits the points with an x_0 coordinate equal to

$$-q(m^2 + 1), -q(m^2 + 2), \ldots, -q(m^2 + m), -q(m^2 + m + 1), \ldots, -q(m^2 + 2m).$$

We shall show that by adding one step it is possible to satisfy (13) for the points $x_0 = -q(m^2 + l)$, $0 < l \leq m$. The second equality of (13) is satisfied only in the case if at the additional position r, the control response $u_r = 0$. The state of the additional position (the rth step) should be selected such as to satisfy the condition

$$[Ex]_{2m+1} - [Ex]_{2m} = ql,$$

i.e., an increase in the ensemble average should compensate for the increase in the initial deviation of the image point. From here we find the value of r. Making use of the transfer matrix, and taking into account that $[Ey]_r = qr$, we write

$$q(qr) + \frac{p}{2}(qr + 1) + \frac{p}{2}(qr - 1) = ql \quad (r = l).$$

Consequently, at $r = l$ the condition

$$[Ex]_{2m+1} = 0$$

is also satisfied.

Similarly, for the points $x_0 = -q(m^2 + l)$, $m < l \leqslant 2m$, we get $K_m = 2m + 2$, $r_1 = m + 1$, $r_2 = l$, $u_{r_1} = u_{r_2} = 0$. Finally we have

$$K_m = \begin{cases} 2m+1, & -qm^2 > x \geqslant -qm(m+1), \\ 2m+2, & -qm(m+1) > x \geqslant -q(m+1)^2. \end{cases} \tag{17}$$

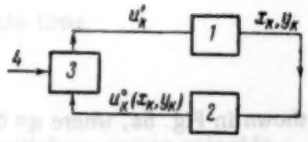

Fig. 7. Block diagram of optimum pulsed relay control system. 1) Control member; 2) algorithm of u_k^* production from x_k, y_k; 3) transfer matrix; 4) disturbance.

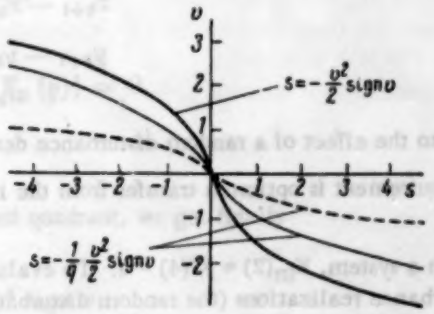

Fig. 8. Optimum switching curves in a second-order relay system in the presence of random disturbances.

The equations (14), (15), and (17) differ from the corresponding equations in the absence of random disturbances in that they have the factor q in front of the values x and y. Therefore, after substituting the variables $\xi = x/q$, $\eta = y/q$, the further analysis can be carried out in the same manner as shown in [4] and [5]. On the phase plane (ξ, η) the equations of the switching curves (10) maintain their validity. In the (x, y) coordinates there occurs a displacement of the switching curves in conformity with the equations

$$\frac{x}{q} = F_1\left(\frac{y}{q}\right), \quad \frac{x}{q} = F_2\left(\frac{y}{q}\right), \tag{18}$$

i.e., in the fourth quadrant the switching curves are defined by the expression

$$x = F_{1q}(y) = -\frac{1}{2q}(y^2 + 4qy + q),$$
$$x = F_{2q}(y) = -\frac{1}{2q}(y^2 + 2qy - q). \tag{19}$$

In the second quadrant of the phase plane the switching curves are displaced in an analogous manner.

The duration of the process at optimum control is determined by the expression

$$K_m(x_0) = K^\circ\left(\frac{x_0}{q}\right). \tag{20}$$

The presence of random effects described by other types of matrices leads to similar results, i.e., to a displacement of the switching curves.

From the fact that after the substitution of the variables ξ and η, at a selected criterion for optimality, the problem under discussion reduces to the well-known problem of optimum control in the absence of disturbances, it follows that the block diagram of a second-order optimum pulsed relay system in the presence of disturbances does not change (Fig. 7), the change affecting merely the algorithm of control.

It is of interest to point out another peculiarity of the optimum pulsed relay system in the presence of random disturbances. In an ordinary system without disturbances, the control law, in principle, becomes apparent as soon as the initial conditions are specified. On the other hand, in a system with disturbances, in determining the final minimum variance at given initial values, it is possible to obtain only the first value of the control response. The following commands can be selected only after the actual state of the system following on the preceding step has

become known, i.e., the magnitude of the subsequent commands depends upon the realization of the disturbance over the first steps. In this way, the optimum control-response sequence in such a system is of a random nature, dependent on the concrete realization of the disturbance.

If a predetermined control-response set, for instance (16), is used as a control device, the equality (13) will be satisfied as before; the variance, $P_{K_m}(i, j)$, however, will increase.

The foregoing can be illustrated by the following example. Let a system described by the equations

$$x_{k+1} - x_k = y_k + \frac{u_k}{2},$$

$$y_{k+1} - y_k = u_k,$$

$$u_k = \{+1, 0, -1\},$$

be subjected to the effect of a random disturbance described by the matrix shown in Fig. 5a, where q = 0.5.

The requirement is optimum transfer from the initial conditions $x_0 = 2$, $y_0 = 0$ to the origin of the phase-space coordinates.

For such a system, $K_m(2) = K^*(4) = 4$. To evaluate the control results, use was made of the averaging of 50 random-disturbance realizations (the random disturbance being given from a table of random numbers). The following results were obtained:

For an optimum closed system, the mean values were equal to

$$\bar{x}_4 = 0.32, \quad \bar{y}_4 = -0.36,$$

while the squared values of $\underline{x}$ and $\underline{y}$ were

$$\bar{x}_4^2 = 7.94, \quad \bar{y}_4^2 = 1.20.$$

Thirteen trajectories terminated in the point (0, 0).

For a control system with a predetermined sequence of control response, irrespective of whether the disturbance was concretely realized or not, in conformity with (16), we have

$$u_k' = u_k^\circ\left(\frac{x_0}{q}\right) = u_k^\circ(4)$$

or

$$u_1 = u_2 = -u_3 = -u_4 = 1.$$

In this case, for the same 50 realizations of random disturbance, we have the following results:

$$\bar{x}_4 = -0.46, \quad \bar{y}_4 = -0.12,$$
$$\bar{x}_4^2 = 23.18, \quad \bar{y}_4^2 = 2.96.$$

One trajectory terminates in the point (0, 0).

From this simple example it can be seen that while the values for $\bar{x}$ and $\bar{y}$ correlate well with the theoretical zero values in both cases, the final variance differs widely. Optimum control provides for smaller variance.

Optimum Relay System

With a decrease in the repetition period ($T \to 0$), the pulsed relay system resolves to an ordinary relay-type system. Let the transfer matrix in such a system retain its previous form, and the distortions be independent as before. In this case, according to the law of large numbers, at given initial conditions, in the system there will be realized a single trajectory which differs from the phase trajectory in a system without disturbances.

The expression for the optimum switching curve can be obtained by means of the limit transfer on the basis of the formulas (19) and (5). In the fourth quadrant of the phase plane we have for F_1

$$\frac{s(nT)}{NT^2} = -\frac{1}{2q}\left[\frac{v^2(nT)}{N^2T^2} - 4q\frac{v(nT)}{NT} - q\right].$$

As $T \to 0$ we get

$$s = -\frac{v^2}{2qN}.$$

At the same time

$$\lim_{T\to 0}[F_1(y) - F_2(y)] = 0,$$

i.e., the switching curves coincide.

Using the equation of the switching curve in the second quadrant, we get finally

$$s = -\frac{1}{2qN}v^2 \operatorname{sign} v.$$

As $q \to 0$, when the disturbance increases in strength, the switching curve approaches the $\underline{s}$ axis to an unlimited proximity (Fig. 8). The duration, T^*, of the optimum transfer process for the initial conditions s_0; $v_0 = 0$, is defined by the expression

$$T^* = 2\sqrt{\frac{|s_0|}{qN}}.$$

In the absence of disturbances ($q = 1$), we arrive at the well-known formulas of optimum control in a second-order relay system; at $N = 1$, we have

$$s = -\tfrac{1}{2}v^2 \operatorname{sign} v, \quad T = 2\sqrt{s_0}.$$

SUMMARY

Optimum control in second-order pulsed relay (number) systems can be realized by plotting switching curves that divide the phase plane into zones in each of which the control response is constant. The number of discrete control-response levels is defined by the accuracy requirements imposed upon the optimum response.

The optimizing algorithm of control in the presence of disturbances consists of the utilization of switching curves shifted with respect to their position in the absence of disturbances. The magnitude of the shift increases with increasing strength of the disturbance.

LITERATURE CITED

1. A. A. Fel'dbaum, Computers in Automatic Systems. Fizmatgiz, 1959.
2. N. N. Krasovskii, Concerning a Certain Problem of Automatic Control. Prikl. Matem. i Mekh. v. 21, No. 5, 1957.
3. Ya. Z. Tsypkin, Theory of Sampled Data Systems. Fizmatgiz, 1959.
4. V. N. Novosel'tsev, Optimum Response in Second-Order Pulsed Relay Systems. Avtomatika i Telemekhanika, V. 21, No. 5, 1960.
5. V. N. Novosel'tsev, Optimum Control in Second-Order Pulsed Relay Systems. Sb. "Avtomaticheskoe regulirovanie i upravlenie." Izd-vo AN SSSR, 1961.

THE DESCRIPTION OF MULTIDIMENSIONAL LINEAR SYSTEMS IN MATRIX FORM

I. Matyáš and Y. Silhánek

(Pardubice, Czechoslovakia)

Translated from Avtomatika i Telemekhanika, Vol. 22, No. 7,
pp. 876-884, July, 1961
Original article submitted November 19, 1960

The paper derives matrix relationships that describe the behavior of multidimensional linear systems. These relationships coincide formally with the generally known formulas for describing unidimensional linear systems. The results are applied in the solution of the problem involving the synthesis of shaping filters for the generation of m stationary random processes.

Statement of the Problem

Figure 1 shows the conditional representation of a unidimensional system. The output quantity u = u(t) of the system is the convolution of the input quantity v = v(t) and the pulse transient response W = W(t):

$$u(t) = \int_{-\infty}^{\infty} v(t-\tau)\, W(\tau)\, d\tau,$$

which shall be expressed in the form

$$u = v * W, \tag{1}$$

where the symbol * denotes convolution.

Then we shall use the definition

$$L\{v\} = V,\ L\{u\} = U,\ L\{W\} = Y, \tag{2}$$

where L is the Laplace transform operator. Evidently Y is the transfer function of the system. After applying the Laplace transform we obtain from (1)

$$U = VY. \tag{3}$$

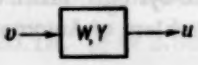

Fig. 1

If the input quantity v = v(t) is a stationary random process, then the output quantity will also be random. We introduce the following statistical characteristics.

Definition 1. The correlation and mutual correlation functions Φ for the stationary random process v and u are determined from the relationships

$$\Phi_{vv} = \varphi = \varphi(\tau) = M\{v(t)\, v(t+\tau)\},$$
$$\Phi_{vu} = \eta = \eta(\tau) = M\{v(t)\, u(t+\tau)\},$$
$$\Phi_{uv} = \bar{\eta} = \eta(\tau) = M\{u(t)\, v(t+\tau)\},$$
$$\Phi_{uu} = \psi = \psi(\tau) = M\{u(t)\, u(t+\tau)\}, \tag{4}$$

where M is the mathematical expectation (averaging operator). It is not difficult to prove the fact that

$$\eta = \varphi * W, \tag{5}$$
$$\psi = \bar{\eta} * W = \bar{W} * \varphi * W, \tag{6}$$

where $\bar{W}(\tau) = W(-\tau)$.

Definition 2. The proper and mutual spectral densities $\mathcal{S}$ of the stationary random processes $\underline{v}$ and $\underline{u}$ will be defined using the relationships

$$\mathcal{S}_{vv} = S = S(j\omega) = F\{\varphi\},$$
$$\mathcal{S}_{vu} = H = H(j\omega) = F\{\eta\},$$
$$\mathcal{S}_{uv} = \bar{H} = \bar{H}(j\omega) = F\{\bar{\eta}\}, \tag{7}$$
$$\mathcal{S}_{uu} = G = G(j\omega) = F\{\psi\},$$

where F is the Fourier transform operator.

Note. Certain authors define the correlation functions by means of the relationship

$$\Phi_{vu}(\tau) = M\{v(t+\tau)\, u(t)\}$$

and the spectral densities

$$u_{vu}(j\omega) = kF\{\Phi_{vu}(\tau)\},$$

where the constant $\underline{k}$ acquires the values $1/2\pi$, $2/\pi$ etc. (cf., for example, [2]). Under these conditions it is evident that all the formulas derived in this paper remain valid.

We shall apply the operator F to Eq. (5) and (6) and obtain

$$H = SY, \tag{8}$$
$$G = \bar{H}Y = \bar{S}\bar{Y}Y = \bar{Y}SY, \tag{9}$$

where $\bar{Y}(s) = \bar{Y}(-s)$, $s = j\omega$.

System with several inputs and outputs (Fig. 2) shall be called multidimensional. Assume now that a multidimensional linear system C is specified whose conditional representation is given in Fig. 2. The input quantities $v_1, v_2, \ldots, v_n$ form the row-vector

$$v = v(t) = [v_1(t), v_2(t), \ldots, v_n(t)] \tag{10}$$

and the column-vector

$$v' = v(t)' = \begin{bmatrix} v_1(t) \\ v_2(t) \\ \ldots \\ v_n(t) \end{bmatrix} \tag{11}$$

(the prime denotes transposition). Analogously, the output quantities $u_1, u_2, \ldots, u_m$ form the vectors

$$u = u(t) = [u_1(t), u_2(t), \ldots, u_m(t)], \tag{12}$$

$$u' = u(t)' = \begin{bmatrix} u_1(t) \\ u_2(t) \\ \ldots \\ u_m(t) \end{bmatrix}. \tag{13}$$

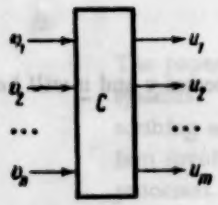

Fig. 2

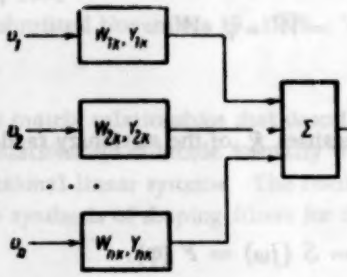

Fig. 3

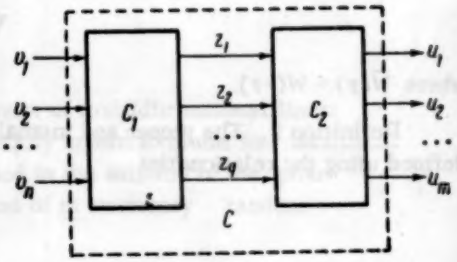

Fig. 4

Figure 3 shows that portion of the system C which corresponds to the kth output $W_{ik} = W_{ik}(t)$ is the pulse transient response, and $Y_{ik} = Y_{ik}(s) = L\{W_{ik}\}$ is the transfer function for the block between the ith input and the kth output of the system C. The characteristics W_{ik} form the pulse transient function matrix

$$W(t) = W = \begin{bmatrix} W_{11}W_{12}\ldots W_{1m} \\ W_{21}W_{22}\ldots W_{2m} \\ \ldots\ldots\ldots\ldots \\ W_{n1}W_{n2}\ldots W_{nm} \end{bmatrix}, \tag{14}$$

and the characteristics Y_{ik} form the transient function matrix for the system

$$Y(s) = Y = \begin{bmatrix} Y_{11}Y_{12}\ldots Y_{1m} \\ Y_{21}Y_{22}\ldots Y_{2m} \\ \ldots\ldots\ldots\ldots \\ Y_{n1}Y_{n2}\ldots Y_{nm} \end{bmatrix}. \tag{15}$$

Making use of the matrix and vector notation cited above, it is possible to represent the multidimensional system C (Fig. 2) in schematic form in just the same way as we do for a unidimensional system (Fig. 1).

Our problem is to derive the matrix relationships that describe the behavior of multidimensional systems and are a generalization of formulas (1), (3), (5), (6), (8) and (9), which describe the behavior of unidimensional systems. The derived results demonstrate that matrix calculus is a very useful means for investigating multidimensional systems.

Matrices When They are Subjected to Operators

Definition 3. Assume that there exist the matrices $A = [A_{ik}]$, $B = [B_{ik}]$ and the operator K which converts the elements A_{ik} of the matrix A into corresponding elements B_{ik} of the matrix B:

$$K\{A_{ik}\} = B_{ik}. \tag{16}$$

The effect of the operator K on the matrix A is defined by the equation

$$K\{A\} = B. \tag{17}$$

Thus, applying the Laplace transform operator L to the matrix W, we obtain

$$L\{W\} = Y. \tag{18}$$

Analogously, we obtain the following results for the Laplace transforms of the vectors of the input and output quantities for the system C:

$$\begin{aligned} U &= L\{u\}, \quad V = L\{v\}, \\ U' &= L\{u'\}, \quad V' = L\{v'\}. \end{aligned} \tag{19}$$

Henceforth we shall apply various forms of operators to the matrices in accordance with Definition 3.

Systems with Definite Input Quantities

Definition 4. The symbol $A * B$, where A and B are matrices whose elements A_{ik}, B_{ik} are functions, denotes the matrix

$$C = A * B, \tag{20}$$

whose elements are determined by the relationships

$$C_{ik} = \sum_j A_{ij} * B_{jk}. \tag{21}$$

It is obvious that the matrix C is a "product" of the matrices A, B, where the "product" of the elements denotes their convolution.

The output quantities $u_1, u_2, \ldots, u_m$ of the system C can be written in the known form

$$u_k = \sum_{i=1}^{n} v_i * W_{ik}, \quad k = 1, 2, \ldots, m. \tag{22}$$

In accordance with Definition 4 the system (22) can be written in matrix form as follows:

$$u = v * W. \tag{23}$$

The Laplace transform of the convolution is the product of the transforms of the functions entering into the convolution. Thus, applying the Laplace transform to Eq. (23), we obtain the known formula

$$U = VY. \tag{24}$$

Formulas (23) and (24), which describe the behavior of multidimensional systems with definite input signals, evidently coincide formally with Eq. (8) and (10), which describe the behavior of unidimensional systems.

The Serial Connection of Multidimensional Systems

Assume that the system B can be represented in the form of a serial connection of two multidimensional systems (Fig. 4); the first of these (C_1) has n inputs and q outputs, and the second (C_2) has q inputs and m outputs. Expressing the vectors z and Z in terms of v and V, respectively, it is possible to write the following relationships on the basis of the formulas cited above:

$$z = v * W_1, \quad u = z * W_2, \; Z = VY_1, \quad U = ZY_2, \tag{25}$$

where W_1, Y_1 are the corresponding matrices for the system C_1; W_2, and Y_2 are the corresponding matrices for the system C_2. Performing a substitution, we obtain

$$u = v * W_1^* W_2, \qquad U = VY_1Y_2. \tag{26}$$

If in general the system C is a serial connection of $\underline{k}$ systems $C_1, C_2, \ldots, C_k$, then we can write

$$u = v * W_1 * W_2 * \ldots \quad *W_k, \quad U = VY_1Y_2 \ldots Y_k. \tag{27}$$

Making use once more of the relationships (23) and (24), we obtain the following expression for the matrices W, Y of the system C:

$$W = W_1 * W_2 * \ldots * W_k, \tag{28}$$

$$Y = Y_1Y_2 \ldots Y_k. \tag{29}$$

The Correlation Functions and the Spectral Densities

The correlation functions of the input random processes form a quadratic matrix of order $\underline{n}$,

$$\varphi = [\varphi_{ik}] = \begin{bmatrix} \varphi_{11} \cdots \varphi_{1n} \\ \cdots\cdots\cdots \\ \varphi_{n1} \cdots \varphi_{nn} \end{bmatrix}, \tag{30}$$

where in accordance with Definition 1

$$\varphi_{ik}(\tau) = M\{v_i(t)\, v_k(t+\tau)\}. \tag{31}$$

Analogously, we denote the matrix for the mutual correlation functions of the input and output quantities by

$$\eta = [\eta_{ik}] = \begin{bmatrix} \eta_{11} \cdots \eta_{1m} \\ \cdots\cdots\cdots \\ \eta_{n1} \cdots \eta_{nm} \end{bmatrix} \tag{32}$$

and the matrix for the correlation functions of the output quantities by

$$\psi = [\psi_{ik}] = \begin{bmatrix} \psi_{11} \cdots \psi_{1m} \\ \cdots\cdots\cdots \\ \psi_{m1} \cdots \psi_{mm} \end{bmatrix}, \tag{33}$$

where

$$\eta_{ik}(\tau) = M\{v_i(t)\, u_k(t+\tau)\}, \tag{34}$$

$$\psi_{ik'}(\tau) = M\{u_i(t)\, u_k(t+\tau)\}. \tag{35}$$

In accordance with Definition 3, these matrices may be written as

$$\varphi(\tau) = M\{v(t)'\, v(t+\tau)\}, \tag{36}$$

$$\eta(\tau) = M\{v(t)'\, u(t+\tau)\}, \tag{37}$$

$$\psi(\tau) = M\{u(t)'\, u(t+\tau)\}. \tag{38}$$

For the matrices of the spectral densities S, H, G we obtain

$$S = [S_{ik}] = [F\{\varphi_{ik}\}] = F\{\varphi\} = F\{M\{v(t)'\, v(t+\tau)\}\}, \tag{39}$$

$$H = [H_{ik}] = [F\{\eta_{ik}\}] = F\{\eta\} = F\{M\{v(t)'\, u(t+\tau)\}\}, \tag{40}$$

$$G = [G_{ik}] = [F\{\psi_{ik}\}] = F\{\psi\} = F\{M\{u(t)'\, u(t+\tau)\}\}. \tag{41}$$

Systems with Random Input Signals

In this section we derive matrix expressions which describe the relationship between the characteristics of multidimensional systems (the matrices W, Y) and between the statistical characteristics of random quantities at the inputs and outputs (the matrices φ, η, ψ; S, H, G).

a) The matrices for the correlation functions.

Substituting into (37), we obtain

$$\eta(\tau) = M\left\{v(t)' \int_{-\infty}^{\infty} (v(t+\tau-x)\, W(x))\, dx\right\} = \int_{-\infty}^{\infty} \varphi(\tau - x)\, W(x)\, dx \tag{42}$$

from (23) and (36).

Therefore,

$$\eta = \varphi * W. \tag{43}$$

From formula (38) we find

$$\psi(\tau) = \int_{-\infty}^{\infty} \bar{\eta}'(\tau - x)\, W(x)\, dx \tag{44}$$

in similar fashion.

The matrix $\bar{\eta}'$ can be written as

$$\bar{\eta}' = \bar{W}' * \bar{\varphi}' = \bar{W}' * \varphi. \tag{45}$$

Substituting in to (44), we finally obtain

$$\psi = \bar{W}' * \varphi * W. \tag{46}$$

Relationships (43) and (46) describe the relationship between the matrices for the correlation functions and the matrix for the pulse transient function of multidimensional linear systems. For the case n = 1, m = 1 these relationships evidently coincide with the formulas for unidimensional systems.

b) The matrices for the spectral densities.

We shall now apply the operator F to the matrix relationships (43) and (46). For the matrix of the mutual spectral densities we obtain

$$F\{\eta\} = F\{\varphi * W\} = F\{\varphi\}\, F\{W\}. \tag{47}$$

From this we have

$$H = SY. \tag{48}$$

In similar fashion we can write

$$F\{\psi\} = F\{\overline{W}' * \varphi * W\} = F\{\overline{W}'\}\, F\{\varphi\}\, F\{W\}. \tag{49}$$

for the matrix G.

Therefore the matrix G for the spectral densities of the output quantities is determined by the relationship

$$G = \overline{Y}'SY. \tag{50}$$

Formulas (48) and (50) describe the relationship between the matrix of the transfer functions Y of multidimensional systems and the matrices for the spectral densities of the input and output random quantities. For the case n = 1, m = 1 these matrix relationships evidently coincide with the generally known formulas that describe unidimensional systems.

By comparing the matrices in the left and right sides of (48) and (50), we obtain known relationships for the spectral densities H_{ik}, G_{ik} (cf., for example, [2]). Thus these simple formulas are actually complex systems of equations.

Shaping Filters

In investigating dynamic systems whose input quantities are random functions we often use simulators. In that case the simulators must be used to generate the required family of random signals with the specified statistical properties.

For stationary random signals this problem can be reduced to the following: It is required to determine the transfer function of a linear system with m inputs for which the desired random quantities appear at m outputs when m uncorrelated white noise signals are applied to its input. In that case it is obvious that the matrix S for the spectral densities of the input quantities is a unit matrix.

Thus we obtain

$$\overline{Y}'Y = G, \tag{51}$$

from (50), where G is the matrix for the spectral densities of the desired processes and Y is the matrix for the transfer functions of the shaping filters.

Thus the problem of generating m stationary random processes reduces to solving the matrix equation (51) for Y. It is not difficult to prove that Eq. (51) has an infinite set of solutions rather than one solution.

The problem of designing the shaping filters for m stationary random processes is treated in [3], where formulas are derived that represent a particular solution of (51).

In the Appendix to this paper we describe certain properties of the general solution for Eq. (51).

The basic property of the general solution of (51) consists of the following: If Y_1 is a particular solution and Y is any solution of (51), then there exist quadratic matrices N, M of order m which satisfy the conditions

$$\overline{N}'N = E, \qquad \overline{M}'GM = G \tag{52}$$

(E denotes the unit matrix), which are such that

$$Y = NY_1 = Y_1M. \tag{53}$$

Thus the matrices N and M are matrices for transfer functions. In accordance with (52), N is the matrix for the transfer functions which reconverts m uncorrelated white noise signals back into m uncorrelated white noise signals, and M is the matrix of transfer functions which converts the input random processes with the spectral density matrix G into output processes with the same spectral density matrix G.

Making use of formula (29), we find from (53) that the system of shaping filters can always be represented in the form of a serial connection of the systems N and Y_1 or Y_1 and M in that order. This property of the general solution for (51) reflects the physical meaning of formula (53). It is not difficult to prove that the matrix NY_1M is also a solution of (51); thus it is a matrix of the transfer functions for the shaping filters.

For n = 2 we shall cite one form of the matrix N which does not coincide with the unit matrix. Assume h_1, h_2, h_3 are any functions that satisfy the conditions

$$\overline{h}_i h_i = 1, \qquad i = 1,2,3.$$

In other words, assume h_i are the transfer functions for phase-shifting filters. Then the quadratic matrix

$$N = \frac{1}{\sqrt{2}} \begin{bmatrix} h_1 & h_2 \\ -\frac{\overline{h}_2}{\overline{h}_3} h_1 & h_3 \end{bmatrix} \tag{54}$$

evidently satisfies the first condition of (52).

Example. The spectral density matrix G for the desired processes is specified in the form

$$G = \begin{bmatrix} \frac{2}{4 - s^2} & \frac{1}{(1+s)(2-s)} \\ \frac{1}{(1-s)(2+s)} & \frac{1}{1-s^2} \end{bmatrix}.$$

Using the method described in [3], we determine the matrix for the transfer functions of the shaping filters

$$Y_1 = \frac{1}{\sqrt{2}} \begin{bmatrix} \frac{1}{2+s} & \frac{1}{1+s} \\ 0 & \frac{1}{1+s} \end{bmatrix}.$$

Using the matrix

$$N = \frac{1}{\sqrt{2}} \begin{bmatrix} 1 & 1 \\ 1 & -1 \end{bmatrix},$$

which is a particular case of (54), we find

$$Y_2 = NY_1 = \begin{bmatrix} \frac{1}{2+s} & \frac{1}{1+s} \\ \frac{1}{2+s} & 0 \end{bmatrix}$$

from (53).

It is obvious that Y_2 also satisfies Eq. (51), and therefore it is a matrix of the transfer functions for the shaping filters which generate the desired random processes. In certain cases we can use formula (53) to simplify the matrix of the transfer functions for the shaping filters.

In practice the problem of generating random processes with a singular spectral density matrix G is also important. The problem of solving Eq. (51) with a singular matrix G is analyzed in [4].

If we use r to denote the rank of the matrix G (r < m), then the solution of (51) can be sought in the form of a matrix Y with the dimensions s, m, where $s \geq r$. Therefore this solution should always be sought in the form of a matrix Y with the dimensions r, m.

After ordering the quantities u_i and correspondingly ordering the matrix G (cf. [4]), it is possible to seek the particular solution of (51) by the method described in [3]. The properties of the general solution in that case are completely analogous to the properties cited above for the case of a nonsingular matrix.

SUMMARY

The input and output quantities for multidimensional systems can be represented in the form of vectors $\underline{v}$ and $\underline{u}$. The pulse transient functions W_{ik} and the transfer functions Y_{ik} form the matrices W and Y. The behavior of multidimensional linear systems in matrix form is determined from formulas (23), (24). Equations (28), (29) express the law for serial connection of multidimensional systems.

If the input quantities $\underline{v}$ for the system are random, then the correlation functions for the input and output quantities form the matrices φ, η, ψ, and the spectral densities form the matrices S, H, G. In this paper we derive the matrix expressions which describe the interrelationship between these matrices and a) the matrix for the pulse transient functions of the system; b) the matrix for the transfer functions of the system. Thus, for example, the matrix G for the spectral densities of the output quantities is given by the relationship

$$G = \overline{Y}'SY .$$

The derived matrix relationships make it possible to describe the behavior of multidimensional linear systems using a very simple form which is the generalization of a description of unidimensional systems. Therefore matrix calculus is a very useful means for investigating multidimensional linear systems.

The derived formulas are used for solving problems in designing shaping filters for $\underline{m}$ stationary random processes. This problem can be reduced to solving the matrix equation (51). The properties of the general solution of this equation are described in the Appendix. It is demonstrated that the system of shaping filters can always be represented as a serial connection of several systems.

APPENDIX

The Solution of the Matrix Equation $\overline{Y}'Y = G$

The problem of determining the transfer functions of the shaping filters reduces to solving Eq. (51) relative to the matrix Y; here G is a Hermitian matrix (the matrix for the spectral densities of the desired processes).

The solution of this equation can be sought in the form of matrices with the dimensions $\underline{s}$, $\underline{m}$, where $s \geq m$. Here we shall limit ourselves to the case of quadratic matrices Y ($s = m$).

It is not difficult to prove that this problem does not have one but an infinite set of solutions among quadratic matrices of order $\underline{m}$. One particular solution is cited in [3] where the process of computing it is demonstrated.

The family of matrices Y [which are solutions of Eq. (51)] and the basic properties of these matrices are described by the following theorem.

Theorem. The quadratic matrix Y is a solution of the equation

$$\overline{Y}'Y = G, \tag{55}$$

where G is a nonsingular Hermitian matrix only for the case where it can be written as

$$Y = NY_1M, \tag{56}$$

where Y_1 is any particular solution of (55) and the matrices N, M satisfy the equations

$$\overline{N}'N = E, \quad \overline{M}'GM = G \tag{57}$$

(E denotes a unit matrix).

The proof of this theorem is simplified by Lemmas 1, 2.

Lemma 1. If the matrix Y_1 is a solution of Eq. (55), then the matrix $Y = NY_1M$, where N, M are arbitrary matrices that satisfy Eq. (57), is also a solution of (55).

Proof. From the statement of the lemma it follows that

$$\bar{Y}'_1 Y_1 = G.$$

By transposing the matrix Y we obtain $\bar{Y}' = \bar{M}'\bar{Y}'_1\bar{N}'$, and therefore $\bar{Y}'Y = \bar{M}'\bar{Y}'_1N'NY_1M$. The use of conditions (57) converts this equation to the form (55), which proves the lemma.

Lemma 2. Assume Y_1 is a particular solution and Y is an arbitrary solution of Eq. (55). Then there exist the matrices N, M which satisfy (57) and are such that

$$Y = NY_1, \tag{58}$$

$$Y = Y_1M. \tag{59}$$

Proof. From the statement of the lemma it follows that $\bar{Y}_1^{-1}Y_1 = \bar{Y}'Y = G$. Since G is a nonsingular matrix, it follows that Y_1 and Y are also nonsingular. Therefore $\bar{Y} = (\bar{Y}')^{-1}Y'_1Y_1$. The matrix $N = (\bar{Y}')^{-1}Y'_1$ evidently satisfies the first condition in (57). Assuming $M = Y_1^{-1}Y$, we immediately obtain (59). It is not difficult to prove that M satisfies (57), and thus Lemma 2 has been proved.

By combining the statements of both lemmas we obtain the proof of the theorem cited above.

LITERATURE CITED

1. F. R. Gantmakher, Theory of Matrices [in Russian] (State Technical Press, Moscow, 1954).
2. V. S. Pugachev, The Theory of Random Functions and its Applications to Problems in Automatic Control [in Russian] (State Technical Press, 1957).
3. I. Matyáš and Ya. Silhánek, "A generator which produces random process, with a specified spectral density matrix," Avtomatika i Telemekhanika, 21, 1 (1960).
4. Matyáš, J. Tvarovací filtry pro generování skupiny stacionárních náhodnych procesu s předepsanými statistickymi charakteristikami. Aplicace matematiky, No. 4 (1961).

THE ANALYSIS OF PERIODIC STATES DUE TO LEVEL QUANTIZATION OF SIGNAL IN AUTOMATIC DIGITAL SYSTEMS

Yu. M. Korshunov

(Ryazan')

Translated from Avtomatika i Telemekhanika, Vol. 22, No. 7,
pp. 885-895, July, 1961
Original article submitted December 19, 1960

A method is presented of determining the amplitude and the frequency of periodic states due to level quantization of signals in ADS, the method being based on the describing function approach. Graphical evaluations are shown. The accuracy of the method is estimated by comparing it with numerical solutions of simultaneous difference equations.

The level quantization of the signal in a closed-loop automatic system can lead to oscillations whose magnitude may considerably exceed the quantization step magnitude. In [1] an easy method was given of determining the highest possible error value caused by level quantization and conditions were found under which periodic states are feasible in the system. In this paper a method is presented leading to the determination of such periodic states by using the describing function approach [2].

1. Equivalent Block Diagram for Analyzing Periodic States in an ADS

One can assume when investigating periodic states in an ADS that only the output quantitity is level quantized, as the output quantity is taken as zero. In order to obtain more general results it is useful to take the magnitude of one quantization step as the unity of measurement of the signal level, and also the time interval T_0 of quantization as the unit of time measurement, i.e., to introduce the nondimensional time $\tau = t/T_0$. Under these assumptions one is able to study the periodic states due to level quantization via an equivalent relay-pulse system shown in Fig. 1. There the pulse element PE produces instantaneous signal value $\varepsilon(\tau)$ at discrete time moments $\tau = n$, that is, it transforms the signal $\varepsilon(\tau)$ into a lattice-type function $\varepsilon[n]$. The clamper Cl complements the holding of the measured level in the time interval between consecutive measurements. The release of discrete levels from the signals ε_c is effected by a relay element RE with a multistep characteristic shown in Fig. 2a.

It is convenient for our purpose to assume that the level quantization is implemented by single-step relay elements. A characteristic of such an element with dead zone Δ_k is shown in Fig. 2b. By putting $\Delta_k = k - 0.5 (k = 1, 2, \ldots)$, we can represent the output quantity of a multistep relay element in the form

$$G = \sum_{k=1}^{\infty} G_k, \tag{1}$$

which is equivalent to parallel single-step relays with dead zones $\Delta_1, \Delta_2, \ldots$, respectively.

It is a particular feature of the relay-pulse systems that the switching (operation) can only take place in the relay at integral values of τ. Consequently the period T of a periodic state must be an integer. The output of each relay is in the form of a rectangular train pulse of unit height, the pulses being separated by blanks. The duration of a pulse, as well as of a blank, will again be a whole number.

It will be assumed in the sequel that the continuous part CP of the system contains at least one integrator. Moreover, in the case of a periodic state the signal $G(\tau)$ cannot have a constant component. We shall limit ourselves to the symmetric state of the operation of a single-step relay in which the width of the positive and the negative pulse is the same for each relay and is subsequently denoted by δ. The set of values of δ for all single-step relays, together with their period T, characterizes fully the form of the periodic state.

2. Describing Function Approach in Relay-Pulse Systems

The describing function approach can be used to investigate periodic states in nonlinear systems which occur in the absence of the input signal:

$$x(\tau) = 0, \qquad \varepsilon(\tau) = -v(\tau). \tag{2}$$

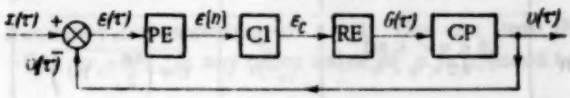

Fig. 1

In [3] an account was given of the application of this method to an approximation of a general periodic state in systems with a nonlinear pulse element.

Let a signal

$$\varepsilon(\tau) = |\varepsilon| \sin(\Omega\tau + \Phi), \tag{3}$$

be sent to the input of a pulse element, where $\Omega = 2\pi/T$ is the angular frequency. The complex amplitude of the signal is

$$\dot{E} = |\varepsilon| e^{j\varphi}. \tag{4}$$

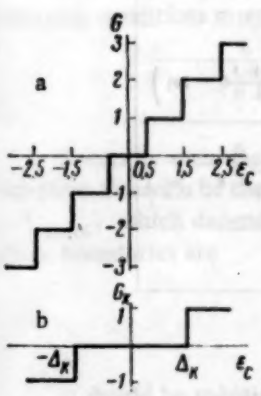

Fig. 2

At the output of the relay element a non-sinusoidal but periodic signal $G(\tau)$ is obtained whose fundamental harmonic, denoted in the sequel by $\Gamma(\tau)$, is

$$\Gamma(\tau) = \gamma \sin(\Omega\tau - \alpha) = A \sin \Omega\tau + B \cos \Omega\tau. \tag{5}$$

The complex amplitude of the fundamental harmonic is

$$\dot{\Gamma} = \gamma e^{-j\alpha} = A + jB. \tag{6}$$

In view of the relation (1), the quantity $\dot{\Gamma}$ can be represented in the form

$$\dot{\Gamma} = \sum_{k=1}^{\infty} \dot{\Gamma}_k, \tag{7}$$

where

$$\dot{\Gamma}_k = \gamma_k e^{-j\alpha_k} = A_k + jB_k \tag{8}$$

is the complex amplitude of the fundamental harmonic of the $G_k(\tau)$ signal.

The nonlinear element is characterized by an equivalent complex gain N; we define it as a ratio of the complex amplitudes of the fundamental harmonics of the input and the output signals respectively, the signals coming from and to the nonlinear part only:

$$N = \frac{\dot{\Gamma}}{\dot{E}} = \frac{\gamma}{|\varepsilon|} e^{-j(\varphi+\alpha)}. \tag{9}$$

TABLE 1. Limiting Values of $|\varepsilon|$ and the Values of $\dot{\Gamma}$ for Relays with Single-Step Characteristic

T	δ	φ	$\dot{\Gamma}$	$\lvert\varepsilon\rvert_{\min}$	$\lvert\varepsilon\rvert_{\max}$
$4Q$ $(Q=1,2,\ldots)$	0	$-\theta/2 < \varphi < +\theta/2$	0	0	$\dfrac{\Delta}{\cos\lvert\varphi\rvert}$
	even	$0 < \varphi < +\theta/2$ $-\theta/2 < \varphi < 0$	γ $\gamma e^{-j\theta}$	$\dfrac{\Delta}{\cos\left(\frac{\delta\theta}{2} - \lvert\varphi\rvert\right)}$	$\dfrac{\Delta}{\cos\left(\frac{\delta\theta}{2} + \lvert\varphi\rvert\right)}$
	odd	$-\theta/2 < \varphi < +\theta/2$	$\gamma e^{-j\theta/2}$	$\dfrac{\Delta}{\cos\left(\frac{\delta-1}{2}\theta + \lvert\varphi\rvert\right)}$	$\dfrac{\Delta}{\cos\left(\frac{\delta+1}{2}\theta - \lvert\varphi\rvert\right)}$
	$T/2$	$0 < \varphi < +\theta/2$ $-\theta/2 < \varphi < 0$	γ $\gamma e^{-j\theta}$	$\dfrac{\Delta}{\sin\lvert\varphi\rvert}$	∞
$4Q+2$ $(Q=0,1,\ldots)$	0	$-\theta/2 < \varphi < +\theta/2$	0	0	$\dfrac{\Delta}{\cos\left(\frac{\theta}{2} - \lvert\varphi\rvert\right)}$
	even	$-\theta/2 < \varphi < +\theta/2$	$\gamma e^{-j\theta/2}$	$\dfrac{\Delta}{\cos\left(\frac{\delta-1}{2}\theta + \lvert\varphi\rvert\right)}$	$\dfrac{\Delta}{\cos\left(\frac{\delta+1}{2}\theta - \lvert\varphi\rvert\right)}$
	odd	$0 < \varphi < +\theta/2$ $-\theta/2 < \varphi < 0$	γ $\gamma e^{-j\theta}$	$\dfrac{\Delta}{\cos\left(\frac{\delta\theta}{2} - \lvert\varphi\rvert\right)}$	$\dfrac{\Delta}{\cos\left(\frac{\delta\theta}{2} + \lvert\varphi\rvert\right)}$
	$T/2$	$0 < \varphi < +\theta/2$ $-\theta/2 < \varphi < 0$	γ $\gamma e^{-j\theta}$	$\dfrac{\Delta}{\sin\lvert\varphi\rvert}$	∞
odd	arbitrary	$-\theta/4 < \varphi < +\theta/4$	$\gamma e^{-j\theta/2}$	$\dfrac{\Delta}{\cos\left(\frac{2\delta-1}{4}\theta + \lvert\varphi\rvert\right)}$	$\dfrac{\Delta}{\cos\left(\frac{2\delta+1}{4}\theta - \lvert\varphi\rvert\right)}$
		$\theta/4 < \varphi < +\theta/2$ $-\theta/2 < \varphi < -\theta/4$	γ $\gamma e^{-j\theta}$	$\dfrac{\Delta}{\cos\left(\frac{2\delta+1}{4}\theta - \lvert\varphi\rvert\right)}$	$\dfrac{\Delta}{\cos\left(\frac{2\delta-1}{4}\theta + \lvert\varphi\rvert\right)}$

Remark. $\gamma = \frac{4}{\pi}\sin\frac{\delta\theta}{2}$ for even T, $\gamma = \frac{4}{\pi}\cos\frac{\theta}{4}\sin\frac{\delta\theta}{2}$ for odd T.

In computations it is of greater practical value to use the reciprocal of this quantity:

$$Z = -\frac{1}{N} = -\frac{\dot{E}}{\dot{\Gamma}} = -\frac{|\varepsilon|}{\gamma}e^{j(\varphi+\alpha)}. \tag{10}$$

The transfer function of the system's continuous part is denoted by W(q), where the appearance of the operator $q = pT_0$ is due to the introduced nondimensional time τ. When the sinusoidal signal $\Gamma(\tau)$ is the input to the continuous part, the output is also sinusoidal, say $v(\tau)$, and its complex amplitude is

$$\dot{V} = \dot{\Gamma}W(j\Omega). \tag{11}$$

The condition governing the existence of a periodic state in the case of (2) can, in view of (10) and (11), be written in the complex form as

$$W(j\Omega) = Z. \tag{12}$$

The easiest way to obtain the points where the condition (12) is satisfied is to find the common points in the complex plane of the characteristics $W(j\Omega)$ and of Z.

We examine the form of the Z characteristic in the case of a single-step relay with dead zone Δ. The input signal (3) at the moments of the pulse element operation is

$$\varepsilon[n] = |\varepsilon| \sin(n\theta + \varphi), \tag{13}$$

where $\theta = 2\pi/T$ is the angular frequency corresponding to $\tau = 1$. One can limit the investigation to the initial phase lying within the band from $-\theta/2$ to $+\theta/2$, as any other value of φ is reduced to these values by an appropriate choice of the initial ordinate.

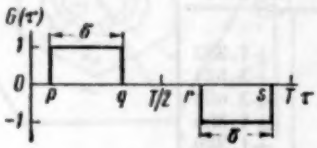

Fig. 3

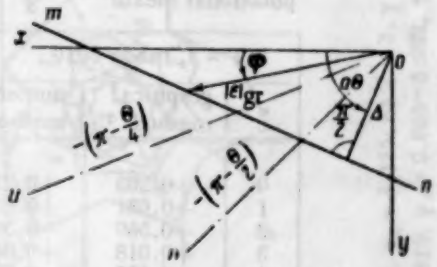

Fig. 4. Construction of the boundary line of the $-\dot{E}$ domain.

The relay output signal is shown in Fig. 3. In order that the positive and negative pulses be of length δ, the following conditions must be satisfied:

$$\varepsilon[p] > \Delta, \quad \varepsilon[q] < \Delta, \quad \varepsilon[r] < -\Delta, \quad \varepsilon[s] > -\Delta. \tag{14}$$

Generally speaking, the conditions (14) will be satisfied not only for one value of $|\varepsilon|$ and φ, but for some complete intervals of these values. To each oscillation mode $G_k(\tau)$ correspond two limiting values, $|\varepsilon|_{\min}$ and $|\varepsilon|_{\max}$, which depend on Δ and φ; they determine in the complex plane the admissible domain of values of $\dot{E}$ whose boundaries are

$$\dot{E}_{\min} = |\varepsilon|_{\min} e^{j\varphi} \qquad \dot{E}_{\max} = |\varepsilon|_{\max} e^{j\varphi}. \tag{15}$$

It should be mentioned that to facilitate the computation of the Z characteristic one should form the domain of $-\dot{E}$ instead of the domain of the admissible values of $\dot{E}$. The values of $|\varepsilon|_{\min}$ and of $|\varepsilon|_{\max}$ for a range of values of T and δ were computed in [4] in the case of a single-step relay characteristic. A summary of these results is given in Table 1.

The output signal $G(\tau)$ of a relay with a multistep characteristic is determined by the entire set of values δ_k, each corresponding to a separate step of the characteristic; it is known how the domain of the admissible values of $-\dot{E}$ should be formed for each step. The common part in the complex plane of all the domains thus obtained gives the domain of admissible values of $-\dot{E}$, which determines the mode of oscillations of $G(\tau)$. The domain of admissible values of Z obtained with the aid of the formula (10) will correlate with the latter domain.

The domains of admissible values of Z are needed for all possible combinations of δ and at the same time for different values of T. It has proved advisable to combine groups of domains into one general domain in order to reduce the number of graphs. We shall construct the general domains of Z corresponding to the operation of one, two, three or more steps of a multistep characteristic. These will be called the first, second, third, etc. generalized domains. Thus when T = 6, there are six possible combinations of δ corresponding to the operation of the first three steps of the characteristic (when reading from left to right the digits show the number of steps when δ equals three,

TABLE 2. Modes of Periodic States

T	Oscillation mode of $G(\tau)$	γ	α	$\lvert\varepsilon\rvert$	φ
7	0010	0.970	0°	0.704	+24°04′
8	1120	4.185	6°10′	3.875	+20°50′

TABLE 3. The Values of $\varepsilon[n]$ Obtained by Graphical and Computational Means

T = 7, mode 0010			T = 8, mode 1120		
n	graphical method	numerical method	n	graphical method	numerical method
0	+0.293	+0.275	0	+1.381	+1.353
1	+0.681	+0.637	1	+3.543	+3.524
2	+0.560	+0.598	2	+3.630	+3.608
3	+0.018	+0.045	3	+1.589	+1.555
4	−0.537	−0.572	4	−1.381	−1.369
5	−0.690	−0.704	5	−3.543	−3.539
6	−0.323	−0.265	6	−3.630	−3.623
			7	−1.589	−1.570

two or one respectively): 030, 021, 120, 111, 201, 102 (see Appendix 1). Six Z domains will correspond to these combinations. When T = 6 the third generalized Z domain is obtained as the external boundary of these domains.

It should be noted that the generalized Z domains, corresponding to the operation of a large number of steps of the characteristic, are mainly to be found within the domains corresponding to the operation of a smaller number of steps. As the occurrence of periodic states with a large amplitude usually proves inadmissible, one is able in practice to limit the investigation to the construction of a small number of generalized Z domains, say from one to five. The fifth generalized domain will then correspond to the operation of five or more steps on the characteristic.

3. Construction of Domains for $-\dot{E}$ and Z.

As can be seen from Table 1, the boundaries of the domains are formed by a straight lines whose equation can be written in the form

$$-\dot{E}_{gr} = -|\varepsilon|_{gr} e^{j\varphi} = -\frac{\Delta}{\cos(a\theta + \varphi)} e^{j\varphi}. \tag{16}$$

The straight line mn is shown in Fig. 4. In order to construct such a boundary straight line it is enough to find the points where it intersects the ox and oy axes, or the ou and ov axes, the latter forming an angle with ox of $\left(\pi - \frac{\theta}{4}\right)$ and $\left(\pi - \frac{\theta}{2}\right)$ respectively. The axis of ox is a symmetry axis for the $-\dot{E}$ domain, because the expressions for $|\varepsilon|_{min}$ and $|\varepsilon|_{max}$ remain the same when replacing φ by $-\varphi$.

One starts by constructing first the boundary lines of the $-\dot{E}$ domain for a single-step characteristic with dead zone Δ. Then by putting $\Delta = \Delta_k = k - 0.5$, and by giving k the values 1, 2, . . . , we obtain the boundary lines for the $-\dot{E}$ domain with a multistep characteristic. The set of δ values for any of these domains is determined by finding all single-step characteristic domains to which the considered domain belongs.

When T is even, one can compute for each set of δ values the quantities γ' and γ'', which are the sums of γ_k values corresponding to even or odd δ_k respectively. When $T = 4Q$ and $0 < \Phi < \theta/2$, we obtain from Table 1

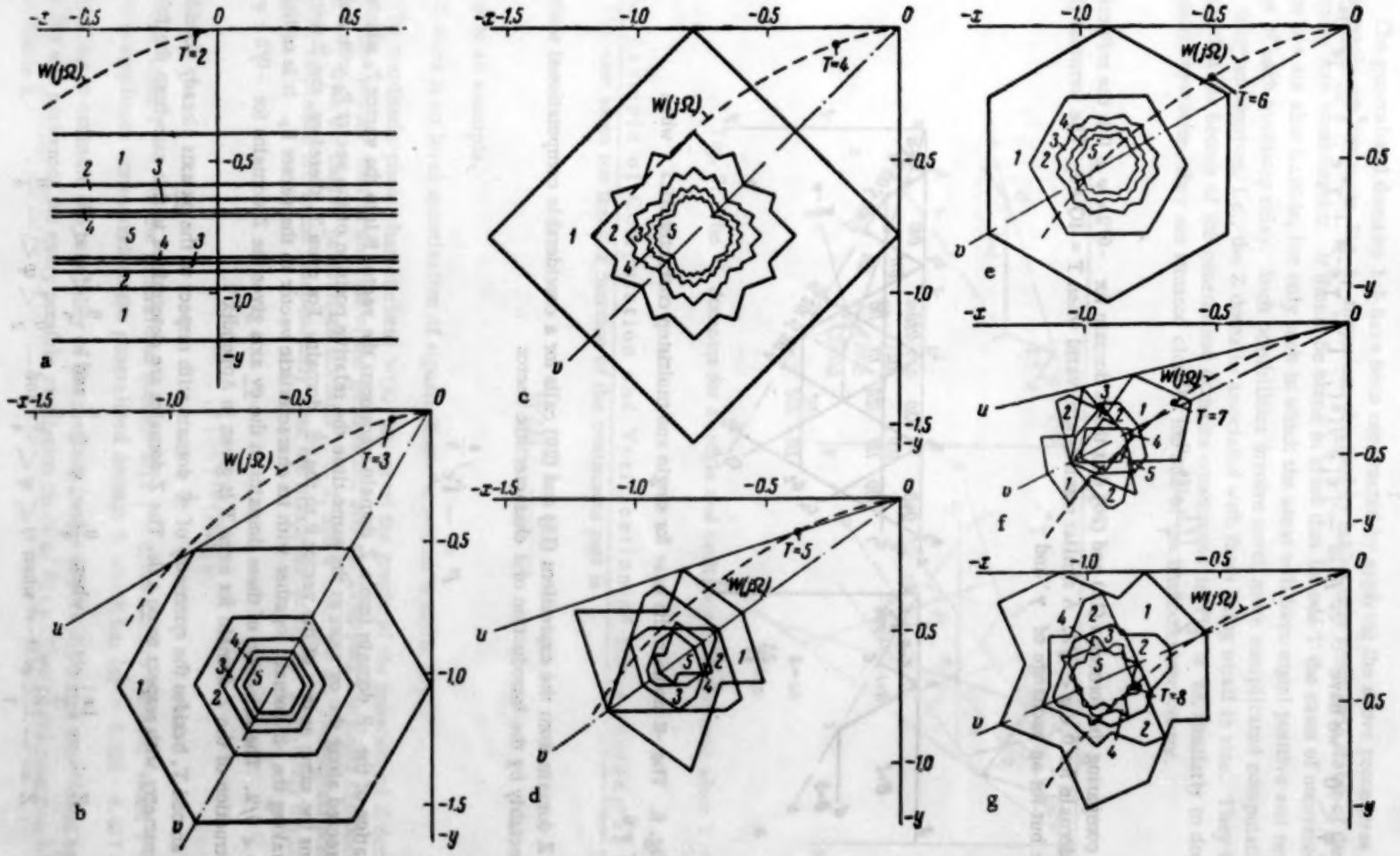

Fig. 5. Graphs of generalized Z domains: a) T = 2, $\gamma_1 = 1.273$, $\gamma_2 = 2.548$, $\gamma_3 = 3.820$, $\gamma_4 = 5.093$, $\gamma_5 = 6.370$; b) T = 3, $\gamma_1 = 0.955$, $\gamma_2 = 1.210$, $\gamma_3 = 2.865$, $\gamma_4 = 3.820$, $\gamma_5 = 4.775$; c) T = 4, $\gamma_1 = 0.900-1.273$, $\gamma_2 = 1.800-2.546$, $\gamma_3 = 2.700-3.819$, $\gamma_4 = 3.600-5.092$, $\gamma_5 = 4.500-6.365$; d) T = 5, $\gamma_1 = 0.712-1.152$, $\gamma_2 = 1.864-2.304$, $\gamma_3 = 3.041$, $\gamma_4 = 3.778-4.193$, $\gamma_5 = 4.930$; e) T = 6, $\gamma_1 = 0.637-1.273$, $\gamma_2 = 1.685-2.295$, $\gamma_3 = 2.545-3.370$, $\gamma_4 = 3.545-4.460$, $\gamma_5 = 4.460-5.525$; f) T = 7, $\gamma_1 = 0.539-1.210$, $\gamma_2 = 1.749-2.180$, $\gamma_3 = 2.719-3.390$, $\gamma_4 = 3.930-4.360$, $\gamma_5 = 4.900$; g) T = 8, $\gamma_1 = 0.487-1.273$, $\gamma_2 = 1.663-2.352$, $\gamma_3 = 2.520-3.290$, $\gamma_4 = 3.326-4.437$, $\gamma_5 = 4.502-5.450$.

$$\dot{\Gamma} = \gamma' + \gamma'' e^{-j\frac{\theta}{2}} = \gamma e^{-j\alpha}. \tag{17}$$

In this case the expression for Z assumes the form

$$Z = -\frac{|\varepsilon|}{\gamma} e^{j(\varphi+\alpha)}. \tag{18}$$

But when $-\frac{\theta}{2} < \varphi < 0$ we have $-\dot{E} = -|\varepsilon| e^{-j|\varphi|}$, $\dot{\Gamma} = \gamma' e^{-j\theta} + \gamma'' e^{-j\frac{\theta}{2}} = \gamma e^{-j(\theta-\alpha)}$, (19)

and therefore

$$Z = -\frac{|\varepsilon|}{\gamma} e^{j[\theta-(|\varphi|+\alpha)]}. \tag{20}$$

We note when comparing the formulas (18) and (20) that the Z domain for $-\theta/2 < \varphi < 0$ is the reflection in the ov axis of the Z domain for $0 < \varphi < \theta/2$. A similar result is also valid when T = 4Q + 2. The formulas (17)-(20) remain the same but for an exchange of γ' and γ''.

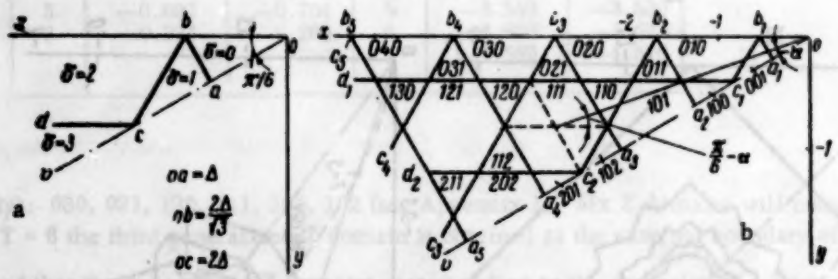

Fig. 6. The $-\dot{E}$ domain the case for single and multistep characteristics when T = 6.

To obtain the Z domain from the expressions (18) and (20) calls for a considerable computational work. It can be reduced appreciably by the introduction of a characteristic vector

$$P = -\dot{\Gamma} e^{j\frac{\theta}{2}} \tag{21}$$

for each $-\dot{E}$ domain.

The transformation of the $-\dot{E}$ domain into a Z domain transforms the vector P into the vector P_0 which has unit length and is directed along the ov axis; at the same time the relative position of the vector P_0 with respect to the Z domain remains the same as that of the vector P to the $-\dot{E}$ domain. For even T, therefore, the Z domain is obtained simply by taking the $-\dot{E}$ domain together with its characteristic vector to the vector P_0. It is sufficient to perform it for $0 < \varphi < \theta/2$. The refection of these domains in the ov axis gives the Z domains for $-\theta/2 < \varphi < 0$. An example of the construction of the Z domain for even T is given in Appendix 1.

In the case of an odd T, besides the symmetry of $-\dot{E}$ domain with respect to the ox axis already considered, there exists also a symmetry with respect to ou axis. The Z domains are determined in this case from the following expressions:

$$Z = -\frac{|\varepsilon|}{\gamma} e^{j\varphi} \quad \text{when } \frac{\theta}{4} < \varphi < \frac{\theta}{2} \text{ and } -\frac{\theta}{4} < \varphi < 0, \tag{22}$$

$$Z = -\frac{|\varepsilon|}{\gamma} e^{j(\theta-\varphi)} \text{ when } 0 < \varphi < \frac{\theta}{4} \text{ and } -\frac{\theta}{2} < \varphi < -\frac{\theta}{4}. \tag{23}$$

Here the quantity γ represents the sum of γ_k of separate steps of a multistep characteristic. We see from these expressions that when T is odd, the Z domains can be obtained from the -Ė domains which are situated in the sector between the ou and the ov axes, that is, when $\theta/4 < \varphi < \theta/2$, by reflecting them in the ov axis and by magnifying them afterwards γ times. An example of a Z domain construction when T is odd will be found in Appendix 2.

The generalized domains 1-5 have been constructed by applying the above procedures for T = 2, 3, 4, 5, 6, 7, 8. Their graphs are shown in Fig. 5; they were obtained by taking only symmetric states of the operation of each single-step relay into consideration. It should be borne in mind that for odd T the cases of nonsymmetric operation of single-step relays are also feasible, but only such in which the areas will have equal positive and negative signals at the output of each multistep relay. Such possibilities involve much more complicated computations being at the same time fairly uncommon, i.e., the Z domains associated with them being small in size. They will be found in most cases within the bounds of the generalized domains constructed in Fig. 5 as, similarly to domains associated with symmetric operation, they are situated close to the end of the characteristic vector.

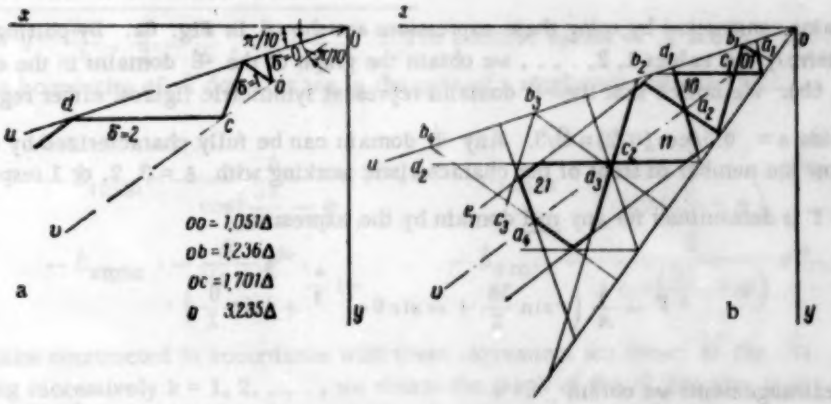

Fig. 7. The -Ė domains for a single and multistep characteristic when T = 5.

4. An Example of Computation and Verification of the Accuracy of the Procedure

The case when the transfer function of the continuous part is

$$W(q) = \frac{1.6}{q(1+2.5q)}$$

is taken as an example.

If there is no level quantization of signals, then the system is stable [5].

The amplitude-phase characteristic $W(j\Omega)$ drawn on the graphs of the generalized Z domains is shown in Fig. 5. One notices that in the case of the generalized domain 1 the periodic states can occur in the system when T = 7, or in the case of generalized domains 1, 2, 3, and 4 when T = 8. The highest possible values of the oscillation amplitude are found independently from the maximum values of γ for every domain according to the formula

$$|\varepsilon| = |W(j\Omega)|\gamma.$$

Thus, when T = 7, for the generalized domain 1, $|\varepsilon| = 0.726 \cdot 1.210 = 0.878$. When T = 8, the largest oscillation amplitude corresponds to the generalized domain 4, which has $|\varepsilon| = 0.926 \cdot 4.437 = 4.110$.

In order to estimate the reliability of the method, modes of periodic states were found by using the Z-domains graphs; this was performed for every possible oscillation mode of $G(\tau)$. Two of the nine possible periodic states are given in Table 2.

Numerical calculations were performed for the same states by solving the system difference equations with the initial conditions chosen in an appropriate manner. The values of $\varepsilon[n]$ obtained both ways are cited in Table 3. One notices that the graphical means used of the describing function approach give results sufficiently close to the exact numerical calculations, especially in cases of large oscillation amplitudes.

APPENDIX I

Construction of the Z Domains when T = 6

This is the case of $T = 4Q + 2$ with $Q = 1$. Then $\theta = \pi/3$, $\theta/2 = \pi/6$. We find from Table 1 the equations of the bounding lines of the $-\dot{E}$ domain in the case of a single-step characteristic for values of $\delta = 0, 1, 2$ and 3 when $0 < \varphi < \frac{\theta}{2}$:

$$-\dot{E}_{01} = -\frac{\Delta e^{j\varphi}}{\cos\left(\frac{\theta}{2} - \varphi\right)}, \quad -\dot{E}_{12} = -\frac{\Delta e^{j\varphi}}{\cos\left(\frac{\theta}{2} + \varphi\right)}, \quad -\dot{E}_{23} = -\frac{\Delta e^{j\varphi}}{\cos\left(\frac{3\theta}{2} - \varphi\right)}.$$

The $-\dot{E}$ domains constructed by using these expressions are shown in Fig. 6a. By putting $\Delta = \Delta_k = k - 0.5$ and giving k successively the values 1, 2, . . . , we obtain the graph of the $-\dot{E}$ domains in the case of a multistep characteristic (Fig. 6b). We notice that the $-\dot{E}$ domains represent symmetric figures, either regular hexagons or triangles with the side $a = 0.5/\cos(\theta/2) = \sqrt{3}/3$. Any $-\dot{E}$ domain can be fully characterized by three numbers r, m and l, and they show the number of steps of the characteristic working with $\delta = 3, 2$, or 1 respectively.

The quantity Γ is determined for any rml domain by the expression

$$\dot{\Gamma} = \frac{4}{\pi}\left(r \sin\frac{3\theta}{2} + m \sin\theta e^{-j\frac{\theta}{2}} + l \sin\frac{\theta}{2}\right).$$

After a few rearrangements we obtain

$$\dot{\Gamma} = \frac{3}{\pi}\left(\frac{4r + 3m + 2l}{3} + \frac{m}{\sqrt{3}} e^{-j\frac{\pi}{2}}\right) = \gamma e^{-j\alpha},$$

where

$$\gamma = \frac{3}{\pi}\sqrt{\left(\frac{4s + 3m + 2l}{3}\right)^2 + \frac{m^2}{3}}, \quad \alpha = \arctan\frac{\sqrt{3}\, m}{4r + 3m + 2l}.$$

The characteristic vector is obtained from the expression (21),

$$P = -\frac{3}{\pi}\left(\frac{4r + 3m + 2l}{3} e^{j\frac{\theta}{2}} + \frac{m}{\sqrt{3}} e^{-j\left(\frac{\pi}{2} - \frac{\theta}{2}\right)}\right) = \frac{3}{\pi} H.$$

It is easy to verify by calculation that the vector H is the radius vector of the center of gravity of the rml domain. In this case the non-symmetric figures, adjacent to ox or ov axes, should be considered as the halves of the corresponding symmetric figures. In this case it is preferable to use vector H instead of the characteristic vector P. The vector H is given by the expression

$$H = \frac{\pi}{3} P = -\frac{\pi}{3} \dot{\Gamma} e^{j\frac{\theta}{2}}.$$

When the $-\dot{E}$ domains have been transformed into Z domains, the transformed vector of the center of gravity is

$$H_0 = \frac{H}{\dot{\Gamma}} = -\frac{\pi}{3} e^{j\frac{\theta}{2}},$$

that is, the center of gravity of the Z domain is situated on the ov axis at a distance of π/3 from the origin of the coordinate system. The construction of the Z domains is reduced therefore to referring the -Ė domain to a new center of gravity. This operation consists in amplifying the unit of measurement γ times and preserving simultaneously the positions relative to the radius-vector of the center of gravity; the latter can be characterized by the angle α or β = (θ/2) - α.

The kth generalized Z domain is obtained as an external boundary of analogously transformed -Ė domains between the straight lines $a_k b_k$ and $a_{k+1} b_{k+1}$. Constructing in this manner one can neglect the triangular -Ė domains as the corresponding Z domains are within the hexagonal domains.

APPENDIX II

Construction of the Z Domain when T = 5

In this case $\theta = \frac{2\pi}{5}$, $\frac{\theta}{2} = \frac{\pi}{5}$, $\frac{\theta}{4} = \frac{\pi}{10}$. The possible values of δ are 0, 1 or 2. For $\frac{\theta}{4} < \varphi < \frac{\theta}{2}$ the equations of the boundaries of -Ė domains are, in the case of a singlestep characteristic,

$$-\dot{E}_{1\min} = -\frac{\Delta}{\cos\left(\frac{3\theta}{4} - \varphi\right)} e^{j\varphi}, \qquad -E_{1\max} = -\frac{\Delta}{\cos\left(\frac{\theta}{4} + \varphi\right)} e^{j\varphi},$$

$$-\dot{E}_{2\min} = -\frac{\Delta}{\sin\varphi} e^{j\varphi}, \qquad -\dot{E}_{2\max} = -\frac{\Delta}{\cos\left(\frac{3\theta}{4} + \varphi\right)} e^{j\varphi}.$$

The -Ė domains constructed in accordance with these expressions are shown in Fig. 7a. By putting $\Delta = \Delta_k = k - 0.5$, and taking successively k = 1, 2, . . . , we obtain the graph of the -Ė domains in the case of a multistep characteristic. The domains and their reflections in the ov axis are shown in Fig. 7b.

The Z domains are obtained from the -Ė domains by contracting the dimensions γ times. The value of γ is easily found for all values of δ for each domain. Thus, for the domain 21 we have

$$\gamma = \frac{4}{\pi} \cos\frac{\theta}{4}\left(2\sin\theta + \sin\frac{\theta}{2}\right) = 3.041.$$

LITERATURE CITED

1. Ya. Z. Tsypkin, Otsenka vliyaniya kvantovaniya po urovnyu na protsessy v tsifrovykh avtomaticheskikh sistemakh. Avtomatika i Telemekhanika, Vol. 21, No. 3 (1960).
2. L. S. Gol'dfarb, Metod issledovaniya nelineinykh sistem regulirovaniya, osnovannyi na printsipe garmonicheskogo balansa. Trudy Vtorovo Vsesoyuzn. Soveshch. po Teorii Avtomaticheskogo Regulirovaniya, Vol. 1, Izd-vo AN SSSR (1955).
3. M. M. Simkin, Periodicheskie rezhimy v sistemakh s nelineinymi impul'snymi elementami, Doklady AN SSSR, 131, No. 6 (1960).
4. S. K. Chow, Contactor Servomechanisms Employing Sampled Data, AIEE Trans. 73, Pt. II (1954).
5. H. M. James, N. B. Nichols, and R. S. Phillips, Theory of Servomechanisms, McGraw-Hill (1947) [Russian translation] (1953).

INVESTIGATING NONSTEADY - STATE PROCESSES IN A PULSE SYSTEM WITH A STEP MOTOR

V. M. Kolesnikov
(Moscow)

Translated from Avtomatika i Telemekhanika, Vol. 22, No. 7,
pp. 896-906, July, 1961
Original article submitted January 4, 1961

The paper formulates the basic problems involved in an investigation of step systems in nonsteady-state modes; the methods of solving these problems are cited, and the formulas for the electromagnetic torque are obtained when the boundary conditions and the optimal parameters are taken into account for a step system with capacitive current commutation in the motor winding.

Step systems are an effective means of automatizing the most varied engineering units and technological processes.

The basic problems which arise in designing a step system are the following:

1) achieving the required speed of response, which is determined by the maximum control pulse frequency for which the rotor of the motor will enter into synchronism from a rest state without losing a step;

2) determining the dependence of the electromagnetic torque of the motor on the frequency of the control pulses;

3) finding the limiting motor torque.

The latter problem reduces to finding the maximum static torque which must be added to the initial torque corresponding to a steady-state mode without causing the rotor to arrive at the nearest position of unstable equilibrium (this would lead to loss of a step).

The solution of the problems posed above can be given only after determining the dependence of the electromagnetic torque corresponding to nonsteady-state modes on the network parameters when the boundary conditions are taken into account and the equations for the dynamics of the system are analyzed.

Determining the electromagnetic torque reduces in the final analysis to determining the current in the motor winding in transient modes.

In [1] it was demonstrated that the power applied to a motor winding for arbitrary current and voltage wave shapes can be represented in the form of the following sum, by analogy with circuit theory, when harmonic signals are used: the resistive component

$$p_a = ri^2 + \frac{i^2}{2}\frac{dx}{d\varphi}\frac{d\varphi}{d\theta}$$

and the reactive component

$$q_p = i\left(\frac{i}{2}\frac{dx}{d\varphi} + x\frac{di}{d\varphi}\right)\frac{d\varphi}{d\theta}.$$

In these expressions i is the current in the winding; $x = \omega L(\varphi)$ is the instantaneous value of the winding reactance; r is the resistance of the winding circuit; φ is the angle of rotation of the rotor; $\theta = \omega t$; ω is the angular frequency of the pulses.

In studying the energy balance in the system it is possible to neglect the reactive power drawn by the winding, since its average value is equal to zero and it is usually compensated in the network.

For the majority of motor designs which are used, the winding reactance can be expressed approximately by the following formula when there is no saturation:

$$x = \frac{x_{min} + x_{max}}{2} - \frac{\Delta x}{2}\cos\alpha,$$

where x_{min}, x_{max} represent the minimum (for $\alpha = 0$) and maximum ($\alpha = 180°$) values of reactance; $\alpha = 2l\varphi$; l is the number of pairs of poles; $\Delta x = x_{max} - x_{min}$.

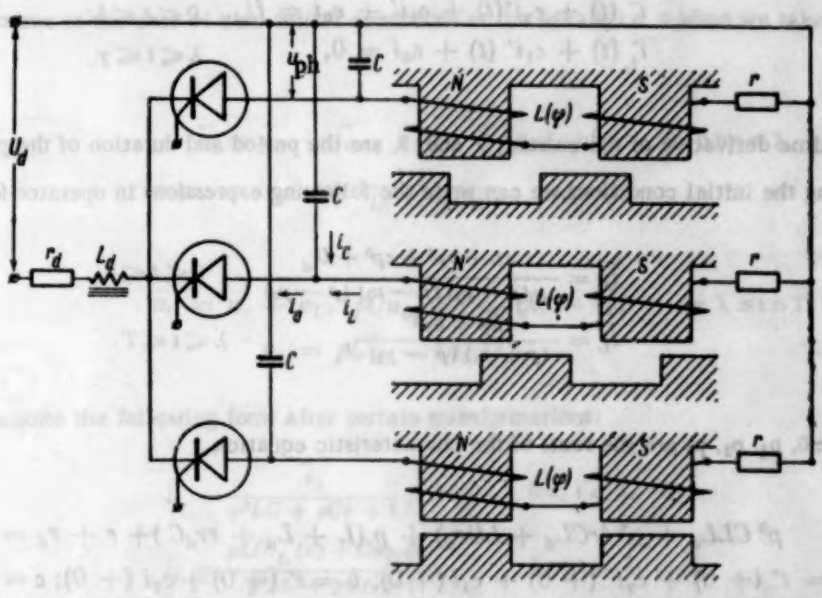

Fig. 1. The electrical circuit for a stepped drive. L_d, r_d represent the inductance and resistance in the circuit of the rectified current; r is the resistance in the motor winding circuit; $L(\varphi)$ is the inductance of the motor winding.

For zero boundary conditions we can write the following relationship [1] for the resistive current drawn from the source and the electromagnetic torque for an arbitrary supply circuit:

$$i = \frac{2\omega u}{\Delta x l \vartheta \sin\alpha + 2\omega r}, \tag{1}$$

$$M_e = \frac{2\Delta x l \omega u^2 \sin\alpha}{[\Delta x l \vartheta \sin\alpha + 2\omega r]^2}, \tag{2}$$

where u is the voltage across the winding and ϑ is the angular velocity.

The angle of rotation and the angular velocity which appear in expressions (1), (2) are determined from the dynamics equation for the step motor when the remaining parameters are specified. However, the substitution of (2) into the dynamics equation leads to a nonlinear transcendental equation which in the general case is not solvable. The effect of the first term in the denominator of (1) and (2) at low frequencies and at the initial instant of motor start is small at high frequencies and can be neglected. In steady-state and almost steady-state modes it is possible to replace the velocity with the independent variable $\vartheta \approx \omega/l$. The error which is caused by this is not difficult to determine if we assume that at the initial instant the motor develops the maximum possible torque

$$M_e = \frac{\Delta x l u^2 \sin\alpha}{\omega r^2};$$

then we substitute this expression into the dynamics equation for the step motor and solve the resulting nonlinear classical equation relative to the velocity by one or another known method.

For a steady-state mode and a specific supply circuit the solution of this equation is cited in [1]. We shall study the nonsteady-state processes in the circuit shown in Fig. 1 for the case where thyratrons or silicon transistors with thyratron characteristics are used.

The circuit under study is one variant of networks with capacitive commutation which have found their greatest practical application in stepped drives. The method of investigation used in this paper can also be applied to the analysis of other similar networks when their specific nature is taken into account.

The differential equations for the current in the motor winding for a conducting and nonconducting rectifier can be written as

$$i_L'''(t) + c_2 i''(t) + c_1 i' + c_0 i = U_d, \quad 0 \leqslant t \leqslant \lambda; \tag{3}$$

$$i_L'''(t) + c_1 i'(t) + c_0 i = 0, \quad \lambda \leqslant t \leqslant T, \tag{4}$$

where i' is the time derivative of the current; T and λ are the period and duration of the plate current i_a.

Introducing the initial conditions, we can write the following expressions in operator form:

$$\overline{i_L} = \frac{ap + bp^2 + cp^3 + U_d}{p(p - p_1)(p - p_2)(p - p_3)}, \quad 0 \leqslant t \leqslant \lambda; \tag{5}$$

$$\overline{i_L} = \frac{ap + bp^2}{(p - p_1)(p - p_2)}, \quad \lambda \leqslant t \leqslant T, \tag{6}$$

where for $\lambda \geq t \geq 0$, p_1, p_2, p_3 are the roots of the characteristic equation

$$p^3 CLL_d + p^3 (rCL_d + LCr_d) + p(L + L_d + rr_d C) + r + r_d = 0;$$

$$a = i''(+0) + c_2 i'(+0) + c_1 i(+0); \; b = i'(+0) + c_2 i(+0); \; c = i(+0)$$

and c_0, c_1, c_2 are the coefficients of Eq. (3); for $T \geq t \geq \lambda$, p_1, p_2 are the roots of the characteristic equation $p^2LC + rpC + 1 = 0$; $a = i'(\lambda) + c_1 i(\lambda)$; $b = i(\lambda)$; and c_0, c_1 and c_2 are the coefficients of Eq. (4).

The equations written above are nonlinear, since $L = L(\varphi)$, and in the general case are not solvable. Moreover, in order to obtain the current corresponding to nonsteady-state modes, it is necessary to solve a third order equation for each of the instantaneous circuits while successively "accumulating" the results. This method leads to extremely cumbersome expressions that are difficult to analyze even when the value of the winding inductance is averaged. Our objective is achieved more rapidly if we make use of a discrete Laplace transform [2]. However, the direct application of the theory of pulse systems in the problem under study is also associated with definite difficulties. For the purposes of further simplication we shall study certain laws governing the network.

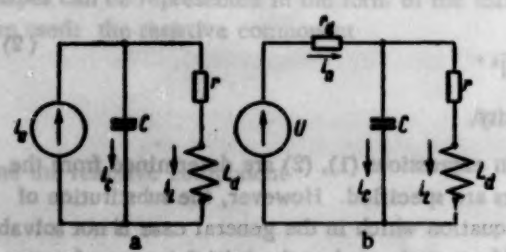

Fig. 2. Instantaneous equivalent circuits for a current source (a) and a voltage source (b).

In [1] it has been demonstrated that there are no conditions and circuit parameters for which the duration of the rectifier plate current can exceed 120°. Moreover, experimental verification was given of the fact that for $L_d \geq$

$\geq L(\varphi)$ the rectifier plate current can be assumed rectangular within the limits of a step. The amplitude of this current is determined by the frequency of the pulses and the parameters of the circuit. Here we shall cite a theoretical verification of this proposition.

In order to increase the efficiency it is expedient to reduce the resistors r_d and r; the effect that this produces on the dynamics of the system requires a special analysis.

We shall distinguish between two extreme cases where $L_d = \infty$ and $L_d = 0$. Such a separation achieves two things: 1) It simplifies the general solution of the problem. 2) It is necessary to clarify the expediency of one or another form of "ballast" (r, r_d or L_d) which assures commutation that is optimal in the sense of achieving the best system dynamics.

In the first case we arrive at a current source, and in the second case we arrive at a voltage source (Fig. 2).

For a current source in the case of zero initial conditions at the instant t = 0, when we take into account the equations

$$\bar{i}_a = \bar{i}_L + \bar{i}_C, \quad \bar{u}_C = \bar{i}_L (r + pL), \quad \text{for } 0 \leq t \leq \lambda,$$

and

$$\bar{i}_C = pC\bar{u}_C$$

$$\bar{u}_C = \bar{u}_r + \bar{u}_L, \quad pC\bar{u}_C = Cu_C(\lambda) - \bar{i}_L, \quad \text{for } \lambda \leq t \leq T,$$
$$u_L = pL\bar{i}_L - Li_L(\lambda),$$

expressions (5), (6) acquire the following form after certain transformations:

$$\bar{i}_L = \frac{\bar{i}_a}{p^2LC + pCr + 1}, \qquad 0 \leqslant t \leqslant \lambda, \tag{7}$$

$$\bar{i}_L = \frac{pLCi_L(\lambda) + Cu_C(\lambda)}{p^2LC + pCr + 1}, \qquad \lambda \leqslant t \leqslant T. \tag{8}$$

Correspondingly, for a voltage source when the equation

$$U_d = pr_d (\bar{i}_C + \bar{i}_L) + \bar{i}_L (r + pL)$$

is taken into account, in the interval $0 \leq t \leq \lambda$

$$\bar{i}_L = \frac{U_d}{p[p^2Cr_dL + p(L + rr_dC) + r + r_d]}. \tag{9}$$

It is evident that for the case under study Eq. (8) remains in force in the interval $0 \leq t \leq \lambda$. We shall assume that the steady-state current in the windings is the basic quantity for both sources; under these conditions

$$i(\infty) = i_i(\infty) = i_u(\infty) = \lim_{p \to 0} p\bar{i}_i(p) = \lim_{p \to 0} p\bar{i}_u(p) = \frac{U_d}{r + r_d} = I,$$

where i_i and i_u are the currents in the motor windings in the cases of current and voltage sources, respectively.

Assuming $i_a = I$, $i(\lambda) = I$, $u_C(\lambda) = rI$, we convert Eq. (7), (8) and (9) to the form

$$\frac{i_i}{i(\infty)} = \frac{1}{p(p^2\nu_i^2 + 2p\xi_i\nu_i + 1)}, \qquad 0 \leqslant t \leqslant \lambda;$$

$$\frac{i_i}{i(\infty)} = \frac{pCL + rC}{p^2\nu_i^2 + 2p\xi_i\nu_i + 1}, \qquad \lambda \leqslant t \leqslant T;$$

$$\frac{i_u}{i(\infty)} = \frac{1}{p(p^2\nu_u^2 + 2p\xi_u\nu_u + 1)}, \quad 0 \leqslant t \leqslant \lambda;$$

$$\frac{i_u}{i(\infty)} = \frac{i_i}{i(\infty)}, \quad \lambda \leqslant t \leqslant T.$$

In both cases the characteristic equation is written as

$$p^2\nu^2 + 2p\xi\nu + 1 = 0,$$

where for $L_d = \infty$ we have

$$\nu = \nu_i = \sqrt{LC}, \quad \xi = \xi_i = \frac{r}{2}\sqrt{\frac{L}{C}}, \tag{10}$$

and for $L_d = 0$ we have

$$\nu = \nu_u = \sqrt{k}\nu_i, \quad \xi = \xi_u = \frac{1 - k(1 - 4\xi_i^2)}{4\xi_i\sqrt{k}},$$

$$k = \frac{1}{\frac{r}{r_d} + 1}. \tag{11}$$

In practice the quantity ξ lies within the limits $0 < \xi < 1$ for $k = 1$.

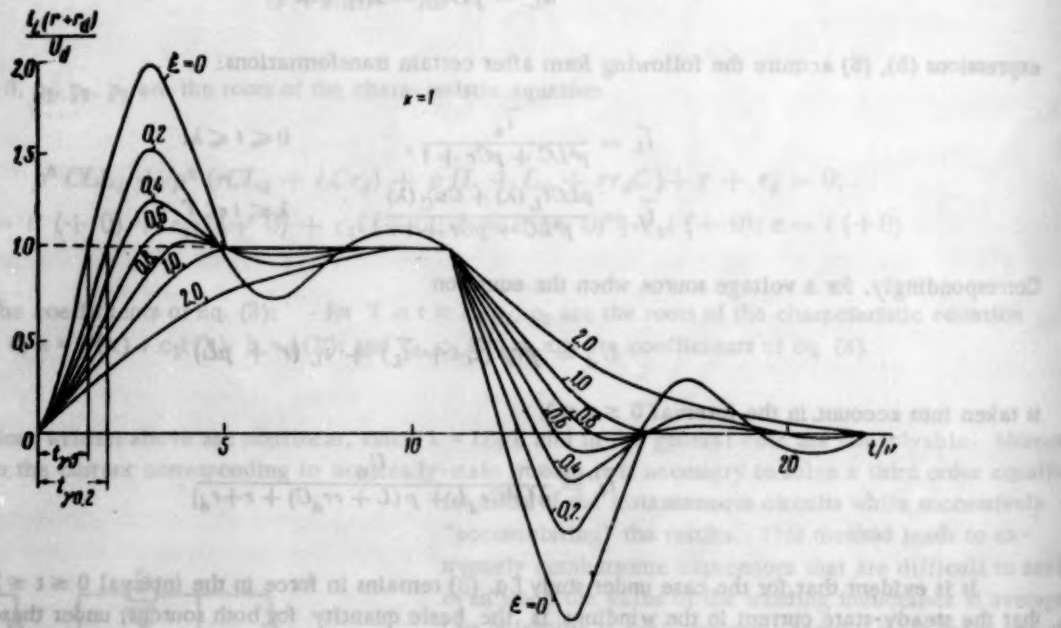

Fig. 3. Family of curves for the relative values of current in the motor winding.

Making use of the family of curves plotted in Figs. 3 and 4, the functions for t_δ and t_γ can be approximated in the form

$$t_\delta = (2.8\xi_i^3 + 0.5\xi_i)\,\tau, \quad t_\gamma = (6.6\xi_i^3 + 3.2\xi_i)\,\tau, \tag{12}$$

where t_δ is the time required for deionization of the rectifier after quenching; t_γ is the time during which the currents in the commutated windings overlap; τ is the time constant for the winding.

From (12) we find the approximate results

$$\xi_i = \frac{2t_\delta}{\tau}, \quad \text{hence} \quad t_\delta = \frac{1}{4}\sqrt{LC}.$$

The overlap time is found from the formula

$$t_\gamma = \left(6{,}4 + 52{,}8\,\frac{t_\delta^2}{\tau^2}\right) t_\delta. \tag{13}$$

Analogously, we can obtain the functions for the case $k \neq 1$ and $L_d = 0$. The variation of $\underline{k}$ and ξ_u is bounded by the intervals $1 \geqslant k > 0$, $\infty \geqslant \xi_u > \xi_i$. . The nature of the variation of the current and voltage in relative units for various $\underline{k}$ is clear from Fig. 5. The rate of rise of the relative voltage u_{ph} drops for a reduction in $\underline{k}$; therefore, for specified ξ_i and ν_i the lead time increases. However, under these conditions the rate of current rise in the winding decreases; this, as demonstrated in [1], decreases the electromagnetic torque on the motor shaft. Moreover, for small $\underline{k}$ the operating conditions of the rectifier deteriorate, since at the initial instant of conduction (for $t \to 0$) the current $i_a = U_d/r_d$ may appreciably exceed the magnitude of its average value. The decrease in the rate of current rise cannot be compensated by decreasing the capacitance without causing a deterioration in the characteristic of the system, since a reduction of C is equivalent to reducing $\underline{k}$ [cf. formulas (10), (11)].

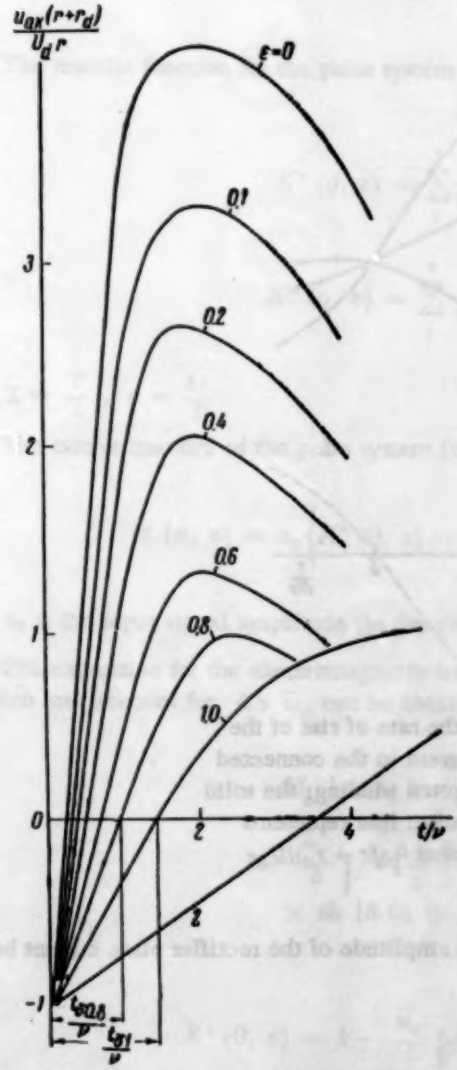

Fig. 4. Family of curves for the relative values of voltage between the anode and cathode of the rectifier after it is quenched.

By increasing the capacitance it is possible to accelerate the current rise; however, when this is done, the rate of current decay decreases and this is turn leads to a deterioration of the dynamic qualities of the system. Thus for improving the dynamics of the system, the case where $L_d \neq 0$ is more favorable.

Such a conclusion can be explained by the presence of a constant energy reserve in the inductance L_d, irrespective of the commutation of the current and the nature of the processes which occur in the system. The resulting relationships make it possible to draw another important conclusion.

In existing motors the maximum deviation of the inductance from the average value comprises a magnitude of the order of ± 20%.

Expression (13) makes it possible approximately to determine the magnitude of the error caused by the assumption that the quantity L maintains its average value. Thus for $2 \cdot 10^{-4} \geq t_\delta > 0$ and $\tau > 2 \cdot 10^{-3}$ (i.e., for the interval which encompasses practically the entire range that is characteristic of the operation of a power drive), this error does not exceed 10% and increases when these intervals are altered (cf. Fig. 6).

Note that the resulting relationships for $k = 1$ are valid in practice for $L_d \approx L$, since even in this case the plate current can be assumed independent of the angle of rotation.

In determining the optimal magnitude of the capacitance from the average value of the inductance, the maximum deviation of the real lead time from the specified value is equal to ± 10%. A reduction of t_s compared to the specified value can be compensated by a corresponding increase in the design capacitance by 20%.

The derived relationships make it possible to study each motor stator with its supply circuits for a three-stator motor (or each phase for a single-stator motor) as a single pulse system whose pulse element forms rectangular current pulses with a variable amplitude that depends only on the pulse frequency and the parameters of the circuit.

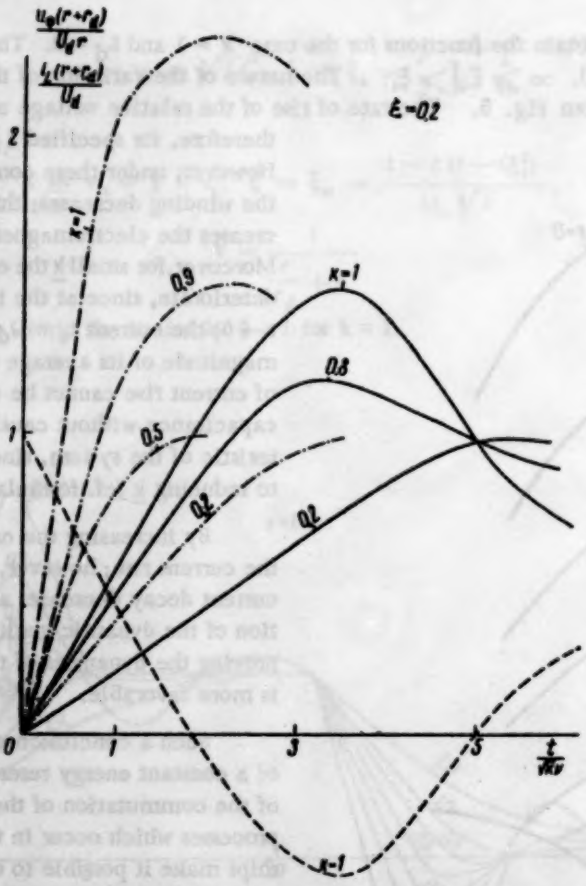

Fig. 5. The effect of the quantity k on the rate of rise of the relative voltage and current. i_1 is the current in the connected winding; i_2 is the current in the disconnected winding; the solid lines represent $i_1(r+r_d)/U_d$; the broken line represents $i_2(r+r_d)/U_d$. ; the dash-dot line represent $u_{ph}(r+r_d)/U_d r$

When the above is taken into account, the expression for the amplitude of the rectifier plate current becomes

$$I_a = \frac{2(U_d - \Delta u)}{\Delta x + 2(r + r_d)},$$

where U_d is the rectified voltage and Δu is the arc drop voltage of the rectifiers.

The transfer function for the continuous section of the system is found on the basis of expression (7):

$$K_c(p) = \frac{1}{p^2\nu^2 + 2p\xi\nu + 1}.$$

Introducing relative quantities, we obtain

$$K_C(q) = \frac{P_C(q)}{Q_C(q)} = \frac{\bar{\omega}_c^2}{q^2 + 2\beta q + \bar{\omega}_c^2},$$

where

$$q = \frac{2\pi p}{\omega}, \quad \beta = \frac{2\pi\xi}{\omega\nu}, \quad \bar{\omega}_c = \frac{2\pi}{\omega\nu}.$$

The poles of the transfer function are equal to

$$q_{1,2} = -\beta \pm j\bar{\omega}_1, \text{ where } \bar{\omega}_1 = \sqrt{\bar{\omega}_c^2 - \beta^2} \quad (\bar{\omega}_c > \beta);$$
$$q_{1,2} = -\beta \pm \delta, \text{ where } \delta = \sqrt{\beta^2 - \bar{\omega}_c^2} \quad (\beta > \bar{\omega}_c).$$

The transfer function for the pulse system under study can be written as [2]

$$K^*(q, \varepsilon) = \sum_1^2 \frac{P_C(q_{1,2})}{Q_C'(q_{1,2})\, q_{1,2}} \frac{e^q - e^{q_{1,2}(1-\chi)}}{e^q - e^{q_{1,2}}} e^{q_{1,2}\varepsilon}, \quad 0 \leqslant \varepsilon \leqslant \chi;$$
$$K^*(q, \varepsilon) = \sum_1^2 \frac{P_C(q_{1,2})}{Q_C'(q_{1,2})\, q_{1,2}} \frac{e^q (e^{q_{1,2}} - 1)}{e^q - e^{q_{1,2}}} e^{q_{1,2}(\varepsilon-\chi)}, \quad \chi \leqslant \varepsilon \leqslant 1,$$

where $\chi = \frac{T}{\lambda}$, $\varepsilon = \frac{\Delta t}{T}$.

The output quantity of the pulse system (the current in the motor winding) is equal to

$$z[n, \varepsilon] = x_0 \left\{ K^*(0, \varepsilon) - \sum_1^2 \frac{P_C(q_{1,2})}{Q_C'(q_{1,2})\, q_{1,2}} \frac{1 - e^{-q_{1,2}\chi}}{1 - e^{q_{1,2}}} e^{q_{1,2}(n+1+\varepsilon)} \right\},$$

where x_0 is the input signal amplitude (in the given case the amplitude of the plate current) and n = 1, 2, 3, ...

The expression for the electromagnetic torque in the nonsteady-state mode, when the boundary conditions are taken into account, for $\beta > \bar{\omega}_c$ can be obtained after performing certain transformations:

$$M_e[n, \varepsilon] = \frac{2\Delta x l (U_d - \Delta u)^2 \sin\alpha}{\omega [\Delta x + 2(r + r_d)]^2} \{K^*(0, \varepsilon)$$
$$- \frac{\bar{\omega}_c}{\delta} \sqrt{\frac{1 - 2e^{-\beta\chi} \operatorname{ch} \delta\chi + e^{-2\beta\chi}}{1 - 2e^{-\beta} \operatorname{ch} \delta + e^{-2\beta}}}\, e^{-\beta(n+1+\varepsilon-\chi)}$$
$$\times \operatorname{sh} [\delta(n + 1 + \varepsilon - \chi) + \psi_1 + \psi_2 + \psi_3]\}^2, \qquad (14)$$

where

$$K^*(0, \varepsilon) = 1 - \frac{\bar{\omega}_c}{\delta} \sqrt{\frac{1 - 2e^{-\beta(1-\chi)} \operatorname{ch}[\delta(1-\chi)] + e^{-2\beta(1-\chi)}}{1 - 2e^{-\beta} \operatorname{ch} \delta + e^{-2\beta}}}$$
$$\times e^{-\beta\varepsilon} \operatorname{sh} (\delta\varepsilon + \psi_1 - \psi_2 + \psi_3) \text{ for } 0 \leqslant \varepsilon \leqslant \chi,$$
$$K^*(0, \varepsilon) = 1 + \frac{\bar{\omega}_c}{\delta} \sqrt{\frac{1 - 2e^{-\beta\chi} \operatorname{ch} \delta\chi + e^{-2\beta\chi}}{1 - 2e^{-\beta} \operatorname{ch} \delta + e^{-2\beta}}}$$
$$\times e^{-\beta(\varepsilon-\chi)} \operatorname{sh} [\delta(\varepsilon - \chi) + \psi_1 + \psi_2 - \psi_3] \quad \text{for} \quad \chi \leqslant \varepsilon \leqslant 1.$$

In a steady-state mode

$$M_{st}[n, \varepsilon] = \frac{2\Delta x l (U_d - \Delta u)^2 \sin\alpha}{\omega [\Delta x + 2(r + r_d)]^2} \times \left[1 - \frac{\overline{\omega}_c}{\delta} \sqrt{\frac{1 - 2e^{-\beta(1-\chi)} \operatorname{ch}[\delta(1-\chi)] + e^{-2\beta(1-\chi)}}{1 - 2e^{-\beta} \operatorname{ch}\delta + e^{-2\beta}}}\right] \times e^{-\beta\varepsilon} \operatorname{sh}(\delta\varepsilon + \psi_1 - \psi_3 + \psi_4)]^2 \quad \text{for} \quad 0 \leqslant \varepsilon \leqslant \chi, \tag{15}$$

$$M_{st}[n, \varepsilon] = \frac{2\Delta x l (U_d - \Delta u)^2 \sin\alpha}{\omega [\Delta x + 2(r + r_d)]^2} \left\{1 + \frac{\overline{\omega}_c}{\delta} \sqrt{\frac{1 - 2e^{-\beta\chi} \operatorname{ch}\delta\chi + e^{-2\beta\chi}}{1 - 2e^{-\beta} \operatorname{ch}\delta + e^{-2\beta}}}\right. \times e^{-\beta(\varepsilon-\chi)} \operatorname{sh}[\delta(\varepsilon - \chi) + \psi_1 + \psi_2 - \psi_3])^2 \quad \text{for} \quad \chi \leqslant \varepsilon \leqslant 1. \tag{16}$$

In expressions (15) and (16),

$$\psi_1 = \operatorname{arc\,th}\frac{\delta}{\beta}, \quad \psi_2 = \operatorname{arc\,th}\frac{e^{-\beta\chi} \operatorname{sh}\delta\chi}{1 - e^{-\beta\chi} \operatorname{ch}\delta\chi},$$

$$\psi_3 = \operatorname{arc\,th}\frac{e^{-\beta} \operatorname{sh}\delta}{1 - e^{-\beta} \operatorname{ch}\delta},$$

$$\psi_4 = \operatorname{arc\,th}\frac{e^{-\beta(1-\chi)} \operatorname{sh}\delta(1-\chi)}{1 - e^{-\beta(1-\chi)} \operatorname{ch}\delta(1-\chi)}.$$

The expressions for the case $\overline{\omega}_c > \beta$ are obtained by sustituting $\overline{\omega}_1$ for $j\delta$.

By changing the parameter ε continuously, we obtain the value of the torque over any time interval for a specified control pulse frequency and all possible network parameters.

In order to obtain the resultant torque of the shaft of the motor in a given case, it is necessary to sum the torques developed by each stator separately. Here we must keep in mind the fact that in the commutation interval for the currents in the motor windings, the resultant torque on the shaft of the motor is equal to the difference between the torques developed by each stator separately. This can easily be seen from Fig. 1.

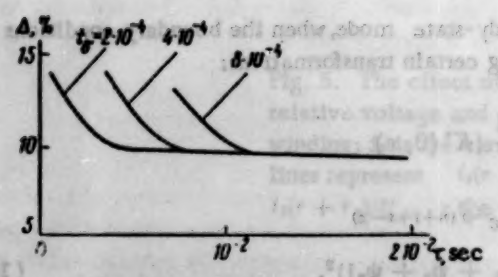

Fig. 6. The error curves which were obtained for the assumptions L = L(φ).

When the expression found for the electromagnetic torque is substituted into the equation of motion, it is possible to determine the speed of rotation of the rotor for any mode of motor operation.

The expression (14) can be written in the form

$$M_e[n, \varepsilon] = \frac{\Delta x l}{2\omega} i_L^2 [n, \varepsilon] \sin\alpha.$$

Note that the interval $\chi \leq \varepsilon \leq 1$ corresponds to overlap of the current in the windings. For an approximate determination of the average torque on the motor shaft we can make use of the value $i[n, \varepsilon]$ only in the interval $0 \leq \varepsilon \leq \chi$.

Denoting the average value of the current in this interval by $\overline{i_L[n, \varepsilon]}$, we obtain the following formula for a shaft torque which is averaged with respect to the current:

$$\overline{M_e[n, \varepsilon]} = \frac{\Delta x l}{2\omega} \overline{i_L^2[n, \varepsilon]} \sin\alpha, \quad 0 < \varepsilon < \chi. \tag{17}$$

Substituting expression (17) into the dynamics equation, we arrive at the classical nonlinear transcendental equation in descrete form:

$$J\alpha'' + k\alpha' + M_{sr} = \frac{\Delta x l}{2\omega} \overline{i^2[n, \varepsilon]} \sin\alpha, \quad 0 < \varepsilon < \chi, \tag{18}$$

where J is the moment of inertia of the moving masses coupled with the rotor; k is the coefficient of friction; M_{sr} is the static resistance torque; α', α'' are the first and second time derivatives of the angle.

In particular, for a large current pulse duration and $M_{sr} = 0$, the movement of the rotor in the step motor is described by the equation for a mathematical pendulum as the stepping process is performed:

$$M_e \sin\alpha = J\alpha'' + k\alpha'; \tag{19}$$

the solution of this equation, as we know, yields attenuating fluctuations of the angle relative to the equilibrium position.

In expression (19) we can assume that

$$M_e = \frac{I_{st}^2 \Delta x l}{2\omega},$$

where I_{st} is the steady-state value of the current in the winding.

Solving Eq. (18) by known methods of numerical integration or by some other method, it is possible to determine the speed of response (i.e., the maximum frequency which the motor can handle without losing a step) as well as the limiting torque which the motor can develop without dropping out of synchronism.

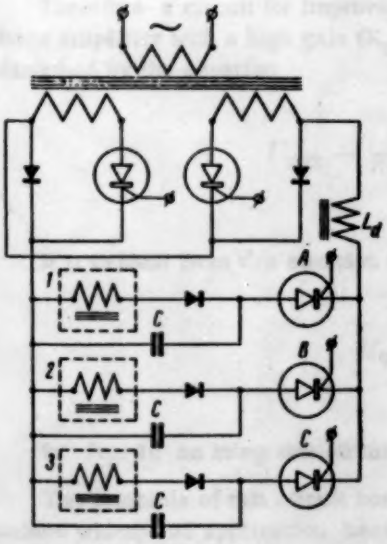

Fig. 7. Circuit for a stepped drive with a controlled dc source.

In particular, in order to determine the conditions governing the appearance of resonant modes which cause the step motor to "stall" when the resistance forces which limit the maximum rate of operation of the step motor are taken into account, it is possible to use [3].

For a constant supply source and constant network parameters the motor has a dropping characteristic $M_e = f(\omega)$. In practice it is possible to achieve any slope of the characteristic $M_e = f(\omega)$ for various frequencies by changing the supply voltage correspondingly. Especially great possibilities in this regard are offered by the networks described in [1, 5], where a choke instead of a resistance is used as the "commutation ballast." This conclusion derives from the fact that the choke produces virtually no voltage losses and it is therefore possible to produce a sufficient voltage margin at low frequencies; this margin is realized when the frequency is increased. The derived expressions for torque permit easy determination of the required law governing the variation of this voltage for variable frequencies in order to achieve the specified characteristic.

In that case the dc supply for the amplifier can be expediently realized using the networks in [4]. These networks assure a high power coefficient, a lighter mode of operation for the rectifiers, and continuous current for large regulation.

A variant of one of these networks is shown in figure 7. The experimental verification of the correctness of our theoretical assumptions is given in [1].

The author thanks A. A. Bulgakov and Ya. Z. Tsypkin for their useful advice.

LITERATURE CITED

1. V. M. Kolesnikov, "Investigation of a thyratron pulse converter with a step motor," Avtomatika i Telemekhanika, 22, 5 (1961).
2. Ya. Z. Tsypkin, Theory of Pulse Systems [in Russian] (Physics and Mathematics State Press, 1958).
3. S. D. Borisov and A. E. Kobrinskii, "On the dynamics of a step motor," Izvestiya Akad. Nauk SSSR, Otdel. Tekh. Nauk, Avtomatika i Énergetika, 6 (1960).
4. V. M. Kolesnikov, "Full-wave rectification with zero anodes and its application in the excitation of excitons," Élektrichestvo, 9 (1960).
5. V. M. Kolesnikov, "The circuit for connecting a motor of the step type," Patent Application No. 132717, Byulleten' Izobretenii, 20 (1960).

PRECISION TRANSISTOR INTEGRATOR

Yu. L. Kurkin and N. S. Kurkina

Translated from Avtomatika i Telemekhanika, Vol. 22, No. 7,
pp. 907-913, July, 1961
Original article submitted January 5, 1961

A circuit for an integrator composed of transistors is proposed. This circuit is shown to be in better agreement with transistor qualifications for amplifying devices than the customary Miller circuit, and, consequently, provides better utilization of the transistors.

A computation of the integrator's operation is given, an expression for the transfer function is derived, and limitations imposed by the finite time constant of the amplifier are pointed out.

Errors introduced by the diodes used for protection against circuit overloading are discussed.

In modern electronic prototype and simulator devices, integration of potentials over time intervals is widely used. The basic means usually employed for integration consists of an RC circuit loop (Fig. 1a). An RC circuit, however, does not provide sufficiently accurate integration, because there is a retroactive action of the output voltage across the capacitor C upon the input current of the circuit. This is clear from the equation

$$U_{out} + \frac{1}{RC}\int_0^t U_{out}\,dt = \frac{1}{RC}\int_0^t U_{in}\,dt.$$

Therefore a circuit for improvement of the integrating properties of the original RC circuit by means of a voltage amplifier with a high gain (K_u) has been proposed. This scheme is called the Miller circuit (Fig. 1b) and is described by the equation

$$U_{out} + \frac{1}{RC\,(1+K_u)}\int_0^t U_{out}\,dt = -\frac{K_u}{RC\,(1+K_u)}\int_0^t U_{in}\,dt.$$

It is evident from this equation that

$$U_{out} \to -\frac{1}{RC}\int_0^t U_{in}\,dt \text{ when } K_u \to \infty.$$

In Fig. 1c an integrator circuit is shown, using an amplifier with a voltage gain of $K_u = 1$.

The principle of this circuit has been known for quite a long time, but, employing vacuum tubes, it has not obtained widespread application because without providing any special advantages it requires an additional separate power supply. When transistors are used in the circuit, this shortcoming is less important [1, 2], and the advantages are appreciable since with a gain of $K_u = 1$ it is easy to obtain a high input resistance $r_i \gg r_c$.

Transistors by their nature are current amplifiers and have low input resistances. A high input resistance r_i is obtained by introduction of a series-parallel feedback at the expense of only a low voltage amplification gain K_u. Therefore, when using transistors it is disadvantageous to build a Miller integrator according to the customary vacuum tube circuit, requiring use of the highest possible values for the gain K_u of the order of 10^5 to 10^6. A transistor integrator designed according to the block diagram of Fig. 1c is more acceptable, since with $K_u = 1$ it is easy to obtain a high input resistance ($r_i \gg r_c$).

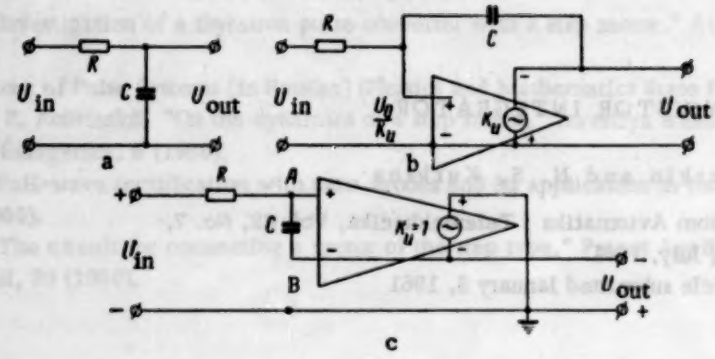

Fig. 1. a) Quasiintegrating circuit; b) Miller integrator ($K_u \to \infty$); c) integrator with voltage amplification gain $K_u = 1$.

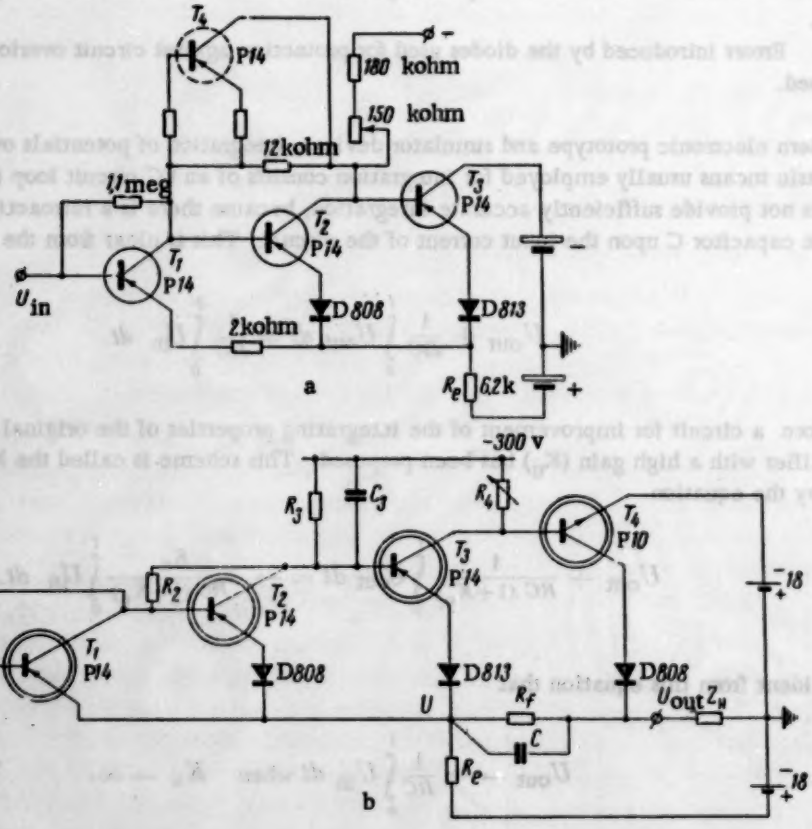

Fig. 2. Amplifier circuits: a) With gain $K_u \leq 1$; b) with $K_u \geq 1$.

It is essential that the obtained high input resistance be determined only by the resistance R_e of the feedback (Fig. 2) and by the current amplification in the circuit, and does not depend upon the small input resistances of the transistors which vary with temperature and other conditions. It is well known that current amplification is one of the most stable parameters of a transistor. The circuit of an amplifier having a $K_u = 1$ and a high input resistance of 100 meg is presented in Fig. 2a. The integration error in a device according to Fig. 1b is proportional to $1/K_u$, and in a device according to Fig. 1c the error depends upon how close the condition $K_u = 1$ is fulfilled. Since the transistor is basically a current amplifying device, the use of some small minimum of current in the input to a transistor integrator is unavoidable; this current is the larger, the smaller the amplifier gain (all other conditions

being equal). The presence of this current is equivalent to the connection of a leakage resistance r_i in parallel with the integrating capacitor (Fig. 1c) and brings about an error similar to that of the Miller integrator. In the Miller integrator this source of error can not be eliminated. In the scheme proposed here (Fig. 1c), however, the leakage through r_i can be compensated for by a small increase of the voltage gain K_u in the amplifier.

The amplifier whose circuit diagram is given in Fig. 2b provides stable operation with any predetermined voltage gain K_u; among others, values of K_u slightly higher than one are also feasible, and these are the ones that are necessary to compensate for the discharge of the condenser, as is evident from the following equations:

$$K_u = \frac{1 + \frac{\alpha_1 R_f}{R_e} + \frac{\alpha_4 R_f}{r_{c3}(1-\alpha_3)}}{1 + \frac{(1-\alpha_4)R_f}{Z_u} + \frac{R_f}{r_{c4}}} \approx 1 + \frac{\alpha_4 R_f}{R_e}.$$

For the circuit of Fig. 1c with leakage it can be shown that

$$\frac{U_{out}}{U_{in}} = \frac{K_u}{RC\left(p + \frac{\frac{1}{r_i} - \frac{K_u - 1}{R}}{C}\right)},$$

that is, the time constant of the integrator is

$$\tau = \frac{C}{\frac{1}{r_i} - \frac{K_u - 1}{R}}.$$

The needed value of $K_u = 1 + \frac{R}{r_i}$ can be obtained by proper choice of the ratio R_f/R_e.

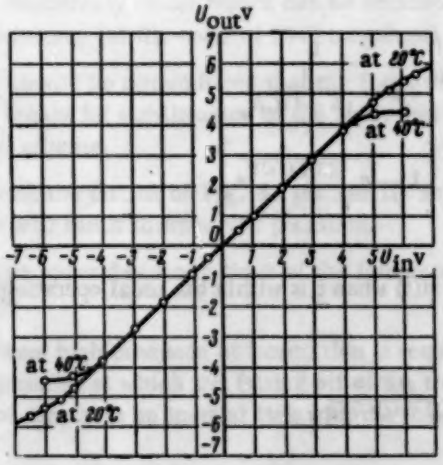

Fig. 3. Dynamic characteristics of the amplifier.

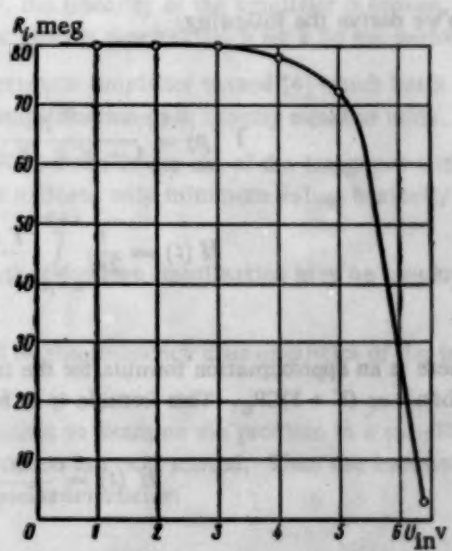

Fig. 4. Input resistance of the amplifier versus input signal voltage.

Let us point out that the circuit remains stable even when a little overcompensated. In that case the integration error changes its sign with respect to the error of the Miller integrator.

The value of K_u must not change throughout the entire range of operational voltages, that is, the amplifier must possess a high degree of linearity. The amplitude characteristics of an amplifier built according to Fig. 2a is presented in Fig. 3.

It is not difficult to see from Fig. 1c that the impedance of the device looking in at the points A and B equals zero within the entire working range of voltages: the circuit at these points possesses infinite capacitance. Certain characteristics of practical interest for this circuit are shown in Fig. 4 and Fig. 5.

Thus this integrator operates with positive feedback and is distinguished from known integrators of this type by the fact that as an amplifier component a three transistor current amplifier with a $K_u = 1$ is used [3]. A circuit diagram of a complete integrator of this type is shown in Fig. 6.

Transistors T_1, T_2, and T_3 (Fig. 2b), all of type П14, form a current amplifier having a nonlinear temperature characteristic; this is compensated for by transistor T_4. The standard operational characteristics of the consecutive amplifier stages are obtained by use of the proper resistances R_1, R_2, and R_3. By proper choice of R_3, an adjustment of the integrator to zero is also obtained. It is essential that R_1 and R_2 be connected not in the power supply line, but in the collector loops of the respective transistors: it is not difficult to see that insertion of R_1 in the power supply line would be equivalent to connecting it in parallel with the integrating capacitance C. The potential increments at the collectors of T_1 and T_2 during the integration process are practically equal to zero because the collectors of T_1 and T_2 are connected to zero potential (ground) through the low ohmage input circuits of the subsequent transistors. Therefore, R_1 and R_2 do not limit the time constant of the transistor integrator.

Obviously, it is possible first to consider the circuit (Fig. 6b) for $R_H \to \infty$, and then account for any R_H by sustituting $R_e R_H / (R_e + R_H)$ for R_e. We thus obtain for the circuit of Fig. 6b the following:

$$\frac{1}{pC}\left(\frac{U_{in}}{R} - i\right) = U_{out} = R_e\left[-\frac{U_{in}}{R} + i\,(1+K)\right]. \tag{1}$$

From this we derive

$$i = \frac{U_{in}}{R}\,\frac{(1+pCR_e)}{1+pCR_e\,(1+K)}.$$

From (1) we derive the following:

$$Y(p) = \frac{K\dfrac{R_e}{R}}{1+pCR_e\,(K+1)} = \frac{K}{(K+1)}\,\frac{1}{RC}\,\frac{1}{p+\dfrac{1}{(K+1)CR_e}}, \tag{2}$$

$$H(t) = \frac{1}{2\pi j}\int_{c-j\infty}^{c+j\infty}\frac{Y(p)e^{pt}\,dp}{p} = \frac{KR_e}{R}\left[1 - e^{-\frac{t}{(K+1)CR_e}}\right]. \tag{3}$$

There is an approximation formula for the transfer function H(t) when t is within the usual operating range, that is, when $t \ll (K+1)CR_e$. This formula is as follows:

$$H(t) = \frac{K}{(K+1)}\,\frac{t}{RC} - \frac{1}{2}\,\frac{t^2K}{(K+1)^2C^2R_eR}. \tag{4}$$

Let us point out that to a first approximation this does not depend upon R_e, that is, upon the load.

The relative error during time t is

$$\delta = \frac{1}{2}\,\frac{t}{CR_e}\,\frac{1}{(K+1)}. \tag{5}$$

In this way, when the acceptable error is given, the maximum of permissible integration time can be calculated. It is not difficult to see (Fig. 6b) that the possible increase of R_e is limited by the output resistance of the current amplifier, which according to the circuit diagram is connected in parallel to R_e.

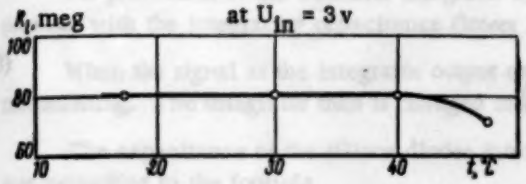

Fig. 5. Input resistance of the amplifier versus temperature.

The drift of the integrator can be estimated when the drift of the current amplifier is known (i_{dr} in Fig. 6b). Solving equation (1) taking into consideration i_{dr}, we obtain

$$U_{out} = \frac{KR_e}{1+pCR_e(K+1)}\left(\frac{U_{in}}{R} + i_{dr}\right).$$

Thus i_{dr} directly enters into the expression under the integration sign along with U_{in}/R, that is, i_{dr} limits the maximum feasible value of R.

Characteristics of such an integrator obtained in practice are given in the following table.

Range of voltages being integrated, v	Zero drift in 100 sec, mv	Decay of charge in 60 sec with maximum of ±5 v in output, % of initial	Characteristic time constant of integrator with C = 8 μf, sec	Integration error for 60 sec in temperature range of 15 to 45°C, in %
+5 to -5	±15, slow drift 20	2-5; with ±4.5 v in output, decay is only 0.3%	1200	0.29

Let us point out that when output voltages exceed ±4.5 v, the linearity of the amplifier is broken, and with an output of +5 v the internal discharge (decay) of the integrator already reaches 2-5% for a 60 sec period.

Considerably better results can be obtained when a four transistor amplifier is used [4] which has a very high input resistance (of the order of 1000 megohms) and a voltage amplification gain exactly equal to unity.

It should be remembered that the figures of the above table pertain to the use of the integrator without any special means for stabilization of the zero; that is, these figures indicate only minimum values basically feasible with this scheme.

With the circuit of Fig. 6, practically any customary method for zero stabilization may be employed [5], and this will result in improved precision.

The upper frequency limit of the integrator is determined by the frequency characteristics of the transistor amplifier.

Since high precision of integration is required, it is reasonable to examine the problem in a simplified manner for frequencies at which the falling off of the transistors' effectiveness has only started. Then the transistor can be regarded simply as an inertial link with the following frequency characteristics:

$$K_i = \frac{\alpha_0}{(1-\alpha_0)} \frac{1}{\left(1 + j\frac{\omega}{\omega_1}\right)} \qquad (\omega \ll \omega_1).$$

Here $\omega_1 = \omega_\alpha(1-\alpha)$ is the cutoff frequency of the transistor with grounded emitter, and ω_α its cutoff frequency with grounded base.

It is known from automatic regulation theory that in a system composed of three stages possessing inertia, the critical gain is the higher, the more widely the time constants of the stages differ from each other. In practice it is sufficient to take two equal transistors and choose the third one with a much higher frequency characteristic, that is, to fulfill the condition $\omega_3 \gg \omega_1$. For a frequency band near ω_1, the transfer function of the amplifier can be written down as follows:

$$K(p) = \frac{K}{\left(1 + \frac{p}{\omega_1}\right)^3}. \tag{6}$$

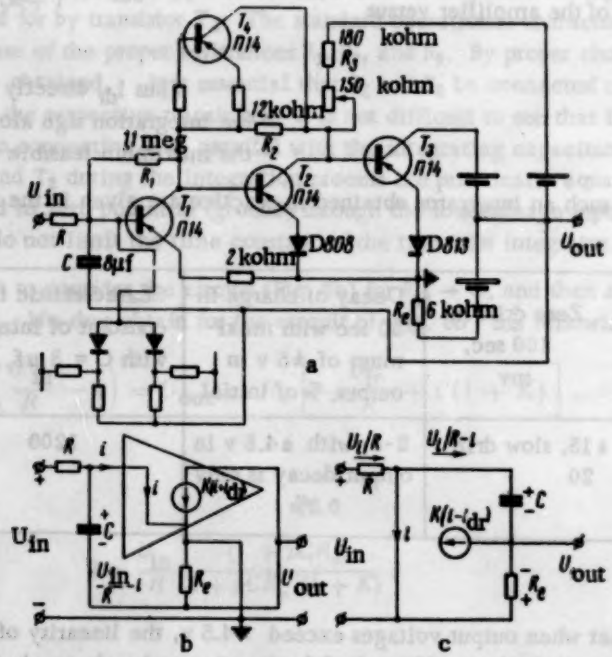

Fig. 6. a) Circuit of complete integrator; b) block diagram of integrator; c) simplified block diagram with K_1 representing current amplification of three transistor amplifier.

Substituting (6) into (2) we obtain the transfer function for the complete integrator in this case:

$$Y(p) = \frac{\frac{K\omega_1^2}{RC}}{\left[p + \frac{1}{(K+1)CR_e}\right]\left[p + \omega_1(1 + j\sqrt{K})\right]\left[p + \omega_1(1 - j\sqrt{K})\right]}.$$

Applying to the input a unit step, we obtain the transfer function for this case:

$$H(t) = \frac{KR_e}{R}\left\{\left[1 - e^{-\frac{t}{(K+1)CR_e}}\right] - \frac{e^{-\omega_1 t}}{\omega_1 CR_e(K+1)}\left[\frac{2\cos(\omega_1\sqrt{K}t)}{(K+1)} + \frac{\sin(\omega_1\sqrt{K}t)}{\sqrt{K}}\right]\right\}.$$

The first member in the curly brackets is the usual transfer function of the integrator when the amplifier has an infinite pass band. The second member represents the damped oscillations which are superimposed upon the integration curve when the pass band of the amplifier is limited by the frequency ω_1.

For protection of the transistor integrator against overloads, silicon diodes are used which are connected in parallel with the integrating capacitance (lower left of Fig. 6a).

When the signal at the integrator output exceeds a certain predetermined value, one of the diodes becomes transmitting. The integrator then is changed into an amplifier having only small gain, and the overload is prevented.

The capacitance of the silicon diodes introduces a perceptible nonlinearity, since it changes with applied voltage according to the formula

$$C_k = S\sqrt{\frac{qEN}{8\pi(U_k + \varphi_k)}},$$

where S is the junction area, N the density of the donors in the base, and φ_k the contact potential difference.

When a required precision of integration is indicated a priori, this effect sets a lower limit to the feasible integrator capacitance C, since we must have $C > C_k/m$, where m is the maximum admissible relative error.

Leakage and polarization of integrator condensers have been neglected, since special condensers of type PGS were used in which these effects have been reduced to a minimum.

In conclusion we shall point out that the described connection of the amplifier in the scheme makes it possible to carry out also other linear operations with given transfer functions. For these purposes, instead of the integrator capacitance, suitable combinations of resistors and capacitances are connected in the circuit.

LITERATURE CITED

1. Use of Isolated Supply Sources in Measuring Devices, Express Information, series VT, 38, No. 116, VINITI, SSSR Acad. of Sc., 1958, translated from J. H. Reaves and J. Walton, Application of isolated power supplies to instr. problems, Nuclear Instruments, Vol. 2, 1958 (North Holland Publ. Co., Amsterdam) pp. 178-181.
2. J. B. Chatterton and D. C. Hollister, Isolation of Power Transformers and Power Supplies, Military Sus. Design, Vol. 3, 1959.
3. Yu. L. Kurkin and N. S. Kurkina, Precision Transistor Integrator for Electronic Simulator Devices. Priority Notice No. 668547/26, May 31, 1960.
4. Yu. L. Kurkin and N. S. Kurkina, Precision Transistor Voltage Amplifier with High (600-2000 meg.) Input Resistance. Priority Notice No. 660213/26, March 28, 1960.
5. G. Korn and T. Korn, Electronic Simulating Devices [Russian translation of "Electronic Analog Computers," McGraw-Hill, New York and London, 1952] Foreign Lit. Press, 1955.

ON THE "REVERSAL" CONDITIONS OF RELAY SEMICONDUCTOR DEVICES

S. V. Kulikov

(Moscow)

Translated from Avtomatika i Telemekhanika, Vol. 22, No. 7,
pp. 914-918, July, 1961
Original article submitted October 3, 1960

A method is presented for finding the "reversal" conditions of semiconductor relay devices from a matrix of the equivalent circuit. The application of the method is shown by an analysis of specific circuits of semiconductor relay devices. Expressions for the "reversal" conditions are derived in terms of a system of parameters from the fourpole amplifier admittances, parameters of the load, of the signal source, and of the positive feedback network between the collector of the output and the base of the input transistors.

1. General Remarks

The problem of finding the "reversal" conditions of semiconductor relay devices leads, in many cases, to the determination of the characteristic equations of the system and to the subsequent analysis of stability with the help, for example, of the Routh-Hurwitz criterion. The characteristic equation can be found either by the method presented in [1] or by the method presented below, for which theoretical bases are included in [2].

The essence of the method is as follows. An impedance or admittance matrix is constructed in a canonical coordinate system for the equivalent circuit corresponding to the conditions of equilibrium. A characteristic equation is obtained by equating to zero the determinant of the matrix (see the demonstration in the Appendix). Further, criteria for stability are used. In a number of cases it is desirable to get an expression for the reversal condition from the fourpole parameters of the amplifier, the parameters of the load, of the signal source, and of the feedback. For the solution of this problem, it is expedient to use the method of separating coordinates with the use of the matrix device [2], thus permitting the fourpole parameters to be found. This method is convenient because the fourpole parameters of an amplifier can often be found experimentally. The method is examined below in examples of the analysis of specific circuits of semiconductor relay devices.

2. Multivibrator with a Collector-Base RC Connection

The general circuit of a multivibrator is shown in Fig. 1. Here R_1 and R_2 are, respectively, the resistances of the control signal source and of the load; C_{FB} is the feedback capacitor (in the present case $R_{FB} = \infty$); T_1 and T_2 are the initial and final transistors of a nonlinear amplifier. The equivalent circuit of the relay device is shown in Fig. 2. Here C_{p1} and C_{p2} are, respectively, parasitic capacities at the input and output of the amplifier; $T_{1,2}$ is a transistor in which the parameters of transistors T_1 and T_2 are embodied.

In order to construct the admittance matrix of the circuit in Fig. 2, we will make the following simplifying assumptions:

a) We will neglect the delay of transistor T_1 with respect to the delay of transistor T_2, since the power of transistor T_1 is usually less than the power of T_2.

b) We will assume that the parameters $Y_{22}^{(1)}$ and $Y_{22}^{(2)}$ of the first and second transistors are equal to zero. This is permissible since in general $Y_{22}^{(1)} \ll Y_{C1}$ and $Y_{22}^{(2)} \ll Y_2$ ($Y_{C1} = 1/R_{C1}$, $Y_2 = 1/R_2$), where $Y_{22}^{(1)}$, $Y_{22}^{(2)}$ are, respectively, the output admittances of the first and second transistors when the input is short circuited.

c) We will assume that the amplifier has the properties of a detector, i.e., $Y_{12}^{(1)}$, $Y_{12}^{(2)} \approx 0$.

d) We will neglect the capacity of the collector junction, assuming that the delay of transistor T_2 depends only on the diffusion process and is characterized by the time constant τ_β.

Taking into consideration the above mentioned assumptions, the circuit matrix in a canonical coordinate system will have the form

$$\begin{array}{c|c|c} & 1 & 2 \\ \hline 1 & Y_1 + Y_{11} + Y_{FB} + (C_{FB} + C_{p1})p & -Y_{FB} - C_{FB}\,p \\ \hline 2 & \dfrac{-Y_{21}}{1+\tau_\beta} - Y_{FB} - C_{FB}\,p & Y_2 + Y_{FB} + (C_{FB} + C_{p2})p \end{array} \qquad (1)$$

where $Y_{11} = Y_{11}^{(1,2)} = Y_{11}^{(1)}$, $Y_{21} = Y_{21}^{(1,2)} = \dfrac{Y_{21}^{(1)} Y_{21}^{(2)}}{Y_{C1} + Y_{11}^{(2)}}$, $\tau_\beta = \tau_\beta^{(1,2)} = \tau_\beta^{(2)} = \dfrac{\beta_0^{(2)}}{2\pi f_{\alpha_0}^{(2)}}$, and $f_{\alpha_0}^{(2)}$ are the common emitter current gain and the amplification cutoff frequency of transistor T_2. The index 1 refers to transistor T_1 and the index 2 to T_2.

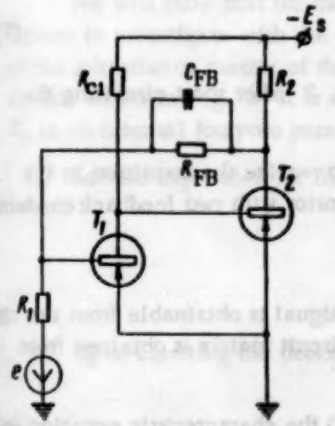

Fig. 1. General circuit for relay semiconductor devices.

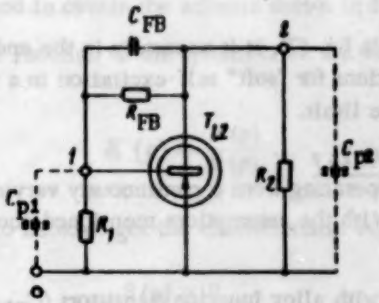

Fig. 2

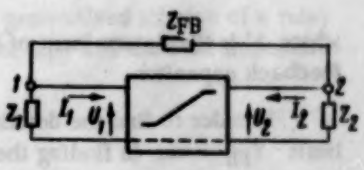

Fig. 3

Fig. 4

During the determination of the parameters of transistor T_1 in the active region at the saturation limit (cutoff) of the first stage, the parameters of transistor T_2 are established in the active region at the cutoff limit (saturation) of the second stage. As studies have shown, in the majority of cases it is sufficient to fulfill the "reversal" conditions obtained below for the limiting parts of the active region.

For the performance of a circuit with alloy junction transistors, we can assume C_{p1}, $C_{p2} \approx 0$. The characteristic equation obtained by equating to zero the determinant of the matrix (1) will in this case have the form

$$\Delta(p) = \tau_\beta C_{FB}(Y_1 + Y_2 + Y_{11})\,p^2 + [\tau_\beta Y_2 (Y_1 + Y_{11}) + C_{FB}(Y_1 + Y_2 + Y_{11} - Y_2)\,p + Y_2 (Y_1 + Y_{11}) = 0. \qquad (2)$$

Applying the Routh-Hurwitz criterion to equation (2), we get the condition for instability corresponding to self-excitation (reversal) of the multivibrator:

$$Y_{21} > \frac{\tau_\beta}{C_{FB}} Y_2 (Y_1 + Y_{11}) + Y_1 + Y_2 + Y_{11}. \qquad (3)$$

For the performance of a circuit with high frequency transistors, we can assume $\tau_\beta = 0$. The characteristic equation will in this case have the form

$$\Delta(p) = [C_{FB}(C_{p1} + C_{p2}) + C_{p1}C_{p2}]p^2 + [C_{p1}Y_2 + C_{p2}(Y_1 + Y_{11}) + C_{FB}(Y_1 + Y_2 + Y_{11} - Y_{21})]p + Y_2(Y_1 + Y_{11}) = 0. \quad (4)$$

The condition of self-excitation of the multivibrator is found from the inequality

$$Y_{21} > \frac{C_{p1}}{C_{FB}}Y_2 + \frac{C_{p2}}{C_{FB}}(Y_1 + Y_{11}) + Y_1 + Y_2 + Y_{11}. \quad (5)$$

For a discontinuous treatment* $\tau_\beta \to 0$, C_{p1}, $C_{p2} \to 0$, $C_{FB} \to \infty$, and the condition of self-excitation will be of the form

$$Y_{21} > Y_1 + Y_2 + Y_{11}. \quad (6)$$

Expression (6) can be obtained from the inequality

$$\Delta' < 0, \quad (7)$$

where Δ' is the determinant of the circuit matrix for the equivalent circuit of Fig. 2 after short circuiting the feedback capacitor.

In order to find the determinant in Eq. (7), it is necessary in the end result to realize the transition in the limit $Y_{FB} \to \infty$. In finding the conditions for "soft" self-excitation in a multivibrator with two feedback condensers, there is no need for the transition in the limit.

3. Bistable Semiconductor Relay

A bistable semiconductor relay operating from a continuously varying input signal is obtainable from the circuit of Fig. 1 if we make $C_{FB} = 0$. With the assumptions mentioned above the circuit matrix is obtained from Eq. (1) after equating C_{FB} to zero.

For the performance of a circuit with alloy junction transistors (C_{p1}, $C_{p2} \approx 0$), the characteristic equation will have the form

$$\tau_\beta[Y_2Y_{FB} + (Y_1 + Y_{11})(Y_2 + Y_{FB})]p + Y_2Y_{FB} + (Y_2 + Y_{FB})(Y_1 + Y_{11}) - Y_{21}Y_{FB} = 0. \quad (8)$$

The reversal condition is found from the inequality

$$Y_{21}Y_{FB} > Y_2Y_{FB} + (Y_1 + Y_{11})(Y_2 + Y_{FB}). \quad (9)$$

Similarly it can be shown that in the performance of a circuit with high frequency transistors, the reversal condition will be given by expression (9). Expression (9) can be obtained from the inequality $\Delta'' < 0$, where Δ'' is the determinant of the circuit matrix obtained from the equivalent circuit (Fig. 2) with $C_{FB} = 0$, when the delay of the transistors and the parasitic capacitors are neglected.

We note that from Eq. (9) it follows that the reversal condition is indepndent of the transistor delay. This result can be considered as the theoretical basis of the calculation method reported by the author in [3], where the delay of the transistors is not considered. From the other direction, experimental studies described in [3] appear to confirm the conclusion indicated. For $C_{FB} \neq 0$ and $\tau_\beta \neq 0$, as follows from an analysis of the coefficients of the complete characteristic equation, this conclusion is wrong if C_{FB} exceeds the value given by the expression

* By discontinuous treatment an idealized condition is implied in which a circuit "reversal" occurs instantaneously, and this is possible when small parasitic circuit elements are neglected.

$$C_{FB}^{max} = \tau_\beta Y_{FB}\left[1 + \frac{Y_{FB}\left(Y_1 + Y_{11}^{(1)} + Y_2\right)}{Y_2\left(Y_1 + Y_{11}^{(1)}\right)}\right]. \quad (12)$$

SUMMARY

The method presented for investigating the reversal conditions of semiconductor relay devices makes it very easy to find relations among the circuit parameters from the matrix of the equivalent circuit. The method can be extended also to relay devices built of other amplifying elements. The relations derived can be used to analyze relay devices having more complicated amplifiers. For this the values of the fourpole admittance parameters of the amplifier are required. The latter can be found experimentally.

In conclusion the author takes this opportunity to express thanks to B. S. Sotskov for valuable advice while doing this work.

APPENDIX

Development of the Characteristic Circuit Equations

We will show that for the determination of the "reversal" conditions of semiconductor relay devices, it is sufficient to investigate with the Routh-Hurwitz criterion the equation obtained by equating to zero the determinant of the admittance matrix of the circuit in a canonical coordinate system. In the generalized scheme of a relay device shown in Fig. 3 it is always possible to refer both the feedback impedance Z_{FB} and the load impedance Z_2 to an internal fourpole parameter, and to obtain the scheme shown in Fig. 4.

Let the expression for the transfer function of the system have the form

$$K(p) = \frac{A(p)}{B(p)}. \quad (I)$$

Upon equating the denominator to zero, we get the characteristic equation of the system

$$B(p) = 0. \quad (II)$$

If only one of the roots of Eq. (II) has a positive real part, the system will be unstable. In relay systems under the specified conditions there develops, in this case, an avalanche process of "reversal."* The presence of a root with a positive real part can be detected, for example, by the use of the Routh-Hurwitz criterion. Equation (II) can be obtained immediately by equating to zero the admittance matrix of the circuit.

Actually, the admittance matrix of the circuit in Fig. 4 with the terminal connected to the base has the form

$$|Y| = \begin{array}{c|c|c} & 1 & 2 \\ \hline 1 & \dot{Y}_1 + \dot{Y}_{11} & Y_{12} \\ \hline 2 & \dot{Y}_{21} & \dot{Y}_2 + \dot{Y}_{22} \end{array}$$

The voltage transfer function at no load is written in the form** [2]

$$K(p) = \frac{\Delta_{13}(p)}{\Delta_{33}(p)},$$

* In the general case the instability condition can correspond not only to an avalanche reversal but to an oscillatory type of transfer from one state to the other, a composite (avalanche with oscillations in certain regions) process and so forth.

** When determining the transfer function, the point of connection of the signal source is the input, and the collector of transistor T_2 is the output.

where $\Delta_{13}(p)$ and $\Delta_{33}(p)$ are determinants obtained from the circuit of Fig. 4 after crossing out the appropriate rows and columns. Thus, in order to find the reversal condition, it is necessary to examine the equation $\Delta_{33}(p) = 0$.

The determinant $\Delta_{33}(p)$ is obtained from the basic matrix of the circuit in Fig. 4:

	1	2	3
1	$\dot{Y}_1 + Y_{11}$	$\dot{Y}_{12}$	$-\dot{Y}_1$
2	$\dot{Y}_{21}$	$Y_{22} + Y_2$	
3	$-Y_1$		$\dot{Y}_1$

by crossing out the third row and the third column. Yet connecting terminal 3 to the base 0 also leads to the diminished (abridged) matrix obtained by crossing out the third row and the third column. And connecting terminal 3 to the base leads to the basic circuit of the relay device; consequently, the matrix of the latter is identical with the $\Delta_{33}(p)$.

Similar demonstrations can be carried out for multipole schemes (more than two poles) and also for an impedance matrix in a canonical system of coordinates.

LITERATURE CITED

1. É. V. Zelyakh, On the Stability Analysis of Vacuum Tube Circuits and of Transistor Circuits, Élektrosvyaz', No. 7 (1960).
2. V. P. Sigorskii, Methods of Analysis of Electric Circuits with Multipole Elements. Izd-vo AN USSR (1958).
3. S. V. Kulikov, Design of a Semiconductor Relay. Radiotekhnika, No. 4 (1960).

DETERMINING THE OPTIMAL PARAMETERS FOR CERTAIN TYPES OF MAGNETIC LOGIC ELEMENTS*

N. P. Vasil'eva and I. Gashkovets

(Moscow and Prague)

Translated from Avtomatika i Telemekhanika, Vol. 22, No. 7,
pp. 919-933, July, 1961
Original article submitted October 18, 1960

The paper determines the relationships between core parameters when saturable-reactor magnetic logic elements have a maximum gain under conditions of maximum power output and limitations on the amount of heating; the conditions required for a stable characteristic are taken into account.

Three basic saturable-reactor logic repeaters are quantitatively compared for operation at 50 and 400 cps.

Among the most common two-cycle logic elements, it is expedient to isolate two groups of networks. The first of these includes networks in which a reversal of the magnetic state of the cores in the controlling element causes a simultaneous reversal of the magnetic state of the controlled element. Such elements perform the function of repeaters. The other group of networks includes those where the reversal of the magnetic state of the core in the controlling element does not permit reversal of the magnetic state of the core in the controlled element; the non-reversal of its magnetic state, which is due to saturation, causes a reversal of the magnetic state of the core in the controlled element. These networks can be called networks with self-exclusive reversal of the magnetic state of the cores. They perform the function of inverters.

One of the basic parameters which characterize magnetic logic elements is their gain (i.e., the maximum number of elements which can be controlled by one logic element).

The selection of all the parameters in a logic element network must be based on obtaining the specified number of controlled elements for stable operation with any number of elements within limits up to the maximum number, while simultaneously taking into account the requirements of economy and small size.

This paper is devoted to determining the relationships between the core parameters and gain of elements and to selecting the optimal parameters of element networks for the purpose of obtaining the maximum gain when the conditions required for a stable static characteristic of the elements are satisfied.

Two-Cycle Elements Which Have Simultaneous Reversal of the Magnetic States of the Cores and Are Supplied from a Voltage Source**

The most frequently used two-cycle logic elements with simultaneous reversal of the magnetic states of the cores and supply from a voltage source include networks which are based on a repeater cell which is decoupled by controlled diodes (Fig. 1) or by resistors (Figs. 2 and 3).

We shall study the controllability conditions for networks with simultaneous magnetic state reversal for the cores in the controlling and controlled elements.

We shall call that half-cycle of supply voltage which causes conduction of the rectifiers in the controlling or output circuit the controlling half-cycle; the half-cycle which cuts off the rectifiers in the controlling or output circuit is called the non-working half-cycle.

* This paper was presented at the All-Moscow Seminar in Contactless Magnetic Elements on October 12, 1960.

** We shall study logic elements with one core having two windings.

For a minimal signal at the output, the core of element I in the networks shown in Figs. 1, 2, 3 will be demagnetized, and then during the next controlling half-cycle it will be magnetized. The maximum signal at the input of the element I, conversely, will not permit demagnetization of the core; therefore during the next controlling half-cycle the core of the element I will be saturated during the entire half-cycle.

When the core of a controlling element is magnetized, its output voltage is minimal, and the core of the controlled element II must be demagnetized simultaneously with magnetization of the core of element I due to the supply voltage in the controlling circuit.

If, however, the core of element I is saturated during the controlling half-cycle, then its output voltage must be sufficient to prevent a reversal in the magnetic state of the core in the controlled element.

For an increase in the number of controlled elements, the conditions for simultaneous reversal of the magnetic state of the cores do not deteriorate as the number of elements increases, since an increase in the number of elements causes a decrease in the minimal output voltage from the controlling element. But the conditions for simultaneous "non-reversal of the magnetic state" of the cores as the number of controlled elements increases deteriorates, since a reduction in the maximum output voltage of the controlling element leads to a situation where (beginning at a certain limiting number of elements) the output voltage is no longer sufficient to avoid at least partial demagnetization of the cores of the controlled elements. That number of controlled elements for which demagnetization of the cores does not yet occur when the core of the controlling element is saturated shall be assumed to be the maximum possible number.

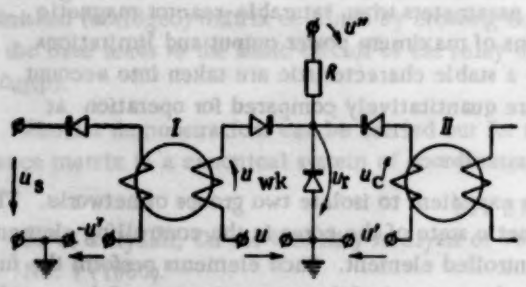

Fig. 1. Network of repeaters with diode decoupling.

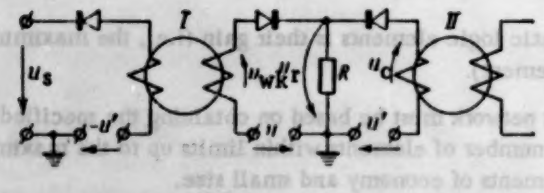

Fig. 2. Network of repeaters with resistor decoupling.

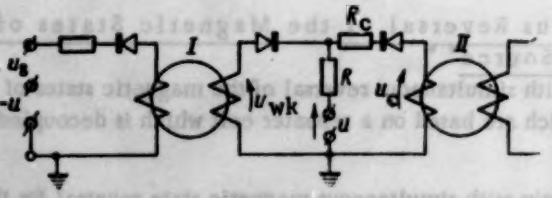

Fig. 3. Network of repeaters with resistor decoupling and a common supply voltage.

In [1] it was demonstrated that in order to obtain a stable characteristic for logic elements of the types under study, it is necessary that the core of the controlled element begin to magnetize later than, and reach complete demagnetization sooner than, the magnetization of the controlling-element core begins and ends. In this paper we do not determine the exact quantitative relationships between these quantities, since in practice they may vary over rather wide limits and depend on the quality of the rectifiers and the core material. We shall demonstrate only that the choice of the optimal relationships in the networks shown in Figs. 1, 2, and 3 is directly related to obtaining a stable characteristic for the elements; thus this choice must be performed while taking stability into account.

We shall make a more detailed study of the network cited above under conditions where the cores have a rectangular hysteresis loop.

A Repeater with Decoupling by Means of Controlled Rectifiers (Network I)

For a minimal signal U_s in the control circuit of the controlling element (Fig. 4a), the core of the controlling element and the cores of the controlled elements must experience a reversal of their magnetic states during a controlling half-cycle. Neglecting the voltage drop across the resistance of the windings and the forward resistance of the rectifiers caused by the current that reverses the magnetic state of the core, it is possible to write the following expressions:

$$U \approx U_{wk}, \tag{1}$$

$$U' \approx k_c U_c, \tag{2}$$

where U_{wk} and U_c are the average values of the voltages required for complete reversal of the magnetic state of the cores during a controlling half-cycle (Fig. 4b). In order to obtain a stable characteristic (cf. [1]) the voltage U_c is produced by a source that generates a sinusoidal voltage U' that is cut off at α_0 at the beginning of the controlling half-cycle. We assume that the voltage U' is chosen in such a way that the core is completely demagnetized for $\alpha_{sat} = \pi - \alpha_0$. Thus, the coefficient k_c, which is associated with an increase in the core demagnetization rate in comparison to its magnetization rate, characterizes the stability of this network.

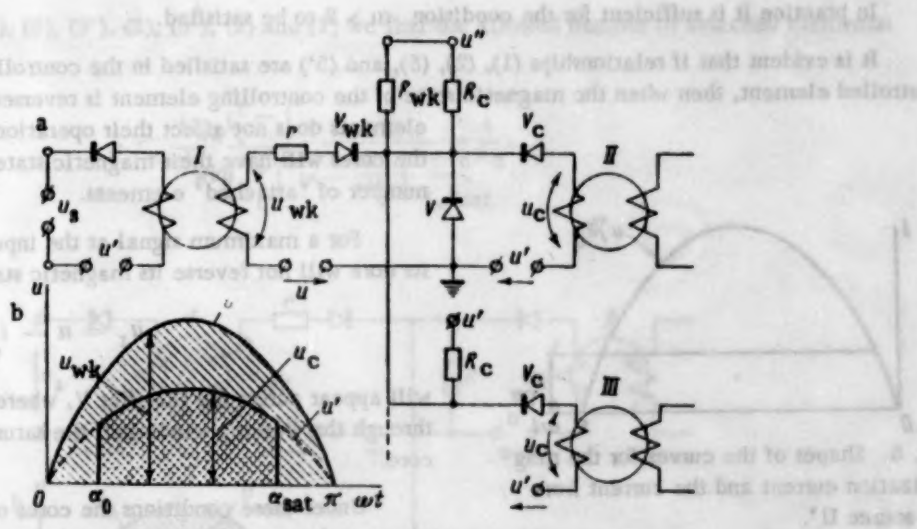

Fig. 4. a) Repeater network with decoupling by a diode loaded with several repeaters; b) relationship between the voltages in the output circuit of the controlling element and the input circuit of the controlled element during a working half-cycle.

For identical cores,

$$\frac{U_{wk}}{U_c} = \frac{w_{wk}}{w_c} = k_w \tag{3}$$

and

$$I_{wk\mu} w_{wk} = I_{c\mu} w_{c\mu} \tag{3'}$$

where $I_{wk\mu}$ is the current required for reversing the magnetic state of the working circuit of the element; $I_{c\mu}$ is the current required to reverse the magnetic state of the controlling circuit of the element.

In order for the coupling rectifier V to remain open during the entire controlling half-cycle, the instantaneous values of the currents from the source U" through the resistances R_{wk} and R_c during this half-cycle must be greater than the currents which reverse the magnetic states of the corresponding elements:

$$\frac{u''}{R_{wk}} \geqslant I_{wk\mu}, \tag{4}$$

$$\frac{U''}{R_c} \geqslant I_{c\mu}. \tag{4'}$$

The voltage u" is usually produced by an ac source and varies sinusoidally. Therefore expressions (4) and (4') cannot, rigorously speaking, be satisfied during the entire half-cycle (Fig. 5), since the magnetizing currents are constant quantities for cores with a rectangular hysteresis loop. In order for the equality conditions to be satisfied

in expressions (4) and (4') during the greater portion of the half-cycle, the average value of the current from the sinusoidal source must be greater than the average value of the magnetizing current (Fig. 5).

We shall denote the ratio between the average values of the currents from the source U" and the magnetizing currents by the coefficient m; then

$$\frac{U''}{R_{wk}} \geqslant I_{wk\mu} m, \tag{5}$$

$$\frac{U''}{R_c} = I_{c\mu}\, m. \tag{5'}$$

In practice it is sufficient for the condition $m > 2$ to be satisfied.

It is evident that if relationships (1), (2), (5), and (5') are satisfied in the controlling element and in each controlled element, then when the magnetic state of the controlling element is reversed the number of controlled elements does not affect their operation. Thus for a minimal signal the cores will have their magnetic state reversed irrespective of the number of "attached" elements.

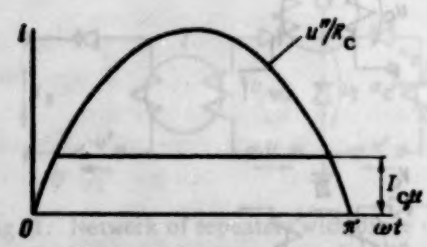

Fig. 5. Shapes of the curves for the magnetization current and the current from the source U".

For a maximum signal at the input of the controlling element, its core will not reverse its magnetic state, and the voltage

$$u_r = u - i_{wk} r \tag{6}$$

will appear across the rectifier V, where i_{wk} is the current passing through the working winding of the saturated controlling-element core.

Under these conditions the cores of the controlled elements must not demagnetize in a properly operating network. This condition will be satisfied if the maximum value of the current in the circuit of each controlled element is less than its magnetization current: $I_{c\mu} \leq I_{c\mu st}$, where $I_{c\mu st}$ is the current for reversing the magnetic state on the static hysteresis loop.

In terms of average values this condition is written as

$$I_c \frac{\pi}{2} = \frac{I_{c\mu}}{k_d}, \tag{7}$$

where $k_d \geq \dfrac{I_{c\mu}}{I_{c\mu st}}$.

Based on this condition, it can be assumed that

$$v_r \approx u' \tag{8}$$

when the resistance of the control circuit is small.

When condition (7) is satisfied, the current i_{wk} is equal to the difference between the currents from the source U" and the currents in the control circuits of all the attached elements, i.e.,

$$I_{wk} = n\left(\frac{U'' + U'}{R_c} - \frac{2I_{c\mu}}{\pi k_d}\right). \tag{9}$$

We shall introduce the substitution $U''/U_{wk} = k''_{sat}$ and shall express U' in terms of U" by using (1) and (2): $U' = U'' \dfrac{k_c}{k_w k''_{sat}}$.

Making use of (5), we obtain

$$\frac{U'' + U'}{R_c} = \frac{U''}{R_c}\left(1 + \frac{k_c}{k_w k''_{sat}}\right) = \left(1 + \frac{k_c}{k_w k''_{sat}}\right) I_{c\mu}{}^m,$$

whence

$$I_{wk} = nI_{c\mu}\left[m\left(1 + \frac{k_c}{k_w k''_{sat}}\right) - \frac{2}{\pi k_d}\right]. \tag{9'}$$

From expressions (8), (6), (9'), (3), (3'), (2) and (1) we find the allowed number of attached elements:

$$n \leqslant \frac{\frac{k_w}{k_c} - 1}{rI_{wk\mu}\left(\frac{k_w}{k_c}\right)^2} \frac{1}{m - \frac{2}{\pi k_d} + \frac{mk_c}{k_w k''_{sat}}} \frac{1}{k_c}. \tag{10}$$

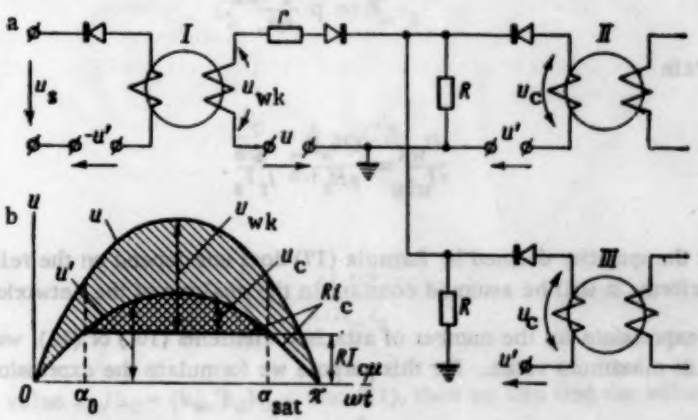

Fig. 6. a) Repeater network with resistor decoupling and a load consisting of several repeaters; b) relationships between the voltages in the output circuit of the controlling element and the input circuit.

If $k''_{sat} \gg 1$ (i.e., if the diode V is supplied from a current source), then expression (10) is simplified and becomes

$$n \leqslant \frac{\frac{k_w}{k_c} - 1}{rI_{wk\mu}\left(\frac{k_w}{k_c}\right)^2} \frac{1}{\left(m - \frac{2}{\pi k_d}\right) k_c}. \tag{10'}$$

These expressions can also be represented in the form of power ratios computed in average values if we use the substitutions

$$I_{wk\mu} U_{wk} = P_\mu \tag{11}$$

and

$$\frac{U^2_{wk}}{4r} = P_{max}, \tag{12}$$

where P_μ is a quantitity proportional to the power expended in reversing the magnetic state of the core (with an accuracy of up to the shape coefficient of the hysteresis loop), and P_{max} is the maximum output power of the controlling element computed in average values.

Making use of (10'), (11), and (12), we obtain

$$n \leqslant \frac{P_{max}}{P_\mu} \frac{\frac{k_w}{k_c} - 1}{\left(\frac{k_w}{k_c}\right)^2} \frac{4}{\left(m - \frac{2}{\pi k_d}\right) k_c}. \tag{13}$$

We shall demonstrate that the quantity $U_{wk}/rI_{wk\mu} = 4(P_{max}/P_\mu)$ depends on the dimensions, shape and material of the core and is independent of the network relationships. We know that

$$U_{wk} = 4fw_{wk} B_m s_s 10^{-8}, \tag{14}$$

$$I_{wk\mu} = \frac{H_s l_s}{w_{wk}}, \tag{15}$$

$$r = \rho \frac{l_r w_{wk}^2}{s_0 k_3}. \tag{16}$$

From this we obtain

$$\frac{U_{wk}}{rI_{wk\mu}} = \frac{4fk_3 B_m}{\rho H_s 10^8} \frac{s_s s_0}{l_r l_s}. \tag{17}$$

It is obvious that the quantity defined by formula (17) does not depend on the relationships between the network parameters; henceforth, it will be assumed constant in the analysis of the networks.

Returning to the expressions for the number of attached elements (10') or (13), we find the optimal value of k_w/k_c for which n has its maximum value. For this purpose we formulate the expression

$$\frac{\partial n}{\partial \left(\frac{k_w}{k_c}\right)} = 0,$$

whence

$$\left(\frac{k_w}{k_c}\right)_{opt} = 1 + \sqrt{1 + \frac{m}{k_d''} \frac{1}{\left(m - \frac{2}{\pi k_d}\right)}},$$

which for large k_{sat}'' yields $(k_w/k_c)_{opt} = 2$. Under these conditions,

$$n_{opt} = \frac{U_{wk}}{4rI_{wk\mu}} \frac{1}{\left(m - \frac{2}{\pi k_d}\right) k_c} = \frac{P_{max}}{P_\mu} \frac{1}{\left(m - \frac{2}{\pi k_d}\right) k_c}. \tag{18}$$

The expressions cited above were obtained without considering the heating of the cores. However, beginning with certain values of output power from the elements, the heating of the working winding of the cores does not permit the use of the elements in the maximum-output mode.

The conditions governing maximum output for the network under study are obtained for $k_w/k_c = (k_w/k_c)_{opt}$. In this case the losses in the core of the controlling element are equal to the output power. If this amount of loss is impermissibly great based on the heating conditions, then in order to obtain the maximum possible n, the element must have a smaller value of k_w/k_c. This new value of $(k_w/k_c)_{all}$ may be determined as follows.

From (6), (8), (1), (2), and (3) we find the relationship between k_w/k_c and I_{wk}:

$$U_{wk}\left(1-\frac{k_c}{k_w}\right)=I_{wk}r. \tag{19}$$

If we denote the current density by Δ, then

$$k_f\frac{I_{wk}}{2}w_{wk}=\Delta s_0 k_{sp}, \tag{20}$$

where $k_f = \pi/2$, and $I_{wk}/2$ is the average value of the working current over a cycle.

Making use of (14), (16), and (20) we find that

$$\frac{k_c}{k_w}=1-\frac{\rho l_r 10^8}{\pi f B_m s_s}\Delta \tag{21}$$

or

$$\frac{k_c}{k_w}=1-C\Delta,$$

where

$$C=\frac{\rho l_r 10^8}{\pi f B_m s_s}. \tag{22}$$

If we substitute the value $k_w/k_c = (k_w/k_c)_{opt}$ into (21), then we can find the value of Δ_{opt} for which the element has the maximum power output.

Thus, for $k''_{sat} \gg 1$, $k_w/k_c = 2$, we have

$$\Delta_{opt}=\frac{\pi f B_m s_s}{2\rho l_r 10^8}. \tag{23}$$

If this value $\Delta_{opt} \leq \Delta_{all}$, where Δ_{all} is the allowable current density, then we can choose $k_w/k_c = (k_w/k_c)_{opt}$ and the number of "attached" elements will be equal to n_{opt} in accordance with (18).

However, if $\Delta_{opt} > \Delta_{all}$, then the quantity k_w/k_c must be determined from the allowable current density given by (21) and the number of attached elements can be determined from formulas (10), (10'), or (13).

In the case where k_w/k_c is not chosen in accordance with expression (21), we will have a situation where for a specified current density the network will not operate in a limiting mode, and the number of attached elements will be less than the number found for formulas (10), (10'), or (13).

A Repeater with Resistor Decoupling (Network II)

The network for such a repeater with a load that also consists of repeaters is shown in Fig. 6a.

Figure 6b shows the distribution of the voltages among the network elements when the magnetic state of the cores is reversed.

For a sinusoidal voltage this network (due to the presence of the resistor R_c) can operate without any special cutoff in the supply voltage U' for the control circuit, since before the cores of the controlled elements begin to

demagnetize (i.e., for $\omega t < \alpha_0$), the flux in the core of the controlling element increases by the amount $\Delta\Phi$, where $\Delta\Phi = \frac{1}{w_{wk}\omega}$; after complete demagnetization of the controlled-element cores (i.e., for $\omega t > \alpha_{sat}$) the flux in the core of the controlling element will continue to increase up to $+\Phi_s$, and the relationship $\Delta\Phi = \frac{1}{w_{wk}\omega}\int_{\alpha_{sat}}^{\pi}(u-u')\,d\omega t$. will again be valid. The ratio $\Phi_s/(\Phi_s - \Delta\Phi)$ in essence determines the stability of the element characteristic, since the greater its ratio, the greater the slope of the characteristic u_{out}/u_{in} for the element.

In the network under study this ratio is determined by the area (Fig. 6b) bounded by the curves $\underline{u}$ and u' from 0 to α_0 and from α_{sat} to π, and by the area bounded by the curves $\underline{u}$ and i_cR which is proportional to U_{wk}. It depends both on the value $k_w = U_{wk}/U_c$ and on the choice of the coefficient

$$k_c = \frac{U'}{U_c}, \tag{24}$$

which determines the angles α_0 and α_{sat}. The stability increases with an increase in k_w and k_c. In the network under study it is not expedient to choose k_w less than 2; however, a growth in k_c also causes a growth of the losses in the resistor R and increases the power drawn by the logic elements.

Just as in the preceding network, for a minimum signal U_s in the control circuit of the controlling element, the cores of all the elements in the network shown in Fig. 6a must simultaneously be subjected to a reversal of the magnetic state. Neglecting the voltage drop caused a) by the currents which flow through the winding resistance and rectifiers and cause the reversal of magnetic state and b) by the current $I_{wk\mu}$, it is possible to write the following relationships for the controlling half-cycle:

$$u = u_{wk} + i_cR, \tag{25}$$

$$u' = u_c + i_cR. \tag{26}$$

As in the case cited above [formulas (3) and (3')],

$$\frac{U_{wk}}{U_c} = k_w, \qquad l_{c\mu}w_c = l_{wk\mu}w_{wk}.$$

If the parameters of all the elements are chosen in such a way that Eq. (25) and (26) are satisfied, then, when the core of the controlling elements is subjected to a reversal of magnetic state, all the remaining elements will be subjected to a reversal of magnetic state irrespective of their number; this follows since it is a fact that, just as in the preceding network, the elements do not affect one another when their magnetic states are reversed.

For a maximum control signal the core of the controlling element remains saturated during the entire controlling half-cycle.

For proper operation of the network, the cores of all attached (controlled) elements must also remain in a saturated state. The condition for this is that the maximum current flowing through the control winding of each controlled element must remain less than the demagnetization current $I_{c\mu st}$ on the static hysteresis loop, i.e., [cf. formula (7)]

$$\frac{\pi}{2}I_{c,sat} = \frac{I_{c\mu}}{k_d}.$$

Neglecting the voltage drop across the control windings of the cores and across the rectifiers, we obtain the following equations for the saturated state of the cores (the subscript "sat" denotes the saturated state of the cores):

$$ri_{wk,sat} = n - (i_{wk,sat} + i_{c,sat}\,n)\frac{R}{n}, \tag{27}$$

$$0 = u' - (i_{wk,sat} + i_{c,sat} n) \frac{R}{n}, \tag{28}$$

where the current $i_{wk,sat}$ is the current in the working winding of the saturated core of the controlling element.

Making the transition to average values and substituting expression (7) into (27) and (28), we obtain the limiting value for the number of controlled elements:

$$n = \frac{U - U'}{r\left(\frac{U'}{R} - \frac{2}{\pi k_d} I_{c\mu}\right)}. \tag{29}$$

From (25) we find the following result for the average values of the currents and voltages:

$$R = \frac{U' - U_c}{I_{c\mu}} k_a \tag{30}$$

where $k_a = \frac{I_{c\mu}}{I_c} > 1$ (cf. Fig. 6b); from (25), (26), and (3) we obtain

$$U - U' = U_{wk}\left(1 - \frac{1}{k_w}\right). \tag{31}$$

From (29) we obtain

$$n \leqslant \frac{U_{wk}}{rI_{wk\mu}} \frac{k_w - 1}{k_w^2} \frac{1}{\frac{k_c}{(k_c - 1)k_a} - \frac{2}{\pi k_d}}, \tag{32}$$

while taking (30), (31), (24), and (3) into account, or if we use (11) and (12) we obtain

$$n \leqslant \frac{P_{max}}{P_\mu} \frac{k_w - 1}{k_w^2} \frac{4}{\frac{k_c}{(k_c - 1)k_a} - \frac{2}{\pi k_d}}. \tag{33}$$

An analysis of these expressions demonstrates that $\underline{n}$ will increase as k_c increases for $k_c > 1$. For $k_c < 1$, expression (33) does not have any physical meaning, since in such a case the core cannot be fully demagnetized.

It is evident that the maximum value of $\underline{n}$ is achieved for

$$k_{w\,opt} = 2. \tag{34}$$

For a sufficiently large k_c and $k_w = k_{w,opt}$, expressions (32) and (33) become simplified and are written as

$$n_{opt} = \frac{U_{wk}}{4rI_{wk\mu}} \frac{1}{\frac{1}{k_a} - \frac{2}{\pi k_d}}, \tag{35}$$

$$n_{opt} = \frac{P_{max}}{P_\mu} \frac{1}{\frac{1}{k_a} - \frac{2}{\pi k_d}}. \tag{35'}$$

If we again introduce limitations for the heating, then k_w must be chosen in accordance with the following reasoning.

From expressions (27), (28), and (31) we obtain the relationship between k_w and I_{wk} which is analogous to the relationship for the preceding network:

$$I_{wk}r = U_{wk}\left(1 - \frac{1}{k_w}\right).$$

Performing the same transformation, we again obtain

$$\frac{1}{k_w} = 1 - C\Delta,$$

where

$$C = \frac{\rho l_r 10^6}{\pi f B_m s_s}$$

and for $k_w = k_{w,opt}$.

$$\Delta_{opt} = \frac{f B_m s_s \pi}{\rho l_r 10^6 2}.$$

If $\Delta_{opt} < \Delta_{all}$, where Δ_{all} is the allowable current density, then it is possible to choose $k_w = 2$; the number of attached elements will be equal to n_{opt} in accordance with (32). If $\Delta_{opt} > \Delta_{all}$, then the quantity k_w must be determined from the allowable current density in accordance with (21),and the number of attached elements can be determined from (32).

However, if k_w from (21) is found to be less than two, then (as was shown at the beginning of this section) the stability of the network deteriorates. Therefore it is expedient to choose $k_w > 2$. This leads to a situation where the number of attached elements must be less than the limiting number which we derive from the condition of maximum output. Thus, since the number of attached elements will be less than the limiting number, the voltage across the coupling resistor will exceed u' and the rectifier V_c in the control circuit will be cut off. This means that coefficient k_d in expression (32) is equal to ∞; therefore, the limiting value of $\underline{n}$ decreases to the value determined from (32) for $k_d = \infty$,and the allowable value of $\underline{n}$ will be less than the limiting value by a factor of Δ/Δ_{all}, where Δ is the value of the current density obtained from (21) for the chosen value of k_w. Thus

$$n = \frac{U_{wk}}{r I_{wk\mu}} \frac{k_w - 1}{k_w^2} \frac{k_c - 1}{k_c} k_a \frac{\Delta_{all}}{\Delta}.$$

Substituting Δ into this expression from (21), we obtain

$$n = \frac{U_{wk} C \Delta_{all}}{r I_{wk\mu}} \frac{(k_c - 1) k_a}{k_c k_w}.$$

Making use of (14), (16), and (22), we find

$$n = \frac{4 k_{sp} s_0 \Delta_{all}}{\pi I_s l_s} \frac{(k_c - 1) k_a}{k_c k_w} = \frac{4}{\pi} \frac{A_{max}}{A_\mu} \frac{(k_c - 1) k_a}{k_c k_w}, \quad (36)$$

where A_{max} represents the maximum allowable ampere turns on the working winding of the core on the basis of heating considerations, and A_μ is the number of coercive ampere turns of this winding.

In expression (36) the value of k_c must be chosen to be the same as k_w while considering stability requirements.

The choice of k_c also determines the choice of the relationship between the supply voltage and the voltage U_{wk} across the working winding which causes a reversal of magnetic state. We shall use the substitution $k_{sat} = U/U_{wk}$. On the basis of expression (31),

$$U = \frac{k_c}{k_w} U_{wk} + \left(1 - \frac{1}{k_w}\right) U_{wk}$$

or

$$k_{sat} = \frac{k_c - 1}{k_w} + 1.$$

A Repeater with Resistor Decoupling and One Supply Source (Network III)

The network for such a repeater with a load that also consists of repeaters is shown in Fig. 7a.

Figure 7b shows the distribution of voltages among the network elements when the magnetic state of the cores is reversed. For a sinusoidal supply voltage this network may be stable due to the presence of the resistances R and R_c (this is analogous to the situation prevailing for the preceding network).

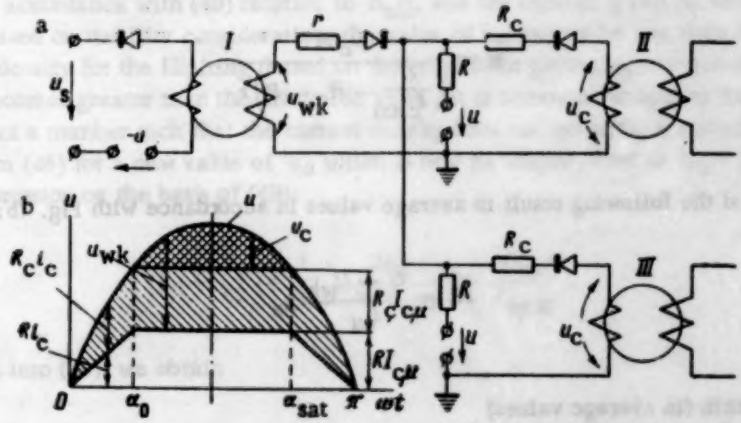

Fig. 7. a) Repeater network with a common supply voltage and resistor decoupling which is loaded with several repeaters; b) relationship between the voltages in the output circuit of the controlling element and the input circuit of the controlled elements during the working half-cycle.

The conditions governing a reversal in the magnetic state of the cores of the controlled elements when a core of the controlling element reverses its magnetic state are written as

$$u - u_{wk} \approx i_c R, \tag{37}$$

$$u_{wk} - u_c \approx i_c R_c \tag{38}$$

$$\frac{u_{wk}}{u_c} = k_w.$$

The satisfaction of these conditions, as in the preceding networks, depends not on the number of controlled elements, but only on the proper relationships between U, R and R_c for specified cores and a definite relationship between the number of turns on their windings.

The condition governing the possibility of controlling n logic elements when the core of the controlling element reverses its magnetic state is also based on the relationship

$$I_{cm} \leqslant I_{c\mu}/n$$

or, in terms of average values,

$$\frac{\pi}{2} I_{c,sat} = \frac{I_{c\mu}}{k_d}$$

and on the relationships between the parameters of the working and controlling circuits:

$$r i_{wk,sat} = R_c i_{c,sat} \tag{39}$$

$$R_c i_{c,sat} = u - (i_{wk,sat} + i_{c,sat} n) \frac{R}{n}. \tag{40}$$

Making the transition to average values, we obtain

$$I_{wk} = \frac{R_c I_{c,sat}}{r}, \tag{41}$$

from (39) and

$$n = \frac{R_c R}{\left(\frac{U}{I_{c,sat}} - R_c - R\right) r}. \tag{42}$$

from (40) and (41).

From (37) we find the following result in average values in accordance with Fig. 7b:

$$R = \frac{U - U_{wk}}{I_{c\mu}} k_a \tag{43}$$

where $k_a = I_{c\mu}/I_c$.

From (38) we obtain (in average values)

$$R_c = \frac{U_{wk} - U_c}{I_{c\mu}} k_a = \frac{U_{wk}\left(1 - \frac{1}{k_w}\right)}{I_{c\mu}} k_a \tag{44}$$

In our subsequent analysis we also introduce the coefficient

$$k_c = \frac{U}{U_c}, \tag{45}$$

which together with k_w determines the stability of the characteristics for the elements.

The choice of k_c determines the angles α_0 and α_{sat} and the termination of the process involving the reversal of magnetic state for the cores of the controlled elements. As k_c and k_w increase, the stability also increases; however, the losses in the resistances R and R_c increase (i.e., the power drawn from the supply sources increases).

Substituting the relationships (7), (3), (43), (44), and (45) into (42), we find

$$n = \frac{U}{r I_{wk\mu}} \frac{k_w - 1}{k_w^2} \frac{1 - \frac{k_w}{k_c}}{\frac{\pi k_d}{2 k_a} + \frac{1}{k_c} - 1}. \tag{46}$$

The value of n increases as k_c increases and has a maximum as a function of k_w for

$$k_{w,opt} = \frac{2}{1 + \frac{1}{k_c}}. \tag{47}$$

For large k_c we have $k_{w,opt} = 2$.

We shall now proceed to a determination of the heating limitations. From (41) and (44) we obtain

$$I_{wk}\, r = U_{wk}\left(1 - \frac{1}{k_w}\right)\frac{2k_a}{\pi k_d}. \tag{48}$$

Making use of (20), (14), (16), and (48), we find

$$\frac{1}{k_w} = 1 - \frac{\pi k_d}{2k_a} C\Delta, \tag{49}$$

where C is determined from (22).

From this we can find Δ_{opt} if we make the substitution $k_w = k_{w,opt}$. In the case where $\Delta_{opt} > \Delta_{all}$, the choice of k_w may be made in accordance with (49) relative to Δ_{all}, and the number n can be determined in accordance with (46). However, based on stability considerations, the value of k_w cannot be less than two. But since under these conditions the current density for the limiting (based on the conditions governing non-reversal of the magnetic state) number of elements becomes greater than the allowable value, it is necessary to retreat from the limiting number of elements and connect a number such that the current density does not exceed the allowable value. This number can be determined from (46) for a new value of k_d which is now no longer equal to $I_{c\mu} / I_{c\mu st}$ but is determined from the following expression on the basis of (49):

$$k_d = \left(1 - \frac{1}{k_w}\right)\frac{2k_a}{\pi C \Delta_{all}} > \frac{I_{c\mu}}{I_{c\mu st}}. \tag{50}$$

Substituting (50) into (46), we obtain

$$n = \frac{U_{wk}}{r I_{c\mu}} \frac{k_w - 1}{k_w^2} \frac{1 - \frac{k_w}{k_c}}{\frac{k_w - 1}{k_w C \Delta_{all}} + \frac{1}{k_c} - 1}. \tag{51}$$

We shall use numerical examples to compare the networks studied above for characteristic operating modes.

In order to compare the networks for operation at a frequency of 50 cps we perform a computation for cores having the following data: material 50 NP, H_s = 0.2 amp/cm, B_m = 15000 gauss, l_s = 8.3 cm, l_r = 5 cm, s_s = = 0.18 cm^2, s_0 = 1.8 cm^2, k_{sp} = 0.3.

In accordance with (17),

$$\frac{4P_{max}}{P_\mu} = 200.$$

In accordance with (22),

$$C = 0.0021 \text{ cm/amp}.$$

We shall compute the number of elements which can be controlled by one element (i.e., the gain of an element) for identical values of k_{sat} and values of k_w close to the optimum values for each network.

a. For network I, $(k_w/k_c)_{opt} = 2$. For stable operation it is sufficient that $k_c = 1.5$, and therefore we choose $k_c = 1.5$; $k_w = 3$, $m = 2$, $k_d = 2$, $k^*_{sat} = 2$. Then according to expression (10),

$$n \approx 15.$$

b. For network II we choose $k_w = 3$, $k_d = 2$; then $k_c = 4$. For these values $k_a \approx 4/3$ (this relationship is determined by graphical plotting in a manner analogous to that shown in Fig. 6b). In accordance with expression (33),

$$n \leqslant 65.$$

We shall verify the conditions governing the heating in such networks. For both networks the current density for $k_w = 3$ is determined from expression (21):

$$\Delta = 315 \text{ amp/cm}^2.$$

For cores with the selected dimensions, $\Delta_{all} = 400$ amp/cm^2. Thus, networks I and III can operate for an optimal value of k_w, i.e., for maximum output.

c. For the network III we have $k_c = 4$ and $k_{w,opt} = 1.8$ from (47) for $k_d = 2$. However, based on the stability conditions we should not choose k_w to be less than 2; we choose $k_w = 2$, and $k_a = 4/3$. Then from (46) we have

$$n \leqslant 15.$$

For this network the current density is

$$\Delta_{opt} = 100 \text{ amp/cm}^2,$$

for the chosen value $k_w = 2$, i.e., $\Delta_{opt} < \Delta_{all}$ and the network can operate for the chosen value of k_w.

The examples cited above clearly show the advantages of network II over networks I and III, which were computed for optimal parameters with respect to the maximum gain. The gains for network II are more than four times the gains for networks I and III.

Here the power loss in the coupling resistors in network II is less than the power loss in the resistors R_c in network I and in the resistors R and R_c in network III.

In order to compare the networks for operation at a frequency of 400 cps, we shall perform the computation for cores with the following data: $H_s = 0.4$ amp/cm, $B_m = 14500$ gauss, $l_s = 6$ cm, $l_r = 4$ cm, $s_s = 0.1$ cm^2, $s_0 = 1.2$ cm^2, $k_{sp} = 0.3$.

In accordance with (17),

$$\frac{4P_{max}}{P_\mu} = 500.$$

In accordance with (22),

$$C = 3.85 \cdot 10^{-4}.$$

First we shall compute the number of elements which one element can control for identical values of k_{sat} and values of k_w which are optimal from the viewpoint of maximum power output.

a. For network I $(k_w/k_c)_{opt} = 2$, where from the stability conditions $k_c = 1.5$; therefore, $k_w = 3$, $k_c = 3$, $k^*_{sat.} = 2$.

Making use of (10), we find

$$n_{opt} \leqslant 36.$$

Under these conditions we obtain

$$\Delta_{opt} = 1350 \text{ amp/cm}^2$$

from (21).

Since $\Delta_{opt} > \Delta_{all}$, we find that the allowable value $(k_w/k_c)_{all}$ for a limiting mode of operation is

$$\frac{k_c}{k_{w\,all}} = 1 - C\Delta_{all} = 0.846;$$

this yields

$$k_{w\,all} = 1.76.$$

for $k_c = 1.5$.

Under these conditions we have

$$n = 16.$$

Thus, when the heating effect is taken into account, one element in this network can control only 16 elements.

b. For network II we have $k_{w,opt} = 2$, $k_d = 3$; thus, according to the stability conditions, we have $k_c = 4$, and $k_{sat} = 2.5$. When heating is not taken into account,

$$n \leqslant 142.$$

Under these conditions $\Delta_{opt} = 1350$ amp/cm^2. We shall find the allowable k_w for which $\Delta_{all} = 400$ amp/cm^2.

Based on (21),

$$\frac{1}{k_{w\,all}} = 1 - C\Delta_{all} = 0.846, \qquad k_w = 1.2.$$

However, for the value $k_w = 1, 2$, it is not possible to obtain a stable characteristic for the elements. From the stability conditions for this network, it is expedient to choose k_w no less than two. In accordance with (36), we obtain

$$n = 22.$$

c. For network III we choose $k_d = 3$, as before. From the stability conditions we choose $k_c = 4$, and then $k_{w,opt} = 1.6$. Therefore, we have

$$n = 22.$$

Under these conditions

$$\Delta_{opt} = \left(1 - \frac{1}{k_w}\right) \frac{2k_a}{\pi C k_d} = 380 \text{ amp/cm}^2,$$

i.e., $\Delta_{opt} < \Delta_{all}$ and the network can still operate in a limiting mode.

SUMMARY

From a comparison of the derived formulas, whose use has been illustrated by means of several examples, we can draw the following conclusions.

1. The optimal choice of parameters is determined in the same way as it is in linear networks or by the condition governing the matching of the input and output resistances of the elements; this condition leads to a mode that is close to maximum power output from the controlling element or to a limitation of the output power by the heating effect in the controlling element.

In the first case (for maximum power output) the ratio k_w between the number of turns on the working and controlling windings is confined within the limits 2 to 3; in networks II and III this makes it possible to achieve a stable characteristic for a ratio k_c (the ratio between the control circuit supply voltage and the voltage which produces a reversal in the magnetic state of the controlling winding) that is confined within the limits 4 to 8. In network I stability is achieved by choosing k_c in the range 1.2 to 1.5.

In the second case, for a limitation based on the heating effect, the value of k_w in network I is chosen in accordance with requirements governing the operation of a network with the limiting number of elements, and the stability is assured by choosing k_c within the range 1.2 to 1.5; in networks II and III the value of k_w must be chosen from the condition governing the achievement of a stable characteristic, and thus it can be no less than two. Under these conditions, the limiting operating mode for networks II and III cannot be achieved, and the number of controlled elements must be determined from the allowable current density on the basis of expressions (36) and (51), which take into account the deviation from the limiting operating mode.

2. Of the networks studied above, the most useful are networks II and III, which yield the maximum values of $\underline{n}$. Network III may be preferable to networks I and II for operation with heating limitations.

3. The derived formulas make it possible not only to determine the gain $\underline{n}$ for specified core parameters, but to determine the core dimensions for a specified $\underline{n}$. Here from expressions (10), or (32) and (34), or (36) and (51), it is possible to determine the value of P_{max}/P_μ or A_{max}/A_μ; then from formulas (17) or (36) we choose the corresponding dimensions and other parameters for the element.

Here in the cases of networks II and III it is necessary to find P_{max}/P_μ or A_{max}/A_μ from the formulas which determine $\underline{n}$ on the basis of the conditions of maximum power output and from the formulas which take heating into account; then we choose the largest value.

4. Since the chief purpose of this paper was a comparison of various networks on the basis of the maximum gain for stable operation, we did not take into account certain factors which would have complicated the analysis substantially. These factors include fluctuations in the supply voltage, a spread in the parameters of the cores and resistors, the effect of the actual rectifier characteristics, and variation of the demagnetization current with the demagnetization rate. Therefore, when the formulas cited above are used for computation purposes, we should treat the values of $\underline{n}$ derived above as the upper limit.

LITERATURE CITED

1. I. Gashkovets and N. P. Vasil'eva, "Problems involving the stability of operation for closed (or "long") networks which make use of several types of logic elements," Avtomatika i Telemekhanika, 21, 6 (1960).

A TRANSMITTING DEVICE FOR PULSE-FREQUENCY TELEMETERING

I. A. Lyubinskii, V. A. Milyutina, and N. V. Pozin

(Moscow)

Translated from Avtomatika i Telemekhanika, Vol. 22, No. 7,
pp. 934-938, July, 1961
Original article submitted December 29, 1960

The paper describes a transmitting unit for a pulse-frequency telemetering system; the unit is based on semiconductor elements. The unit employs a new type of dc to ac converter – a magnetic modulator with transverse excitation. The range of variation for the output frequency from the unit is 5 to 15 cps. Due to the high sensitivity of the unit (the input signal power is 10^{-8} w) the unit can be used for transmitting readings from dc transducers which have a low output power.

The pulse-frequency telemetering unit "ChTI-1" designed in the Institute of Automation and Remote Control of the USSR Academy of Sciences is designed for measuring low dc voltages. The "ChTI-1" transmitter produces rectangular pulses with a duty ratio of two and a repetition frequency proportional to the measured voltage. The pulses from the output of the transmitter can be transmitted directly over communication line wires or over frequency division channels. The increased noise immunity requirements of modern telemetering transmission using frequency channels gives rise to the problem of narrowing the frequency band in pulse-frequency telemetering. For this reason the range of variation for the pulse repetition frequency is chosen between 5 and 15 cps. A further lowering of the upper frequency by modern engineering means, including the use of transistors, would lead to an impermissible reduction of the operating stability of the unit.

For telemetering transmission over frequency division channels, the pulses from the transmitter modulate the generator producing the sub-carrier frequency. The chosen frequency range (upper frequency 15 cps) makes it possible to achieve extremely narrow-band transmission (this therefore results in a high noise immunity). The "ChTI-1" unit is matched to a simple narrow-band frequency division unit [1] which was developed in the Institute of Automation and Remote Control of the USSR Academy of Sciences; this makes it possible to transmit telemetering data over a band 40 cps wide in any section of the total range.

We can use any one of numerous frequency metering networks as the receiver in the pulse-frequency telemetering unit "ChTI-1." For example, a number of modern designs of transistorized capacitor frequency meters are available which have a stabilized supply voltage [2]. Because of this the network for the receiver is not cited in this paper.

The Block Diagram for the Transmitter

The "ChTI-1" transmitter operates according to the compensation method and is essentially a rectangular pulse generator with a pulse duty ratio equal to two; it is controlled by the measured voltage and is encompassed with a large negative feedback. The transfer coefficient for the closed system is approximately equal to $1/\beta$ for large values of $k\beta$.* Therefore the stability of the transfer coefficient will be determined basically by the feedback circuit which is much easier to make highly stable than is the direct channel. The block diagram for the unit (Fig. 1) consists of a low-pass filter 1, a dc amplifier 2 containing a modulator-converter that converts a dc signal to an ac signal, an ac amplifier and a rectifier, a pulse generator 3, and a block 4 which performs the reverse conversion of a frequency to a voltage.

* Here k is the transfer coefficient for the direct channel; β is the transfer coefficient for the feedback circuit.

The position of the filter in the direct channel permits a substantial simplification of the amplifier circuit (the phase-detecting stage* can be eliminated) due to the fact that there is no inertial section in the feedback circuit. This is possible, of course, in the case where voltages which do not change sign are measured. When there is no phase-detecting stage it is necessary to choose the filter parameters correctly in order to achieve stable operation of the network. We shall compare the expressions for the transfer functions of the device in two cases:

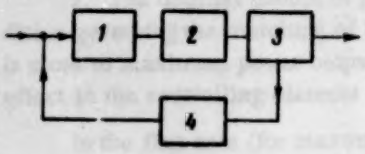

Fig. 1

1) The filter is located in the direct channel:

$$k'(p) = \frac{k_1(p)k_2k_3}{1 + k_1(p)k_2k_3\beta} = k_2k_3\frac{1}{ap^2 + bp + c + k_2k_3\beta};$$

2) the filter is located in the feedback circuit:

$$k''(p) = \frac{k_2k_3}{1 + k_1(p)k_2k_3\beta} = k_2k_3\left(1 - \frac{k_2k_3\beta}{ap^2 + bp + c + k_2k_3\beta}\right).$$

Here $k_1(p) = \frac{1}{ap^2 + bp + c}$ is the transfer function for a two-section RC filter; k_2 is the amplifier gain; k_3 is the voltage to frequency coefficient. The transient functions which determine the nature of the transient responses are equal to the following expressions in the first and second cases, respectively:

$$h'(t) = \frac{k_2k_3}{c + k_2k_3\beta}\left(1 - \frac{p_1e^{-p_2t} - p_2e^{-p_1t}}{p_1 - p_2}\right),$$

$$h''(t) = k_2k_3\left(\frac{c}{c + k_2k_3\beta} + \frac{p_1e^{-p_2t} - p_2e^{-p_1t}}{p_1 - p_2}\right),$$

where p_1 and p_2 are the roots of the equation $ap^2 + bp + c + k_2k_3\beta = 0$.

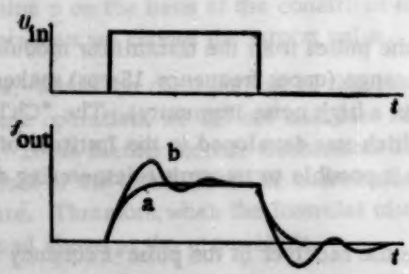

Fig. 2. Response of the unit with the filter in the direct channel to a rectangular pulse. a) Aperiodic mode; b) oscillatory mode.

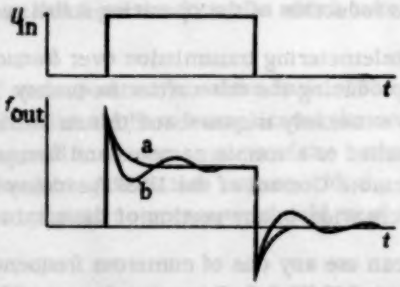

Fig. 3. Response of the unit with the filter in the feedback circuit to a rectangular pulse.

Making use of the relationships derived above, we plot the curves for the variation of the frequency at the output of the unit when it is subjected to a rectangular input signal (Figs. 2 and 3). The difference between the time characteristic for the output frequency and the time characteristic for the voltage at the modulator input involves only a constant coefficient. Therefore, if we choose the system parameters in such a way that the response to a rectangular input signal has the shape of curve a in Fig. 2, the voltage at the modulator input will always be of the same sign. Thus when the filter is located in the direct channel and the transient responses are aperiodic, the system can operate without a phase-detecting stage.

* The phase-detecting stage is usually employed in networks which amplify a direct current by converting the direct current to alternating current, since the phase of the ac current at the output of the converter depends on the polarity of the direct current at its input.

In the case of a two-section low-pass RC filter, it is easy to derive relationships from which it follows that stable operation of the network requires the time constant of the first section to be much greater than the time constant of the second section. In view of the fact that the filter must achieve good filtering of very low frequencies (from 5 cps up), it has appreciable inertia. However the inertia of the filter has little effect on the speed of response of the system, since the "hard" negative feedback reduces this inertia by a factor of $(1 + k\beta)$.

One of the advantages of the block diagram we have chosen is the fact that due to compensation of the input signal by the feedback voltage in the measured-voltage circuit* it is possible to increase appreciably the input resistance of the unit.

Circuit Diagram

The circuit diagram for the "ChTI-1" transmitter is shown in Fig. 4. The device which converts the dc imbalance voltage at the filter output into a dc voltage is a new type of magnetic modulator with transverse excitation [3]. The magnetic fields of the excitation current and the measured current are spatially separated in the core of the modulator M (the windings W_1 and W_2, respectively); therefore, it is possible to achieve a sharp increase in null stability. The transfer coefficient of the modulator is equal to approximately 0.8-0.9 and does not depend on wide variations in the voltage and frequency of the supply source and in the temperature of the ambient medium. The modulator is practically inertialess.

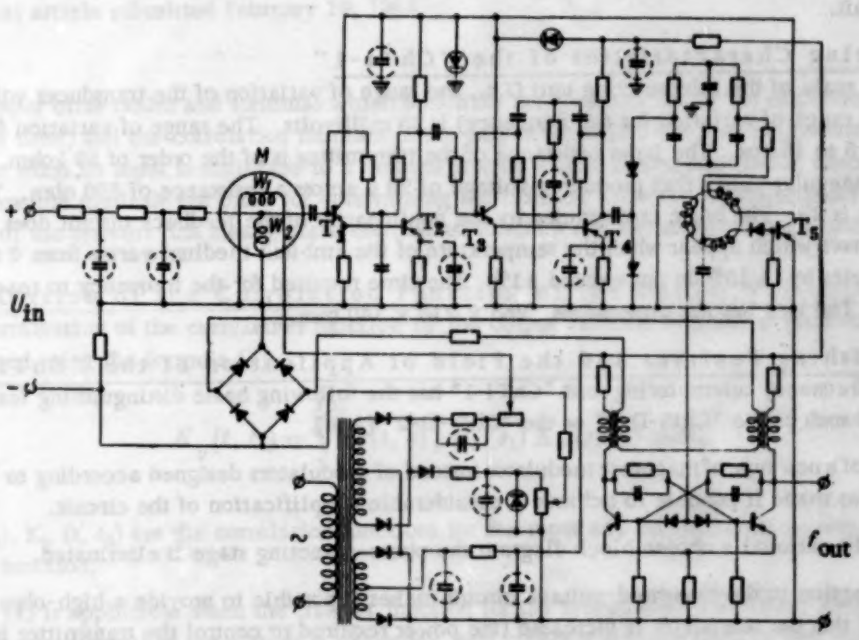

Fig. 4

The ac amplifier consists of two paired stages of transistors "P13B" and "P14" (these are the transistors T_1, T_2 and T_3, T_4 in the circuit shown in Fig. 4). The first transistor in such a stage uses a common-collector connection. The input impedance of the stage is sufficiently high, and therefore the stages can be connected together by means of RC coupling. Such interstage coupling permits us to achieve temperature stabilization easily.

The rectified and filtered output voltage from the amplifier controls the frequency of a blocking oscillator (the transistor T_5). The use of a blocking oscillator as a voltage-to-frequency converter is based first on its high

* In contrast, for example, to magnetic flux compensation in the cores of null-elements in pulse-frequency telemetering systems of the type "ChIS-D-1" and "ChIS-D-2" developed by the Central Laboratory and Experimental Workshop of Electrical and Measuring Instruments [2, 4].

sensitivity with respect to the controlled voltage (in order to change the frequency from minimum to maximum we require a voltage of 2 v across a 50 kohm resistor), and second on the possibility of achieving temperature stabilization in simple fashion (temperature stabilization is achieved with a silicon diode and a shunting resistor in the base circuit; stabilization with respect to the supply voltage is achieved by using a silicon stabilizing diode).

A trigger consisting of transistors of the types "P2B," "P25," or "P26" is used to shape the output pulses; the primary windings of the differentiating transformers are connected in the collector circuits of these transistors. The voltage from the secondary windings of the transformers is rectified by diodes and becomes a pulsating voltage with a dc component that is proportional to the repetition frequency of the pulses; this voltage is then applied to the input of the unit in order to compensate the input voltage. The voltage which acts at the input of the unit as a result of the conversion of the lowest frequency (5 cps) is compensated by a special tributary voltage that is stabilized by a silicon stabilizing diode.

The "ChTI-1" unit was subjected to laboratory tests whose basic results are reflected in the engineering characteristics of the unit.

The Engineering Characteristics of the "ChTI-1"

The entire scale of the telemetering unit (i.e., the range of variation of the transducer voltage which corresponds to the full range of variation for the frequency) is 25 millivolts. The range of variation for the pulse repetition frequency is 5 to 15 cps. The input resistance of the transmitter is of the order of 50 kohm. The output signal consists of dc rectangular pulses that produce a voltage of 20 v across a resistance of 800 ohm. The gain of the open-loop system is 25. The basic error caused by the nonlinearity of the feedback circuit does not exceed ± 1%. The additional errors which appear when the temperature of the ambient medium varies from 0 to +40°C and the supply voltage varies by ± 15% do not exceed ±1%. The time required for the frequency to reach a steady-state value is 0.5 sec. The unit has the dimensions 255 x 215 x 140 mm.

The Distinguishing Features and the Field of Application of the "ChTI-1"

The pulse-frequency telemetering unit "ChTI-1" has the following basic distinguishing features in comparison to analogous units such as the "ChIS-D-1" or the "ChIS-D-2" [2, 4].

1. The use of a new type of magnetic modulator instead of modulators designed according to the magnetic amplifier principle has made it possible to achieve a considerable simplification of the circuit.

2. Due to the rationally chosen block diagram, the phase-detecting stage is eliminated.

3. Compensation in the measured-voltage circuit makes it possible to provide a high-ohm input for the transmitter; because of this the sensitivity is increased (the power required to control the transmitter is 10^{-8} w), and the range of application of the device is expanded.

The telemetering unit "ChTI-1" can be used for transmitting readings produced by a wide class of dc transducers that have a low output power. These include various transducers in which thermal elements are used: temperature transducers, electric power transducers, etc. Moreover, a small output voltage also characterizes individual tension transducers and other bridge networks such as gas analyzers. An example where a gas analyzer is used as a transducer in a telemetering system is a system for telemetering the methane concentration in mines.

LITERATURE CITED

1. N. V. Pozin, On the Transmission of Telemetered Values over Telephone Channels. Transactions of the Session of the USSR Academy of Sciences on the Scientific Problems of Production Automation, October 5-20, 1956 [in Russian] (USSR Academy of Sciences Press, 1957).
2. A. M. Pshenichnikov, A Static Pulse-Frequency Telemetering System Based on Magnetic and Semiconductor Elements. Scientific-Engineering Conference on the Problems of Design and Production of Remote Control Equipment and Communications Channels for Remote Control [in Russian] (Leningrad, 1958).
3. F. I. Kerbnikov and M. A. Rozenblat, "Magnetic modulators with transverse excitation," Avtomatika i Telemekhanika, 19, 9 (1958).
4. A. M. Pshenichnikov, "A static transmitting unit for a pulse-frequency telemetering system," Avtomatika i Telemekhanika, 18, 5 (1957).

TABLES AND FORMULAS FOR DETERMINING THE ACCURACY CHARACTERISTIC FOR THE OPERATION OF A LINEAR STATIONARY DYNAMIC SYSTEM

A. N. Sklyarevich

(Riga)

Translated from Avtomatika i Telemekhanika, Vol. 22, No. 7,
pp. 939-949, July, 1961
Original article submitted February 10, 1961

The paper cites tables and formulas which facilitate the computation of the dispersion (as a function of time) and the correlation function of the output variable for a linear stationary dynamic system when its input is subjected to a random process with a known correlation function. Certain possible methods are cited for determining the limiting accuracy characteristics for the operation of the system: the steady-state correlation function and the steady-state dispersion.

1. Determination of the Correlation Function of the Output Variable

The determination of the correlation function of the output variable of a linear stationary dynamic system is usually performed using the formula [1]

$$K_y(t, t_1) = \int_0^t \int_0^{t_1} g(t, s)\, g(t_1, s_1)\, K_x(s, s_1)\, ds ds_1, \tag{1}$$

where $K_X(t, t_1)$, $K_Y(t, t_1)$ are the correlation functions for the input and output variables, respectively, and $g(t, s)$ is a weighting function.

Formula (1) is applicable when the transfer function for the system has an arbitrary form; it does not assume that the random input signal of the system is stationary and makes it possible to take into account the time for which the system operates. The shortcomings of (1) are the necessity for the preliminary determination of a weighting function and the complexity which is involved in performing the double integration.

This paper presents a different method for determining the correlation functions of the output variables of a linear stationary dynamic system. This method does not require the determination of a weighting function and eliminates the necessity of integrating. The computations are reduced to performing a series of simple operations.

The basis of the method is the relationship [2, 3]

$$\Phi_{ky}(u, u_1) = W(u)\, W(u_1)\, \Phi_{kx}(u, u_1), \tag{2}$$

in which $\Phi_{kx}(u, u_1)$, $\Phi_{ky}(u, u_1)$ respectively denote the results of two-dimensional Laplace transformations of the correlation functions for the signals at the input and output of the system; $W(p)$ is the transfer function for the system.

First we shall assume that a stationary random signal with the correlation function $K_X(\tau) = K_X(|t-t_1|)$ is applied to the system input. Under these conditions

$$\Phi_{kx}(u, u_1) = \frac{F_x(u) + F_x(u_1)}{u + u_1}, \tag{3}$$

where $F_X(p)$ is a unidimensional transform of the function $K_X(\tau)$,

TABLE 1

Transform $F_x(p)$	Original $K_x(p)$
$\frac{1}{2}$	$\delta(\tau)$
$\frac{1}{p}$	1
$\frac{1}{p+\alpha}$	$e^{-\alpha\tau}$
$\frac{p+\alpha}{(p+\alpha)^2+\beta^2}$	$e^{-\alpha\tau}\cos\beta\tau$
$\frac{(p+\alpha)\cos\gamma-\beta\sin\gamma}{(p+\alpha)^2+\beta^2}$	$e^{-\alpha\tau}\cos(\beta\tau+\gamma)$

$$F_x(p)=\int_0^\infty K_x(\tau)e^{-p\tau}\,d\tau. \tag{4}$$

Table 1 shows the transform for the functions $K_x(\tau)$ that are frequently used in solving practical problems.

It is evident that the function $F_x(p)$ can in many cases be represented by the proper fraction

$$F_x(p)=\frac{M(p)}{N(p)}, \tag{5}$$

where M(p), N(p) are polynomials of degree m and n, respectively, relative to the variable p($m < n$). We shall assume that the function W(p) can also be represented by the proper fraction

$$W(p)=\frac{Q(p)}{R(p)}. \tag{6}$$

The quantities q and r shall be used to denote the order of the polynomials Q(p) and R(p).

The position of the poles of the function W(p) [the zeros of the function R(p)] will be characterized by a system of quantities λ_i for $1 \le i \le r$; the position of the poles for the function $F_x(p)$ [the zeros of the function N(p)] will be characterized by a system of quantities λ_i for $r+1 \le i \le r+n$. During the first stage of our investigation we shall assume that all poles of the function W(p) and $F_x(p)$ are simple and that the position of the poles for the function $F_x(p)$ does not coincide with the position of any of the poles for the function W(p).

We shall represent the function W(p) and the product of the functions $W(p)F_x(p)$ in the form of a sum of simple fractions:

$$W(p)F_x(p)=\sum_{i=1}^{r+n}\frac{A_i}{p-\lambda_i};\quad W(p)=\sum_{j=1}^{r}\frac{B_j}{p-\lambda_j}, \tag{7}$$

where

$$A_i=\frac{Q(\lambda_i)M(\lambda_i)}{[R(\lambda_i)N(\lambda_i)]'};\quad B_j=\frac{Q(\lambda_j)}{R'(\lambda_j)}. \tag{8}$$

Making use of this representation for transforming the formula

$$\Phi_{ky}(u, u_1) = \frac{W(u)\,W(u_1)\,[F_x(u) + F_x(u_1)]}{u + u_1}, \tag{9}$$

which is a corollary of formulas (2) and (3), we obtain

$$\Phi_{ky}(u, u_1) = \sum_{i=1}^{r+n} \sum_{j=1}^{r} A_i B_j F(\lambda_i, \lambda_j), \tag{10}$$

where

$$F(\lambda_i, \lambda_j) = \frac{1}{u + u_1}\left[\frac{1}{(u - \lambda_i)(u_1 - \lambda_j)} + \frac{1}{(u - \lambda_j)(u_1 - \lambda_i)}\right]. \tag{11}$$

Formula (10) in the region of the originals corresponds to the formula

$$K_y(t, t_1) = \sum_{i=1}^{r+n} \sum_{j=1}^{r} A_i B_j f(\lambda_i, \lambda_j). \tag{12}$$

in which

$$f(\lambda_i, \lambda_j) = \frac{1}{-\lambda_i - \lambda_j}(e^{\lambda_i \tau} + e^{\lambda_j \tau})\,[1 - e^{(\lambda_i + \lambda_j) T}], \tag{13}$$

$$\tau = |t - t_1|, \quad T = \min(t, t_1). \tag{14}$$

If all the quantities λ_i are real then the result is final. However, if among the quantities λ_i there are complex quantities then additional transformations will be needed to eliminate the imaginary values.

We can avoid performing additional transformations if we formulate the corresponding table of originals and transforms for the case of a two-dimensional transform. Starting from the formulas

$$W(p)\,F_x(p) = \sum_{s=1}^{k} \frac{c_s p + d_s}{p^2 + a_s p + b_s} + \sum_{i=2k+1}^{r+n} \frac{A_i}{p - \lambda_i},$$

$$W(p) = \sum_{s=1}^{l} \frac{c_{s^*} p + d_{s^*}}{p^2 + a_s p + b_s} + \sum_{j=2l+1}^{r} \frac{B_j}{p - \lambda_j},$$

which are equivalent to formulas (7), and for $b_s > \frac{a_s^2}{4}$ $(1 \leqslant s \leqslant k)$ representing the expansion of functions W(p) and $W(p)F_X(p)$ in simple rational fractions, we can conclude that in the transform column of this table it is necessary to write not only the functions $F(\lambda_i, \lambda_j)$ but also the functions which have a structure analogous to the functions $F(\lambda_i, \lambda_j)$ and contain terms of the form $\frac{cu + d}{u^2 + au + b}$, $\frac{cu_1 + d}{u_1^2 + au_1 + b}$ in various allowed combinations.

The originals corresponding to these transforms can be found using formulas (12), (13) if we first represent each newly introduced tabular transform by the sum of terms of the form $F(\lambda_i, \lambda_j)$.

Table 2 is a correspondence table for the originals and transforms which assure the computation of the probability characteristics for the variable at the output of a stationary dynamic system when there are no multiple roots for the function W(p) and the product $W(p)F_X(p)$.

TABLE 2.

Transform $\Phi(u, u_1)$	Original $K(t, t_1)$
$\frac{1}{u+u_1}$	$\delta(\tau)$
$\frac{1}{(u+u_1)uu_1}$	T
$\frac{1}{(u+u_1)(u-\lambda)(u_1-\lambda)}$	$-\frac{1}{2\lambda}e^{\lambda\tau}[1-e^{2\lambda T}]$
$F(\lambda, \mu)=\frac{1}{u+u_1}\left[\frac{1}{(u-\lambda)(u_1-\mu)}+\frac{1}{(u-\mu)(u_1-\lambda)}\right]$	$f(\lambda, \mu)=-\frac{1}{\lambda+\mu}(e^{\lambda\tau}+e^{\mu\tau})[1-e^{(\lambda+\mu)T}]$
$F(\lambda, -\lambda)=\frac{1}{u+u_1}\left[\frac{1}{(u-\lambda)(u_1+\lambda)}+\frac{1}{(u+\lambda)(u_1-\lambda)}\right]$	$f(\lambda, -\lambda)=T(e^{\lambda\tau}+e^{-\lambda\tau})$
$\frac{1}{u+u_1}\left(\frac{1}{u-\lambda}\frac{cu_1+d}{u_1^2+au_1+b}+\frac{1}{u_1-\lambda}\frac{cu+d}{u^2+au+b}\right)$ for $b>\frac{a^2}{4}$	where $R_1(T)(e^{\lambda\tau}+e^{\alpha\tau}\cos\beta\tau)+R_2(T)e^{\alpha\tau}\sin\beta\tau$, $\alpha=-\frac{a}{2}$, $\beta=+\sqrt{b-\alpha^2}$, $R_1(T)=K[\cos\gamma-e^{(\lambda+\alpha)T}\cos(\beta T+\gamma)]$, $R_2(T)=-K[\sin\gamma-e^{(\lambda+\alpha)T}\sin(\beta T+\gamma)]$, $K=+\sqrt{\frac{bc^2+2\alpha cd+d^2}{\beta^2(\lambda^2-a\lambda+b)}}$, $\tan\gamma=\frac{(b+\alpha\lambda)c+(\alpha+\lambda)d}{\beta(d-c\lambda)}$

(Table 2, continued)

Transform $\Phi(u, u_1)$	Original $K(t, t_1)$
$\frac{1}{u+u_1}\,\frac{cu+d}{u^2+au+b}\,\frac{cu_1+d}{u_1^2+au_1+b}$ for $b>\frac{a^2}{4}$	$R_1(T)\,e^{\alpha\tau}\cos\beta\tau + R_2(T)\,e^{\alpha\tau}\sin\beta\tau$, where $R_1(T)=\frac{bc^2+2acd+d^2}{4\beta^2}\left\{\frac{\cos\gamma}{\sqrt{b}}-\frac{1}{\alpha}-e^{2\alpha T}\left[\frac{\cos(2\beta T+\gamma)}{\sqrt{b}}-\frac{1}{\alpha}\right]\right\}$, $R_2(T)=-\frac{bc^2+2acd+d^2}{4\beta^2\sqrt{b}}\left[\sin\gamma-e^{2\alpha T}\sin(2\beta T+\gamma)\right]$, $\alpha=-\frac{a}{2}$, $\beta=\sqrt{b-\alpha^2}$, $\tan\gamma=\frac{\beta(bc-d^2)}{\alpha bc^2+2bcd+\alpha d^2}$
$\frac{1}{u+u_1}\left(\frac{c_1u+d_1}{u^2+a_1u+b_1}\,\frac{c_2u_1+d_2}{u_1^2+a_2u_1+b_2}+\frac{c_1u_1+d_1}{u_1^2+a_1u_1+b_1}\,\frac{c_2u+d_2}{u^2+a_2u+b_2}\right)$ for $b_1>\frac{a_1^2}{4}$, $b_2>\frac{a_2^2}{4}$. 1. In all cases it is necessary to take into account the signs of $\sin\gamma$ and $\cos\gamma$ in determining the angle γ; these signs coincide with the signs of the numerator and denominator, respectively, of the right side of the formula which determines the value of $\tan\gamma$.	$R_1(T)\,(e^{\alpha_1\tau}\cos\beta_1\tau+e^{\alpha_2\tau}\cos\beta_2\tau)+R_2(T)\,e^{\alpha_1\tau}\sin\beta_1\tau+R_3(T)\,e^{\alpha_2\tau}\sin\beta_2\tau$, where $\alpha_1=-\frac{a_1}{2}$, $\beta_1=\sqrt{b_1-\alpha_1^2}$, $\alpha_2=-\frac{a_2}{2}$, $\beta_2=\sqrt{b_2-\alpha_2^2}$. $R_1(T)=K_1\cos\gamma_1+K_2\cos\gamma_2-e^{(\alpha_1+\alpha_2)T}\{K_1\cos[(\beta_1+\beta_2)T+\gamma_1]+K_2\cos[(\beta_1-\beta_2)T+\gamma_2]\}$, $R_2(T)=-K_1\sin\gamma_1-K_2\sin\gamma_2+e^{(\alpha_1+\alpha_2)T}\{K_1\sin[(\beta_1+\beta_2)T+\gamma_1]+K_2\sin[(\beta_1-\beta_2)T+\gamma_2]\}$, $R_3(T)=-K_1\sin\gamma_1+K_2\sin\gamma_2+e^{(\alpha_1+\alpha_2)T}\{K_1\sin[(\beta_1+\beta_2)T+\gamma_1]-K_2\sin[(\beta_1-\beta_2)T+\gamma_2]\}$, $K_1=+\frac{1}{2\beta_1\beta_2}\sqrt{\frac{(b_1c_1^2+2a_1c_1d_1+d_1^2)(b_2c_2^2+2a_2c_2d_2+d_2^2)}{b_1+b_2+2a_1\alpha_2+2\beta_1\beta_2}}$, $K_2=+\frac{1}{2\beta_1\beta_2}\sqrt{\frac{(b_1c_1^2+2a_1c_1d_1+d_1^2)(b_2c_2^2+2a_2c_2d_2+d_2^2)}{b_1+b_2+2a_1\alpha_2-2\beta_1\beta_2}}$, $\tan\gamma_1=\frac{c_1c_2(b_2\beta_1+b_1\beta_2)+(c_1d_2-d_1c_2)(\beta_1\alpha_2-\beta_2\alpha_1)-d_1d_2(\beta_1+\beta_2)}{c_1c_2(b_1\alpha_2+b_2\alpha_1)+c_1d_2(b_1+\alpha_1\alpha_2+\beta_1\beta_2)+c_2d_1(b_2+\alpha_1\alpha_2+\beta_1\beta_2)+d_1d_2(\alpha_1+\alpha_2)}$, $\tan\gamma_2=\frac{c_1c_2(b_1\beta_2-b_2\beta_1)+(d_1c_2-c_1d_2)(\beta_1\alpha_2+\beta_2\alpha_1)+d_1d_2(\beta_1-\beta_2)}{-[c_1c_2(b_1\alpha_2+b_2\alpha_1)+c_1d_2(b_1+\alpha_1\alpha_2-\beta_1\beta_2)+c_2d_1(b_2+\alpha_1\alpha_2-\beta_1\beta_2)+d_1d_2(\alpha_1+\alpha_2)]}$

The method of tables for determining the correlation function of the output variable assumes that the unidimensional transform of the correlation function for the input signal is found; then formula (9) is used to find the two-dimensional transform of the correlation function for the output variable, the transform for the correlation function of the output variable is converted to a sum of tabular transforms, and finally the transition is made into the region of originals.

In accordance with Eq. (12) each pole of the transfer function in the expression for the correlation function of the output variable corresponds to n components. Comparing the values of the individual components, it is possible to establish which of them are the most important (usually it is those corresponding to the smallest values of the parameters λ_i), and thus it is possible to clarify the possibility of replacing the equation that describes the behavior of the specified dynamic system by another simpler equation.

It is evident that this same method for finding the correlation function of the output variable can be extended to apply to the case where a nonstationary random input is applied to the system under conditions where the transform for the correlation function of the signal is represented in the form of a linear combination of tabular transforms. In particular, the problem of investigating the process involved in the passage of a signal through serially connected sections of a dynamic system whose input is subjected to a stationary random process reduces to this case.

If the function W(p) or the product $W(p)F_X(p)$ have multiple poles, then it is impossible to determine the correlation function for the output variable solely by means of Table 2.

2. Determining the Dependence of the Dispersion of the Output Variable on Time

In order to find the dispersion of the output variable of the system, it is necessary to set $t = t_1$ in Eq. (12)-(14). Under these conditions $\tau = 0$, $T = t$, and therefore

$$D_y(t) = K_y(t, t) = 2\sum_{i=1}^{r+n}\sum_{j=1}^{r}\frac{A_i B_j}{-\lambda_i - \lambda_j}\left[1 - e^{(\lambda_i + \lambda_j)t}\right]. \tag{15}$$

Formula (15) determines the dependence of the dispersion for the output variable of the system on time for a known position of the poles of the functions W(p) and $F_X(p)$. However, very frequently the position of the poles of the functions W(p) and $F_X(p)$ is unknown, and therefore it is expedient to transform formula (15) to the expression

$$D_y(t) = 2\int_0^t x_1(u)\, x_2(u)\, du, \tag{16}$$

where

$$x_1(t) = \sum_{i=1}^{r+n} A_i e^{\lambda_i t}, \quad x_2(t) = \sum_{j=1}^{r} B_j e^{\lambda_j t}. \tag{17}$$

Comparing Eq. (17) with relationships (7), we arrive at the conclusion that the transforms $W(p)F_X(p)$ and W(p) in the region of originals corresponds to the functions $x_1(t)$ and $x_2(t)$. This proves the possibility of using the following method for computing the dependence of the output-variable dispersion on time:

1) Using the tables for correspondence of the formulas when the Laplace transform is used, we find a unidimensional transform for the output-variable correlation functions $F_X(p)$.

2) Using the same tables, we determine the originals $x_1(t)$, $x_2(t)$ corresponding to the transforms $W(p)F_X(p)$ and W(p).

3) Using formula (16), we compute the dispersion $D_y(t)$.

A corollary of formula (16) is the formula

$$D_y = 2\int_0^\infty x_1(u)\, x_2(u)\, du, \tag{18}$$

which expresses the steady-state value of the output-variable dispersion.

We find the unidimensional transform of the function $D_y(t)$. In accordance with the basic properties of a Laplace transform [4], this transform is determined by the formula

$$Д(p) = \frac{1}{\pi j p} \int_{c-j\infty}^{c+j\infty} W(z) F_x(z) W(p-z)\, dz, \tag{19}$$

where c is the abscissa of the absolute convergence for the products $x_1(t)x_2(t)$.

When the input of a definitely stable dynamic system is subjected to a stationary random signal, $c < 0$; therefore formula (19) establishes the value of the function Д(p) at the point $p = 0$. Applying the final-value theorem [4], we obtain

$$D_y = \lim_{p\to 0} pД(p) = \frac{1}{\pi j} \int_{c+j\infty}^{z-j\infty} W(z) F_x(z) W(-z)\, dz. \tag{20}$$

The validity of formulas (19), (20) is proved for the condition that the poles of the transfer function W(p) and the products $W(p)F_X(p)$ have a multiplicity equal to unity. The cases where the functions W(p) and $W(p)F_X(p)$ have multiple poles can be treated as limiting cases with respect to the case treated previously. For the transition in the limit $\lambda_i \to \lambda_j$, the function W(p) and $W(p)F_X(p)$ do not lose their continuity relative to the variable p. Therefore it can be assumed that formulas (19), (20), as well as their corollaries, are valid for an arbitrary multiplicity of the poles of the functions W(p) and $W(p)F_X(p)$. This fact proves the possibility of using the method cited above for determining the function $D_y(t)$ and the value of D_y when the form of the transfer function W(p) is arbitrary and the transform of the correlation function $F_X(p)$ is practically arbitrary.

If the position of the poles of the functions W(p) and $F_X(p)$ is known and the multiplicity of each pole is also known, then it is possible to use the theorem of residues [5] in computing the steady-state dispersion D_y.

In the general case we shall assume that for $1 \le i \le k$ the quantities λ_i characterize the position of the poles of the function W(p), and the quantity m_i determines the multiplicity of the poles λ_i. Performing summation over the poles of the function W(-p) that are located symmetrically with respect to the poles of the function W(p) relative to to the point $p = 0$, we can use the theorem of residues to obtain

$$D_y = \sum_{i=1}^{k} \frac{2}{(m_i-1)!} \frac{d^{m_i-1}}{dz^{m_i-1}} [W(z) W(-z) F_x(-z)(z-\lambda_i)^{m_i}]_{z=\lambda_i}. \tag{21}$$

The formula

$$D_y = 2 \sum_{i=1}^{r} \frac{Q(-\lambda_i) M(-\lambda_i) Q(\lambda_i)}{R(-\lambda_i) N(-\lambda_i) R'(\lambda_i)} \tag{22}$$

is a particular case of formula (21) and determines the steady-state dispersion of the output variables of the system when all poles of the transfer function W(p) have a multiplicity equal to unity (for $k = r$).

3. Determining the Steady State Correlation Function of the Output Variable

From table 2 it follows that when a stationary random signal is applied to the input of a linear stationary dynamic system the output signal theoretically cannot be assumed stationary. If the transfer function of the system has a pole at the point $p = 0$, or if it has poles at the points $p = \pm\lambda$ (λ is an arbitrary number), then the quantity T is included in one of the components of the function $K_y(t, t_1)$ as a multiplier; therefore the output signal does not become stationary from a practical point of view even for the case where the preliminary operating time of the system is large (a large value of T). The signal cannot be considered stationary for a large value of T at the output of an unstable dynamic system, since in this case an unlimited increase in certain of the components of the function $K_y(t,t_1)$ occurs due to the positive nature of the real part of at least one of the parameters λ_i for $T \to \infty$.

If the dynamic system is definitely stable, then for a sufficiently large preliminary operating time of the system (large T) the nonstationary parts of the components of the function $K_y(t,t_1)$ become small in absolute magnitude; therefore we can assume that the output signal is practically stationary.

The correlation function and dispersion of the output variable of a definitely stable dynamic system approach their limits for an unbounded increase in the preliminary operating time for the system (when $T \to \infty$): they approach the values of the steady-state correlation function and the steady-state dispersion [1]. In many cases involving the solution of practical problems it is expedient to find precisely these characteristics of the operational accuracy of the system.

At the present time we usually make use of the following formulas [1] in determining the steady-state characteristics for the operational accuracy of a linear stationary dynamic system:

$$S_y(\omega) = |W(j\omega)|^2 S_x(\omega), \tag{23}$$

$$K_y(\tau) = \int_{-\infty}^{+\infty} S_y(\omega)\cos\omega\tau\, d\omega, \quad D_y = \int_{-\infty}^{+\infty} S_y(\omega)\, d\omega, \tag{24}$$

where $S_x(\omega)$, $S_y(\omega)$ are the spectral densities of the signals at the input and output of the system, respectively. Finding the steady-state accuracy characteristic by means of Eq. (23), (24) is usually associated with computing complex integrals.

We shall demonstrate that from relationships (12), (13) we obtain relatively simple formulas that express the results of the integrations indicated by (24).

If the system is definitely stable (all the quantities λ_i, λ_j have negative real parts) and if the preliminary operating time for the system is sufficiently great (the value of T is large), then on the basis of Eq. (13) the function $f(\lambda_i, \lambda_j)$ can be expressed with a sufficient degree of accuracy by the formula

$$f(\lambda_i, \lambda_j) = \frac{1}{-\lambda_i - \lambda_j}\left(e^{\lambda_i \tau} + e^{\lambda_j \tau}\right), \tag{25}$$

whose components are independent of the nonstationary quantity T.

We shall substitute (25) into formula (12) and take into account the fact that for large values of T the correlation function of the output variable depends solely on the value of τ. After simple transformations we obtain

$$K_y(t, t_1) = K_y(\tau) = \sum_{i=1}^{r+n}\sum_{j=1}^{r} \frac{B_j A_i}{-\lambda_i - \lambda_j} e^{\lambda_i \tau} + \sum_{j=1}^{r}\sum_{i=1}^{r+n} \frac{A_i B_j}{-\lambda_j - \lambda_i} e^{\lambda_j \tau}. \tag{26}$$

But, in accordance with (7),

$$\sum_{i=1}^{r+n} \frac{A_i}{-\lambda_j - \lambda_i} = W(-\lambda_j) F_x(-\lambda_j), \quad \sum_{j=1}^{r} \frac{B_j}{-\lambda_i - \lambda_j} = W(-\lambda_i),$$

and therefore we can write the following formula if we take (5), (6), and (8) into account:

$$K_y(\tau) = \sum_{i=1}^{r} \frac{Q(\lambda_i) Q(-\lambda_i)}{R'(\lambda_i) R(-\lambda_i)}\left[\frac{M(\lambda_i)}{N(\lambda_i)} + \frac{M(-\lambda_i)}{N(-\lambda_i)}\right] e^{\lambda_i \tau} + \sum_{i=r+1}^{r+n} \frac{Q(\lambda_i) Q(-\lambda_i) M(\lambda_i)}{R(\lambda_i) R(-\lambda_i) N'(\lambda_i)} e^{\lambda_i \tau}. \tag{27}$$

A corollary of formula (27) is the formula

$$D_y = K_y(0) = \sum_{i=1}^{r} \frac{Q(\lambda_i)\,Q(-\lambda_i)}{R'(\lambda_i)\,R(-\lambda_i)} \left[\frac{M(\lambda_i)}{N(\lambda_i)} + \frac{M(-\lambda_i)}{N(-\lambda_i)}\right] + \sum_{i=r+1}^{r+n} \frac{Q(\lambda_i)\,Q(-\lambda_i)\,M(\lambda_i)}{R(\lambda_i)\,R(-\lambda_i)\,N'(\lambda_i)}, \tag{28}$$

which expresses the steady-state dispersion of the output variable and is equivalent to formula (22). Usually formula (28) is more complex than formula (22).

In the particular case where white noise is applied to the system input, the function $F_X(p)$ has no poles. Under these conditions we obtain the following equation from formulas (24), (27):

$$\frac{1}{2\pi}\int_{-\infty}^{\infty} \left|\frac{Q(j\omega)}{R(j\omega)}\right|^2 \cos\omega\tau\, d\omega = \sum_{i=1}^{r} \frac{Q(\lambda_i)\,Q(-\lambda_i)}{R'(\lambda_i)\,R(-\lambda_i)}\, e^{\lambda_i \tau}; \tag{29}$$

this formula is valid when the multiplicity of all the poles of the function W(p) is equal to unity.

The use of Eq. (27)-(29) is possible if the position of the poles of the functions W(p) and $F_X(p)$ is known. If this is known, then the steady-state characteristics for the operational accuracy of the dynamic system can be found by another method.

Starting from formula (27), we find the unidimensional transform for the steady-state correlation function $K_y(\tau)$ of the output variable. Denoting this transform by $F_y(p)$, we shall prove the validity of the equation

$$F_y(p) + F_y(-p) = W(p)\,W(-p)\,[F_x(p) + F_x(-p)] \tag{30}$$

by means of simple transformations for an arbitrary location of the poles of the functions W(p) and $F_X(p)$. Relationship (30) is a generalization of formula (23), since in accordance with the definitions of the functions $F_X(p)$, $F_y(p)$, $S_X(\omega)$, $S_y(\omega)$,

$$F_x(j\omega) + F_x(-j\omega) = 2\pi S_x(\omega),\quad F_y(j\omega) + F_y(-j\omega) = 2\pi S_y(\omega). \tag{31}$$

Originating from the proof of formula (30), the following method for determining the steady-state correlation $K_y(\tau)$ and the steady-state dispersion D_y can be proposed:

1) We find the transform $F_X(p)$ of the correlation function for the input signal.

2) We represent the function

$$W(p)\,W(-p)F_x(p) = \frac{Q(p)}{R(p)}\frac{Q(-p)}{R(-p)}\frac{M(p)}{N(p)}$$

in the form of a sum of simple fractions:

$$W(p)\,W(-p)F_x(p) = \frac{S(p)}{R(p)\,N(p)} + \frac{S_1(p)}{R(-p)}$$

then, using the method of indeterminate coefficients, for example, we find the functions S(p) and $S_1(p)$.

3) In accordance with the formula

$$F_y(p) = \frac{S(p)}{R(p)\,N(p)} + \frac{S_1(p)}{R(p)}$$

we determine the function $F_y(p)$.

4) Using the known transform $F_y(p)$ we determine the original $K_y(\tau)$.

5) Using the initial-value theorem [4], we compute the steady-state dispersion of the output variable without resorting to tables or to integration on the basis of the formula

$$D_y = K_y(0) = \lim_{p \to \infty} p\, F_y(p).$$

In determining the originals and transforms we can use the tables of operational calculus formulas with the appropriate correction; these tables differ from the tables of Laplace transform formulas in that the transform is multiplied by the argument p.

Examples

1. White noise is applied to a system that is described by the equation

$$(p^2 + 10p + 100)\, x = f(t).$$

It is required to determine the correlation function for the signal at its output.

In this case

$$W(p) = \frac{1}{p^2 + 10p + 100},\quad K_x(\tau) = \delta(\tau),\quad F_x(p) = \frac{1}{2},$$

and therefore

$$\Phi_{ky}(u, u_1) = \frac{1}{(u + u_1)(u^2 + 10u + 100)(u_1^2 + 10u_1 + 100)}.$$

In accordance with the data in Table 2, the transform $\Phi_{ky}(u, u_1)$ corresponds to the correlation function

$$K_y(t, t_1) = R_1(T)\, e^{-5\tau} \cos 5\sqrt{3}\tau + R_2(T)\, e^{-5\tau} \sin 5\sqrt{3}\tau,$$

where we have

$$R_1(T) = 1.6 \cdot 10^{-4} \left\{3 - 2e^{-10T}\left[2 - \cos\left(20\sqrt{3}T + \frac{\pi}{3}\right)\right]\right\},$$

$$R_2(T) = 1.6 \cdot 10^{-4} \left[\sqrt{3} - 2e^{-10T} \sin\left(20\sqrt{3}\,T + \frac{\pi}{3}\right)\right]$$

after transformations.

2. A nonstationary random signal with the correlation function

$$K_x(t, t_1) = \frac{1}{2\lambda} e^{-\lambda\tau}(1 - e^{-2\lambda T}) \quad (\lambda > 0)$$

is applied to the input of an aperiodic section.

It is required to determine the correlation function for the process at the output of the section.

In this case

$$W(p) = \frac{k}{p + a}$$

and in accordance with the data in Table 2,

$$\Phi_{kx}(u, u_1) = \frac{1}{(u + u_1)(u + \lambda)(u_1 + \lambda)}.$$

Therefore

$$\Phi_{ky}(u, u_1) = \frac{k^2}{(u+u_1)(u+\lambda)(u+a)(u_1+\lambda)(u_1+a)}$$

or

$$\Phi_{ky}(u, u_1) = \frac{k^2}{(\lambda-a)^2}[F(-a, -a) + F(-\lambda, -\lambda) - F(-a, -\lambda)].$$

Performing the transition to the region of originals by means of the formulas in Table 2, we find the function $K_y(t, t_1)$.

3. A stationary random process with the correlation function $K_x(\tau) = D_x e^{-a\tau}$ is applied to the input of a section with the transfer function $W(p) = 1/(p + a)$. It is necessary to determine the time dependence of the output-variable dispersion.

In this case

$$F_x(p) = \frac{D_x}{p+a}, \quad W(p) F_x(p) = \frac{D_x}{(p+a)^2}.$$

In making use of the tables for operational calculus formulas [6] with the appropriate correction, we find the originals $x_1(t)$, $x_2(t)$:

$$x_1(t) = D_x t e^{-at}, \quad x_2(t) = e^{-at}.$$

On the basis of formula (16) we obtain

$$D_y(t) = 2D_x \int_0^t u e^{-2au} du = \frac{D_x}{2a^2}(1 - e^{-2at} - 2ate^{-2at}).$$

Assuming $t \to \infty$, we find the steady-state value for the dispersion of the output variable

$$D_y = \frac{D_x}{2a^2}.$$

4. White noise is applied to the input of a section with the transfer function $W(p) = 1/(p + a)^2$. It is required to determine the steady-state dispersion of the output variable.

In this case the function $W(p)$ has one pole $\lambda_1 = -a$ with the multiplicity $m_1 = 2$, and the function $F_X(p)$ has no poles. Therefore we find

$$D_y = \frac{d}{dz}\left[\frac{1}{(a-z)^2}\right]_{z=-a} = \frac{1}{4a^3}$$

by making use of formula (21).

5. We shall study the problem which was cited and partially solved in [1]: a random signal with the correlation function

$$K_x(\tau) = D_x e^{-c\tau}$$

is applied to the input of an oscillatory section.

It is necessary to determine the steady-state correlation function and the steady-state dispersion of the output signal.

In this case

$$W(p)=\frac{1}{p^2+ap+b},\quad F_x(p)=\frac{D_x}{p+c}$$

and therfore Q(p) = 1, $R(p)=p^2+ap+b$, $M(p)=D_X$, $N(p)=p+c$. If $b>a^2/4$, then the poles of the function W(p) are located at the points $\lambda_1=\alpha+j\beta$, $\lambda_2=\alpha-j\beta$, where $\alpha=-\frac{a}{2}$, $\beta=\sqrt{b-\alpha^2}$. The pole of the function $F_X(p)$ is located at the point $\lambda_3=-c$. Making use of formula (27), we obtain

$$K_y(\tau)=\frac{D_x}{(c^2+ac+b)(c^2-ac+b)}\left\{e^{-c\tau}+\frac{c}{ab\beta}e^{\alpha\tau}\left[\beta(c^2-a^2+b)\cos\beta\tau+\frac{a}{2}\times(c^2-a^2+3b)\sin\beta\tau\right]\right\}$$

after a series of transformations.

Assuming $\tau=0$, we find

$$D_y=\frac{(a+c)D_x}{ab(c^2+ac+b)}.$$

If it is necessary to determine only the steady-state dispersion, then it is expedient to make use of the equation

$$W(p)\,W(-p)\,F_x(p)=\frac{D_x}{2ab}\left[\frac{p+a}{(p^2+ab+b)(p+c)}+\frac{a+c}{(c^2+ac+b)(p+c)}+\frac{-(a+c)p+a^2+ac-b}{(c^2+ac+b)(p^2-ap+b)}\right].$$

Therefore

$$F_y(p)=\frac{D_x}{2ab}\left[\frac{p+a}{(p^2+ap+b)(p+c)}+\frac{a+c}{(c^2+ac+b)(p+c)}+\frac{(a+c)p+a^2+ac-b}{(c^2+ac+b)(p^2+ap+b)}\right].$$

Making use of the initial-value theorem, we find

$$D_y=\lim_{p\to\infty}pF_y(p)=\frac{(a+c)D_x}{ab(c^2+ac+b)}.$$

LITERATURE CITED

1. V. S. Pugachev, Theory of Random Functions and its Application to the Problems of Automatic Control [in Russian] (Physics and Mathematics State Press, 1960).
2. V. L. Lebedev, Random Processes in Electrical and Mechanical Systems [in Russian] (Physics and Mathematics State Press, 1958).
3. A. N. Sklyarevich, "On the use of a two-dimensional Laplace transform in determining the correlation function for the output signal of a linear dynamic system," Avtomatika i Telemekhanika, 22, 5 (1961).
4. The Fundamentals of Automatic Control. Theory.- Edited by V. V. Solodovnikov [in Russian] (Machinery Press, 1954).
5. V. I. Smirnov, Course in Higher Mathematics, Vol. 3, Part 2 [in Russian] (State Technical Press, 1949).
6. V. A. Ditkin and P. I. Kuznetsov, Handbook on Operational Calculus [in Russian] (State Technical Press, 1951).

THE SRP-3 INDUSTRIAL REMOTE CONTROL SYSTEM

M. G. Geshelin, B. M. Levin, and A. G. Mamikonov

(Moscow)

Translated from Avtomatika i Telemekhanika, Vol. 22, No. 7,
pp. 950-953, July, 1961
Original article submitted March 11, 1961

An industrial remote control system with a two frequency combination code is described which uses a tone range of frequencies. The apparatus is designed for the remote control of widely distributed groups of objects and provides transmission and reception for a large number of signals. There is described a contactless converter of discrete values of rotational angle into a frequency combination code which is based on scanning the indications by a static induction method.

The SRP-3 remote control system for lumped objects was developed by IAT AN SSSR jointly with VNIIKAneftegaz and served as the basis for a number of the following developments.

The transmission of signals in the SRP-3 system is accomplished by means of a two frequency combination code using a tone frequency range which ensures its universality with regard to communication channels, i.e., the feasibility of operating on physically separate wire lines, frequency multiplexed channels, and radio relay lines. At every control point (CP) there is provision for the remote control of objects, telesignalling their condition, telemetry, and telephone communication. From a dispatching point (DP) to every CP up to 24 signals can be transmitted, and in the reverse direction 36 signals for information and emergency alarms, and 5 of telemetry. There is provision for connecting to one DP up to 10 CPs, so that the total capacity of the system in numbers of signals is 240 issuing from a DP and 410 signals coming in to a DP.

The number of frequencies n employed for the transmission of N signals by means of a two frequency code with sequential transmission of frequencies is determined from the expression

$$n = 0.5(1 + \sqrt{4N + 1}).$$

SRP-3 apparatus was developed for the remote control of interconnected pumping stations in a system for maintaining the stratum pressure in the petroleum industry [1], but it can be used for the remote control of any groups of objects. In the course of industrial operation of an experimental assembly, some changes, which are described in the present article, were introduced.

A block diagram of one-terminal sets for a dispatching and a control point is shown in Fig. 1. There are similar sections in the DP and CP half assemblies: the amplifiers of the receive and transmit channels, the coders, the decoders, and the control sections.

The normal state of all one-terminal sets is a stand-by condition for reception. When it is necessary to transmit a signal, the control section switches amplifiers from receive to transmit. At a DP the control section is switched on from the selector section, and at a CP when one of the information generators is operated. The signal is encoded by a coder which causes voltages of appropriate frequencies to be generated. The sequence and duration of the transmission is determined by the control section.

A signal received at a CP is fed, after amplification, to a decoder, on the output of which control devices are connected.

The transmission of information signals and emergency alarms proceeds in a similar fashion during transmissions from information generators.

During a telemetry call the control section makes a measurement, switches the amplifier to transmit, and connects a measuring generator (for the frequency method of measurement).

A CP coder is shown in Fig. 2a. The networks of the coder control are connected by the information generator contacts. While a signal is passing, voltage is removed from the control networks, and that, in conjunction with the capacitor connected to the relay and their self-blocking, delays a new signal until the completion of the preceding one. Contacts of the A and B relays (a single relay operates simultaneously in each group) connect networks to the RC oscillators (Fig. 2b) thus creating voltages of appropriate frequencies.

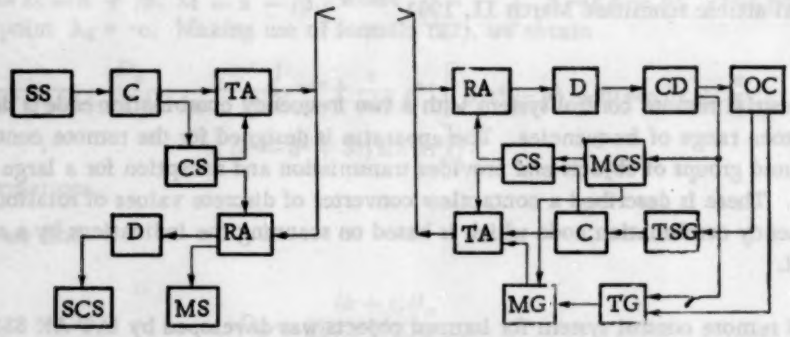

Fig. 1. Block diagram of one-terminal sets at dispatching and control points of the SRP-3 system. SS) Selector section; C) coder; CS) control section; TA) transmit channel amplifier; RA) receive channel amplifier; D) decoder; SCS) signal control section; MS) measuring section; CD) controlling device; OC) object controlled; MCS) measuring control section; TSG) telesignalling information generator; TG) telemetry information generator; MG) measuring information generator.

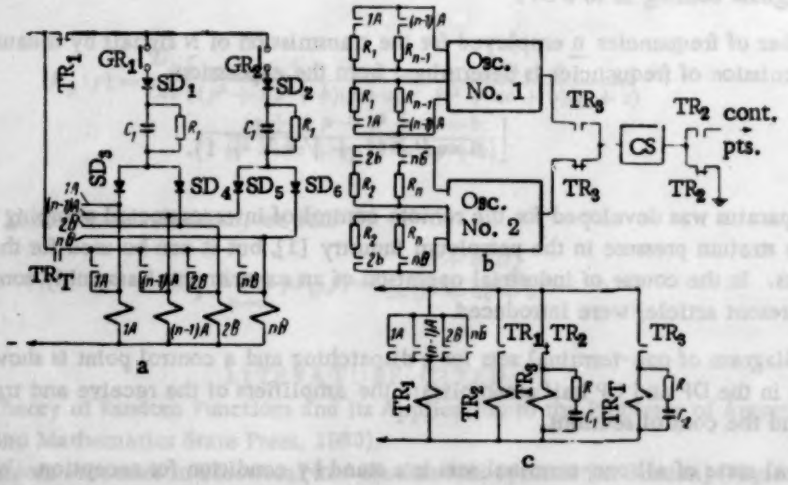

Fig. 2. Transmission sections for signals from CP to DP. a) Coder; b) oscillators; c) control section.

While relays of groups A and B are operated, the control section is connected and performs the following functions.

Relay TR_1 cuts off the voltage from the coder control networks and operates relay TR_2, which, in turn, connects the amplifier of the transmit channel. Relay TR_3 carries out the sequential transmission of the oscillator frequencies.

It is possible to use a single oscillator having the networks connected to it by turns as determined by the contacts of relays A and B. The TR_T relay limits the total time of a signal transmission and restores the circuit to its original state.

The decoder consists of a series of frequency selectors, equal in number to the number of frequencies in the encoded signals which are accepted by the particular decoder. Series resonant LC networks are used as frequency selectors, and the possibility of using K-type filters (Fig. 3) is also provided for. The passband of the selectors is 150 to 170 cps; the attenuation for frequencies in the cutoff region is 4 to 5 nepers.

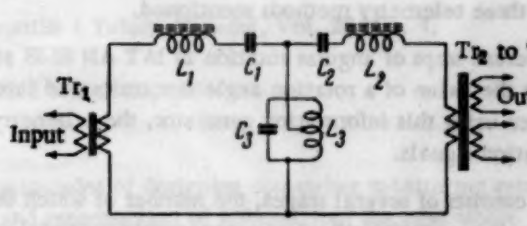

Fig. 3. Basic circuit of a K-type filter.

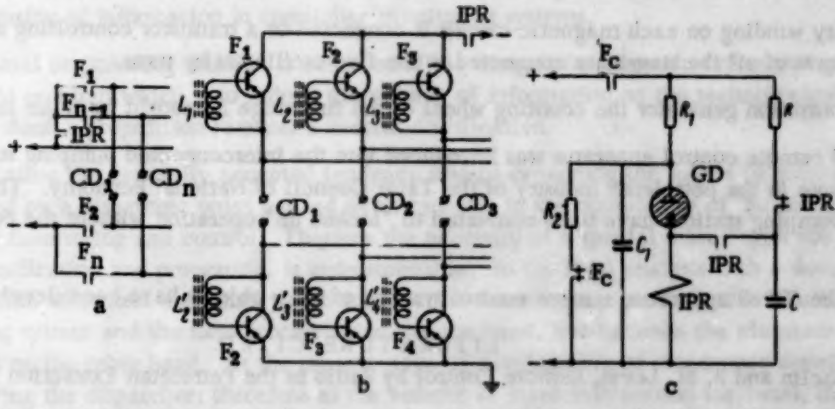

Fig. 4. Receiving sections for signals at a CP. a) Contact decoder; b) contactless decoder; c) interference protection circuit.

The decoder networks were made in two types; contact and contactless. The contact type (Fig. 4a) is distinguished by the small number of contacts. The output of each frequency selector consists of a relay with two make contacts. When two selectors are operated, a circuit is completed to the appropriate control device.

The contactless type (Fig. 4b) differs from the contact type in that transistors, biased to cutoff, replace the relays. Voltages from frequency-selector outputs switch on the transistors so that common paths are produced.

In order to increase the noise immunity of the system there is added to the signal combination a lead frequency which precedes the transmission of code frequencies. The lead frequency pulse passes into a selector ahead of the decoder which has relay F_c for an output. Contacts on F_c turn on a relaxation oscillator (Fig. 4c). The incoming pulse is integrated by network R_1C_1, whose time constant ensures that the interference protection relay IPR operates only on pulses of a specified duration which is appreciably longer than the duration of the expected interfering pulses. During either one or a series of short interfering pulses, the circuit reverts after each pulse to the initial condition by discharging the capacitor through the small resistor R_2. Hence interfering pulses do not accumulate and cannot cause the apparatus to operate.

Upon the arrival of a working pulse of appropriate duration relay IPR operates, locks itself up, and connects, a battery to the output circuits of the decoder.

At the expiration of the time required to receive the signals,relay IPR reverts to the initial condition.

The dependability of the interference protection arrangement was tested with various kinds of real and artificial interference, in particular during operation over radio channels. The tests showed extremely high reliability of operation for the arrangement.

For telemetry transmission no additional control or coding sections are necessary. Provision is made in the SRP-3 system for frequency, time pulse, and code telemetry (frequency combination code).

For the numerical registration of the parameters measured in VNIIKAneftegaz,a numerical converter arrangement was developed which has an output to an electric typewriter with solenoid controls, thus providing printed results in numerical form for the three telemetry methods mentioned.

For the measurement of discrete steps of angular rotation in IAT AN SSSR and VNIIKAneftegaz an information generator was developed in which the value of a rotation angle is transformed into a frequency combination code by the static induction method. When using this information generator, the telemetry signals are no different from the transmission of control or information signals.

The information generator consists of several stages, the number of which determines the accuracy of the measurement. In each stage there is a counting wheel of nonmagnetic material with magnetically permeable strips distributed around the periphery of the wheel. Over each stage there is located a contactless scanner comprising five magnetic circuits with windings which are completed by the magnetically permeable strips of the counting wheel. The positions of these strips causes the completion of two magnetic circuits out of five for every position of the counting wheel, which thus produce a code for a specific number.

A secondary winding on each magnetic circuit is connected to a transistor controlling a fixed frequency oscillator. The scanners of all the stages are connected to the five oscillators by turns.

In the information generator the counting wheel of the first stage is brought up to an integral number of units.

The SRP-3 remote control apparatus was introduced into the interconnected pumping stations which maintain the stratum pressure in the petroleum industry of the Tatar Council of National Economy. The remotely controlled interconnected punping stations have been converted to "locked up" operation without the constant presence of duty personnel.

Based on the SRP-3 apparatus, remote control systems of other objects have been developed for future use.

LITERATURE CITED

1. M. G. Geshelin and B. M. Levin, Remote Control by Radio in the Petroleum Extraction Industry, GOSINTI, 1960.

INFORMATION

MODERN TRENDS IN THE DEVELOPMENT OF DISPATCHER MONITORING ON THE BASIS OF DIGITAL TECHNIQUES

Ya. A. Kupershmidt, V. S. Malov, and I. M. Shenbrot

(Moscow)

Translated from Avtomatika i Telemekhanika, Vol. 22, No. 7,
pp. 954-959, July, 1961
Original article submitted March 22, 1961

The paper studies the principles of designing dispatcher monitoring systems which make use of digital techniques for teletransmission and reproduction of information; the case where information is processed at the dispatcher point is also treated.

At the present time the transmission of data to a dispatcher point and data processing at the dispatcher point are performed almost exclusively on an analog basis. However, the modern state of the techniques available for digital conversion and reproduction provides wide avenues for perfecting methods for transmission, reception, reproduction and processing of information in dispatcher monitoring systems.

The most rational engineering solution is achieved if the design of a dispatcher monitoring system is subordinated to the main problem, which is to reduce the volume of information on the technological process to the required minimum. Such a proposition requires a certain clarification.

At the present time the generally accepted tendency toward expanding the sphere of monitoring and control which is encompassed by a dispatcher point has led to an increase in the complexity of the functions which are involved in dispatcher monitoring and control. Therfore the necessity of a special selection of the essential data, and their automatic classification and processing, is understandable. In the final analysis such a development logically leads to the application of control machines which exclude the intermediate participation of a human operator between the monitoring system and the data processing on the one hand, and between the elements which control the production processes on the other hand. At the present stage of development of monitoring systems, it is still easy to speak of eliminating the dispatcher; therefore as the volume of input information increases, the requirements imposed on the monitoring system involve an ever greater degree of processing for this information [1, 2]. One of the results of processing input data by the system is the operative information which is used by the operator to affect the process directly. It is possible to indicate the following stages of development in formulating the functions which govern the preparation of the operative information.

1. The dispatcher performs simple processing of the received information, estimates the the situation, and adopts operative decisions directly on the basis of the readings of the telemetering instruments and telephone communications.

2. To the degree that the volume of the monitored production process increases, the continuous readings of a large number of instruments are replaced by signals with information on the output of the monitored parameters within the allowed limits. Such a system not only economizes monitoring equipment but also solves the important problem of filtering the information.

3. When signalling a small number of limiting values at each monitored point proves to be inadequate, automatic computing devices are used for processing the data. Using computers, generallized indices of the operating mode of the monitored units are determined and reproduced on the output indicating meters. Thus the dispatcher is freed from performing the operative computing operations, and at the same time the quantity of data monitored by the dispatcher is reduced.

4. A further automatization of the information processing permits the formulation of the control demands to be automatized also. Here the direct participation of a human operator in the operative control of the process is completely or partially eliminated.

Besides the operative information which allows a dispatcher to adopt immediate decisions on direct manipulation of the process, it is usually necessary to acquire statistical information on the process as well. In contrast to operative information, statistical information is subjected to averaging or comparison over a definite time interval (a day, a month, etc.) and must be retained for a prolonged period; it always requires the use of a memory device in which it is recorded.

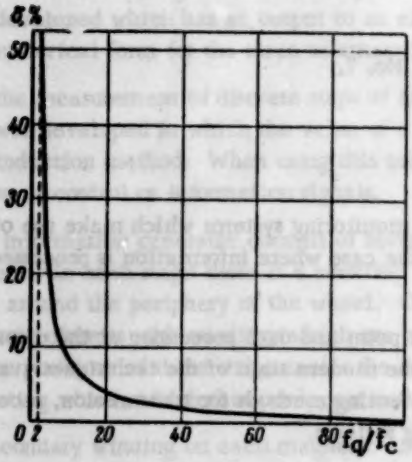

Fig. 1

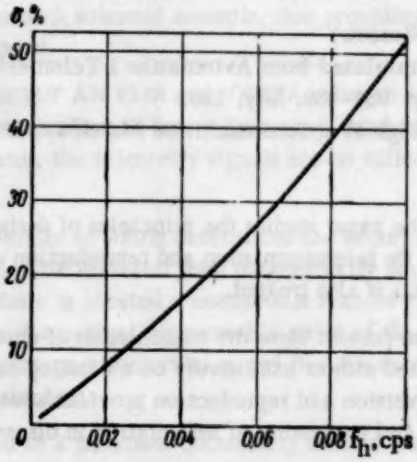

Fig. 2

Digital recording can be used both in the case where the recorded information is designed for subsequent readout by a human operator and in the case where it is designed for machine readout. In both cases the digital form of recording has appreciable advantages. Recording in tabular form is somewhat less convenient than analog diagrams obtained by means of automatic recorders, but it permits us to achieve an appreciably greater accuracy in terms of both the actual measurement and the synchronization of measurements at a large number of points.

Moreover, when compact recording of many parameters is required, digital printing on one blank is definitely the most practical method. For further processing of statistical data in digital computers, only the digital form of recording is a practical method (on punch cards, punched tape, or magnetic tape).

Digital Reproduction of Readings

For purposes of obtaining information in the form of instrument readings, both analog and digital indicators are equally practical. However, analog instruments are in themselves considerably simpler. The advantage is with digital indicators only in those cases when an appreciable noise level in communication channels makes it necessary to transmit information in coded form [3, 4]. Pulse-telemetering systems, as we know, are among those with the highest noise stability. If we also take into account the fact that the noise stability can be appreciably increased by using codes with a high noise immunity, then the advantages of pulse-code systems over telemetering systems with an analog signal is obvious in those cases when noise immunity is the most important property of the system. The comparatively high cost of pulse-code telemetering equipment in one metering channel is lowered when we design a multichannel system with a common coding unit.

When a digital code arrives from a communication channel, the conversion to analog form at the receiving end is, as a rule, completely unjustified. Such a conversion leads to the loss of a number of advantages which a pulse-code telemetering system has; these include the absence of receiver errors, objectivity of readings, and the presence of memory.

We should especially note the memory of digital instruments. In all those cases where information arrives at the instrument at certain time intervals, it is necessary to memorize the readings over a comparatively short period. When the duration of the interval is to any extent appreciable, the solution of this problem by analog techniques is extremely difficult. Only one practical method for memorizing readings in analog form is known—the use of a system with a motor or with a mechanical means for fixing the indicator. However, data in digital form can be

memorized using the simplest means: practically any elements which have two distinguishable states (relays, triggers, etc.) can be used.

The necessity for memorizing the readings in a multichannel telemetering system with time division of the channels may in itself require conversion to the digital form of reproducing readings if the monitored object is inertial and the cycle of measurements is greater than the time constant of the reproducing instrument [1].

The advantages of digital indicators also include the fact that they yield a reading that is easily reproducible by the operator for very small dimensions of the indicators proper; this is due to the rational use of the indicating phase area of such instruments. Thus it is possible to mount such instruments directly in the memo-circuit of the monitored object. Moreover, digital reproduction eliminates subjective errors in taking readings. At present, satisfactory designs for digital indicators are already available (projection indicators, indicators with multielectrode gas tubes, etc.), and work on perfecting them is continuing [5, 6].

The choice of the repetition periodicity of the digital measurements for each parameter is determined by the upper limit of its frequency spectrum. In accordance with the Kotel'nikov theorem, the behavior of the parameter with respect to time can be established in single-valued fashion from the values of individual measurments that are repeated at a frequency which exceeds the upper boundary of the frequency spectrum for the parameter by more than a factor of two. In the case of digital data processing in which the pulse train is not passed through the filter, this requires multiplication of each ordinate by a function of the form sin at/at and addition of the products. Here it is possible to determine the behavior of the measured quantity exactly in the interval between the kth and $(k + 1)$th measurements only after processing the results of a number of subsequent measurements: from the $(k + 1)$th to the $(k + n)$th. The number n is the greater, the higher the required accuracy of computation. Therefore in order to clarify the behavior of the measured parameter with respect to time from the values of individual measurements taken in accordance with the Kotel'nikov theorem, we require both cumbersome computations and a time delay.

If a time delay is impermissible and computations are undesirable, it is necessary to choose a higher quantization frequency than the theorem requires; then horizontal steps are used to approximate the behavior of the function in the intervals between measurements. Under these conditions the relationship between the quantization frequency f_q and the upper boundary f_h for the frequency spectrum of the function depends on the allowable approximation error. Figure 1 shows the analytically derived dependence of the mean-square error δ of the step approximation of the frequency ratio f_q/f_h for the case where the function is random, stationary, and has a uniform energy spectrum from 0 to f_h.

It can be demonstrated that a digital converter can be designed for a number of quantization levels such that the mean-square level quantization error will be of the same order of magnitude as the error of approximating the dependence of the parameter on time. This makes the choice of the number of quantization levels dependent on the time quantization frequency.

The transition to digital reproduction of the parameters is possible in dispatcher systems for inertial industrial objects whose cutoff frequencies are sufficiently small. It is expedient to establish an upper limit for the average frequency with which the readings of the digital indicator change on the basis of the possibilities of human perception. Thus far there is insufficient experimental data, but on the basis of preliminary results it is possible to assume that this frequency is equal to 0.2 cps. Having specified this value, it is possible to use the function shown in Fig. 1 to determine the digital reproduction error for any value of the upper boundary for the spectrum of the monitored process. The corresponding relationship is shown in Fig. 2.

In those cases where it is sufficient to provide the operator with averaged readings of the process flow during comparatively long time intervals, it is possible to use digital reproduction devices which incorporate intermediate conversion to a frequency followed by calculation of the number of oscillations during a fixed time interval.

Returning to the assertion that it is expedient to perform digital conversion of signals received at the dispatcher point from multichannel analog telemetering systems with time division of the channels, we should indicate the comparatively simple engineering realization of this problem. The signal from a frequency or pulse-time telemetering system is in itself already prepared for digital conversion. In fact, it is sufficient to compute the number of oscillations of a frequency telemetering signal over a time interval, or the number of oscillations of a fixed-frequency oscillator over the duration of the signal from a pulse-time telemetering system in order to obtain the numerical value of the parameter. Of course, here it is necessary to make a proper choice of the frequencies and the time required for a reading. The structure of the scaling circuit is determined by the nature of the chosen code.

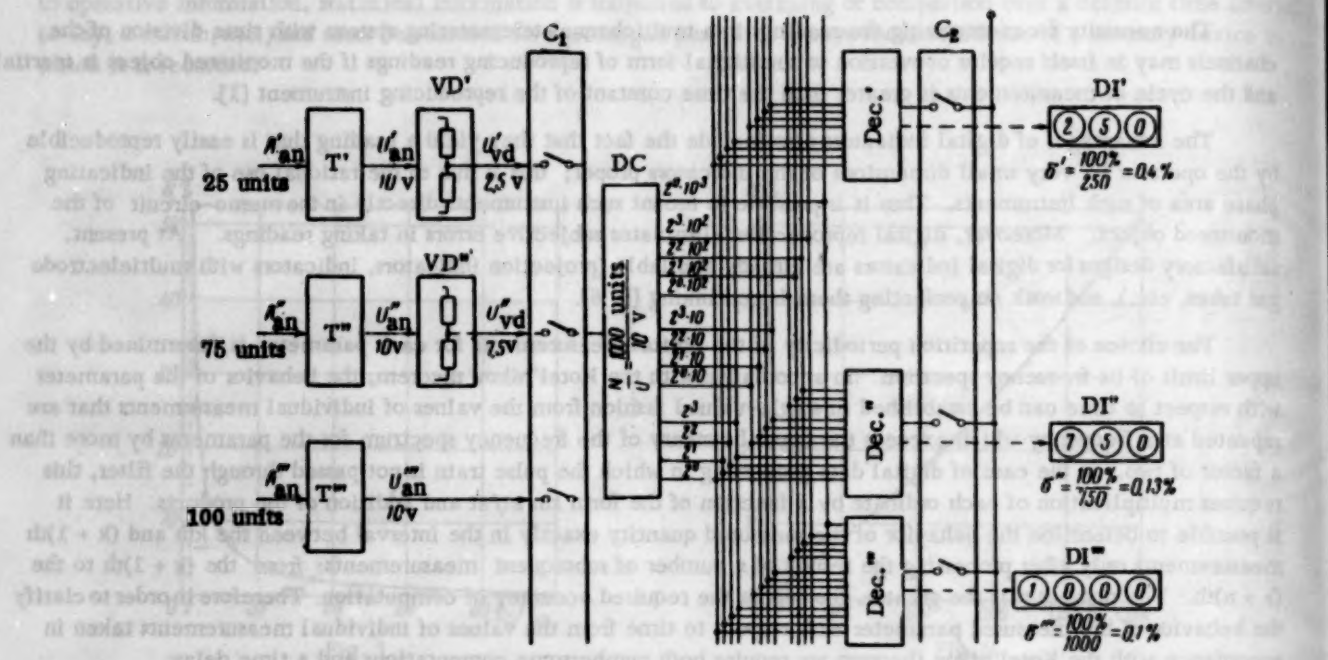

Fig. 3. A circuit for digital conversion with the introduction of scale coefficients by means of voltage dividers. T) Transducer; VD) voltage divider; C_1, C_2) commutators; DC) digital converter; Dec.) decoder; DI) digital indicator.

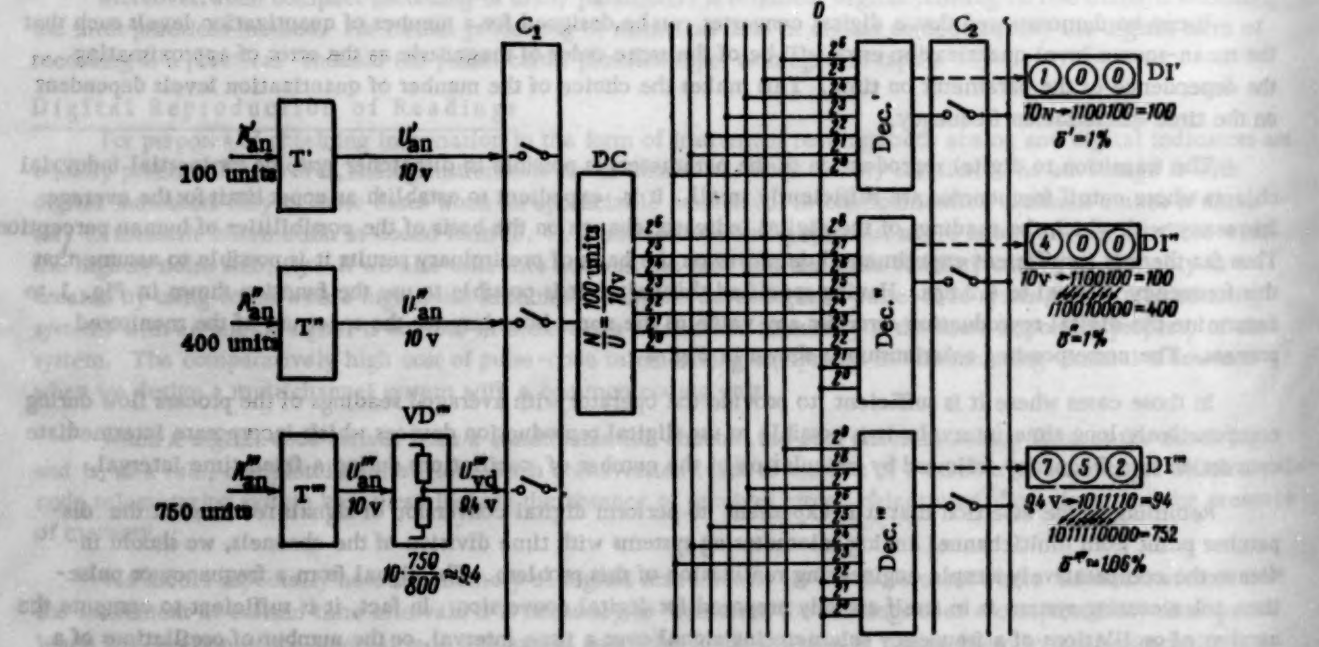

Fig. 4. Circuit for digital conversion with the introduction of scale coefficients by shifting the places of the binary code (the notation is the same as in Fig. 3).

We shall now study certain problems involved in digital conversion for the purposes of both indication and recording.

Since the dispatcher must obtain the digital value of the parameters in a decimal system, it follows that the scaling circuit must be designed either in accordance with the decimal system or in accordance with a system which allows subsequent single conversion of the resulting code to a decimal code. In our opinion this problem can be solved most economically by using a binary-decimal scaling circuit with a simple matrix decoder which converts four binary stages in each decade of the scaling circuit into one of the digits in a decimal number. The digital reproduction is achieved most simply in percentage form, since for various scales corresponding to the variation of the measured parameters, all of these scales are reduced to one nominal at the input of the digital converter. In that case the resulting digit expresses the relative value of the parameter. In individual cases the transition to a percentage scale is permissible. However for the most part we encounter the requirement of reproducing the values of parameters in an absolute digital expression. Under conditions where the dispatcher point does not contain computer devices which permit us to multiply the number by an individual coefficient for each scale, we are left with two possibilities.

It is possible to introduce the scaling coefficient even before introducing the analog parameter into the digital converter. This can be done conveniently using a simple voltage divider if the parameter is represented in the form of a voltage. In that case we obtain a definite relative quantization error for digital conversion. Therefore the digital converter must be designed in such a way that for a minimum nominal for the input analog quantity the quantization error does not exceed the specified value. Under these conditions, increased requirements with respect to the number of digital places are imposed on the digital converter as compared to the case of reproduction in percentage form.

We shall clarify the above on the basis of the example and illustration cited in Fig. 3. Assume that the nominals for the measured parameters have various magnitudes: from 25 to 100 units. If the quantization error for digital reproduction must not exceed $\pm 0.5\%$, then in order to produce the appropriate numbers in percentages we require a coding device incorporating two decimal stages; for producing the appropriate numbers and absolute values we require a digital indicator with three decimal stages for a scale of 25 units. Therefore the same number of stages must be contained in an over-all digital converter.

Of course, if we allow a lower accuracy for the reproduction of the absolute numbers when lower nominals are used, then the digital converter does not become more complicated.

The other possibility for using absolute digital readings without making use of arithmetic units at the output can be simply realized when the digital converter produces a binary code. Shifting a binary code n places to the left is equivalent to multiplication by 2^n. This makes it possible to introduce coefficients which are multiples of the numbers 2, 4, 8, 16, etc. after digital transformation. Under these conditions the relative magnitude of the quantization error remains constant. Since the nominal for the absolute scales do not always differ by a factor of 2^n, it follows that an additional correction can be performed using a divider at the input analog end of the system.

We shall study the example illustrated by Fig. 4. Assume that we have a binary coding device with seven stages. The number of quantization levels in this device is equal to 128. If the range of variation for the analog parameter at the converter input is chosen within the range of from 0 to 100 quantization levels, it follows that the coding will be performed with a normalized quantization error equal to $\pm 0.5\%$. Assume that these 100 conditional units of the analog parameter correspond to an absolute nominal of a hundred units for measured parameter No. 1, an absolute nominal of 400 units for measured parameter No. 2, and an absolute nominal of 750 units for parameter No. 3. In all cases the coding device produces the binary code corresponding to the number 100 for the nominal value of the parameter; this code is equal to 1100100. For the first parameter this code must be retained, and for the second and third parameters it must be altered. In order to multiply this number by 4 (for parameter No. 2) it is sufficient to shift the entire code two places to the left for transfer of the code to the cells of the digital memory for parameter No. 2. We obtain the binary number 110010000 which is equal to 400. For this purpose we need only two extra memory cells. Increasing the number of code places to 9 does not mean a variation in the relative quantization error, since the number will be obtained with an accuracy of up to the third place counting from the lowest place.

As far as parameter No. 3 is concerned, a voltage divider with a division coefficient $750/800 = 15/16$ must be placed after the corresponding transducer. Then the nominal value of the measured parameter will correspond

to (15/16) · 100 conditional units of the analog parameter at the input to the digital converter; with an accuracy of up to integers this will be equal to 94 units, or 1011110 in the binary code. Making a shift of three places to the left for transfer of the code to the memory cells (i.e., multiplying by eight), we obtain 1011110000. This corresponds to the number 752. The accuracy with which parameter No. 3 is reproduced will be slightly lower than the accuracy in the first two cases.

For scales with a suppressed zero the introduction of scale coefficients is extremely complicated, since in this case it is necessary to subtract the particular number corresponding to the parameter in question from the coding result.

Summing up what was said above on the relationship between analog and digital techniques in performing the simplest function of a dispatcher monitoring system (i.e., for the simple reproduction of data), we should note that digital techniques are superior for transmitting information over noisy channels, reproducing signals in multichannel low-frequency telemetering system with time division, and in all other cases where a memory of long duration is required.

Digital reproduction is also convenient to use at a dispatcher point for individual parameters which are transmitted in analog form. In the case under study the convenience of such a solution as far as the dispatcher is concerned is obvious, since it is easier for him to make use of a single mnemo-circuit with digital indicators and a single recording blank. Furthermore, the converse is also probable: For individual parameters whose spectrum contains comparatively high frequencies, it is necessary to use point indicators irrespective of the method by which the signal is transmitted to the dispatcher point. Moreover, if it is important to make it possible to achieve a convenient estimate of the flow of the process over a certain time interval, then analog automatic recorders which trace out a graph are incorporated.

The Equipment for Centralized Monitoring and Processing of Data

In the analysis of a dispatcher monitoring system which we performed above, we did not take into account the problem of filtering the information. Only when this system is augmented by equipment which has become known as centralized monitoring equipment does it become fully usable from the point of view of the minimum-information criterion.

The equipment for centralized monitoring can be designed on the principle of comparing parameters with settings both in digital and analog form. The latter method is realized considerably more easily, but it is applicable only for transmission of the parameters to the dispatcher point in analog form.

The design of centralized monitoring systems using the digital form evidently makes it possible to obtain a universal dispatcher monitoring system which is simpler in design and more successful from the point of view of equipment usage.

When the received information requires more complex processing associated with the performance of mathematical operations, the advantages of complete conversion of dispatcher monitoring systems to the digital basis are even more clearly manifested. Only digital computers have the necessary flexibility and accuracy, and therefore it is precisely these devices which must be used in universal data processing systems. It is logical to design the entire dispatcher monitoring system in such a way that the output data of the monitoring system is introduced directly into a computer without any intermediate conversions.

Thus, digital conversion at the earliest possible stages of information transmission is rational here. This principle is employed most appropriately for transmission of signals over a communication channel in coded form (i.e., in a pulse-code telemetering system). In those cases when the use of comparatively complex and extensive coding equipment at the transmitting end is not justified by cost-engineering considerations (for single-channel systems), the analog telemetering signals which are received at the dispatcher point should be subjected to digital conversion. Such a converter may also service local measurements.

The Transmission of Commands

We shall study methods for transmitting commands from the dispatcher point. Our use of quantized signals for this purpose is based on reliability consideration. Thus it is true that the means for transmitting the control signals will also be basically identical to those used for digital transmission of information from the objects to the dispatcher. This provides broad possibilities for the unification of the engineering means for measurement and control, and for the realization of the block principle in designing equipment for dispatcher systems.

We should make a separate analysis for the case where smooth remote control signals are transmitted (the remote control process). Here we can introduce the following additional arguments in favor of the coded form in choosing between transmission in coded form or analog form.

1. Even for manual transmission of the control pulses (for which there is no direct coupling between the digital system for processing the information and the actuating elements) the use of coding is justified by a considerable increase in the noise immunity of the commands.

2. For automatization of the command function on the basis of digital processing of the information the reverse transition to the analog form of the signal in the final stages of the system is not rational. Therefore it is more expedient to send quantized control signals over the channel. If under these conditions we make use of actuating mechanisms that are controlled by discrete commands (for example, step motors), then digital methods will become most effective.

The argumentation presented above in favor of introducing digital techniques into all the phases of reception, processing, and transmission of information from the dispatcher point makes it possible to conclude that this is the most rational path for achieving the transition to complete automatization based on the use of control machines.

LITERATURE CITED

1. V. S. Malov, A. M. Pshenichnikov, and Ya. A. Kupershmidt, Industrial Telemetering Systems and Digital Engineering, Report to the First International Congress IFAK on Automatic Control [in Russian] (Moscow, 1960).
2. I. M. Shenbrot, Centralized Monitoring and Automatic Processing of Data at Electric Power Stations in the Symposium: "Centralization of control and automation at electric power stations" [in Russian] (State Power Engineering Press, 1960).
3. Ya. A. Kupershmidt, "Coding and decoding units for pulse-code telemetering systems," Avtomatika i Telemekhanika, 19, 9 (1958).
4. V. S. Malov, Remote Control [in Russian] (State Power Engineering Press, 1960).
5. How Digital Readouts Stack Up. Industr. Labs. 10, No. 6 (1959).
6. Numerical Readout Instrum. and Automat. Vol. 31, No. 6 (1958).